Investigation into the regulatory mechanism of BRCA2 stability

Claudia Gruber

University of Oxford
Sir William Dunn School of Pathology
St Cross College

Trinity term 2013

A thesis submitted in partial fulfilment of the requirements for the degree of Doctor of Philosophy at the University of Oxford

To my parents

Abstract

Claudia Gruber
St Cross College

A thesis submitted for the degree of Doctor of Philosophy
University of Oxford
Trinity term 2013.

Investigation into the regulatory mechanism of BRCA2 stability

Inherited mutations in the *BRCA2* gene predispose individuals to the development of breast and ovarian cancers. The BRCA2 protein plays a fundamental role in the repair of DNA double strand breaks by homologous recombination (HR). BRCA2 mediates the recruitment of the RAD51 recombinase to DNA damage sites, which in turn promotes homologous pairing and strand exchange during HR.

It has been reported that increased BRCA2 mRNA levels correlate with poor cancer prognosis, and recently it has been shown that increased levels of BRCA2 suppress HR. As HR is regulated through the cell cycle and can only be employed during S and G2 phases of the cell cycle, in this study, the cell cycle-dependent regulation of BRCA2, as a key player of HR, was investigated.

In this study I report that BRCA2 stability is regulated by the ubiquitin-proteasome system (UPS), which has become increasingly evident as an important regulator of DNA repair. In line with this, I found that BRCA2 can be ubiquitylated *in vivo* and that it interacts with proteins of the UPS. Interestingly, I observed that BRCA2 levels and its ubiquitylation status change during the cell cycle. Using a siRNA-based approach, I identified a candidate E3 ubiquitin ligase, the SCF^{FBXW7} complex, which is also a known major cell cycle regulator. siRNA-mediated knockdown of FBXW7 led to stabilization of BRCA2 and overexpression of FBXW7 resulted in BRCA2 ubiquitylation *in vivo*. Furthermore, I have refined the regions that the SCF^{FBXW7} interacts with on BRCA2, which likely occurs in a phosphorylation-dependent manner.

Taken together, these observations suggest that BRCA2 stability is regulated by the UPS in a cell cycle-dependent manner, which may be an important regulatory mechanism for BRCA2 function.

Acknowledgements

I would like to express my special thanks to:

- my supervisor, Dr. Fumiko Esashi, for the very interesting project and stimulating atmosphere
- Prof. Kevin Hiom and Dr. Eric O'Neill for agreeing to act as my examiners
- My scientific Advisors Prof. Stephen Bell and Prof. Jordan Raff for scientific discussions and support
- my great colleagues Keiko, Chris and Jean-Yves + Sophie for their continuous support, experimental help, the great Lab-atmosphere and food support.
- my friends, who kept me sane in the last 4 years with time, food, running and laughing
- Andy, thank you for your support, the scientific discussions and distraction
- meiner Familie: Ich widme euch diese Arbeit, da es ohne euch und eure unermüdliche Unterstützung nicht möglich gewesen wäre! Danke!

Table of contents

List of Figures

List of Tables

1 Introduction

1.1 Cancer and DNA damage

The development of cancer is a multistep process that is reflected by the occurrence of genetic alterations that lead to transformation of normal cells into highly malignant cells. Tumour cells invariably show genetic alterations and changes in chromosome complement which result in a Darwinian survival advantage, as the succession of mutations lead to growth advantage and thus conversion of normal human cells into cancer cells (Hanahan and Weinberg, 2000; Hao et al., 2007; Kinzler and Vogelstein, 1996).

The genome of cells is constantly exposed to potential DNA-damaging agents from environmental or endogenous sources. These include Ultraviolet light (UV), Ionizing Radiation (IR) or mutagenic reagents such as tobacco or chemicals (Ciccia and Elledge, 2010; Friedberg et al., 2006; Jackson and Bartek, 2009; Li and Hao, 2010). But DNA damage can also arise as a result of normal cellular metabolic processes that create, as by-products, reactive-oxygen species that can damage DNA bases, causing DNA lesions that lead to stalled replication progress and ultimately to DNA double-strand breaks (DSBs) (Chance et al., 1979; Tron et al., 2012). It is estimated that these threats lead to more than 1000 DNA lesions in every cell every day (Hoeijmakers, 2009; Lindahl and Barnes, 2000; Popov et al., 2007; Welcker and Clurman, 2005), which have to be repaired to maintain genome integrity. As the damage interferes with DNA replication and transcription, failure to repair these DNA damages can lead to mutations, genomic instability, premature aging or cancer. Consequently, cells have developed mechanisms to sense the DNA damage and to choose the distinct repair pathway specific for the damage.

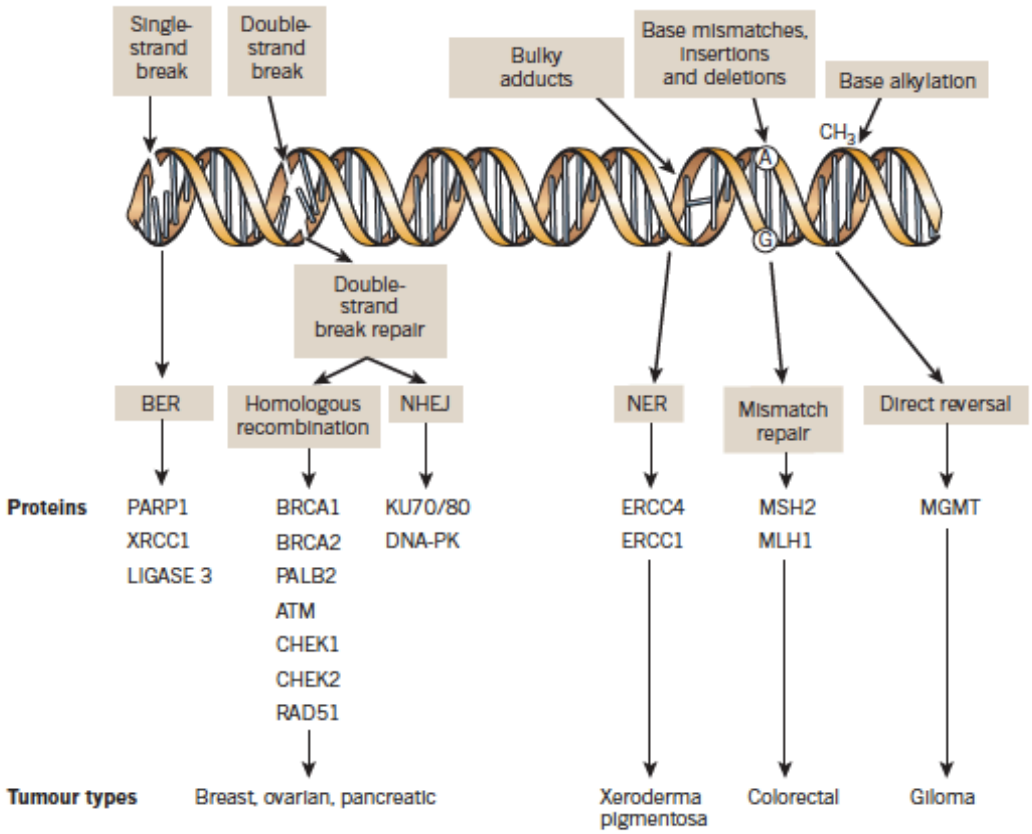

Figure 1.1: Overview of DNA damage and repair mechanisms

DNA is continuously exposed to a variety of DNA damaging agents. The type of DNA damage as well as the stage of cell cycle determines the repair mechanism: base excision repair (BER), homologous recombination (HR), non-homologous end-joining (NHEJ), nucleotide excision repair (NER), mismatch repair and direct reversal (Lord and Ashworth, 2012).

1.2 DNA damage response

The mechanisms that sense the DNA damage and choose the distinct repair pathway are referred to as DNA damage response (DDR). The DDR is classically seen as a signalling cascade that is driven by four groups of proteins. The signal (DNA damage) is detected by the 'sensors' that lead to the activation of the 'transducers' that amplify the signal via 'mediators', triggering the downstream 'effectors' of the DNA damage response, the repair proteins. The DDR signal transduction pathway ultimately leads to cell cycle arrest via activation of the DNA damage checkpoints, DNA damage repair and cell cycle restart or apoptosis. The major drivers of the DDR are members of the phosphatidylinositol 3-kinase like protein kinase (PIKK) family such as the ATM (ataxia-telangiesctasia mutated) and the ATR (ATM and Rad3-related) kinase (Akhoondi et al., 2007; Cimprich and Cortez, 2008; Lovejoy and Cortez, 2009). These kinases phosphorylate down-stream mediator and effector proteins. ATM is activated upon DSBs and phosphorylates the CHK2 (checkpoint kinase 2) whereas ATR is activated in response to single strand breaks and phosphorylates CHK1. Activated CHK1 and CHK2 then phosphorylate and inactivate CDC25 phosphatases which results in inhibition of CDK/cyclin complexes and thus cell cycle arrest in G1/S or G2/M (Bulavin et al., 2003; Mailand et al., 2000; 2002). ATM/ATR activation also leads to phosphorylation and activation of the tumour suppressor protein p53 and its regulator MDM2 which facilitates the expression of CDK inhibitor p21 therefore delaying CDK activation resulting in G1 cell cycle arrest (Agarwal et al., 1995; Harper et al., 1993; Rother et al., 2007).

1.3 DNA double stand break repair

DNA double stand breaks (DSBs) are probably the most toxic lesions within a cell, because, if not repaired, they ultimately can lead to cell death. DSBs can be induced directly by exposure to IR or indirectly as a result of chemical modifications of the DNA, replication fork stalling and collapse.

DSBs can be repaired by 4 different pathways: homologous recombination (HR), non-homologous end-joining (NHEJ), alternative NHEJ (alt-NHEJ) and single strand annealing, whereby HR and NHEJ, are proposed to be the major pathways for DSB repair. NHEJ, in which the Ku complex, consisting of Ku70 and Ku80, are key players, operates throughout the cell cycle and is thought to be a more error-prone repair pathway in comparison to HR. HR uses the genetic information of the complementary, duplicated sister chromatid as a template for the repair during S and G2 phase of the cell cycle when the sister chromatids are lightly packed, in close proximity and accessible. In addition, HR is also regulated during cell cycle by phosphorylation events, for example by CDK phosphorylation. Numerous DNA repair proteins, such as BRCA2, CtIP, RAD51, NBS1, to name a few, have been found to be phosphorylated in a cell cycle-dependent manner (Esashi et al., 2005; Huertas and Jackson, 2009; Yata et al., 2012; Yu and Chen, 2004). BRCA2 is phosphorylated by CDKs on S3291 when cells progress towards mitosis, which blocks interaction with RAD51 and therefore was proposed to possibly act as a terminator of HR repair (Esashi et al., 2005). Besides CDK phosphorylation, also other kinases have been suggested to be involved in the cell cycle-dependent regulation of HR repair, such as PLK1 (polo-like kinase 1), which phosphorylates RAD51 on S14 in a cell cycle and DNA damage-dependent manner. S14 phosphorylation by PLK1 is supposed to prime subsequent RAD51 phosphorylation by CK2 (casein kinase 2) on T13, which in turn triggers binding of RAD51 to NBS1, thus facilitates RAD51 localization to DNA

damage sites (Yata et al., 2012). In addition cell cycle regulation of HR is also reflected in the pathway choice, which will be described in chapter 1.4.2.

1.4 DNA double stand break repair by homologous recombination

1.4.1 Sensing the DSBs and signalling cascade

In homology-directed repair, DSBs can be recognized by the MRE11-RAD50-NBS1 (MRN) complex. The MRN complex consists of three subunits: RAD50, a structural maintenance of chromosome (SMC) protein, which interacts with MRE11 (meiotic recombination 11 homologue) and binds to DNA ends, localizing the MRN complex to sites of DNA damage; MRE11, which is proposed to function as a protector of DNA ends, but also has endo- and exonuclease activities, that are important for the homology-dependent repair and activation of the phosphatidylinositol 3-kinase like protein kinase ataxia-telangiectasia mutated (ATM); and NBS1 (Nijmegen breakage syndrome 1), which interacts with MDC1 (Mediator of DNA damage checkpoint protein 1) in a phosphorylation-dependent manner that facilitates recruitment of MRN to sites of DNA damage and interacts with MRE11 and ATM, resulting in the recruitment of ATM to site of DNA damage and ATM activation by ATM monomerization and autophosphorylation on S1981 (Bakkenist and Kastan, 2003; Chapman and Jackson, 2008; de Jager et al., 2001; Falck et al., 2005; Kitagawa et al., 2004; Lee and Paull, 2005; Uziel et al., 2003). ATM activation initiates a signalling cascade that leads to accumulation of repair factors at DNA damage sites and subsequent protein modification events. In brief, histone variant H2AX, is phosphorylated on serine 139 by ATM (γH2AX) enabling the direct binding of the MDC1 (Rogakou et al., 1998; Stucki et al., 2005). ATM also phosphorylates

MDC1, which in turn recruits the RING-finger (RNF) ubiquitin E3 ligase RNF8 via its forkhead-associated (FHA) domain, that polyubiquitylates H2A and γH2AX together with the E2 enzyme UBC13 in a Lys63 (K63)-linked manner (Galanty et al., 2012; Huen et al., 2007; Kolas et al., 2007; Mailand et al., 2007). The RING finger ubiquitin E3 ligase RNF168 then recognizes and binds the ubiquitin chains via its motifs interacting with ubiquitin (MIU). MIUs form a single amphipathic α-helix which contains a centred alanine that interacts with mono-ubiquitin with an affinity about ~ 30 μM (Lee et al., 2006; Penengo et al., 2006). Together with the E2 ubiquitin-conjugating enzyme UBC13 RNF168 further stimulates K63 ubiquitylation (Doil et al., 2009; Krogan et al., 2004; Stewart et al., 2009; Yin et al., 2012). In turn the formation of K63 polyubiquitin chains leads to the recruitment of the adapter protein RAP80 (receptor associated protein 80). RAP80 selectively recognizes K63 polyubiquitin chains through its ubiquitin interacting motifs (UIMs) and recruits the dimeric E3 ligase complex BRCA1-BARD1, which is bridged by the phosphorylated Abraxas protein (Gudmundsdottir et al., 2007; Kim et al., 2007; Liu et al., 2007; Sobhian et al., 2007; Wang and Elledge, 2007). UIMs also contain one single α-helix with a centred alanine that contacts Ile^{44} of ubiquitin but their α-helix is one turn shorter than that of the MIUs. In contrast to MIUs, UIMs show a lower affinity to mono-ubiquitin and also bind to K6 or K63-linked polyubiquitin chains (Fisher et al., 2003; Swanson et al., 2003; Wang et al., 2005). The RNF168-stimulated ubiquitylation of H2A and γH2AX further facilitates the accumulation of additional repair proteins, such as CtIP (CtBP (C-terminal binding protein) interacting protein), Rad18 (radiation-sensitive 18), 53BP1 (p53 binding protein 1) and the HECT-type E3 ligase HERC2. HERC2 accumulates at DNA damage sites by interaction with the FHA domain of RNF8. Although the function of HERC2 has not been entirely elucidated, it has been suggested that it stabilizes RNF168 and RNF8/UBC13 interaction (Bekker-Jensen et al., 2010) (Fig. 1.4.1).

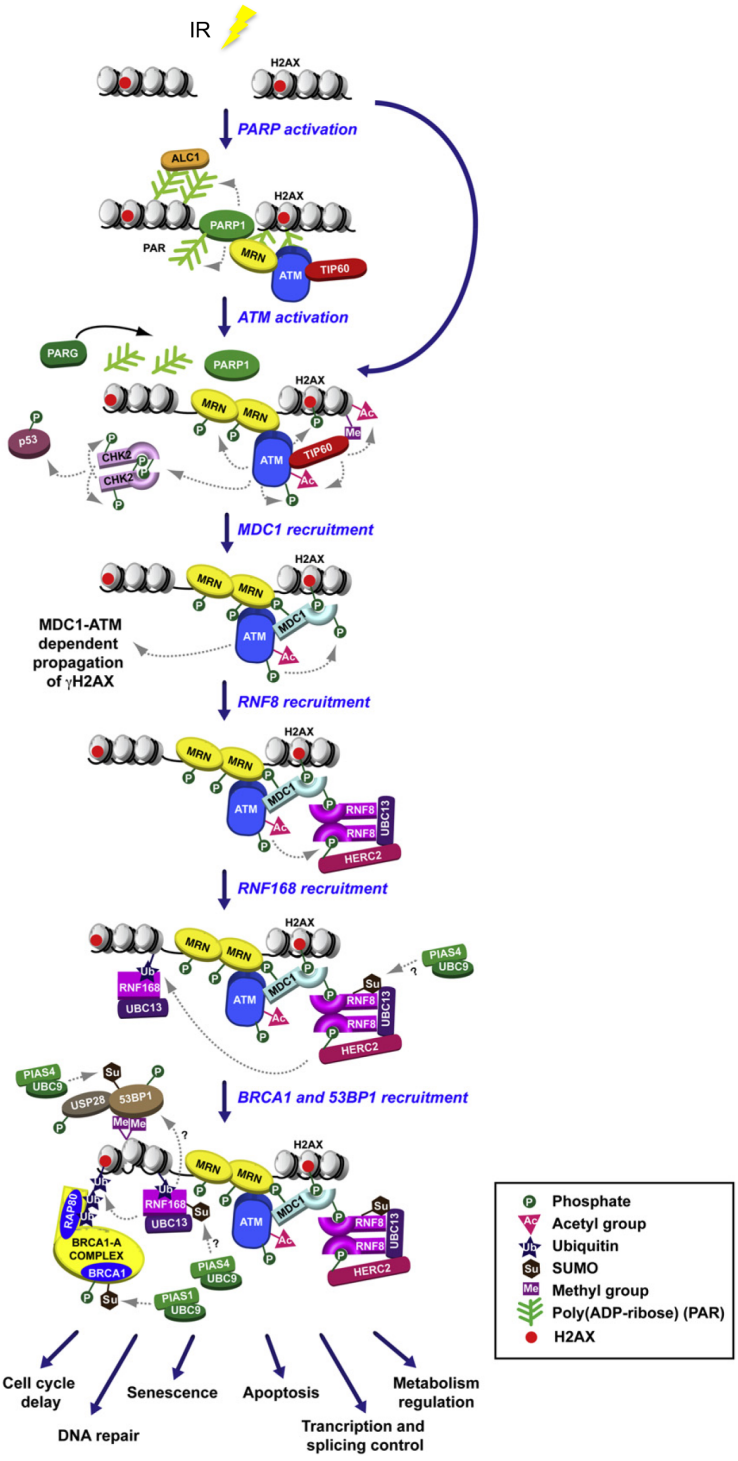

Figure 1.4.1: Schematic representation of IR-induced ATM activation
DNA double strand breaks (DSBs) lead to the activation of PARP1, which mediates the recruitment of the MRN complex and subsequent localization and activation of ATM to DSBs, followed by phosphorylation of CHK2, H2AX and further DNA repair proteins. Phosphorylation of H2AX leads to further accumulation of repair proteins and initiates a signalling cascade. Taken from (Ciccia and Elledge, 2010)

1.4.2. DNA-end resection and repair pathway choice

In the past years it became evident, that the choice of DSB repair pathway is closely controlled during cell cycle. The main factor that is thought to influence the choice of DSB repair pathway is DNA-end resection which has been described to be controlled in cell cycle-dependent manner through CDK phosphorylations (Aylon et al., 2004; Ira et al., 2004; Jazayeri et al., 2006).

Homology-directed repair of DSBs is thought to require extensive DNA-end resection. It has been proposed that phosphorylation of S432 on NBS1 of the MRN complex promotes DNA-end resection (Falck et al., 2012). Nonetheless, another study by Wohlbold et al. observed no changes in DNA-end resection in the absence of S432 phosporylation (Wohlbold et al., 2012). Whether CDK phosphorylation of NBS1 indeed is necessary for DNA-end resection remains to be elucidated. However, there are further evidences for a CDK-dependent regulation of DNA-end resection as CDK-dependent phosphorylation of CtIP on T847 by CDKs is required to promote end resection (Huertas et al., 2008; Huertas and Jackson). In addition, there are some evidences that upon CDK phosphorylation, CtIP can interact with NBS1 of the MRN complex, leading to DNA damage-dependent phosphorylation of CtIP on T859 by ATM, which may contribute CtIP function in end-resection (Huertas and Jackson, 2009; Wang et al., 2013; Yu and Chen, 2004; Yu et al., 2006). In S and G2 phases CtIP can be phosphorylated by CDKs on S327 which has been reported to be necessary for CtIP-BRCA1 interaction (Yu and Chen, 2004; Yu et al., 2006). Though BRCA1-CtIP interaction has been shown to be dispensable for CtIP function in end-resection in mammalian cells, the BRCA1-CtIP complex has been reported to direct the pathway choice towards HR-directed repair by removal of RIF1 from DSBs in S and G2 phases (Escribano-Diaz and Durocher, 2013; Reczek et al., 2013). However, loss of the CDK phosphorylation sites in CtIP impairs end resection and

results in HR defects (Huertas and Jackson, 2009; Limbo et al., 2007; Yun and Hiom, 2009). Thus CDK-dependent phosphorylation of proteins involved in DNA-end resection provide one possible layer of regulation that links the extensive DNA end resection required for HR repair to cell cycle.

After the initial resection by CtIP, extensive resection is carried out by to parallel pathways, one EXO1-dependent and one BLM-dependent pathway (Gravel et al., 2008).

1.4.3. RAD51- mediated homologous Recombination

DSB end resection leads to the formation of 3' ssDNA ends that can be bound by the single strand binding protein Replication protein A (RPA) (Fig. 1.4.3). RPA accumulates on these regions and stabilizes ssDNA. RPA is then subsequently replaced by the RAD51 recombinase, a highly conserved RecA homologue. RAD51 is recruited to the ssDNA areas by BRCA2, the breast cancer protein 2, which facilitates the loading of RAD51 on RPA-coated ssDNA and formation of RAD51 nucleoprotein filaments (Sharan et al., 1997; Thorslund et al., 2007; Yuan et al., 1999). The RAD51 nucleoprotein filaments then invade the homologous template and form displacement loop (D-loop) DNA structures. Within these structures RAD51-dsDNA filaments are formed that consist of the invading and the donor ssDNA strands. RAD51 is then thought to be removed from the D-loop by the RecQ helicase BLM (Bugreev et al., 2007). DNA can be synthesized by DNA polymerases using the invading 3'-OH end as a primer and the 3' invading strand can be elongated using the sister chromatid information as a template. After ligation to the processed second end of the DSB, the D-loop can revert into its original position; this process is called synthesis-dependent strand annealing (SDSA) and is thought to be

promoted by the RTEL helicase (Barber et al., 2008; Youds et al., 2010). In an alternative pathway, the second end of the DSB can be used to stabilize the D-loop formed (second end capture); whereby sister chromatids can exchange DNA strands, forming a structure called Holliday junction, and branch migration can occur. Holliday junctions can be resolved by dissolution, performed by the SGS1/BLM-TOPIIIα complex (Fabre et al., 2002; Wu et al., 2006), or by endonucleolytic cleavage, catalysed by GEN1, MUS81/EME1 or SLX1/SLX4 nucleases (Andersen et al., 2009; Fekairi et al., 2009; Osman et al., 2003; Svendsen et al., 2009).

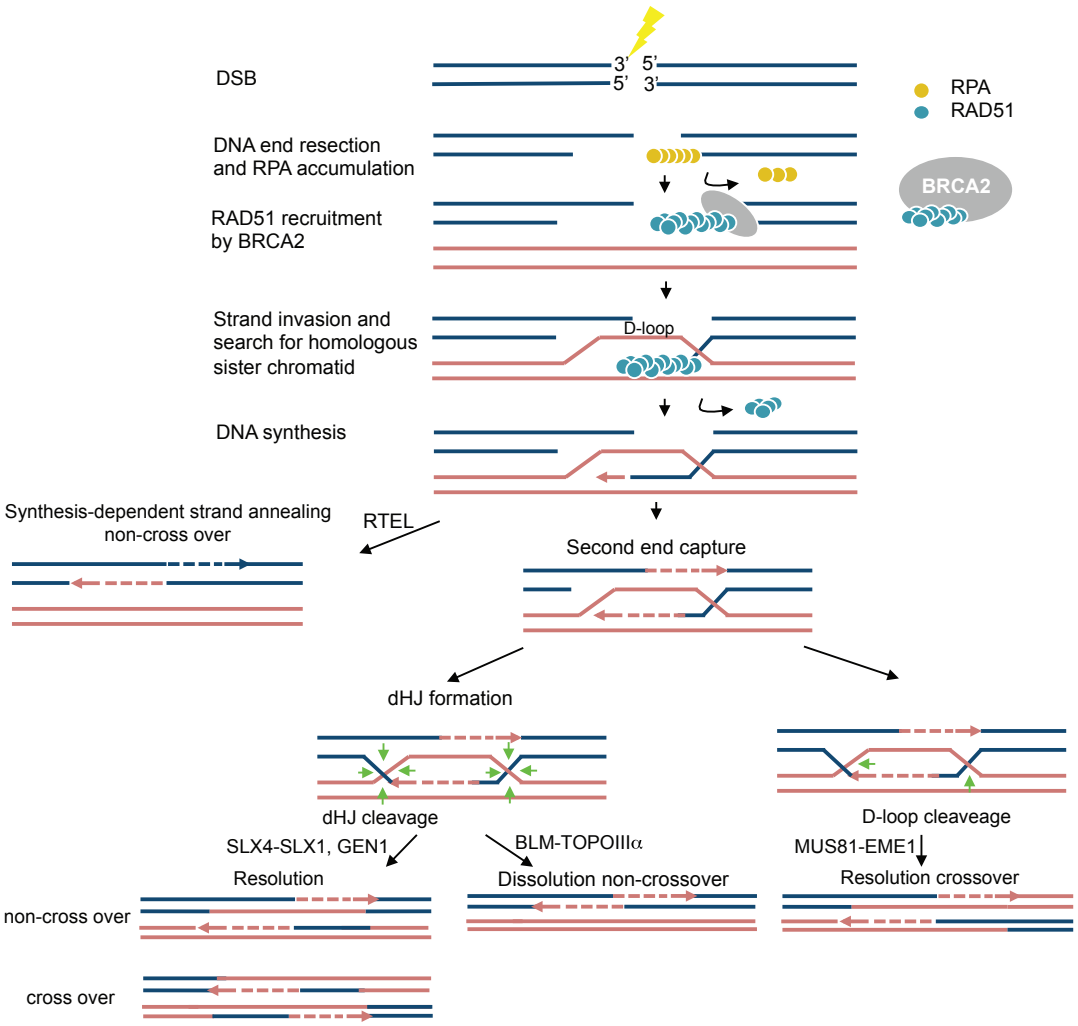

Figure 1.4.3: Schematic figure of DSB repair by homologous recombination

After DNA double-strand breaks (DSBs) have been recognised, DNA ends are resected generating 3' single-stand DNA (ssDNA) overhangs on which the RPA (replication protein A, yellow circles) accumulates. BRCA2 (grey) recruits RAD51 (blue circles) and promotes RAD51 assembly on ssDNA thereby replacing RPA. RAD51 nucleofilaments can then invade the homologous duplex DNA, which is used as a template for DNA synthesis. The resulting DNA structure can be differentially dealt with leading to crossover or non-crossover products. The green arrows indicate where cleavage can occur. (Adapted from (Chapman et al., 2012)

1.5 BRCA2

Germline mutations in the *BRCA2* gene predispose Individuals to the early onset of breast and ovarian cancers as well as pancreatic, prostate and male breast cancers (Couch et al., 1996; Lowenfels and Maisonneuve, 2005; Simard et al., 2003; Venkitaraman, 2002). Women carrying germline mutation in *BRCA2* show loss of heterozygosity (LOH) at this locus, suggesting that BRCA2 protein functions as a tumour suppressor. BRCA2-defective cells exhibit increased sensitivity to IR, accumulation of chromosomal breaks, gross chromosomal rearrangements, and impaired DSB repair by HR (Moynahan et al., 2001; Patel et al., 1998; Sharan et al., 1997). Furthermore, BRCA2 deficiency causes defects in RAD51 foci formation and DNA replication (Lomonosov et al., 2003; Sharan et al., 1997; Yu et al., 2000; Yuan et al., 1999).

More than 1800 mutations in BRCA2 have been found so far (Breast Cancer Information Core database), though the physiological impact of most of these mutations remains unknown. Most of the germ-line mutations found in ovarian cancer cases usually lead to a truncated BRCA2 protein whose functions are impaired. Analyses of BRCA2 mRNA level by RT-PCR or immunocytochemistry revealed that BRCA2 is often overexpressed in sporadic breast, ovarian, pancreatic and prostate cancers and that increased level of BRCA2 mRNA correlates with poor cancer prognosis (Bièche et al., 1999). Whether the overexpression of wild-type BRCA2 is associated with tumourigenesis is still unknown, as the methods used in the previously mentioned studies did not determine whether the overexpressed BRCA2 was a wild-type or a mutant variant of BRCA2. However, recent findings show that overexpression of BRCA2 impairs HR (Magwood et al., 2012). These evidences indicate that de-regulation of BRCA2 could potentially lead to cancerogenic phenotypes.

1.5.1 BRCA2 structure

The *BRCA2* gene encodes for a protein of 3418 amino acids, which shows little homology to known proteins and does not exhibit enzymatic activity (Fig. 1.5.1) (Wooster et al., 1995). In its middle region BRCA2 contains a cluster of eight repetitive sequences of about 35 amino acids (amino acids 1009 – 2083), called the BRC repeats (Bignell et al., 1997; Bork et al., 1996). In the C-terminal region BRCA2 contains a DNA-binding domain (DBD) that binds to single stranded (ss) and double stranded (ds) DNA. The DBD domain consists of 5 components: an α-helical domain of 190 amino acids, three oligonucleotide-binding (OB) folds that can bind ssDNA and subsequently a tower domain (TD) that binds dsDNA (Yang et al., 2002). However, recent reports suggest, that BRCA2 preferably binds ssDNA (Jensen et al., 2010; Thorslund et al., 2010). Furthermore, the C-terminal area of BRCA2 contains a nuclear localization signal (NLS) and is highly conserved throughout mammals.

There are several BRCA2 interaction partners known, i.e. RAD51 recombinase, BRCA1, P300/CBP-associated factor (P/CAF), deleted in spilt hand/spilt foot 1 (DSS1), Disrupted Meiotic cDNA1 (DMC1) recombinase, BRCA2 associated factor 35 (BRAF35), polo-like kinase 1 (PLK1), ubiquitin thioesterase 11 (USP11), the fanconi anemia proteins FANCD2 and FANCG, the androgen receptor, BRCA2 and CDKN interacting protein (BCCIPα)β), the oncoprotein EMSY, PALB2, which localizes BRCA2 to DNA damage sites and acts as a molecular scaffold for the formation of a BRCA1-PALB2-BRCA2 complex (Hughes-Davies et al., 2003; Hussain et al., 2004; 2003; Lee et al., 2004; Lu et al., 2005; Marmorstein et al., 2001; Marston et al., 1999; Schoenfeld et al., 2004; Sharan et al., 1997; Shin and Verma, 2003; Sy et al., 2009; Wang and D'Andrea, 2004; Zhang et al., 2009a; Zhang et al., 2009b).

However, the interaction sites for some BRCA2 interaction partners have been mapped, but for many, the sites of interaction are yet to be determined.

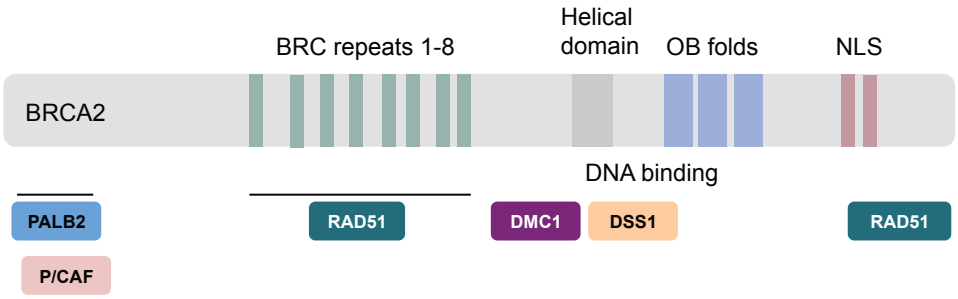

Figure 1.5.1: Schematic figure of BRCA2 domains and interacting proteins
BRCA2 contains 8 repetitive sequences termed BRC motifs 1-8 in the middle region. A helical domain and adjacent OB-folds are located in the C-terminal region, which are both involved in the DNA binding ability of BRCA2. At the C-terminus BRCA2 contains a nuclear localization signal. Binding sites for BRCA2 interaction partners: partner and localizer of BRCA2 (PALB2), P300/CBP-associated factor (P/CAF), RAD51 recombinase, Disrupted Meiotic cDNA1 (DMC1) recombinase, deleted in spilt hand/spilt foot 1 (DSS1) are shown.

1.5.2 BRCA2 function

BRCA2 has been shown to have multiple functions that contribute to the maintenance of genome integrity, such as roles in transcriptional regulation, protection of nascent DNA at stalled replication forks, inhibition of cell proliferation, regulation of cytokinesis, G2/M checkpoint control, and regulation of centrosome duplication (Chen et al., 1999b; Chen et al., 1998a; Daniels et al., 2004; Hughes-Davies et al., 2003; Lomonosov et al., 2003; Milner et al., 1997; Moynahan et al., 2001; Schlacher et al., 2011; Sharan et al., 1997; Shin and Verma, 2003; Tutt et al., 1999; Yu et al., 2000). A very well established function of BRCA2 lies in its involvement in the repair of DSBs by HR. BRCA2 is required for the recruitment of the RAD51 recombinase to sites of DNA damage and the formation of RAD51 foci

after DNA damage (Tarsounas et al., 2003; Yu et al., 2003; Yuan et al., 1999). During HR-directed repair, BRCA2 binds and recruits RAD51 to sites of DNA damage, where it promotes assembly of RAD51 to RPA-covered ssDNA and RAD51-medated strand exchange (Jensen et al., 2010; Liu et al., 2010; Thorslund et al., 2010).

1.5.3 BRCA2 interaction with RAD51

BRCA2 is known to interact with RAD51 through two regions: RAD51 interacts with the middle region of BRCA2 via the BRC motifs that structurally mimic the RAD51 self-association motif (Esashi et al., 2007; Pellegrini et al., 2002; Wong et al., 1997) and via a C-terminal domain, which contains a CDK phosphorylation site that modulates RAD51 binding, and can bind and stabilize RAD51 nucleoprotein filaments (Fig. 1.5.3) (Davies and Pellegrini, 2007; Esashi et al., 2005; Esashi et al., 2007).

Much effort has been put into the understanding of how BRCA recruits RAD51 to sites of DNA damage, in particular the involvement of BRC motifs in this process. *In vitro* interaction assays using GST-tagged BRCA2 fragments showed that RAD51 interacts with fragments containing BRC1-5 but not 5-8 (Chen et al., 1998b; Esashi et al., 2005). More recent analyses revealed that BRC1-4 bind strongly to free RAD51, thereby inhibiting ATP-hydrolysis by RAD51 and stabilizing RAD51-ssDNA complexes, whereas for BRC5-8 a high affinity to RAD51-ssDNA complexes was observed (Carreira and Kowalczykowski, 2011; Carreira et al., 2009). Interestingly, excess of BRC3 and BRC4 was found to disrupt RAD51 filament formation (Chen et al., 1999a; Davies and Pellegrini, 2007; Galkin, 2005). Furthermore, BRC4 and BRC1-8 were found to stabilize RAD51-ssDNA complexes and stimulate RAD51-mediated strand exchange at low concentrations, but increased concentrations of

BRC4 or BRC1-8 resulted in decreased RAD51-mediated strand exchange which suggest that the molecular ratio of RAD51 to BRC4 or BRC1-8 is important (Carreira et al., 2009; Shivji et al., 2006). These findings suggest a possible regulatory mechanism for the BRC motifs in BRCA2-RAD51 interaction in DNA repair.

RAD51 interaction with BRCA2 via the C-terminal interaction site on BRCA2 has been found to play a crucial role in DSB repair. As mentioned above the C-terminal region was shown to interact with and stabilize RAD51 nucleoprotein filaments, which appears to be crucial for DSB repair (Davies and Pellegrini, 2007; Esashi et al., 2005; Esashi et al., 2007; Sharan et al., 1997). Indeed, cells expressing C-terminal truncated BRCA2 are hypersensitive to IR, show a recombination-defective phenotype and have lost the ability to form RAD51 foci in response to IR (Yuan et al., 1999; Moynahan et al., 2001; Tutt et al., 2001; Wang et al., 2004). Fusing BRC3 or BRC4 to the ssDNA-binding domain of RPA rescued the BRCA2-defective phenotype, indicating that the BRC domains together with the C-terminal region are important for the recruitment of RAD51 by BRCA2 to DSBs (Saeki et al., 2006). Nevertheless, the mechanism of how the BRC motifs and the C-terminus of BRCA2 collaborate in RAD51 recruitment still needs to be elucidated.

In addition to the role of the BRCA2 C-terminus in DSB repair, recent reports have observed a role for the BRCA2 C-terminus together with RAD51 in the protection of DNA replication forks (Hashimoto et al., 2010; Lomonosov et al., 2003; Schlacher et al., 2011; Ying et al., 2012). Cells expressing truncated BRCA2 showed increased destabilization of replication forks, which led to the proposal, that BRCA2 is involved in the protection of nascent DNA strands at stalled replication forks (Lomonosov et al., 2003). This was confirmed by more recent reports, which showed that the C-terminal region of BRCA2 is critical to protect the replication fork from MRE11-dependent degradation by facilitation of RAD51 assembly on replication forks and stabilizing RAD51 nucleofilaments (Hashimoto et al., 2010; Schlacher et

al., 2011). However, the exact mechanism of how BRCA2 and RAD51 protect nascent DNA at replication forks is unclear but it has been proposed that the CDK-dependent S3291 phosphorylation of BRCA2 is be involved in this process as a BRCA2 S3291A mutant failed to protect nascent DNA from degradation (Schlacher et al., 2011).

However, BRCA2 interaction with RAD51 is also regulated by posttranslational modifications in a cell cycle and DNA damage-dependent manner. Upon DSB induced by IR, BRCA2 is phosphorylated on the C-terminal T3387 by CHK1 and CHK2, which has been implicated in the recruitment and release of RAD51 to sites of DNA damage. A non-phosphorylatable alanine mutant of the BRCA2 C-terminus (T3387A) failed to release RAD51, even after IR-induced DNA damage (Bahassi et al., 2008). Furthermore, BRCA2 phosphorylation on S3291 by CDK2 blocks interaction with RAD51. After IR-induced DNA damage S3291 phosphorylation of BRCA2 decreased facilitating accumulation of RAD51 (Esashi et al., 2005).

BRCA2 can be modified by a number of kinases, which is proposed to mediate BRCA2 function through regulation of protein interactions (Fig. 1.5.3) (Kim et al., 2008; Lee et al., 2004; Lin et al., 2003; Olsen et al., 2010). Nonetheless, the effects of most of these modifications have yet to be elucidated.

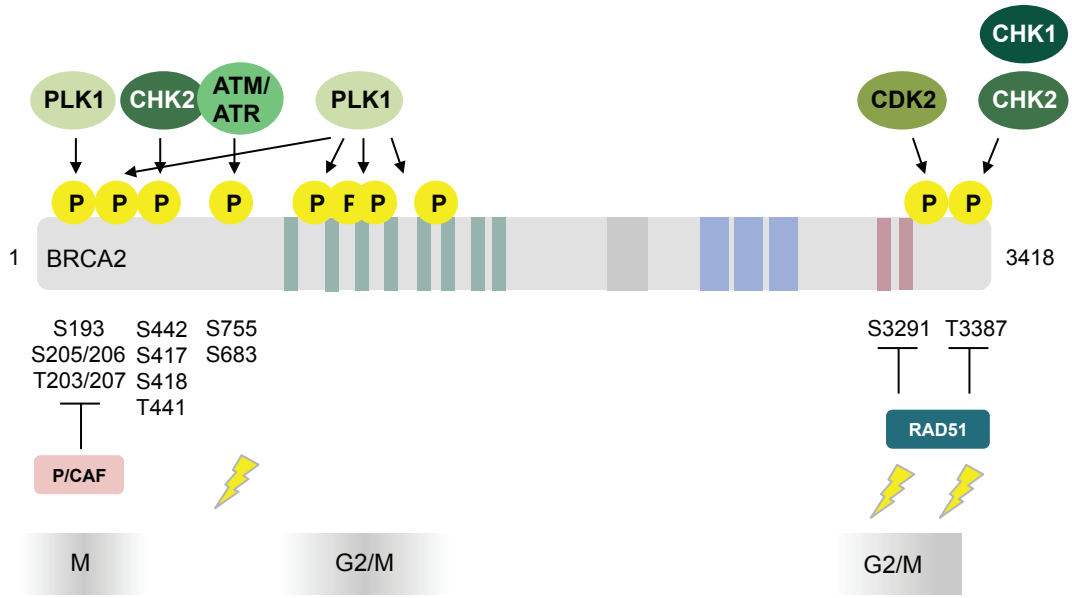

Figure 1.5.3: Schematic figure of BRCA2 post-translational modifications

Kinases are depicted in green ovals: polo-like kinase 1 (PLK1), checkpoint kinase 1 (CHK1) and 2 (CHK2), ataxia-telangiectasia mutated (ATM), ataxia-telangiesctasia and Rad3 related kinase (ATR), cyclin-dependent kinase 2 (CDK2). S represents serine, T represents threonine and numbers represent the amino acid position. Phosphorylation of residues S193, S205/206, T203/207 block p300/CBP-associated factor P/CAF association, phosphorylation of S3291 and T3387 block RAD51 interaction. Yellow flash arrows represent DNA damage-dependent phosphorylation events and in grey background are specific cell cycle phases depicted in which phosphorylations occur.

1.6 The Ubiquitin Proteasome System (UPS)

1.6.1 Mechanism of the UPS

Ubiquitylation is a fundamental process in cells that is involved in the control of protein function, degradation, interactions and their subcellular localization. Therefore, ubiquitylation also controls a variety of cellular processes. The discovery of the ubiquitin proteasome system in the early 1980s by A. Hershko, his PhD student A. Chiechanover, and I. Rose were honoured with the Nobel Prize in 2006 (Ciechanover et al., 1978; (Hershko et al., 1983). Ubiquitin is a small protein of 76 amino acids, that is highly conserved in all eukaryotes (Hershko and Ciechanover, 1998). Ubiquitin is attached to substrates via three enzymes: the ubiquitin-activating enzyme E1, the ubiquitin-conjugating enzyme E2 and the ubiquitin ligase E3 (Fig. 1.6.1) (Ciechanover et al., 1981;(Hershko et al., 1983). In an ATP-dependent process, the ubiquitin-activating enzyme E1 forms a thioester bond via its active cysteine with the C-terminus of the ubiquitin. Then ubiquitin can be transferred to the active cysteine of the ubiquitin-conjugating enzyme E2. Finally, the ubiquitin is added to the target substrate with the aid of the ubiquitin E3 ligase, which forms an isopeptide-linkage between the ubiquitin and the ε-amino group of a lysine of the target substrate. In concert, these enzymes can attach ubiquitin to proteins as a single molecule (monoubiquitylation) or as chains (polyubiquitylations). In humans, two E1 enzymes, ~30 E2 enzymes and hundreds of E3 ligases have been identified to date.

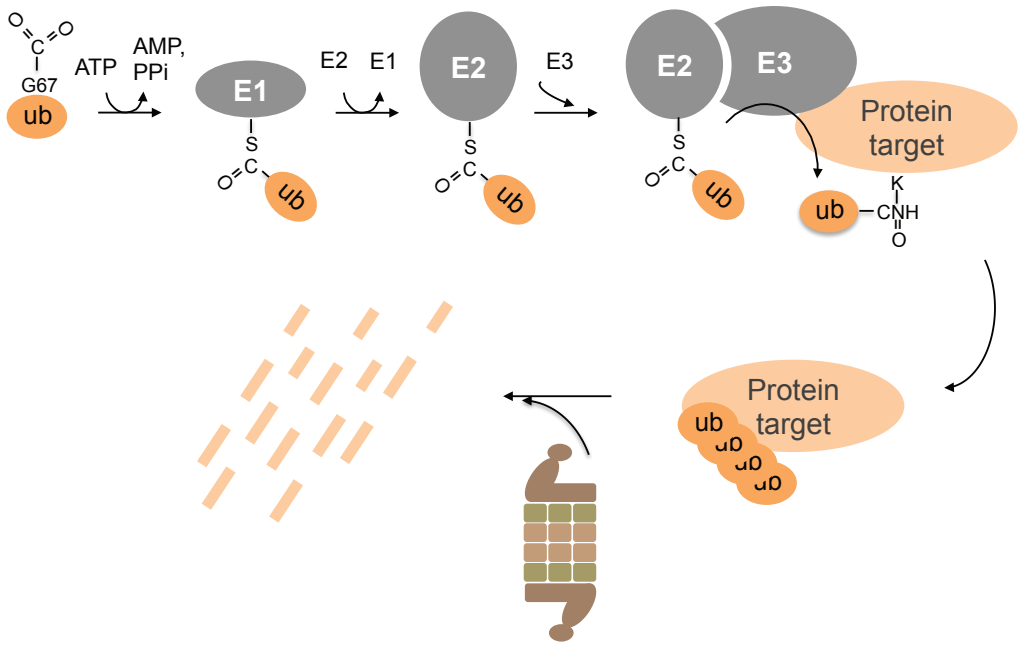

Figure 1.6.1: The Ubiquitin Proteasome system
Ubiquitin is attached to substrates in a three step process. Ubiquitin is activated in an ATP-dependent manner by the ubiquitin-activating enzyme E1, the ubiquitin-conjugating enzyme E2 then transfers the ubiquitin to a protein target in concert with the ubiquitin ligase E3. The ubiquitin chain is elongated by multiple rounds of ligation, and the polyubiquitylated protein can be targeted by the 26S proteasome for degradation.
(Figure Adapted from Cell Signaling Technology. Ubiquitin/Proteasome Pathway. http://www.cellsignal.com/reference/pathway/Ubiquitin_Proteasome.html, 2007)

These ubiquitylations can occur in different variations and are thought to result in different functions. Monoubiquitylation is often involved in endocytosis of membrane proteins, DNA repair and histone activity (Mukhopadhyay and Riezman, 2007; Polo, 2012). Monoubiquitylations can also occur on various lysines in a target substrate, which is called multi-monoubiquitylation and suggested to lead to increased affinity of proteins that contain multiple ubiquitin interaction motifs (UIMs) and has been shown to be involved in endocytosis of membrane proteins (Haglund et al., 2003; Petroski and Deshaies, 2003; Raiborg et al., 2002). Poly-ubiquitin chains

can occur in two structures, which is supposed to lead to specific interaction with some interaction partners (Komander et al., 2009; Rahighi et al., 2009); as linear chains in which an isopeptide bond is formed between the carboxyl group of glycine 76 and a lysine of the previous ubiquitin; or as 'nicked chains' in which ubiquitin forms a peptide bond with the C-terminal glycine of the previous ubiquitin via its N-terminal methionine (Goldknopf et al., 1977;(Kirisako et al., 2006).

Furthermore, chains can be formed through different lysines of the ubiquitin, resulting in different fates for the substrate. Ubiquitin contains seven conserved lysine residues on which chains can be formed: K6, K11, K27, K29, K33, K48 and K63 (Peng et al., 2003). K63-linked chains have been found to act as molecular scaffolds that bring together oligomeric kinase or DNA repair complexes (Deng et al., 2000; VanDemark et al., 2001). K11-, K29- and K48-linked polyubiquitin chains have been shown to mark substrates for proteasomal degradation by the 26S proteasome (Chau et al., 1989; Thrower et al., 2000; Xu et al., 2009). It is speculated that chains linked by the other lysines also target proteins for proteasomal degradation, though the direct evidence has not been reported yet. K6-linked polyubiquitin chains are known to be the rarest linkage structure, which is formed by yet only two identified E3 ligases, BRCA1 and RING1B, and is not involved in proteasomal degradation (Ben-Saadon et al., 2006; Nishikawa et al., 2004).

Ubiquitylation of proteins can also be removed by de-ubiquitylating enzymes (DUBs). More than a hundred DUBs are encoded in the human genome and they are thought to cleave the polyubiquitin chain of substrates, thus rescuing proteins from proteasomal degradation or changing the fate and function of the protein, leading to re-localization or function as docking proteins for other proteins (Cooper et al., 2010; Johnson et al., 1995; Sowa et al., 2009). Furthermore it is thought that with the help of DUBs a wide variety of ubiquitin chain structures can be generated, such as branched or mixed ubiquitin chains.

1.6.2 Ubiquitin E3 ligases

There are two major E3 ligase families, the really interesting new gene (RING) finger domain-containing E3 ligases and the homologous to E5-AP carboxyl terminus (HECT) domain-containing E3 ligases. Both have been implicated in the regulation of cellular processes and shown to target oncoproteins.

HECT E3 ligases have intrinsic catalytic activity and can transfer the ubiquitin to the target protein themselves. They bind directly to the ubiquitin-conjugating enzyme E2, form a thioester interpeptide bond with ubiquitin and then transfer ubiquitin to the target protein. Substrate specificity of HECT E3 ligases is mediated by their protein-protein interaction domains, which divides them into further sub-families: HERC E3 ligases contain RCC1-like domains (RLDs), C2-WW-HECT E3 ligases contain double tryptophan (WW) domains, and SI(ngle)-HECT E3 ligases that lack either RLDs or WW domains (Scheffner and Staub, 2007).

The second major group of E3 ligases contains the RING finger E3 ligases and the RING finger-related E3 ligases, which include plant homeodomain (PHD), leukemia associated protein (LAP) finger proteins and members of the U-box family, and are conserved from yeast to human (Deshaies and Joazeiro, 2009). The human genome encodes for more than 600 RING finger domain containing proteins, of which, to date, around 150 have been found to act as ubiquitin E3 ligases (Li et al., 2008). The consensus sequence of the RING finger domain is Cys-X_2-Cys-$X_{(9-39)}$-Cys-$X_{(1-3)}$-His-$X_{(2-3)}$-Cys-X_2-Cys-$X_{(4-48)}$-Cys-X_2-Cys, whereby X can be any amino acid (Freemont et al., 1991). RING finger E3 ligases act in concert with the ubiquitin-conjugating enzyme E2 to transfer ubiquitin to the target substrate. It is thought that interaction with the RING finger domain induces a conformational change in the E2 enzyme, facilitating the transfer of ubiquitin to the target protein (Brzovic et al., 2003;

Zheng et al., 2000).

The best characterised RING finger E3 ligases are the Cullin-RING ligases (CRLs). CRLs contain a Cullin-family scaffold protein that directly interacts with the RING domain-containing enzyme via its C-terminal domain. The N-terminal Cullin-repeat motifs of the Cullin scaffold protein interact with an adaptor protein that, in turn, recruits one of the 69 known human receptor proteins, which mediates substrate specificity (Petroski and Deshaies, 2005a). The CRLs are the largest family of E3 ligases and their mode of action is exemplified by the SCF complex. RING finger E3 ligases initiate together with their E2 ubiquitin-conjugating enzyme ubiquitin chain formation on a substrate lysine (Williamson et al., 2011).

The human genome encodes for seven Cullin-based E3 ligases (Cullin 1, 2, 3, 4a, 4b, 5 and 7) of which the SKP1-Cullin1-F-box-protein complex (SCF) and the anaphase-promoting complex/cyclosome (APC/C) have been most extensively studied. Both complexes are structurally similar and are thought to regulate each other's activity during cell cycle through sequential and dynamic ubiquitylation events that will be detailed below.

1.6.3 The SKP1-Cullin1-F-box (SCF) protein complex

The SCF complex consists of three invariable components, the Rbx1 RING finger protein, the Cullin1 (CUL1) scaffold protein and the SKP1 (S phase kinase-associated protein 1) adaptor protein, which recruits the variable F-box protein that mediates substrate specificity (Fig. 1.6.3). F-box proteins interact with SKP1 via their N-terminal F-box motif (~ 49 residues) and recruit the target substrates via their C-terminal motifs (Jin et al., 2004). F-box proteins can be divided into three categories according to their C-terminal motifs: FBXW, FBXL and FBXO, which respectively contain WD40 repeats, leucine-rich repeats or other domains (Bai et al., 1996; Jin et

al., 2005). F-box proteins typically recognize a phosphorylated motif, so called phosphodegron motif, in the target protein (Jin et al., 2005; Orlicky et al., 2003). However, recent studies demonstrated that substrate recognition by F-box proteins can also be mediated via non-canonical motifs. These include, unmodified degrons, inducible non-covalent degrons, covalent non-phosphorylated degrons, modification inhibition, and domain-based degrons (Skaar et al., 2013). However, independent of the F-box protein, the SCF complex interacts with the E2 UBE2E1, a K48-specific E2, which leads to proteasomal degradation of the protein target (Li et al., 2007).

There are several mechanisms that regulate SCF E3 ligases. Direct regulation of SCFs occurs by interaction with the F-box proteins, which leads to dimerization of the F-box proteins and ubiquitylation of substrates (Barbash et al., 2008; Li and Hao, 2010; Tang et al., 2007; Welcker and Clurman, 2007; Zhang and Koepp, 2006). Therefore, the availability of the F-box proteins determines the activity of the specific SCF complex. However, the activity of SCF E3 ligases is also positively regulated by the small ubiquitin-like modifier Nedd8/RUB1. Neddylation of CUL1 enhances its association with the RING finger protein, which leads to increased SCF activity and ubiquitin chain elongation (Duda et al., 2008; Saha and Deshaies, 2008). De-neddylation by COP9 signalosome (CSN) was found to inhibit degradation of the SCF substrate cyclin E (Lyapina et al., 2001; Schwechheimer et al., 2001). Another important regulator of SCF activity is CAND1 (Cullin-associated and neddylation-dissociated protein 1), which has been shown to activate SCF (Bosu et al., 2010; Zheng et al., 2002a). However, CAND1 was also reported to have a negative effect on CRL function, since binding of CAND1 blocked the interaction with F-box proteins by inhibiting interactions between CUL1 and SKP1 and prevents neddylation of SCF *in vitro* (Goldenberg et al., 2004; Liu et al., 2002). Recent studies shed light on these paradoxes, and suggested that CAND1 acts as an exchange factor for F-box proteins, as high levels of CAND1 accelerated dissociation of F-box

proteins from the SCF complex (Pierce et al., 2013; Wu et al., 2013; Zemla et al., 2013). Therefore a model was proposed, which suggests a mutual action of neddylation and CAND1 in SCF regulation. If CRLs detect a substrate, neddylation is induced, which stabilizes the substrate receptor protein (F-box) and facilitates CRL activity. When the substrate is processed the CRL becomes de-neddylated by the CSN and CAND1 binds to the F-box protein and forms a transient complex resulting in the release of the F-box protein. Hence, the CRL is free to form a complex with another F-box protein and target a new substrate.

However, the availability of F-box proteins appears central to the regulation of the SCF complex. As the cellular levels of some F-box protein fluctuate during cell cycle, their availability also determines when, during the cell cycle, the SCF complex is active.

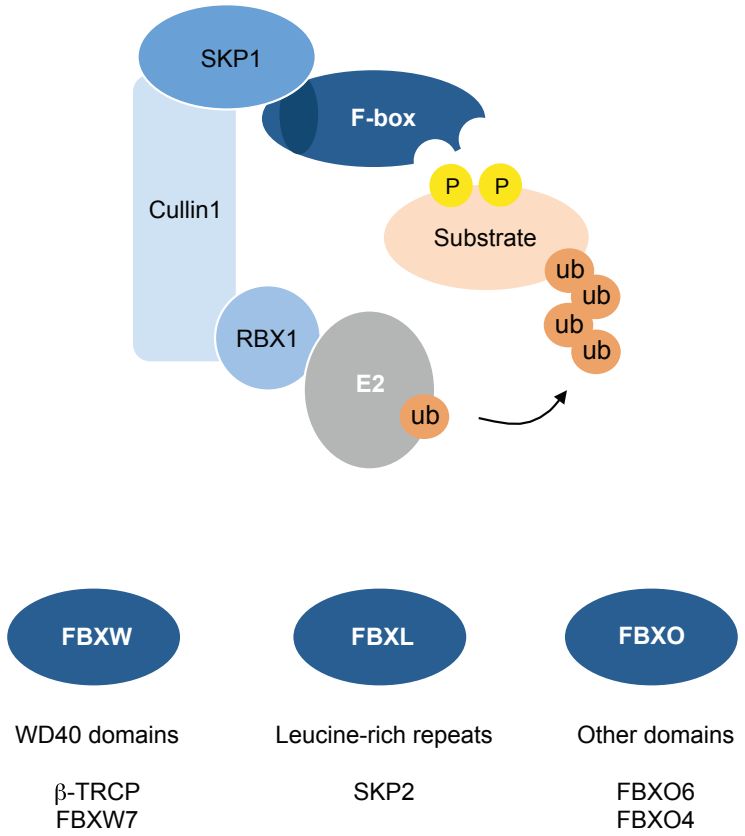

Figure 1.6.3: Schematic representation of the SKP1-Cullin1-F-box protein complex (SCF)

The SCF complex contains the scaffold protein Cullin 1 and the RING finger protein RBX1 that interacts with the ubiquitin-conjugating enzyme E2. Substrate recognition is mediated by F-box proteins, which are recruited by the adaptor protein SKP1. F-box proteins recognize specific phosphorylated degron motifs on target substrates, leading to their ubiquitylation and subsequent degradation. (Adapted from (Teixeira and Reed, 2013)

1.6.4 The anaphase promoting complex/cyclosome (APC/C)

The APC/C is structurally very similar to the SCF complex, though it is composed of at least fourteen different proteins (Fig. 1.6.4). It also consists of invariable units, such as the Apc11 RING finger protein, that interacts with an E2 enzyme and the Cullin-like unit APC2 that serves as the scaffold protein. Substrate recognition is mediated by two receptor proteins: the cell division cycle protein 20 (CDC20) and the CDC20 homolog1 (CDH1) (Dawson et al., 1995; Fang et al., 1998; Kramer et al., 1998; Lim et al., 1998; Lorca et al., 1998; Shirayama et al., 1998; Sigrist et al., 1995; Visintin et al., 1997; Zachariae et al., 1998). Through C-terminal WD40 repeats, both receptor proteins recognize destruction motifs on target substrates. CDH1 recognizes both the D-box (RXXLXXXXN) and the KEN-box (KENXXXN), whereas CDC20 has an intrinsic preference for the D-box motifs (Glotzer et al., 1991; Pfleger and Kirschner, 2000). The APC/C can also recognize substrates via non-canonical motifs, which are thought to require co-factor stimulation but this remains to be elucidated (Carroll et al., 2005; Passmore et al., 2003).

The APC/C acts together with two specific E2 enzymes, UBE2C, which is thought to conjugate the initial ubiquitin to the substrate, and UBE2S that can form K11-linked polyubiquitin chains on this initial ubiquitin (Garnett et al., 2009; Jin et al., 2008; Rodrigo-Brenni and Morgan, 2007; Wickliffe et al., 2011; Williamson et al., 2011; 2009).

APC/C in complex with CDC20 is responsible for promoting sister chromatid separation during anaphase and mitotic exit by targeting securin for degradation as well as cyclins A and B (Cohen-Fix et al., 1996; Fang et al., 1998; Funabiki et al., 1996; Geley et al., 2001). Targeting of securin activates the cysteine protease separase, which then cleaves the cohesion subunit SCC1 which leads to separation

of sister chromatids (Ciosk et al., 1998; Uhlmann et al., 1999). APC/C^{CDH1} targets mitotic cyclins as well as the mitotic kinases Auroa A and PLK1 (Castro et al., 2002; Lindon and Pines, 2004; Stewart and Fang, 2005; Taguchi et al., 2002).

The activity of the APC/C is controlled by the spindle assembly checkpoint (SAC). Until kinetochores are attached to the mitotic spindle, SAC blocks anaphase by inhibiting APC/C (Kulukian et al., 2009; Sudakin et al., 2001). The mitotic checkpoint complex (MCC) consisting of MAD2, BUBR1/MAD3, BUB3 and CDC20 acts as inhibitor of APC/C (Sudakin et al., 2001). MAD2 (mitotic arrest deficient 2) and BUBR1 (budding uninhibited by benzimidazole 1) are loaded onto CDC20 at kinetochores so that CDC20 cannot form a complex with APC/C (Chao et al., 2012; Kulukian et al., 2009). After biorientation of the chromatid pairs on the mitotic spindle, kinetochores experience tension which leads to the disassembly of MCC and APC/C is released and can target securin for degradation.

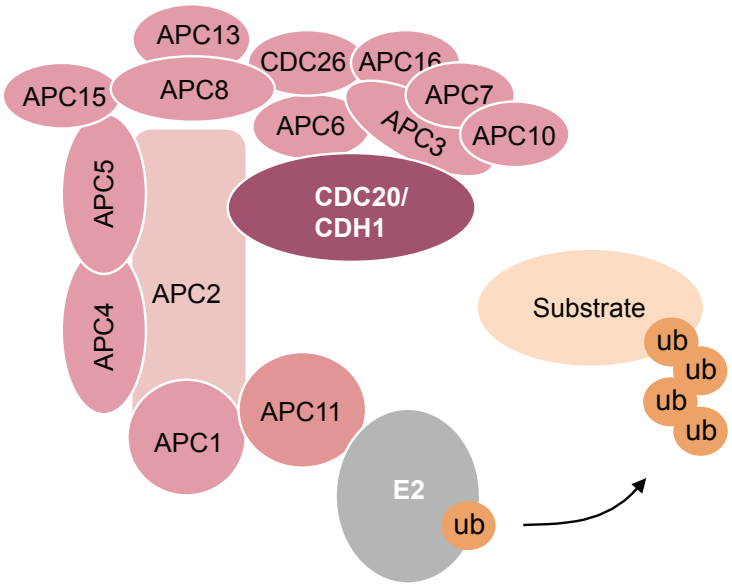

Figure 1.6.4: Schematic representation of the anaphase promoting complex/cyclosome (APC/C)
APC/C consists of the cullin-like protein scaffold protein (APC2) and a RING finger protein (APC11) that interacts with the ubiquitin-conjugating enzyme E2. Substrate binding is mediated by the receptor proteins CDC20 or CDH1. (Adapted from(Teixeira and Reed, 2013)

1.7 Regulation of cell cycle progression

1.7.1 The mammalian cell cycle

The eukaryotic cell cycle consists of four cell cycle phases: gap 1 (G1), synthesis (S), gap 2 (G2) and mitosis (M). (Fig.) The fifth phase, gap 0 (G0) is a quiescent cell cycle state. Cells can exit the cell division cycle into G0, re-enter upon mitogenic stimuli or terminate differentiation and undergo apoptosis. After division, cells are in G1 phase, in which transcription and translation take place to prepare for genome duplication and synthesis of organelles required for cell division. In S phase, DNA replication is performed to generate an exact copy of the chromosomes for the

daughter cell. In G2 phase cells grow and express proteins to prepare for division into two viable daughter cells in M phase.

During interphase, which consists of G1, S and G2 phases cells prepare for cell division and DNA is loosely packed to ensure accessibility for translation and the repair machinery. The M phase can be divided into prophase, prometaphase, metaphase, anaphase and telophase. In Prophase chromosome condensation begins to prevent damage to the DNA, when sister chromatids are equally distributed into the daughter cells. Furthermore, outside the nucleus the mitotic spindle starts to form. During prometaphase the nuclear envelope breaks down and each chromosome consists of two sister chromatids connected by the centromere. The chromosomes become attached to the spindle microtubules via the kinetochores, so that chromosomes can be aligned at the metaphase plate in metaphase. In anaphase, the separation of sister chromatids takes place, where the sister chromatids are drawn to opposite poles of the mitotic spindle, a process which is facilitated by the elongation of the mitotic spindle. In telophase, the migration of chromatids to spindle poles is completed, chromatids are released from the spindle fibres and the new nuclear envelope reforms around the nuclei of the newly formed daughter cells (Reviews et al., 2002).

1.7.2 Regulation of the mammalian cell cycle

The mammalian cell cycle is driven by the temporal activation and inhibition of cyclin-dependent kinases (Fig.1.7.2) (CDKs). There are currently more than 20 CDK family members identified (Malumbres et al., 2009), of which five have been shown to be involved in cell cycle regulation: CDKs 1, 2, 3, 4, and 6. The activity of CDKs is controlled by binding of cyclins to form cyclin/CDK complexes and phosphorylation events by CAKs (CDK-activating kinases). In G1 cyclin D is expressed, which can be

in complex with the CDK4 and CDK6, that stimulate expression of growth factor proteins (Beijersbergen and Bernards, 1996; Bienvenu et al., 2010). The expression of cyclin E in G1 phase and its association with CDK2, together with CAK phosphorylation, promotes the activation of the CDK2/cyclin E complex, which initiates the transition to S phase (Dulić et al., 1992). During S phase, when DNA replication is performed, cyclin A expression continues to increase. In complex with CDK2 cyclin A is involved in the transition from S to G2 phase (Pagano et al., 1992; Rosenblatt et al., 1992). At the end of S phase, cyclin B levels increase, leading to the formation of a CDK1/cyclin B complex that catalyses entry into M phase and predominantly controls mitotic progression (Nigg, 2001). In addition, the CDK3/cyclin C complex has been shown to mediate cell cycle re-entry from G0 phase (Ren and Rollins, 2004; Sage, 2004; Tomashevski et al., 2010).

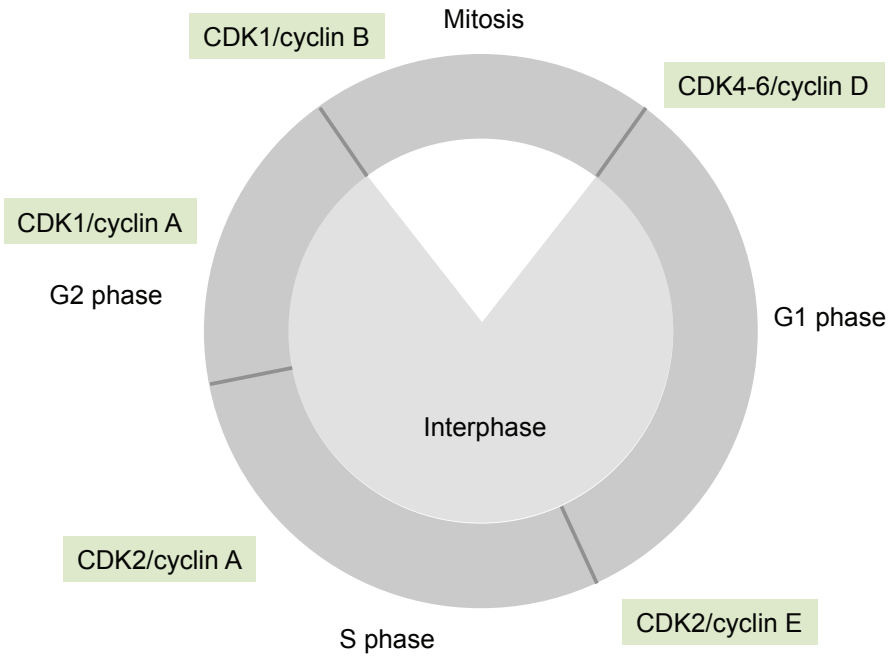

Figure 1.7.2: Classic model of the CDK/cyclin activity
Cyclin D in complex with CDK4 or CDK6 govern entry in and progression through G1 phase. CDK2/Cyclin E is required to initiate S phase, cyclin A in complex with CDK1 or CDK2 are responsible for S phase progression and entry into mitosis. CDK1/cyclin B complexes catalyse mitotic entry.

1.7.3 Regulation of CDKs

The processes mentioned above are carried out in unperturbed cycling cells. However, in response to DNA damage and genotoxic stress DNA damage checkpoints are activated that arrest cell cycle progression to ensure the faithful duplication of the genetic information and to provide time for repair. These checkpoints operate at G1/S phase transition, in S phase and at G2/M phase transition.

The kinase activity of the CDK/cyclin complexes is tightly regulated by CDK inhibitors (CKIs), which promote cell cycle arrest when cells encounter DNA damage. CKIs can be divided into two groups: the INK4 family members and the Cip/Kip family members. The INK4 family members (p16, p15, p18, p14) primarily target CDK4 and CDK6 (Chan et al., 1995; Guan et al., 1994; Hannon and Beach, 1994; Hirai et al., 1995; Serrano et al., 1993). By binding to the CDKs, the inhibitors prevent complex formation with cyclin D, which facilitates G1 arrest. The Cip/Kip family members (p21, p27, p57) target CDK/cyclin complexes, blocking their phosphorylation-dependent activation (Dulić et al., 1994; Gu et al., 1993; Harper et al., 1993; Lee et al., 1995; Matsuoka et al., 1995; Polyak et al., 1994). p21 is triggered by UV, IR, MMS or Cisplatin, and leads to the arrest at the G1/S phase transition, due to the inhibition of the CDK2/cyclin E complex p27 expression inhibits CDK2/cyclin E and CDK2/cyclin A resulting in G1 or G2 cell cycle arrest (Di Leonardo et al., 1994).

However, activity of CDK/cyclin complexes are regulated by phosphorylation events, there are also inhibitory phosphorylation events. The phosphorylation by the inhibitory kinases WEE1 and MYT1 leads to inhibition of CDKs (Lundgren et al., 1991; Russell and Nurse, 1987). WEE1 is active during G1, S and G2 phases and can phosphorylate CDK1/cyclin B, which inhibits phosphorylation of its target substrates. These inhibitory phosphorylations can be removed by the CDC25

phosphatase, which becomes active in G2 (Russell and Nurse, 1986). Removal of these phosphorylations results in abrupt activation of CDK1/cyclin B and transition from G2 into mitosis. In response to DNA damage, the DNA damage checkpoint is activated resulting in inactivation and proteasomal degradation of CDC25. Therefore, the inhibitory phosphorylations on CDK1/cyclin B cannot be removed, which ultimately leads to a cell cycle arrest in G2.

1.7.4 Regulation of the cell cycle by the SCF complex and the APC/C

The SCF complex and APC/C E3 ligases are major cell cycle regulators that are active at distinct stages of the cell cycle. The SCF complex is active from late G1 to early M phase, whilst the APC/C is active from anaphase to late G1. The activities of the SCF complex and the APC/C are controlled by each other through positive and negative feedback actions.

In S phase, cyclin B1 accumulates and forms a complex with CDK1, which is kept inactive by WEE1 kinase-dependent phosphorylation (Parker and Piwnica-Worms, 1992; Parker et al., 1992). When levels of the CDK1/cyclin B1 complex rise WEE1 is phosphorylated and targeted by SCF^{TRCP}_{β} (SCF in complex with the receptor protein β-TRCP) for proteasomal degradation, leading to increased CDK1 activity. CDK1 activation triggers a positive feedback loop, via phosphorylation of the activator CDC25C phosphatase and promotes transition into mitosis (Watanabe et al., 2004). As mentioned above the APC/C is active from early mitosis. Until this point of the cell cycle the APC/C activity is inhibited by different mechanisms: 1. The activity of the APC/C^{CDC20} complex is blocked by the maintenance of the SAC (see chapter 1.6.4) and the early mitotic inhibitor 1 (EMI1) (Reimann et al., 2001); 2. CDH1 is kept in an inactive phosphorylated form, which prevents the association of

CDH1 with the APC/C and thus the formation of an active APC/C^{CDH1} complex (Jaspersen et al., 1999).

First APC/C in complex with CDC20 becomes active. As the activity of CDK1/cyclin B1 complexes and polo-like kinases (PLKs) increase EMI1 is phosphorylated and targeted for degradation by SCF^{TRCP}_{β} (Hansen et al., 2004; Margottin-Goguet et al., 2003). Once every chromosome is properly attached to the mitotic spindle SAC releases CDC20. The release of CDC20 from the SAC inhibition as well as the degradation of EMI1 results in the formation of an APC/C^{CDC20} complex which can be activated by CDK1/cyclin B1 dependent phosphorylation (Kraft et al., 2003; Rudner and Murray, 2000). Active APC/C^{CDC20} targets securin, leading to the activation of the cysteine protease separase, that in turn cleaves cohesin, allowing sister chromatids to separate (Waizenegger et al., 2000). Activation of APC/C^{CDC20} also starts a negative feedback loop, in which APC/C^{CDC20} targets cyclin B for proteasomal degradation and promotes mitotic exit (Kraft et al., 2003; Sudakin et al., 1995). As mentioned above, CDH1 is phosphorylated which prevents the association of CDH1 with the APC/C (Jaspersen et al., 1999). In late mitosis, CDH1 is de-phosphorylated by the CDC14 phosphatase, allowing the formation of an active APC/C^{CDH1} complex (Jaspersen et al., 1999; Visintin et al., 1997). APC/C^{CDH1} then targets CDC20, SKP2 (S phase kinase-associated protein 2, an F-box protein of the SCF complex) and CDC25A for degradation, which leads to accumulation of the CDK inhibitors (CKIs) p21 and p27 and exit of mitosis (Bashir et al., 2004; Fang et al., 1998; Wei et al., 2004). At the G1/S phase transition, active CDK2/cyclin A starts to accumulate and phosphorylates CDH1, resulting in its dissociation from the APC/C. CDH1 can also autoubiquitylate itself, thus leading to its degradation and promotion of APC/C^{CDH1} inactivation (Jaspersen et al., 1999; Listovsky et al., 2004).

Inactivation of APC/C^{CDH1} leads to an increase of SKP2 in G1/S phase (Bashir et al., 2004; Wei et al., 2004) where SCF^{SKP2} can mediate the degradation of the

CKIs p21, p27 and p57. This leads to the increase in the activity of the CDK/cyclin complexes so that cells can progress through S phase. During late G1, SCF in complex with FBXW7 is active, which targets cyclin E for degradation, thereby allowing the transition to S phase.

During late G1, SCF^{FBXW7} becomes active and can target cyclin E for degradation and promote S phase progression (Ekholm et al., 2001).

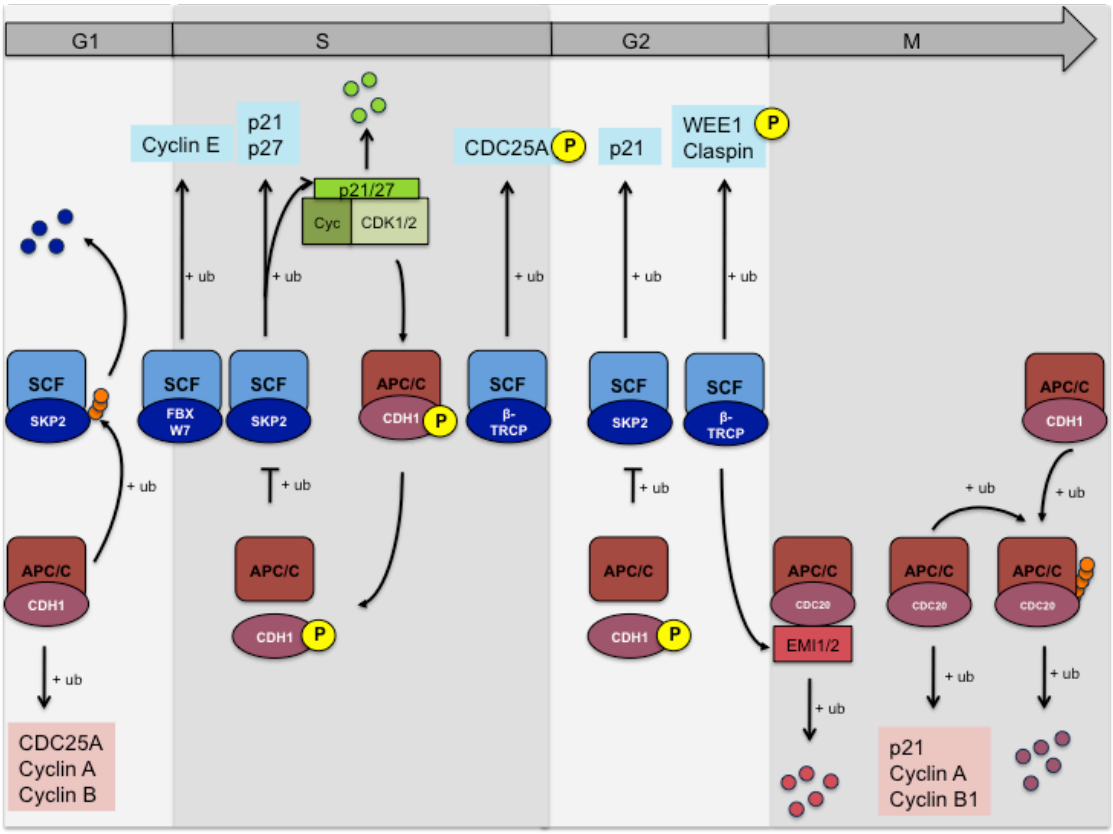

Figure 1.7.4: Functions and interplay of the SCF complex and APC/C during cell cycle

In cell cycle APC/C^{CDH1} and APC/C^{CDC20} attenuate CDK1 activity by degradation of cyclin A and cyclin B. In G1 APC/C^{CDH1} mediates degradation of SKP2 and CDC25A (CDK activator), cyclin A/B causing low activity of CDK1/2. After G1/S transition SCF^{FBXW7} ubiquitylates cyclin E to attenuate CDK activity. SCF^{SKP2} initiates CDK1/2 activity by degradation of CDK1/2 inhibitors p21/p27. Increasing activity of CDK1/2 leads to phosphorylation of CDH1, which separates from APC/C, leading to its inactivation. In unperturbed cell cycle CDK1/2 phosphorylate CDC25A, which is then recognized by SCF_{β}^{-TRCP} and degraded causing inactivation of CDK1. In response to DNA damage SCF_{β}^{-TRCP} arrests cell cycle to allow repair, by degradation of CHK1-phosphorylated CDC25A. In G2 SCF^{SKP2} targets p21 for degradation so that CDK2 activity maintains. SCF_{β}^{-TRCP} activates CDK1 by promoting degradation of Claspin (CHK1 activator) and WEE1 (CDK inhibitor) at G2/M phase. In early mitosis SCF_{β}^{-TRCP} switches CDK1 off by degradation of CDC25A and EMI1/2 (APC/C inhibitor), which leads to activation of APC/C^{CDC20}, that targets p21, cyclin A/B for degradation. In late mitosis APC/C^{Cdc20} itself and APC/C^{Cdh1} ubiquitylate CDC20 so that the APC/C^{CDC20}-complex becomes inactive. Proteins ubiquitylated by APC/C are depicted in red background, proteins ubiquitylated by the SCF complex in blue background. (Adapted from(Nakayama and Nakayama, 2006)

1.8 FBXW7

FBXW7 (F-box/WD40 repeat-containing protein 7, CDC4 in yeast) is a member of the F-box protein family and functions as a substrate receptor protein for the SCF complex, through direct interaction with the adaptor protein SKP1 (Bai et al., 1996). In mammals, alternative splicing produces three FBXW7 isoforms: FBXW7α, FBXW7β and FBXW7γ, which are respectively localized in the nucleus, cytoplasm and nucleolus (Spruck et al., 2002; Welcker et al., 2004a). These isoforms are functionally identical and differ only in their N-terminal regions. Eight tandem WD40 repeats, in the C-terminal region of FBXW7, form a β-propeller structure that recognizes a specific consensus motif, called phospho-degron motif, in the target substrate. Within the β-propeller structure, three arginine residues (R465, R479, R505) are crucial for the substrate recognition (Fig. 1.8.1) (Li and Hao, 2010; Orlicky et al., 2003). FBXW7 contains another functional domain, called D domain, which is located N-terminal of the F-box domain. This D domain facilitates FBXW7 dimerization, which in turn regulates and it thought to increase substrate interaction (Li and Hao, 2010; Tang et al., 2007; Welcker and Clurman, 2007).

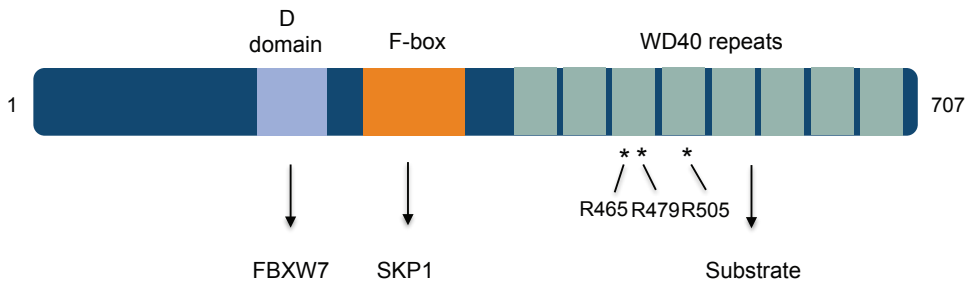

Figure 1.8.1: FBXW7 domain architecture and function
FBXW7 consists of the N-terminal D domain, dimerization domain (first arrow), the F-box domain with which FBXW7 interacts with the SKP1 adapter protein of the SCF complex (second arrow). WD40 repeats in the C-terminus mediate substrate recognition via three arginine residues R465, R479 and R505 (third arrow).

The substrate recognition of FBXW7 has been extensively studied using its substrate cyclin E. The first indication of a phosphorylation-dependent interaction of FBXW7 with its substrates was found in budding yeast, where it was suggested that binding of the FBXW7 homologue CDC4 to its substrate SIC1 requires phosphorylation at six or more CDK1 target sites on SIC1 (Nash et al., 2001). For mammalian substrates, a single or double phosphorylation was shown to be sufficient. Cyclin E can be phosphorylated by CDK2 on S384 and by glycogen synthase kinase 3 (GSK3) at T380 (Koepp et al., 2001; Strohmaier et al., 2001; Ye et al., 2004). It was observed that these phosphorylation events increase the interaction with FBXW7; indeed the di-phosphorylated form of cyclin E can be targeted by monomeric FBXW7, whereas the mono-phosphorylated form of Cyclin E (at T380) requires a dimeric FBXW7 to trigger its proteosomal degradation (Welcker et al., 2003; Ye et al., 2004). Furthermore, GSK3 kinase requires a priming phosphorylation at position +4 to efficiently phosphorylate its targets (Fiol et al., 1987). Therefore, S384 phosphorylation by CDK2 can also act as a priming phosphorylation for T380 phosphorylation by GSK3.

Interestingly, most FBXW7 substrates are phosphorylated by the GSK3 (Fig. 1.8.2). Moreover, for c-myc, sterol regulatory element binding protein (SREBP) and c-Jun, it has been observed that these substrates undergo two sequential phosphorylations of the degron motif by a priming kinase (mitogen activated protein kinase for c-myc and mitogen activated protein kinase 8 for c-Jun) and GSK3 kinase occur (Punga et al., 2006; Welcker et al., 2004b; Yada et al., 2004). Furthermore, increasing evidences suggest, that FBXW7 substrates contain two phospho-degron motifs. For example, besides the above mentioned C-terminal phospho-degron motif, cyclin E also contains a N-terminal phospho-degron motif, which has been found to be less important for cyclin E degradation, but it has been suggested to have a

cooperative function between the two degron motifs to promote substrate degradation (Hao et al., 2007; Ye et al., 2004).

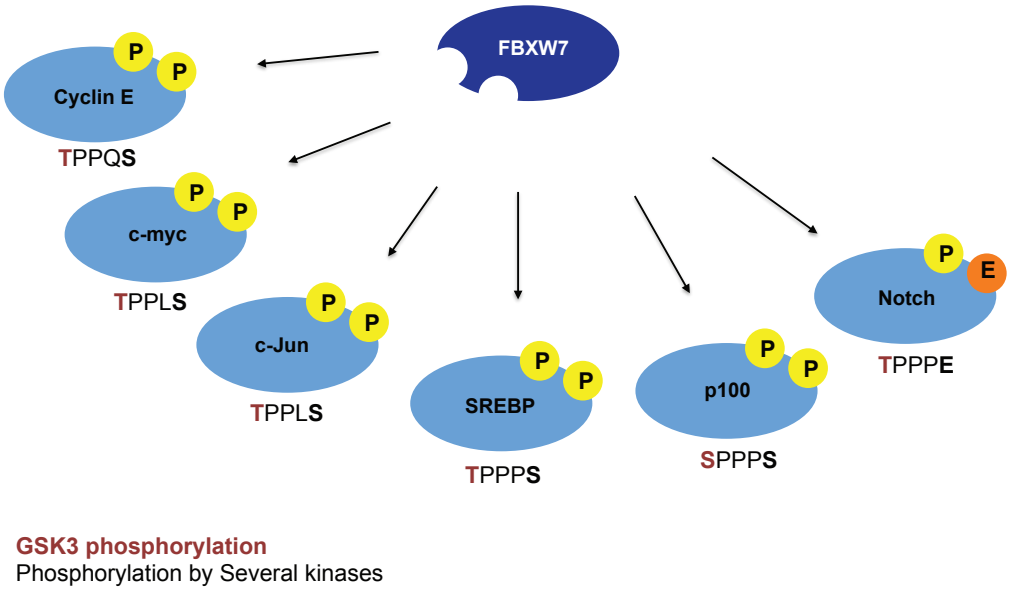

Figure 1.8.2: FBXW7 substrates
FBXW7 substrates contain a phospho-degron motif in which the central phosphorylatable residue can be phosphorylated by GSK3 after pre-phosphorylation at +4 position by another priming kinases. In some substrates, for example Notch, the phosphorylatable residue at +4 position is substituted by a negative charged amino acid, for Notch glutamate. SREBP, sterol regulatory element binding protein. (Adapted from (Welcker and Clurman, 2008)

However, alignment of the phosphodegron motifs of known FBXW7 substrates with the solved crystal structure of FBXW7 led to the proposal of a structure-based phosphodegron motif: ϕ-X-ϕ–ϕ–ϕ-pT/S-P-P-X-pS/T, where ϕ represents hydrophobic residue, X any amino acid, and p a phosphorylated residue (Fig. 1.7.3) (Hao et al., 2007). Nevertheless, variations in the degron motif, such as substitutions of serine and threonine residues or the inclusion of phosphomimicking

amino acids have been observed (Fig. 5.5 A, B and Fig. 1.8.3) (Hao et al., 2007; Orlicky et al., 2003; Welcker et al., 2003; Ye et al., 2004).

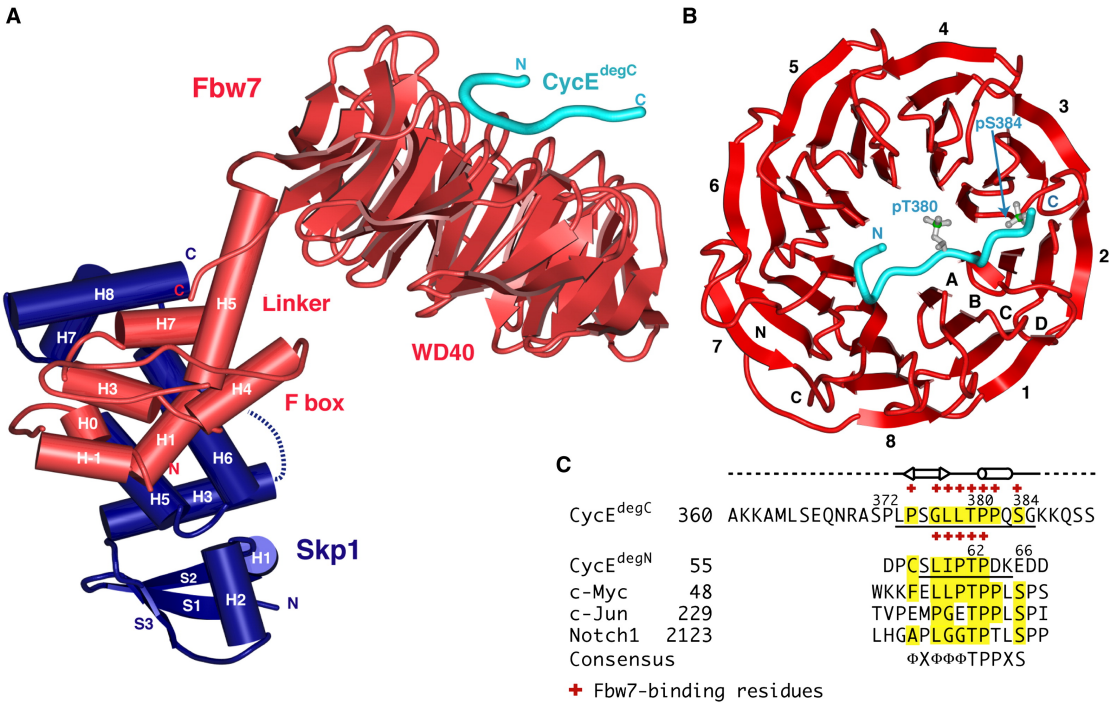

Figure.1.8.3: Ribbon representation of the crystal structure of FBXW7 in complex with cyclin E C-terminal degron motif and alignment of FBXW7 phospho-degron motifs

A) Overall structure of FBXW7 with SKP1 and C-terminal degron (degC) motif of cyclin E. B) Binding of cyclin E C-terminal degC to FBXW7 β-propeller structure. FBXW7 blades are labeled with letters, strands for each blade by numbers. C) Sequence alignment of cyclin E phospho-degron motifs with other motifs of known substrates. Residues that match the structure-based degron motif are highlighted in yellow. (ϕ-X-ϕ–ϕ–ϕ-pT/S-P-P-X-pS/T, where ϕ = hydrophobic residues, X = any amino acid, pT = phosphorylated threonine, pS = phosphorylated serine, P = proline. (Hao B et al., 2007) PDB codes for the SKP1-FBXW7 complex: 2OVP, for the SKP1-FBXW7-CycE^{degC} complex: 2OVR. Taken from (Li and Hao, 2010)

FBXW7 levels are stable throughout the cell cycle, but its activity is regulated. Glomulin is a CRL inhibitor that is proposed to regulate FBXW7 activity in complex with SCF by binding to the RING finger protein Rbx1, which blocks the interaction with E2 (Tron et al., 2012). Another regulator of FBXW7 function is the oncogene SV40 large T antigen, which contains a decoy phosphor-degron motif that leads to FBXW7 binding and subsequently re-locates FBXW7γ to the nucleoplasm and interferes with cyclin E degradation (Welcker and Clurman, 2005). However, for the FBXW7-dependent targeting of substrates, further regulation of FBXW7 ubiquitylation activity has been observed. For example, the FBXW7α isoform promotes interaction between c-myc and the de-ubiquitylating enzyme USP28 thereby stabilizing c-myc (Popov et al., 2007). This indicates not only a regulation of FBXW7 by control of FBXW7 activity but also by control of ubiquitylation of the target protein.

Because increased levels of cyclin E activity are oncogenic, it was suggested that FBXW7 functions as a tumour suppressor, when it was first identified as the E3 ligase that targets cyclin E for proteasomal degradation. Indeed, FBXW7 is frequently deleted in tumours and it is estimated that 6% of cancers have *FBXW7* mutations that cause loss-of-function that correlates with de-regulation of the cell cycle (Akhoondi et al., 2007; Ekholm et al., 2001; Maser et al., 2007). Most *FBXW7* mutations, that have been identified in tumours, are missense mutations in crucial residues, that interfere with substrate recruitment (Akhoondi et al., 2007). In addition to mutations directly affecting FBXW7, the degron motif of oncoproteins, such as c-myc and notch, is often mutated in tumours, which prevents substrate recognition by FBXW7, stabilizes the substrates and results in increased genome instability (Bahram et al., 2000; Rajagopalan et al., 2004; Wei et al., 2005; Weng et al., 2004). These findings support a function of FBXW7 as a tumour suppressor as many of its substrates are oncoproteins, such as cyclin E, c-myc, c-Jun or Notch1, and de-

regulation of these proteins promotes cell proliferation and tumourigenesis (Akhoondi et al., 2007; Mao et al., 2004; Minella et al., 2005).

1.9 The UPS in DNA repair

Increasing evidences suggest a role of the UPS in DNA damage response and repair. As mentioned above ubiquitylation events have crucial functions in modulating the recruitment and interaction of proteins in response to DNA damage (chapter 1.3.1). In contrast to the function in cell cycle regulation, where it primarily targets proteins for proteasomal degradation, the function of the ubiquitylation in damage response and repair is still under debate.

Interestingly, proteasomes localize to sites of DNA damage (Blickwedehl et al., 2008; Ustrell et al., 2002): Components of the 19S and 20S subunits of the proteasome have been found to localize to DNA damage sites (Galanty et al., 2012; Levy-Barda et al., 2011), whereby co-localization of some of the 19S subunits with γH2AX was dependent on RNF8, UBC13 and BRCA1, which are all involved in the DNA damage response (Butler et al., 2012). Treatment of cells with proteasome inhibitor MG132 prior to induction of DNA damage results in persistence of MDC1 repair foci and inhibition of HR repair (Gudmundsdottir et al., 2007; Jacquemont and Taniguchi, 2007; Murakawa et al., 2007; Shi et al., 2008; Wang and Elledge, 2007). Also, depletion of the proteasome subunits 19S and 20S leads to increased genomic instability and decreased RAD51 foci in cells (Ben-Aroya et al., 2010; Jacquemont and Taniguchi, 2007). Thus proteasomes are proposed to promote DNA damage response signalling as well as DNA damage response-dependent protein turnover and HR.

Formation of RAD51 foci at DNA damage sites has been found to depend on RNF4, which targets MDC1 and RPA for proteasomal degradation (Galanty et al.,

2012). Loss of RNF4 led to increased sensitivity to DNA damaging agents and defective loading of RPA and RAD51 on DNA (Yin et al., 2012). Furthermore, the DSS1 protein, a component of the 19S proteasome, has been shown to localize to sites of DNA damage and to be required for efficient DSB repair (Krogan et al., 2004). Significantly, DSS1 also interacts with BRCA2 and is thought to facilitate BRCA2 interaction with DNA, BRCA2-mediated homologous repair as well as BRCA2-mediated replacement of RPA by RAD51 independently of proteasomal degradation (Kojic et al., 2005; Kristensen et al., 2010; Liu et al., 2010; Zhou et al., 2007). It was also shown that BRCA2 can interact with the proteasome subunits RPN7 and RPN3, whereby RPN7 interaction with BRCA2 was independent of DSS1 (Gudmundsdottir et al., 2007). However, an implication of this particular interaction in DNA repair has not been shown. These reports suggest a functional interplay of BRCA2 with the proteasome in DNA repair. This is supported by reports showing that SKP2, an F-box protein of the SCF complex, which has recently been reported to K63-linked poly-ubiquitylate NBS1, thereby facilitating ATM activation, also interacts with soluble and chromatin-bound BRCA2, targeting BRCA2 for ubiquitin-dependent proteasomal degradation (Arbini et al., 2011; Moro, 2006; Wu et al., 2012).

1.10 Aims

This thesis is concerned with a mechanism to regulate the stability of the breast cancer susceptibility protein BRCA2. In particular it investigates how BRCA2 protein stability is regulated in a the cell cycle-dependent.

To address this, the thesis aims to:

- Identify the mechanism that regulates BRCA2 stability
- Identify a potential candidate E3 ligase for BRCA2
- Analyse the interaction of the candidate E3 ligase with BRCA2
- Assess the importance of BRCA2 level regulation on DNA repair

In brief, Chapter 3 studies BRCA2 protein levels during the cell cycle and BRCA2 protein half-life, suggesting an active regulatory mechanism for BRCA2 stability. Chapter 4 investigates the ubiquitylation of BRCA2 and identifies SCF^{FBXW7} as a candidate E3 ligase responsible for targeting BRCA2 for proteasomal degradation. Chapter 5 studies the interaction of BRCA2 with the SCF^{FBXW7} E3 ligase and Chapter 6 analyses the impact of SCF^{FBXW7}-dependent regulation of BRCA2 on DNA damage repair.

Taken together, the results presented in this thesis provide insight into a regulatory mechanism that controls BRCA2 stability.

2 Materials and Methods

Unless otherwise noted, methods described in this thesis were performed or modified according to Sambrook et al. (Sambrook and Russell, 2001).

2.1 Materials

In this thesis chemicals and reagents with purity grade pro analysi (p.a.) were purchased from the companies AppliChem, GE Healthcare, Merck, MWG-Biotech, Qiagen and Sigma. Materials for cell culture (2.2), such as growth media and antibiotics/antimycotics, were ordered from PAA and Invitrogen. Proteins were transferred onto the Whatman nitrocellulose (GE Healthcare). Bound antibodies were detected by chemiluminescence with ECL hyperfilms from GE Healthcare or Biological Industries.

All solutions were prepared with bi-distilled water. As appropriate, solutions were sterilised by autoclaving for 20 min at 121 °C.

2.2 Cell Culture

2.2.1 Cell lines and maintenance

HEK293T, HT1080, HeLa, U2OS-SCR♯18

HEK293T cells are human embryonic kidney cells (HEK293) that constitutively express the simian virus 40 (SV40) large T antigen enabling efficient transfection and high expression of the gene of interest, Ht1080 are human

fibrosarcoma cells (epithelial), HeLa are human cervical adenocarcinoma cells (epithelial), U2OS are human osteosarcoma cells.

Cell lines (HEK293T, HT1080, HeLa, U2OS-SCR♯18) were cultured in Dulbecco's modified Eagle's minimal essential medium (DMEM, Sigma Aldrich), containing 10 % v/v FBS, 0.1 mg/ml Penicillin and Streptomycin (PAA Laboratories GmbH) at 37 °C and 5 % CO_2. U2OS-SCR♯18 was a kind gift from Ralph Scully, described in (Puget et al., 2005; Rouet et al., 1994).

Flp-In™ T-REx-HEK293 FE and FE-BRCA2

Flp-In™ cells (Invitrogen, Germany) are human embryonic kidney cells (Flp-In T-REx™ HEK293) suitable for the integration of the gene of interest at a specific genomic locus. Since the Flp-In system contains a Flp Recombination Target (FRT) in the genome, an expression vector containing the gene of interest can be integrated into the genome by Flp recombinase-mediated DNA recombination at the FRT-site (O'Gorman et al., 1991). The introduction of the Flp-In expression vector also enables high expression levels of the gene of interest.

Flp-In-T-REx-HEK293 (Invitrogen) were transfected with cDNA encoding for FLAG-EGFP-tagged BRCA2 or the FLAG-EGFP-tag (FE). Cells were cultured in Dulbecco's modified Eagle's minimal essential medium (DMEM, Sigma Aldrich), containing 10 % v/v FBS, 0.1 mg/ml Penicillin and Streptomycin (PAA Laboratories GmbH) at 37 °C and 5 % CO_2. Selection for FLAG-EGFP-BRCA2 or FLAG-EGFP was performed using 10 µg/ml Blasticidin and 100 µg/ml Hygromycin (Invitrogen). For conditional expression of FE-BRCA2 or FE in Flp-In-T-Rex-HEK293 cells, cells were incubated with 2 µg/ml of Doxycycline (Sigma) for 48 hours at 37 °C and 5 % CO_2.

HCT116^{WT} and HCT116*FBXW7*$^{-/-}$

HCT116 are human colon cancer cells. HCT116^{WT} and HCT116*FBXW7*$^{-/-}$ isogenic cell lines were cultured in McCoy's 5A (PAA Laboratories GmbH) containing 10 % FBS, 100 µg/ml Penicillin and Streptomycin (PAA Laboratories GmbH) at 37 °C and 5 % CO_2. These cell lines were a generous gift by Bert Vogelstein (Rajagopalan et al., 2004).

DLD-1^{WT} and DLD-1*FBXW7*$^{-/-}$

Duke's type C, colorectal adenocarcinoma cell line (epithelial). DLD-1^{WT} and DLD-1*FBXW7*$^{-/-}$ cell lines were cultured in RPMI (PAA Laboratories GmbH) containing 10 % FBS, 100 µg/ml Penicillin and Streptomycin (PAA Laboratories GmbH) at 37 °C and 5 % CO_2. These cell lines were a generous gift by Bert Vogelstein (Rajagopalan et al., 2004).

2.2.2 Harvesting of cells

Cell lines were grown on 10 cm sterile petri dishes. The generation time of the cells was approximately 24 h. At a density of ~1 x 10^7 cells per 10 cm petri dish, i.e. 90 % confluence, cells had to be transferred onto new petri dishes. Cells were washed with 10 ml PBS (137 mM NaCl, 2.7 mM KCl, 10 mM Na_2HPO_4 x 2 H_2O, 1.8 mM KH_2PO_4 x H_2O, pH 7.5) and incubated in 1 ml trypsin/EDTA (0.05 %/0.02 %; GIBCO) for 5 min at 37 °C. Trypsin detaches the cells by hydrolytic cleavage of adhesion proteins. The enzymatic reaction was stopped with 9 ml of Ca^{2+}-containing growth medium (DMEM, McCoy's 5A, RPMI). The cell number was determined and

approximately ~4 x 10^5 cells were plated onto a new petri dish. The medium was changed every four days.

Cells were counted in a “Neubauer counting chamber”. Cell suspensions were diluted 1:10 and 10 µl were applied to each site of the Neubauer chamber. The cell number from eight squares x dilution factor x10^4 gave the cell number per ml solution.

2.3 Molecular biological methods

2.3.1. Bacterial strains and plasmids

In this thesis *E. coli* strains TOP10F’ (Agilent Technologies), BL21 (Agilent Technologies), and gateway ccdB competent cells (Invitrogen) were used.

Table 2.3.1: The following plasmids were used in this thesis

Plasmid	Size	Resistance	Feature	Promoter	Manufacturer
pcDNA3.1 (+)	5428 bp	Ampicillin (bacterial) Neomycin (mammalian)		CMV	Invitrogen
pENTR1A	2294 bp	Kanamycin	attL1, attL2		Invitrogen
pDEST53	7767 bp	Ampicillin (bacterial) Neomycin (mammalian)	GFP-tag	CMV	Invitrogen
pDEST17	6354 bp	Ampicillin	6xHis	T7	Invitrogen
pEYFP-C1	4731 bp	Neomycin	EYFP-tag	CMV	Clontech

2.3.2 *Escherichia coli (E. coli)* cultures

E. coli cells were cultured sterilised in Luria-Bertani (LB) broth (Lysogeny broth, Calbiochem) with continuous shaking (220 rpm) at 37 ºC.

For selection of *E. coli* cells containing a transformed plasmid, cells were plated onto LB-Agar plates containing the corresponding antibiotic as selection marker during growth at 37 ºC. For, LB-Agar plates, LB-Agar (Calbiochem) was dissolved in dH_2O and sterilised by autoclaving. LB-media was cooled to 50 ºC and antibiotics for collection of plasmid-coded resistance were added and poured into sterile Petri dishes (~25 ml per 10 cm petri dish). *E. coli* cells were plated on antibiotic containing LB-Agar plates and incubated at 37 ºC ON or until colonies were visible. Colonies from *E. coli* cells containing the transformed plasmid were then inoculated in LB medium with antibiotics and grown at constant shaking at 37 ºC, ON. For selection of plasmid-coded antibiotic resistance antibiotics were used at a final concentration: ampicillin (100 µg/ml), kanamycin (50 µ/ml) or spectinomycin (100 µg/ml).

For storage of *E.coli* cultures glycerol-stocks were generated (1:1 mixture of *E.coli* culture with 50 % glycerol) and kept at – 80 ºC.

2.3.3 Heat-shock transformation

Transformation is the non-viral uptake of plasmid DNA by prokaryotes. To transfer plasmids, approximately 50 ng plasmid DNA was added to 100 µl competent TOP10F' *E. coli* cells and incubated for 30 min on ice. *E. coli* cells and DNA were then heat-shocked for 30 sec at 42 ºC and immediately incubated for further 10 min on ice. After adding antibiotic-free LB-medium (1 ml) cells were incubated for 1 h at

37 °C with constant shaking. The cell suspension was then transferred onto LB-agar plates containing 100 µg/ml ampicillin or 50 µg/ml kanamycin or spectinomycin (100 µg/ml) and incubated ON at 37 °C.

2.3.4 Preparation of plasmid DNA

Plasmid DNA was extracted using the Qiagen Mini or Midi prep kit (Qiagen) according to the manufacturer's instructions.

2.3.5 Polymerase chain reaction (PCR)

Polymerase chain reaction was used to amplify DNA fragments. Therefore, two oligonucleotides (primers) flanking the DNA fragment are necessary, that provide free 3'-hydroyl groups for the DNA synthesis and extension.

The PCR reaction consists of three steps which are repeated 20-35 times. First the DNA double strands are denatured by treatment with high temperature (95 ºC), second, the temperature is decreased (55 – 65 ºC) to allow annealing of primers with the complementary DNA sequences, and third, the DNA synthesis, which is executed by a thermostable DNA polymerase extending the 3'-hydroxyl group of the oligonucleotides at 72 ºC. These reactions are repeated multiple times resulting in an exponential increase of the DNA fragment.

Reaction mix:	Reaction program:			
1 x Reaction buffer (5x)	95 ºC	x	3 min	
50 ng Template DNA	98 ºC	x	20 sec	x 25 cycles
0.3 µM 3' oligonucleotide primer	62 ºC	x	15 sec	
0.3 µM 5' oligonucleotide primer	72 ºC	x	1 min	
0.25 mM dNTP mix	72 ºC	x	1 min	
1 U Kappa HiFi DNA Polymerase				

2.3.6 Site-directed mutagenesis

In site-directed mutagenesis targeted changes to a DNA sequence are made, using primers that are complementary to the template DNA but contain amino acid changes that lead to introduction of rendered amino-acids into the newly synthesized DNA by the DNA polymerase.

To perform site-directed mutagenesis the QuikChange kit (Agilent Technologies) was used according to the manufacturer's instructions. In this kit, the DNA Polymerase PfuUltra high-fidelity is used, which extends the primers thus generating a mutated plasmid. After the PCR, the product is treated for 2 h at 37 ºC with DpnI endonuclease which, targets methylated and hemimethylated DNA (5'-G_{m6}ATC-3'), thus digesting the parental template DNA and leaving the newly synthesized DNA plasmid, which can be transformed into competent cells, in which the nicks in the DNA are circularized and repaired. After growth of transformed cells, DNA mini preps (Quiagen) were performed and DNA was sent for sequencing by SourceBioscience. The typical protocol used in this study is outlined below:

Reaction mix:	Reaction program:			
10 x Reaction buffer	95 ºC	x	30 sec	
50 ng Template DNA	95 ºC	x	30 sec	x 16 – 20 cycles
125 ng oligonucleotide primer ♯1	55 ºC	x	1 min	
125 ng oligonucleotide primer ♯2	68 ºC	x	12 min	
1 µl dNTP mix (25 mM each)	37 ºC	x	2 h	
2.5 U PfuUltra HF DNA Polymerase				

2.3.7 Restriction enzyme digestion and DNA ligation

Restriction enzyme digestion was performed in buffer conditions recommended by the supplier. The digestion mix typically contained 3 µg DNA, 1 U/µg DNA restriction enzyme, 100 µg/ml BSA, 1x reaction buffer added by dH_2O to a total volume of 10 µl. The digestion mix was incubated according to the manufacturer's recommendations (NEB) but typically at 37 ºC for 1 h.

For ligation reactions, 1 µg of cut vector was mixed with 3 times molar excess of insert and T4 DNA ligase (NEB) added up to a total volume of 10 – 20 µl with dH_2O and incubated at 16 ºC for 16 h.

2.3.8 Gateway cloning

Gateway cloning was performed using the Gateway cloning kit from Invitrogen according to the manufacturer's instructions. Gateway cloning bases on the site-specific recombination properties of bacteriophage lambda (Landy, 1989). The lambda recombination occurs at specific attachment (att) sites on the interacting DNA molecules. There are two different att sites (aattB and attP) that flank the

recombination sites and between which recombination can occur. It enables a fast way to generate proteins with a distinct tag for expression as there are various Destination vectors available and it is easy to subclone DNA into multiple vectors using this method.

For generation of a Gateway entry clone a BP reaction according to the manufacturer's instructions was performed (Invitrogen).

LR Reaction mix:

1 – 10 µl	Entry clone (50 – 150 ng)
2 µl	Destination vector (150 ng/µl)
4 µl	5x LR Clonase reaction buffer
4 µl	LR Clonase
to 20 µl	TE Buffer, pH 8.0

2.3.9 Agarose gel electrophoresis

DNA fragments can be separated according to their size by electrophoresis in agarose gels. Due to the negatively charged phosphate backbone, DNA molecules migrate towards the anode. The velocity of double-stranded DNA fragments within the agarose gel is inversely proportional to their size. The concentration of the agarose gel determines which size-range of fragments can be well separated.

Table 2.3.9: Separation of DNA in agarose gels

Concentration of agarose [%] (w/v)	Size range of fragments [bp]
0.75	1,000-9,000
1	300-1,000
1.5	< 300

Agarose was dissolved in 1 x TBE buffer in a microwave. After cooling to 60 °C 1 µg/ml ethidium bromide was added to the agarose solution. Ethidium bromide intercalates with nucleic acids, which then can be visualised under ultraviolet light. DNA samples were mixed with 1/4 volume of 5 x sample buffer and loaded onto the gel. Electrophoresis was performed at 85 V in 1 x TBE electrophoresis buffer. For verification of sizes of DNA fragments the 1 kb ladder or 100 bp ladder from NEB were used.

10 x TBE buffer	
1 M	Tris base
1 M	Boric acid
20 mM	EDTA

5 x Sample buffer	
30 % (v/v)	Glycerol
0.25 % (w/v)	Bromophenol blue
0.25 % (w/v)	Xylene cyanol

2.3.10 Quantification of DNA concentration by agarose gel electrophoresis

The quality and quantity of plasmid DNA was analysed using 1 % (w/v) agarose gels. From the purified plasmid solution an aliquot of 5 µl was diluted with 15 µl TE buffer. This solution was mixed with 5 µl loading buffer and aliquots of 2.5 µl, 5 µl and 12.5 µl were separated on the agarose gel. Under UV illumination plasmid

DNA bands were compared according to their size to the 100 bp ladder or 1kb DNA ladder from NEB.

DNA concentration was also quantified using the Nanodrop (Thermo Scientific).

2.3.11 Generation of 6xHis-tagged ubiquitin

pET28c-ubiquitin plasmid DNA was a generously provided by M. Cohen to generate a histidine tagged ubiquitin for mammalian expression. Ubiquitin DNA was amplified by PCR using Esashi_pET28His (GGAAGAATTCATGGGAGCAGCCATCATC) and XhoI-ub primer provided by M. Cohen using the KAPA HiFi polymerase (Kappa Biosystems). Amplified DNA was digested using EcoRI and XhoI, ligated with EcoRI and XhoI digested pcDNA3.1(+) vector and transformed in competent *E. coli* TOP10 by heat-shock and selected on ampicillin-containing LG-Agar plates and send for sequencing.

2.3.12 Generation of GST-TUBE

Tandem UBA repeats were constructed using BglII and XhoI. Tandem UBA domains were cloned in a modified pGEX-4T-3 for FLAG-tag (F. Esashi) or modified to code for 6xHis-tag and then cloned in pGEX-6P-1 (GE Healthcare). Constructs were inducibly expressed in *E. coli* BL21 at 18 ºC ON. Constructs were then purified according to the GST-affinity purification described below.

Table 2.3.13: Primer for generation of self-made GST-TUBE

Primer	Sequence 5'-3'
Esashi_BglII-FLAG-UBA	ACGTAGATCTATGGACTACAAGGACGACGATGACAA ACATCCTCCAAAATCGGATCTG
Esashi_UBA-XhoI-RC	CGATCTCGAGTCAGTCGACCCGGGAATTCGG
Esashi_BglII-6His-UBA	ACGTAGATCTCATCACCACCATCATCATCCTCCAAAA TCGGATCTGGTTCCGCGT

2.3.13 Generation of FBXW7^{R465C}

FBXW7 was received in the gateway entry vector pENTR223 (The ORFeome Collaboration, David E Hill and David E Root). The FBXW7^{R465C} mutant was generated using the primers listed below in a site-directed mutagenesis reaction.

Table 2.3.13: Primer for generation of FBXW7^{R465C}

Primer	Sequence 5'-3'
FBXW7_R465C_s	GGGCATACTTCCACTGTGTGTTGTATGCATCTTCATG
FBXW7_R465C_as	CATGAAGATGCATACAACACACAGTGGAAGTATGCCC

2.3.14 Generation of BRCA2-2 fragment mutants

For generation of BRCA2 B2-2 mutants, site-directed mutagenesis was performed using the primers listed below.

Table 2.3.14: Primers for generation of BRCA2 B2-2 mutants

Primer	Sequence 5'-3'
B2-2_T703A_(2)S	CTACAGTTATTTATTGCCCCAGAAGCTGATTCTCTG
B2-2_T703A_(2)AS	CAGAGAATCAGCTTCTGGGGCAATAAATAACTGTAG
B2-2_T772A_S	CCAGCACTCTTATTTTAGCCCCTACTTCCAAGGATGTTC
B2-2_T772A_AS	GAACATCCTTGGAAGTAGGGGCTAAAATAAGAGTGCTGG
B2-2_S767A_T768A_S	GTCTTTTATATGATCATGAAAATGCCGCCGCTCTTATTTTAGCCCCTA
B2-2_S767A_T768A_AS	GTAGGGGCTAAAATAAGAGCGGCGGCATTTTCATGATCATATAAAAGA
B2-2_T774A_S775A_S	GCACTCTTATTTTAGCCGCTGCTTCCAAGGATGTTCTGTCAAAC
B2-2_T774A_S775A_AS	GTTTGACAGAACATCCTTGGAAGCAGCGGCTAAAATAAGAGTGC

2.3.15 Generation of smaller BRCA2-2 fragments

Smaller BRCA2 fragment B2-2 fragments were generated with BamHI and NotI restriction sites by PCR using the primers listed below. DNA was then digested using BamHI and NotI and ligated with the BamHI and NotI digested pENTR1A.

Table 2.3.15: Primers for generation of smaller BRCA2 B2-2 fragments

Primer	Sequence 5'-3'
B2-2-1 (5')	GGGGGATCCGACCAAAATATTTCAGAAAAAGACCTAT
B2-2-1 (3')	GGGGCGGCCGCTTAATTCTGTGTGGTGGTGGC
B2-2-2 (5')	GGGGGATCCGGTCATATGACTGATCCAAACTTTA
B2-2-2 (3')	GGGGCGGCCGCTTATTTCCTCAGAATTGTCCCAAAAG
B2-2-3 (5)	GGGGGATCCGATTCTGAAGAACCAACTTTGTC
B2-2-3 (3')	GGGGCGGCCGCTTAAATATTTTTGGTTAATTCAACATCAG
B2-2-4 (5')	GGGGGATCCGCATGTCACCCAGTACAACATTC
B2-2-4 (3')	GGGGCGGCCGCTTATCTTAGATTTGTGTTTTGGTTGAATTG
B2-2-5 (5')	GGGGGATCCGGTAACAATTATGAATCTGATGTTG
B2-2-5 (3')	GGGGCGGCCGCTTAAGTATTTCCTAAAGCAAGATTATTCCT

2.4 Biochemical methods for *in vitro* analyses

2.4.1 Expression of recombinant proteins in *E. coli*

Expression of recombinant proteins was performed in *E.coli* BL21. Cultures were grown in LB-medium, supplemented with the appropriate antibiotics at 37 ºC and 220 rpm until an OD_{600} of 0.7 was reached. Cultures were cooled down and protein expression was induced by addition of 0.1 mM IPTG. GST-B2-2 and GST-B2-9 were expressed at 18 ºC for 6 h and then purified using GST-affinity purification.

2.4.2 Protein GST-affinity purification

For 100 ml bacterial culture, 5 – 10 ml extraction buffer and 100 µl GST-affinity resin (Glutathione Sepharose 4 Fast Flow, GE Healthcare) were used. Cultures were spun down at 2000 g for 20 min. After decanting the supernatant and the pellet was resuspended in extraction buffer and incubated on ice for 30 min. After mild sonication (3 x 15 seconds) the lysates were spun down at 10 krpm for 45 min at 4 ºC. 100 µl GST-affinity resin was added to the supernatant an incubated on rotating wheel ON at 4 ºC.

Lysates with beads were spun down at 500 g for 5 min and supernatant was taken off. Beads were then washed three times in extraction buffer, 3 times with ATP-Mg buffer and 3 times with equilibration buffer. Then beads were three times incubated with 100 µl elution buffer for 15 min on a rotating wheel at 4 ºC. From each elution fraction 5 µl were incubated with LDS sample buffer and denatured for 5 min at 95 ºC and separated on SDS-PAGE to determine protein concentration.

Extraction buffer
50 mM Tris pH 7.5
150 mM KCl
10% Glycerol
1 mM EDTA
2 mM $MgCl_2$
1 x Protease inhibitor cocktail
2 mM Benzamidine-HCl
2 mg/ml Lysozyme
0.2 % Trition-X-100
Benzonase

ATP-Mg buffer
50 mM Tris-HCl pH 7.5
0.5 M KCl
20 mM $MgCl_2$
10% Glycerol
5 mM ATP
2 mM DTT

Equilibration buffer
50 mM Tris-HCl
150 mM KCl
10% Glycerol
2 mM DTT

Elution buffer
50 mM Tris-HCl pH 7.5
150 mM KCl
10% Glycerol
20 mM glutathione
0.1% Triton-X-100

2.4.3 *In vitro* kinase assays

2.4.3.1 CDK2/cyclin A phosphorylation assay

Reactions were typically performed in a total volume of 20 µl. 0.5 mg/ml substrate was incubated with 1 µl CDK2/cyclin A, 500 µM ATP, 10 mM DTT in CDK kinase buffer (10 mM HEPES (pH 7.6), 50 mM β-Glycerophosphate, 50 mM NaCl, 10 mM $MgCl_2$ 10 mM $MnCl_2$). The phosphorylation reaction was incubated for 15 min at 30 ºC. To terminate the reaction 7 µl 4 x LDS buffer (NuPAGE) was added and samples were boiled at 95 ºC for 10 min.

2.4.3.2 GSK3α phosphorylation assay

Reactions were usually performed in a total volume of 25 µl. 0.5 mg/ml substrate was incubated with 1 µl GSK3α (Millipore), 5 µl GSK3 kinase buffer (2 mM MOPS/NaOH (pH 7.0), 0.01 mM EDTA, 0.5 % Glycerol, 0.001 Triton-X-100, 0.01 % β-mercaptoethanol, 0.1 mg/ml BSA) and 10 µl ATP buffer (10 mM MgAc, 0.1 mM ATP 1 µCi γ^{32}P ATP) and added to a total volume of 25 µl with dH_2O. The phosphorylation reaction was incubated for 10 min at 30 ºC and terminated by addition of 7 µl 4 x LDS buffer and boiling at 95 ºC for 10 min.

2.4.3.3 Phosphorylation assay using HeLa whole cell extract

Phosphorylation reactions using whole cell extract were performed in a total volume of 20 µl. First whole cell extracts, maintaining functional kinases were generated using HeLa cells. 80 – 90 % confluent HeLa cells were harvested and lysed using Kinase extraction buffer. After 30 min incubation on ice, extracts were spun down at 30.000 rpm for 45 min at 4 ºC and the supernatant was taken off carefully without taking in of the lipid layer on the top of the supernatant and kept on ice. The extract was then diluted to 150 mM KCl and spun down again. 1 or 2 µl of this extract were then used in a phosphorylation reaction in a total volume of 25 µl. 0.5 mg/ml substrate was incubated with 1 µl or 2 µl of whole cell extract with 12.5 µl 2 x kinase buffer and 2.5 µl 10 x ATP buffer in the presence of 1 µCi γ^{32}P ATP. The phosphorylation reaction was incubated for 10 min at 30 ºC and the kinase reaction was terminated by the addition of 7 µl 4 x LDS buffer and boiling at 95 ºC for 10 min.

Kinase extraction buffer

20 mM	HEPES-NaOH pH 7.3
2 mM	EGTA
1.5 mM	$MgCl_2$
0.5%	NP-40
10%	Glycerol
20 mM	β-Glycerol phosphate
50 mM	NaF
1 mM	Na_3VO_4
1 mM	DTT

1 x Protease inhibitor cocktail

Kinase buffer

10 mM	HEPES pH 7.6
50 mM	NaCl
10 mM	$MgCl_2$
10 mM	$MnCl_2$
50 mM	β-glycerophosphate
1 mM	DTT

10 x ATP buffer

50 µM	ATP
10 mM	DTT

2.5 Biochemical methods for *in vivo* analyses

2.5.1 Transient protein expression in mammalian cells

2.5.1.1 jetPRIME transfection

Plasmid DNA was obtained using the Qiagen Midiprep Kit and was transfected into cells using the jetPRIME transfection reagent (Source BioScience). According to the manufacturer's instructions 10 µg or 1µg of DNA was used for 60 % confluent 100 mm dishes or 20 mm dishes of cells respectively and incubated for 4 hours at 37°C in 5 % CO_2. After 4 hours the medium was exchanged with fresh medium and cells were incubated for further 20 h at 37°C in 5 % CO_2.

Table 2.5.1.1: Plasmid DNA of dominant negative Cullin variants

DN Cullin variant	No.	Vendor
pcDNA3-DN-hCul1-FLAG	Plasmid 15818	Addgene
pcDNA3-DN-hCul2-FLAG	Plasmid 15819	Addgene
pcDNA3-DN-hCul3-FLAG	Plasmid 15820	Addgene
pcDNA3-DN-hCul4a-FLAG	Plasmid 15821	Addgene
pcDNA3-DN-hCul4b-FLAG	Plasmid 15822	Addgene
pcDNA2-DN-hCul5-FLAG	Plasmid 15823	Addgene

2.5.1.2 PEI transfection

The day before transfection cells were seeded to gain 70 % confluence the next day. For 10 mm or 20 mm dishes 2 µg or 10 µg of plasmid DNA was transfected respectively using 5.9 nM PEI (Sigma #408727) and added to the cells maintained in antibiotics- and serum-free DMEM. After incubation for 4 hours at 37°C, 5 % CO_2 the medium was exchanged to DMEM containing 10 % FBS, 100 µg/ml Penicillin and Streptomycin (PAA Laboratories GmbH) and incubated for another 20 hours before performing analyses. Plasmid DNA for transfections was purified using the Quiagen Midiprep Kit.

2.5.2 Dharmafect siRNA transfections

siRNA transfections were performed according to the manufacturer's instructions (Thermo Scientific) using DharmaFECT®1. For 80 % confluent cells in 6 well plates a final concentration of 100 nM siRNA 40 nM siRNA for down-regulation of RAD51 was used. siRNA was complexed with the reagent and incubated 20 min at room temperature. The complex was then added to HT1080 cells and incubated for 24 hours incubation. Cells were harvested using trypsin and proteins were extracted using Laemmli buffer. For down regulation of BRCA2 a 1:1 mixture of the siRNAs BRCA2-387 and BRCA2-3401 was used. Rad51 was downregulated using siRNAs RAD51_3'UTR1 and RAD51_3'UTR2 in a 1:1 ratio.

Table 2.5.2: siRNAs

siRNA	Sequence 5'-3'	Vendor
BRCA2-387	CAACAAUUACGAACCAAACdTdT	GENOSYS
BRCA2-3401	CUGAGCAAGCCUCAGUCAAdTdT	GENOSYS
RAD51_3'UTR1	GACUGCCAGGAUAAAGCUU	GENOSYS
RAD51_3'UTR2	GUCCUGCAGCCUAAUGAGA	GENOSYS
PALB2 #1	GGAAAGAGCCGGUUGUAAAdTdT	[31]
PALB2 #2	GGAGAAAUUAGCAUUCUUGdTdT	[31]
CUL1	ON-TARGET plus SMARTpool Human CUL1	Thermo scientific Dharmacon
SKP2	ON-TARGET plus SMARTpool Human SKP2	Thermo scientific Dharmacon
CDC20	ON-TARGET plus SMARTpool Human CDC20	Thermo scientific Dharmacon
FBXW7	ON-TARGET plus SMARTpool Human FBXW7	Thermo scientific Dharmacon
FBXO6	ON-TARGET plus SMARTpool Human FBXO6	Thermo scientific Dharmacon
FBXO40	ON-TARGET plus SMARTpool Human FBXO40	Thermo scientific Dharmacon
CDH1	ON-TARGET plus SMARTpool Human FZRI	Thermo scientific Dharmacon
BTRC (β-TRCP)	ON-TARGET plus SMARTpool Human BTRC	Thermo scientific Dharmacon
FBXW7 1	GGGCACCAGUCGUUAACAA[dT][dT]	Thermo scientific Dharmacon
FBXW7 1 as	UUGUUAACGACUGGUGCCC[dT][dT]	Thermo scientific Dharmacon
FBXW7 2	GUGAGUGGAUCUCUUGAUA[dT][dT]	Thermo scientific Dharmacon
FBXW7 2 as	UAUCAAGAGAUCCACUCAC[dT][dT]	Thermo scientific Dharmacon

FBXW7 3	GGAGUUGUGUGGCGGAUCA[dT][dT]	Thermo scientific Dharmacon
FBXW7 3 as	UGAUCCGCCACACAACUCC[dT][dT]	Thermo scientific Dharmacon
FBXW7 4	CAACAACGACGCCGAAUUA[dT][dT]	Thermo scientific Dharmacon
FBXW7 4 as	UAAUUCGGCGUCGUUGUUG[dT][dT]	Thermo scientific Dharmacon

2.5.3 Determination of protein half-life

To determine protein half-life in cells, HT1080 cells were treated with 10 µM cycloheximide (CHX) dissolved in dH_2O (Sigma) for up to 18 h at 37°C and 5 % CO_2. Incubation times are indicated for the different experiments.

2.5.4 Protein extraction from mammalian cells

Cells were harvested by trypsination, washed twice with 1 x PBS and proteins were extracted using HEPES-based extraction, Laemmli or NETN150 extraction buffer. Cells were incubated with the above mentioned extraction buffers for 30 min on ice and spun down for 10 min at 16 krpm to pellet cell debris. The supernatant was decanted and the protein concentration was measured according to Bradford at 595 nm (Bradford, 1976). Proteins were separated via gel electrophoresis.

For protein extraction using RIPA, cells were harvested by trypsination, washed twice with 1 x PBS and incubated in 10 µl 2 mM $MgCl_2$ with 5U/10 µl Benzonase for 10 min on ice. Then 100 µl RIPA buffer per 10 mg cells was added and incubated for another 30 min on ice before the extract was spun down for 10 min at 16 krpm to pellet cell debris. The supernatant was decanted and the protein concentration was measured using the D/C protein assay (Biorad) at 750 nm.

HEPES-buffer

150 mM	KCL
20 mM	HEPES pH 7.6
2 mM	EGTA pH 8
1.5 mM	$MgCl_2$
50 mM	NaF
0.1 %	NP-40
10 %	Glycerol
1 mM	Na_3VO_4
20 mM	β-glycerophosphate
1 mM	DTT
250 U/µl	Benzonase
1x	Sigma protease inhibitors

NETN150/300

50 mM	Tris HCl pH 7.5
150/300 mM	NaCl
2 mM	$MgCl_2$
0.2 %	NP-40
1x	Sigma Protease inhibitors
10 mM	Benzamidine Hydrochloride
50 mM	NaF
1 mM	Na_3VO_4
20 mM	Na-β-Glycerophosphate
0.5 M	DTT

RIPA

50 mM	Tris HCl pH 7.5
150 mM	NaCl
1%	NP-40
0.1 %	SDS
0.5 %	DOC
10 %	Glycerol
1 x	Sigma Protease inhibitors

Laemmli

2%	SDS
10%	Glycerol
60 mM	Tris HCl pH 6.8

2.5.5 Immunoprecipitation (IP) and Pull-down of endogenous proteins

2.5.5.1 FLAG-Immunoprecipitation of dominant negative Cullin variants

Immunoprecipitation of DN Cul variants was performed using Anti-FLAG-Agarose-M2 beads (A2220, Sigma). 20 µl of FLAG-beads were washed with HEPES-based extraction buffer, treated with 100 mM Glycine pH 3.5 and incubated with 0.1 % BSA/HEPES-buffer to block the beads. Afterwards beads were equilibrated in HEPES-based extraction buffer and added to 0.5 ml cell extracts containing 0.9 mg/ml protein. Incubation was performed ON at 4 °C with gentle rotation. After the incubation, samples were spun for 2 min at 1 k rpm to separate FLAG-beads from the extracts and washed 3 times with HEPES-based extraction buffer. 4 x LDS sample buffer was added and samples were boiled for 10 min at 95 °C and loaded onto 3-8 % Tris-Acetate gels and separated for detection by western blotting. As optimization DN Cul variants were extracted in NETN150 buffer and IP was performed as above but instead of HEPES-based extraction buffer NETN150 buffer was used. Bound proteins were eluted using by boiling beads with the same volume of 2 x LDS buffer at 95 °C for 10 min.

2.5.5.2 Immunoprecipitation of proteins using antibodies cross-linked to beads

For each sample 2.5 µg of BRCA2 antibody (OP95, Calbiochem) or 2.5 µg FBXW7 (NB100-88139, Novus Biologicals) were cross-linked to 10 µl of Affi-Prep Protein A Support (BioRad). Protein A beads were washed twice in 1 x PBS and incubated with antibody for 3 h at RT. After 3 washes with 1 x PBS the antibody –

Protein A sepharose beads were washed twice with Coupling buffer (0.1 M Sodium Tetraborate, 0.1 M Boric acid, pH 9), washed with DIM-PIM buffer (0.125 g Dimethyl Pimelimidate Dihidrochlordie in Sodium Tetraborate pH 8.5 – 9) and incubated ON rotating at 4 °C. Beads were then washed 3 times with coupling buffer, 2 times with Tris pH 9.0. For storage, beads were washed 3 times with storage buffer (0.1 M Sodium Tetraborate, 0.1 M Boric acid, pH 8.0). For direct use beads were washed quickly with 100 mM Glycine pH 3.5, twice with 1 M Tris pH 9.0 and incubated with 5 mg/ml BSA in PBS for at least 1 h at 4 °C before incubating with cell lysate for 4 h or ON. Bound proteins were eluted by boiling beads with the same volume of 2 x LDS buffer at 95 °C for 10 min

2.5.5.3 Pull-down of proteins using GFP-Nanotrap

GFP-pull-downs were performed for pull-down of GFP-tagged BRCA2 fragments. Cells were extracted in NETN150 extraction buffer. Per sample 7.5 µl GFP-Nanotrap beads (Chromotek) were washed once with 1 x PBS and equilibrated by three washes with the extraction buffer (NETN150) and incubated with protein extracts of a concentration of 1 mg/ml for 2 h on a rotating wheel at 4 °C. Beads incubated with cell extracts were washed three times with extraction buffer and bound proteins were eluted by boiling beads with the same volume of 2 x LDS buffer at 95 °C for 10 min.

2.5.5.4 GST-pull-down of proteins using GST-TUBE

GST-pull-down of ubiquitylated proteins using GST-TUBE 2 (Lifesensors) (Hjerpe et al., 2009) was performed according to the manufacturer's instructions. 100 µg/ml (1.5 µM) GST-TUBE 2 was added to 500 µl lysis buffer and proteins were extracted in GST-TUBE 2 containing lysis buffer for 1 h on ice. After centrifugation at <14000 x g at 4°C for 20 min the supernatant was collected and incubated with equilibrated Glutathione affinity resin for at least 2 h at 4ºC on a rotating wheel. Beads were collected by centrifugation <1000 x g, 4°C for 5 min and were washed with TBS-T containing 2 mM DTT. The resin was resuspended in 2 x LDS sample buffer and boiled at 95 ºC for 5 min.

Lysis buffer		TBS-T
150 mM	KCl,	20 mM Tris-HCl pH 8.0
20 mM	HEPES (pH 7.6)	150 mM NaCl
2 mM	EGTA	0.1 % Tween-20
1.5 mM	$MgCl_2$	
50 mM	NaF	
0.1 %	NP-40	
10 %	Glycerol	
1 mM	Na_3VO_4	
20 mM	β-glycerophosphate	
1 mM	DTT	
25 U	Benzonase	
1 mM	Benzamidine-HCl	
1x	Sigma protease inhibitors	

2.5.6 *In vivo* ubiquitylation assay

2.5 x 10^6 HEK293 T-Rex Flp-In cells were seeded on 10 cm dishes the day before transfection. A total of 5 µg DNA (2.5 µg 6xHis-ubiquitin, 2.5 µg pcDNA3.1 (+)) was transfected using PEI methodology and incubated for 4 hours at 5% CO_2, 37 ºC. After 4 hours the medium was exchanged with the culture medium containing 2 µg/ml Doxycycline. 24 hours later the medium was exchanged with fresh medium containing 2 µg/ml Doxycycline and incubated another 24 - 48 hours. 48 - 72 hours after transfection cells were incubated with 10 µM MG132 for 4 hours and then harvested using trypsin and washed twice with PBS.

20 % of the cell suspension was separated, directly extracted and protein concentration was determined using the Bradford assay and used for the Input in Western blot analysis. The remaining 80% of cells were extracted in 6 ml

Guanidinium-HCl extraction buffer at RT on a rotating wheel. In the meantime 10 µl His-Talon beads (Clontech) were equilibrated Guanidinium-HCl extraction buffer and added to whole cell extracts and incubated for 4 h at RT on a rotating wheel. Afterwards beads were washed excessively with 750 µl of the following buffers: 1 x washing buffer I, 2 x washing buffer II, 3 x washing buffer III, 3 x washing buffer IV, 3 x washing buffer V. For elution of ubiquitylated proteins, beads were incubated with 30 µl of Elution buffer ON at RT.

Lysis buffer
150 mM NaCl
50 mM Tris/HCl pH 8.0
5 mM EDTA
200 mM $MgCl_2$
1 % NP-40
2 mM DTT
1x Protase inhibitor cocktail
10 mM Benzamidine HCL

Guanidinium-HCL extraction buffer
6 M Guanidinium-HCl
0.1 M Na_2HPO_4/NaH_2PO_4 pH 8.0
0.01 M Tris/HCl pH 8.0
10 mM β-mercaptoethanol
100 m $MgCl_2$
Benzonase

Washing buffer I
6 M Guanidinium-HCl
0.1 M Na_2HPO_4/NaH_2PO_4 pH 8.0
0.01 M Tris/HCl pH 8.0
10 mM β-mercaptoethanol

Washing buffer II
8 M Urea
0.1 M Na_2HPO_4/NaH_2PO_4 pH 8.0
0.01 M Tris/HCl pH 8.0
10 mM β-mercaptoethanol

Washing buffer III
8 M Urea
0.1 M Na_2HPO_4/NaH_2PO_4 pH 6.3
0.01 M Tris/HCl pH 6.3
10 mM β-mercaptoethanol
0.2 % Triton X-100

Washing buffer IV
8 M Urea
0.1 M Na_2HPO_4/NaH_2PO_4 pH 6.3
0.01 M Tris/HCl pH 6.3
10 mM β-mercaptoethanol

Washing buffer V	Elution buffer
8 M Urea	200 mM Imidazole
0.1 M Na_2HPO_4/NaH_2PO_4 pH 6.3	0.15 M Tris/HCl pH 6.7
0.01 M Tris/HCl pH 6.3	20 % glycerol
10 mM β-mercaptoethanol	0.72 mM β-mercaptoethanol
0.1 % Triton X-100	

2.5.7 λ-phosphatase treatment

To test the phosphorylation dependent interaction of GFP-BRCA2 fragment B2-2 with FBXW7, GFP-IP of B2-2 was performed first. GFP-pull down was performed as above. After three washes with the extraction buffer, beads were equilibrated in PMP buffer containing 1 mM $MnCl_2$ and incubated with 1000 U λ-phosphatase (NEB) at 30 ºC for 45 min with regular shaking. Beads were washed three times with Protein MetalloPhosphatase (PMP) buffer and boiled with similar volume of 2 x LDS buffer for 10 min at 95 ºC.

To test the phosphorylation dependent interaction of BRCA2, GFP-BRCA2 fragment B2-6, B2-9 and TR1, and TR2 with FBXW7 cells were extracted in extraction buffer and protein concentration was measured. Protein extracts at a concentration of 1 mg/ml were incubated with 1000 U of λ-phosphatase for 45 min at 30 ºC. After phosphatase treatment Affi-Prep Protein A Support beads cross-linked to FBXW7 were added to the samples and further incubated at 30 ºC for 30 min. Afterwards, samples were transferred for gentle shaking on a rotating wheel at 4 ºC for further 3 hours. Samples were washed three times with 1 x PMP buffer and proteins were eluted by boiling beads with the same volume of 2 x LDS buffer for 10 min at 95 ºC and proteins were separated by electrophoresis.

Extraction buffer		Protein MetalloPhosphatase (PMP) buffer	
50 mM	HEPES pH 7.6	50 mM	HEPES pH 7.6
150 mM	NaCl	100 mM	NaCl
2 mM	$MgCl_2$	2 mM	DTT
0.1%	NP-40	0.01%	NP-40
1x	Sigma Protease inhibitors		
1 mM	DTT		

+ kinase inhibitors

10 mM	Benzamidine-HCl
50 mM	NaF
1 mM	Na_3VO_4
20 mM	β-Glycerophosphate

2.5.8 Kinase inhibitor treatments

For inhibition of kinases in cells, cells were treated with kinase inhibitors dissolved in DMSO for 4 h. CDK1 activity was inhibited using 10 µM RO-3306 (Calbiochem); CDK1 and CDK2 were inhibited using 60 µM NU6102 (generous gift by M. Nobel, Newcastle University (Davies et al., 2002) and GSK-3 kinase was inhibited using 10 µM IX (Calbiochem). In simultaneous inhibitions, the same concentrations of inhibitors were used.

2.6 General biochemical methods

2.6.1 Quantification of protein concentration

2.6.1.1 Quantification of protein concentration by Bradford (1976)

For quantification of total protein concentration the Bradford assay from BioRad was used and protein concentration was determined according to the manufacturer's instruction. In an acidic solution the absorption maximum of Coomassie Brilliant Blue G-250 bound to proteins shifts from 495 nm to 595 nm.
After whole cell extraction, 1µl of the whole cell extract was added to 1 ml of the Bradford reagent solution, mixed and incubated for 15 min at RT. Protein concentration was measured at 595 nm (E_{595}) and protein concentration of the probe was determined by comparison to a calibration curve obtained with defined concentrations of BSA (0, 1, 2, 4, 6, 8, 10). Calculation was performed according to Beer-Lambert Law:

$$E = \varepsilon \times c \times d$$

E = extinction at 595 nm

ε = coefficient of absorbance (1/mol * cm)

c = concentration (mol/l)

d = thickness of cuvette (cm)

2.6.1.2 Quantification of protein concentration by D/C Assay (BioRad)

Quantification of proteins using RIPA as extraction buffer was performed using the D/C Assay (BioRad) as this assay is compatible to the high concentrations of SDS (0.1%) and NP-40 (1%). The assay was performed according to the manufacturer's instructions and protein concentration was determined in comparison to a BSA-calibration with defined protein amounts.

2.6.1.3 Quantification of protein concentration on SDS-PAGE by Coomassie staining

For quantification of proteins on SDS-PAGE gels were stained with Instant blue (Expedeon) or ProtoSafeBlue (Geneflow). The staining intensity of the protein of interest was compared with staining intensities of bands with a defined of protein amounts (BSA-calibration).

2.6.2 Electrophoretic separation of proteins under denaturing conditions (SDS-PAGE)

In a denaturating Sodiumdodecylsulfate-Polyacrylamide gel electrophoresis (SDS-PAGE) according to Laemmli proteins are separated by their molecular weight in an electric field (Laemmli, 1970). SDS is an anionic and denaturing detergent that binds to proteins in a rather constant mass ratio of 1.4:1. This results in a negative net charge of the proteins which allows determination of the apparent molecular weight of the proteins rather precisely.

Proteins were denatured by boiling at 95 ºC for 10 min in the presence of LDS sample buffer and equal amounts of proteins were loaded on 3-8 % NuPAGE Tris-Acetate gel (Invitrogen) or 4-12 % Bis-Tris gel (Invitrogen) according to the size of the protein of interest. 3-8 % Tris-Acetate gels proteins were separated at 85 V for 1 h 40 min in Tris-Acetate SDS running buffer (50 mM Tricine, 50 mM Tris base, 0.1 % SDS) or for 4-12 % Bis-Tris gels at 100 V for 2 h in MOPS SDS running buffer (50 mM MOPS, 50 mM Tris base, 0.1 % SDS, 1 mM EDTA) as recommended by Invitrogen.

NuPAGE LDS sample buffer
106 mM Tris-HCl
141 mM Tris base
2 % lithium dodecyl sulfate
10 % Glycerol
0.51 mM EDTA
0.22 mM SERVA Blue G250
0.175 mM Phenol Red
pH 8.5

2.6.3 Immunoblotting

Electrophoretically separated proteins were transferred onto nitrocellulose membrane (Millipore) at 35 V for 14 h at 4 °C or at 100 V for 2 h in Transfer buffer (25 mM Glycine, 25 mM Tris, 10 % MeOH) for antibody staining. After transfer of proteins onto nitrocellulose membranes, membranes were blocked in 5 % dried milk in PBS containing 0.02 % Tween (PBST) for 1 h at room temperature. Then, membranes were probed with primary antibodies diluted in 5 % PBST either ON at 4 °C or for 4 h at room temperature. After 3 washes with PBST for 15 min, the

secondary Horseradish peroxidase (HRP) -conjugated antibody, diluted 1:1000 in 5 % dried milk/PBST, was added and incubated for 1 h at room temperature. Detection was performed with ECL Plus reagents (GE Healthcare, Biological Industries). The membrane was incubated with ECL reagent for 3 min at RT, and autoradiography was performed.

The molecular size of proteins was determined using the pre-stained BLUeye protein marker (Geneflow) or the pre-stained protein marker (Expedion).

Table 2.6.3: Antibodies for immunological protein detection

Antigen	**Origin/Dilution**	**Product no.**	**Source**
Primary antibodies			
Anti-BRCA2	Mouse (1:1000)	OP95	Calbiochem
Phospho Histone H3	Rabbit (1:1000)	382159	Calbiochem
γ phospho Histone H2AX	Mouse (1:2000)	05-636	Millipore
Histone H2A	Rabbit (1:1000)	2578	Cell Signaling
RAD51 (FBE2)	Rabbit (1:2000)		Kindly provided by Steve West
RAD51 (7646)	Rabbit (1:2000)		Self-made F. Esashi
GAPDH	Rabbit (1:5000)	G9545	Sigma-Aldrich
LaminA	Rabbit (1:5000)	L1293	Sigma Aldrich
Skp2	Rabbit (1:1000)	ab19877	Abcam
FLAG	HRP-coupled (1:1000)	A8592	Sigma
FBXW7	Rabbit (1:600)	NB100-88138/39	Novus Biologicals
FBXW7	Mouse (1:600)	FB407	Sigma
GFP, N-Terminal	Rabbit (1:5000)	G1544	Sigma
β-TRCP	Rabbit (1:1000)	D13F10	Cell Signaling
Cullin 1	Rabbit (1:1000)	NBP1-40523	Novus Biologicals
Cyclin E	Rabbit (1:1000)	Sc-481	Santa Cruz
6xHis	Mouse (1:1000)	631212	BD Biosciences
GST (B-14)	Mouse (1:1000)	Sc-138	Santa Cruz
Myc	Mouse (1:1000)	CBL-430	Millipore
Secondary antibodies			

Rabbit IgG HRP	Goat (1:1000)	PO448	DaKo Cytomation
Mouse IgG HRP	Goat (1:1000)	PO447	DaKo Cytomation
Protein A/G Peroxidase conjugated	(1:1000)	32490	Thermo Scientific

2.7 Cellular and phenotypic analysis

2.7.1 Synchronization of cells using double thymidine block

Cells were synchronized using thymidine. Thymidine inhibits synthesis of deoxynucleotides, therefore DNA synthesis cannot be performed and cells are arrested at the end of G1 phase. 2.5 x 10^5 cells were seeded on 10 cm dishes and incubated for at least 4 h at 37 °C and 5 % CO_2 so that cells did attach. Cells were then incubated in 2 mM thymidine-containing medium for 16 h at 37 °C and 5 % CO_2, washed twice with PBS and incubated with fresh medium for 9 h and incubated again in 2 mM thymidine-containing medium for 12 h at 37 °C and 5 % CO_2. Then cells were released in fresh medium and cell cycle analysis was performed.

2.7.2 Gene conversion assay

As a measurement for the repair of DNA double strand breaks the occurrence of gene conversion was measured in U2OS-SCR18 cells, generous gift by Ralph Scully (Puget et al., 2005). U2OS-SCR cells contain a reporter plasmid containing a truncated donor GFP gene in which the first 12 amino acids of the ORF are deleted. The receiving GFP gene has a CMV promoter but is inactive due to an insertion of the I-SceI recognition site 5'-TAGGGATAACAGGGTAAT-3'. Using the I-SceI nuclease a site-specific double strand break is introduced, which can be repaired by homology-directed repair using the donor GFP gene. Because of the orientation of the GFP gene copies successful repair of the DNA double strand break can occur via gene conversion between this two copies, resulting in a functional GFP gene. Therefore, successful repair can be measured by detection of GFP positive cells.

To analyse the impact of FBXW7 on HR-repair, siRNA-mediated knockdown of BRCA2 with control (universal negative control, Invitrogen), FBXW7 (Dharmacon SMARTpool or mixed individual siRNAs FBXW7 1- 4) with control and BRCA2 with FBXW7 was performed in U2OS-SCR cells. After 24 h cells were transfected with pCBA-I-SceI Nuclease plasmid using jetRPIME and incubated for 4 h, before re-plating cells into 10 cm dishes. 96 h later cells were harvested using trypsin and washed twice with 1 x PBS. 50 % of cells were fixed in 4 % paraformaldehyde for 15 min at RT, washed three times with 1 x PBS and gene conversion was determined by measuring GFP positive cells by FACS analysis using Cyan ADP analyser (Beckman Coulter).

2.7.3 Clonogenic survival assay

500 or 100 FBXW7^{WT}, FBXW7$^{-/-}$ HCT116 or FBXW7^{WT}, FBXW7$^{-/-}$ DLD-1 cells were plated on 10 cm dish format and incubated for 4 h at 37 °C and 5 % CO_2 to attach. Cells were then irradiated at 1, 2 and 4 Gy from a $_{137}$Cs-source of a GRAVITON RX 30/55 irradiator and further incubated for 14 days. Cells were fixed and stained with Coomassie stain and colonies of >50 were counted.

Coomassie stain
0.1% Brilliant Blue R-250
7% Acetic Acid
50% Methanol
43% H_2O

2.8 Cell sorting and imaging

2.8.1 Propidium Iodide staining for fluorescence-activated cell sorting (FACS)

Synchronized HT1080 cells were harvested using trypsin. After washing with 1 x PBS, cells were fixed in 70 % ice cold ethanol for at least 15 min or kept at -20 C until analysis. Fixed cells were washed 3 times with 1 x PBS and incubated in 0.5 ml PBS containing 5 µg/ml Propidium Iodide (PI, Sigma) and RNase (0.2 mg/ml) for x min at x C. Analyses were performed using Cyan ADP Analyzer (Beckmann Coulter).

2.8.2 Fluorescence-based immunocytochemical detection of proteins

1 x 10^5 cells were seeded per well containing a glass coverslip in a 12 well plate the day before treatment and incubated at 37 ºC with 5 % CO_2. After treatment with IR and incubation for the indicated times, cells were washed three times with 1 x PBS and incubated with hypotonic swelling solution (80 mM NaCl, 3 mM $MgCl_2$) for 10 min at room temperature (RT). Cells were then fixed with 4 % Paraformaldehyde for 10 min at RT and washed with 1 x PBS three times. For permeabilization of cells, cells were incubated with 0.5 % Triton-X-100 (Sigma Aldrich) in 1 x PBS for 5 min. After three washes with 1 x PBS, cells on coverslips were blocked with Antibody dilution buffer (5 % BSA (Sigma Aldrich), 0.2 % Cold Fish Skin Gelatin (Sigma Aldrich), 10 % goat serum (Sigma Aldrich) and 0.05 % Triton-X-100 in 1 x PBS) for 30 min at RT. Cells were then incubated with the primary antibody diluted in Antibody dilution buffer for 1 h at RT or ON at 4 ºC, washed three times with 0.05 % Triton-X-100 in 1 x PBS and incubated with the secondary fluorescent-coupled antibody diluted in Antibody dilution buffer for 30 min – 1 h at RT. Coverslips were washed

three times with 0.05 % Triton-X-100 in 1 x PBS and mounted using DAPI-containing mounting media (ProLong Gold Antifade Reagent, Life Technologies) for observation.

Table 2.8.2: Antibodies for immunocytochemical protein detection

Antibodies	Isotype	Dilution (in ADB)	Product no.	Vendor
Goat-α-rabbit	Goat, Alexa Fluor 555 linked	1:500	A21430	Life Technologies
Goat-α-mouse	Goat, Alexa Fluor 488 linked	1:500	A11017	Life Technologies

2.9 Software

- Quantification of protein amount in western blots was performed using Image6J.
- PRISM (Version 6.0; GraphPad, San Diego, USA) was used for statistical analyses.
- Flow cytometric data analysis on CyAn ADP Analyzer (BeckmanCoulter) was performed with Summit.
- Data gained from Flow cytometric analyses were plotted using FlowJo.
- For alignments ClustalW EMBO was used.

3 BRCA2 protein levels change in cells

3.1 Preface

BRCA2 is a key regulator of DNA double strand break repair by homologous recombination (HR), which takes place during S and G2 phases of the cell cycle. Previously, it has been shown that BRCA2 mRNA levels vary in a variety of sporadic breast cancers (Bièche et al., 1999) and that loss of BRCA2 or expression of dysfunctional BRCA2 lead to genome instability and impaired repair by HR (Connor et al., 1997; Moynahan et al., 2001; Patel et al., 1998; Sharan et al., 1997; Tutt, 2001; Tutt et al., 1999; Xia et al., 2001; Yang et al., 2002; Yu et al., 2000; Yuan et al., 1999). However, BRCA2 mRNA overexpression has also been found in rapidly proliferating cells (Rajan et al., 1996) and increased BRCA2 mRNA levels correlate with a poor cancer prognosis (Egawa et al., 2002). Furthermore, Magwood et al. showed that high levels of BRCA2 suppress RAD51-mediated HR (Magwood et al., 2012). These findings indicate that the loss of BRCA2 function as well as increased BRCA2 levels impair the repair of DNA damage by HR. Since HR is directly regulated during the cell cycle by major cell cycle regulators, such as CDKs (Aylon et al., 2004; Huertas and Jackson, 2009; Ira et al., 2004; Limbo et al., 2007; Yun and Hiom, 2009; Zierhut and Diffley, 2008), and the interaction of BRCA2 with RAD51 is also cell cycle-regulated (Esashi et al., 2005), the aim of the work described in the following chapter was to investigate BRCA2 protein levels during the cell cycle.

3.2 BRCA2 protein levels during the cell cycle

To investigate BRCA2 protein levels during the cell cycle, HT1080 and HeLa cells were synchronized by double thymidine block and samples were taken at regular intervals following cells cycle re-entry. Thymidine inhibits the synthesis of deoxynucleotides (Ives et al., 1963), thus arrests cells at G1/S phase transition. Cell cycle progression was monitored by quantification of cellular DNA content by PI staining in fluorescent associated cell sorting (FACS). To perform quantitative analysis of BRCA2 protein during the cell cycle, Western blot analyses were carried out and intensities of bands detected by antibodies against BRCA2 and a loading control (GAPDH or α-tubulin) were densitometrically analysed and normalized. Membranes were also blotted against cell cycle markers as described below, to further confirm the respective cell cycle stages of the samples. Phosphorylation of Histone H3 on Ser10 (pH3) indicates when cells are in mitosis (Wei et al., 1999), and as the amount of individual cyclins vary in the different phases of the cell cycle, probing against cyclin A and cyclin B indicates when cells are in S/G2 phases or at G2/M phase transition, respectively. As controls, asynchronous cells and nocodazole-treated cells, which are arrested in mitosis, were also analysed.

First, HT1080 cells were synchronized and the cell cycle analysis showed that HT1080 cells progressed through one whole cell cycle within 12 h after release from thymidine block (Fig. 3.2 A). Cells already entered S phase 2 h after the release, reached M phase after 7 h, and progressed into G1 at 9 h after release. This is in agreement with the Western blot analysis shown in Fig. 3.2 B, in which a signal for pH3 was detected around 7 h, confirming that cells enter mitosis. For the quantitative analyses of BRCA2 levels during cell cycle, BRCA2 levels detected by Western blotting were normalized against the loading control α-tubulin (Fig. 3.2 C). The

quantitative analysis showed that BRCA2 levels change during the cell cycle. At the G1/S phase transition (1 h) BRCA2 levels decreased two-fold and remained at this level until the end of S phase (6 h). In G2 (6 – 7 h) BRCA2 levels increased, peaked in mitosis (8 h) and decreased again as cells progressed through G1 (9 - 12 h) towards the next cell cycle.

To test whether other cell lines display similar patterns of BRCA2 protein levels during the cell cycle, HeLa cells were synchronized using double thymidine block and analysed as mentioned above (Fig. 3.2 D – F). The cell cycle analysis showed a longer doubling time for HeLa cells compared with HT1080 cells (Fig. 3.2 D). This is in agreement with a previous report estimating a doubling time for HeLa cells around 20 h (Boisvert et al., 2012). After release from the thymidine block HeLa cells progressed into G2/M phase around 8 – 10 h, began to exit mitosis at 14 h and entered G1 phase at 16 h. A change in BRCA2 levels during the cell cycle was also observed in HeLa cells. The quantitative analysis of the BRCA2 level revealed that BRCA2 levels decreased approximately two-fold at the G1/S phase transition (2 h), remained stable until after 6 h when cells are in late S phase or begin to enter G2 phase, gradually increased and peaked in mitosis (12 -14 h), then decreased in G1 phase and remained low throughout G1 (16 – 22 h) (Fig. 3.2 F).

In both HT1080 and HeLa cells, a similar pattern for BRCA2 protein levels during the cell cycle was observed (Fig. 3.2 C and 3.2 F). It has been reported that BRCA2 mRNA levels are low in G0 and G1 phases, increase at G1/S phase transition and remain high during S phase (Vaughn et al., 1996b; Wang et al., 1997). These reports differ from our analyses of BRCA2 protein levels during the cell cycle. BRCA2 is a key player of HR but at the same time it is proposed that high levels of BRCA2 block HR mediated repair (Magwood et al., 2012). These results suggest an

additional regulatory level of HR through the regulation of BRCA2 protein levels, which will be discussed in chapter 3.3.

I and others in lab observe a decrease in BRCA2 levels after nocodazole treatment, which arrests cells in mitosis. Also here, in both cell lines, cells treated with nocodazole showed a decrease in BRCA2 protein in comparison to the non-treated or synchronized cells. Previous observations showed, that treatment with nocodazole induces DNA damage (Dalton et al., 2007; Wong and Stearns, 2005). Therefore, together with the data obtained in Figure S2 the decrease in BRCA2 protein levels here could be a result of DNA damage-induced degradation of BRCA2.

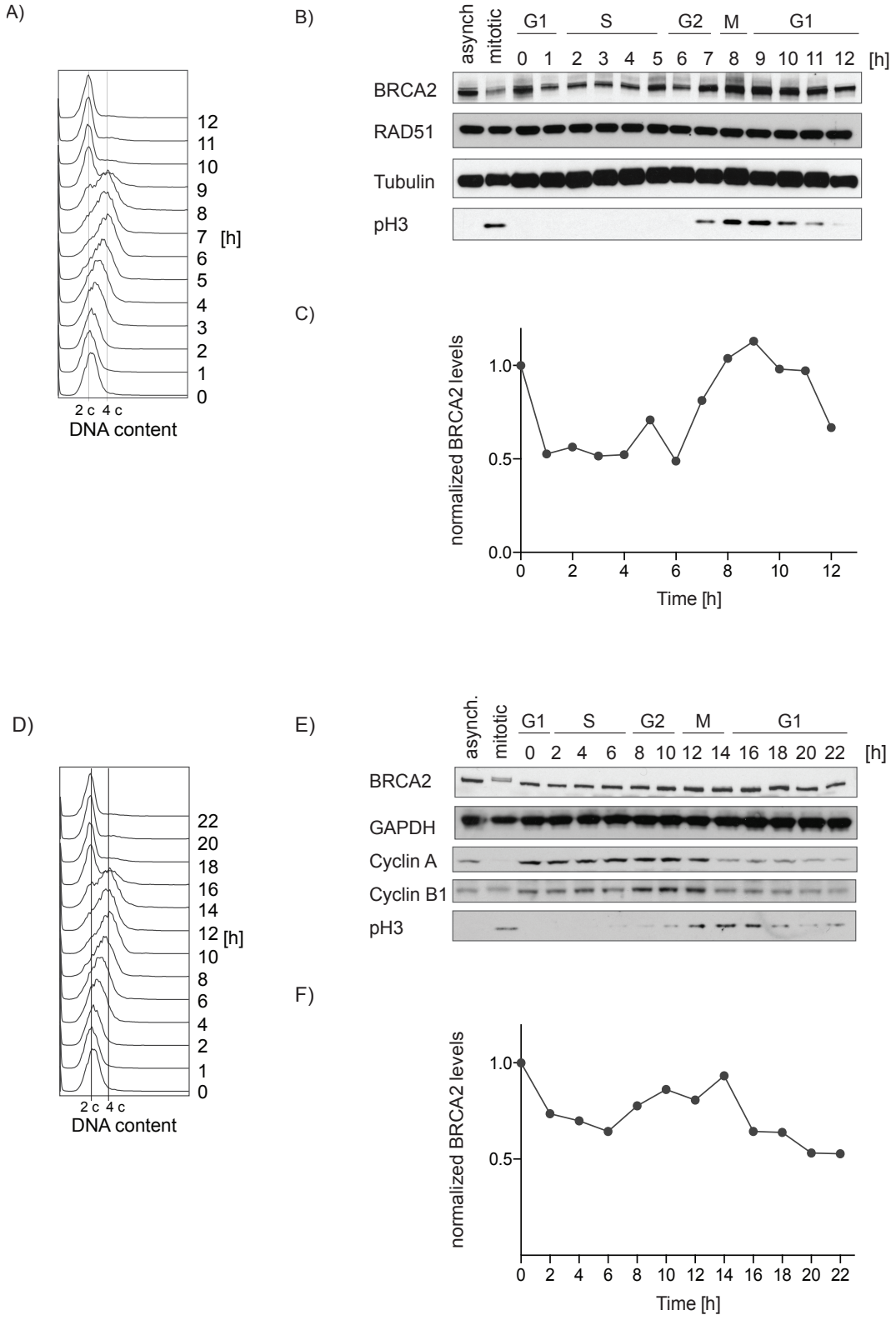

Figure: 3.2 BRCA2 protein levels change during cell cycle progression

(see next page for description)

Figure 3.2: BRCA2 protein levels change during cell cycle progression
A, B, C) HT1080 cells were synchronized using double thymidine block. Samples were taken every hour to analyse protein levels and DNA content was analysed using FACS (A), Western blot (B) and quantitative analyses of Western blots (C) were performed. D, E, F) HeLa cells were synchronized using double thymidine block methodology and samples were analysed as described in (A). FACS cell cycle analysis (D), Western blot (E) and quantitative analyses of E (F) were carried out as above. asynch. = asynchronous cells, mitotic = mitotic cells after treatment with nocodazole (2 µM, ON), pH3 (phosphorylated Histone H3).

3.3 Determination of BRCA2 half-life

As mentioned above, several reports observed that BRCA2 mRNA levels are low in G0 and G1 phases, are high at G1/S phase transition and remain high during S phase (Vaughn et al., 1996b; Wang et al., 1997). This is in contrast to the results obtained from the cell cycle analysis of BRCA2 protein levels, performed in section 3.2, which showed that BRCA2 levels decreased nearly two-fold at G1/S transition, remained stable until late S/G2 phase, increased in mitosis, and decreased and remained low in the following G1 phase. One major regulatory mechanism of protein expression in cells is the control of protein synthesis, which is reflected by mRNA level. The discrepancies between mRNA and protein levels presented here suggest the existence of an additional active mechanism that controls BRCA2 protein stability. To investigate this, the half-life of BRCA2 was tested at the protein level.

To this end, HT1080 and HEK293T cells were treated with cycloheximide (CHX), a bacterial toxin that inhibits protein synthesis by blocking translational elongation. Following addition of CHX, samples were taken at the indicated time points and BRCA2 protein levels were assessed by Western blotting (Fig. 3.3 A and C). This quantitative analyses (Fig. 3.3 B and D) revealed that BRCA2 protein levels decreased when *de novo* protein synthesis was inhibited by CHX. From this study, the BRCA2 protein half-life is estimated to be about 6 h in both HT1080 and HEK293T cell lines. To investigate whether BRCA2 is degraded by a proteasome-dependent mechanism, HT1080 cells were also treated with the proteasome inhibitor MG132 together with CHX, and BRCA2 protein levels were assessed as above (Fig. 3.3 E, F). As above, using CHX alone, a BRCA2 half-life of 6 h was estimated. Simultaneous treatment with MG132 stabilized BRCA2, with a mild decrease of BRCA2 levels after 6 h and a three-fold prolonged BRCA2 half-life of about 18 h.

These results suggest a proteasome-dependent regulatory mechanism for controlling BRCA2. Recent studies have shed some light on the proteasome-dependent turnover rate of proteins, with some variation reported between them. Yen et al. estimated the average 50% turnover rate for over 8000 GFP-tagged proteins to be between 30 min to 2 h (Yen et al., 2008). Eden et al. discovered protein half-lives ranging from 45 min to 22.5 h in H1299 human non-small lung cancer cell lines. Using YFP-tagged proteins in a bleach-chase assay they determined that the half-life of most proteins is between 5 to 10 h (Eden et al., 2011). In agreement with this, Boisvert et al. detected an average half-life of proteins about ~ 20 h, whereas 60% of proteins in HeLa cells showed a half-life of about 5 h (Boisvert et al., 2012). Therefore, the estimated half-life of BRCA2 of about 6 h can be ranked in the middle range of protein turnover rate.

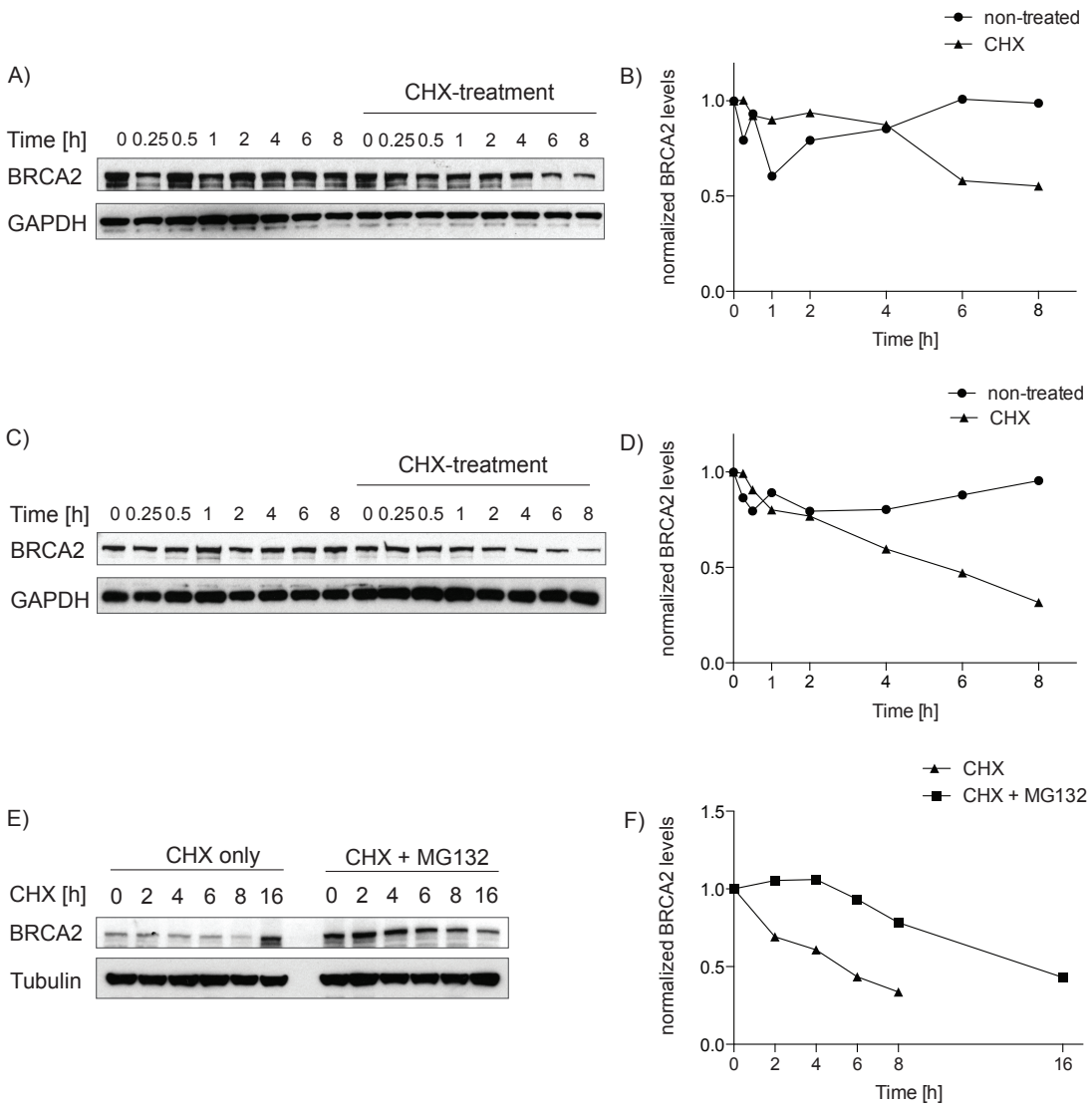

Figure 3.3: Analysis of BRCA2 half-life

See next page for description

Figure 3.3: Analysis of BRCA2 half-life

HT1080 and HEK293T cells were treated with 10 μM CHX. At the indicated incubation times (15 min, 30 min, 1 h, 2 h, 4 h, 6 h and 8 h) cells were harvested and Western blot analyses performed. For determination of BRCA2 half-life, quantitative analyses were performed in which detected BRCA2 was normalized against the loading control GAPDH. Graphs display the non-treated samples (circles) and CHX treated samples (triangles) plotted against time. A) Western blot analysis of BRCA2 extracted from HT1080 cells non-treated and treated with CHX. B) Quantitative analysis of A. C) Western blot analysis of proteins extracted from HEK293T cells. D) Quantitative analysis of C. E) HT1080 cells were treated with 10 μM CHX and 10 μM MG132 simultaneously for 2 h, 4 h, 6 h, 8 h and 18 h. At the indicated times cells were harvested and BRCA2 half-life analyses were performed as above. F) Quantitative analysis of E. Graphs display CHX treated samples (triangles) and simultaneous CHX with MG132 treated samples (squares).

3.4 Summary and Discussion

The analyses of BRCA2 protein levels showed that BRCA2 levels changed during the cell cycle (Fig. 3.2). Surprisingly, BRCA2 levels decreased two-fold at the end of G1 phase, just before entering S phase, the cell cycle stage when cells are able to carry out homologous recombination. The BRCA2 level remained at this lower level throughout S phase, then during G2 phase BRCA2 levels began to increase and peaked in mitosis. This pattern, found for BRCA2 levels during the cell cycle presented here differs from previous reports of BRCA2 mRNA levels during the cell cycle as mentioned above. However, the prediction of protein expression from mRNA abundance is inefficient and the correlation can be as little as 40% (de Sousa Abreu et al., 2009; Gygi et al., 1999; Maier et al., 2009; Vogel and Marcotte, 2012). Therefore, mRNA levels were not investigated here. Furthermore, the abrupt two-fold decrease in BRCA2 levels at the G1/S transition indicates that regulation at the mRNA level is unlikely; rather, it suggests an alternative mechanism of controlled protein degradation, e.g. by the ubiquitin-proteasome system.

To investigate the possibility of an alternative mechanism responsible for BRCA2 stability, such as ubiquitin-dependent proteasomal degradation, the stability of BRCA2 protein by analysis of BRCA2 half-life was investigated (Fig. 3.3). The analysis revealed a BRCA2 protein half-life of 6 h, which was increased by addition of the proteasome inhibitor MG132. *In vivo* analyses of protein half-life revealed half-lives in a range from 45 min to 22.5 h, with increased occurrence of protein half-lives between 5 – 10 h (Boisvert et al., 2012; Eden et al., 2011). This was also estimated for BRCA2 with a half-life of 6 h. The two to three-fold increase in BRCA2 half-life in the presence of MG132, indicates a role for the ubiquitin-proteasome system in BRCA2 regulation.

4 BRCA2 is ubiquitylated and SCF^{FBXW7} is a candidate E3 ubiquitin ligase for BRCA2

4.1 Preface

Recent studies have shown that BRCA2 interacts with components of the proteasome such as DSS1, RPN3 and RPN7 (Gudmundsdottir et al., 2007) and that BRCA2 is ubiquitylated *in vivo* and can interact with the de-ubiquitylating enzyme USP11 *in vivo* (Schoenfeld et al., 2004). Furthermore, it has been suggested that BRCA2 is ubiquitylated by the SCF^{Skp2} complex and targeted for ubiquitin-dependent proteasomal degradation, though the direct ubiquitylation of BRCA2 by SCF^{Skp2} complex has not been demonstrated (Arbini et al., 2011; Moro, 2006). Consistently, previous results obtained in section 3.3 also suggest a role for the ubiquitin-proteasome system in BRCA2 regulation. In this chapter, to analyse ubiquitylation of BRCA2 by a specific E3 ligase several approaches were employed. First, ubiquitylation of BRCA2 was tested using different methods, second, BRCA2 protein stability after siRNA-mediated knockdown of E3 ligase complexes was investigated, and third, ubiquitylation of BRCA2 by a candidate E3 ligase complex was tested.

4.2 Detection of ubiquitylated BRCA2

To address the notion that BRCA2 is ubiquitylated, I first attempted to detect the ubiquitylation of BRCA2 *in vivo*. To this end, HT1080 (Fig. 4.2 A) and HEK293T (Fig. S1) cells were treated with 10 µM of the proteasome inhibitor MG132 and

collected for analysis at the indicated times. After immonuprecipitation (IP) of BRCA2 the samples were subjected to Western blot analysis. Blotting against ubiquitin revealed for both cell lines, bands at the expected molecular weight of BRCA2, indicating ubiquitylated species of BRCA2, which peaked at 4 h of MG132 treatment. For this reason, in subsequent analyses where MG132 was used, samples were collected 4 h after addition of the drug.

To overcome the fact that polyubiquitylated proteins are not stable in cells, Hjerpe et al. developed a tool consisting of tandem ubiquitin binding entities (TUBEs), that stabilizes ubiquitylated proteins and allows detection and isolation of polyubiquitylated proteins using three different tags, namely GST, 6xHis and SV5-tag (Hjerpe et al., 2009). In this analysis GST-TUBE 2 (Lifesensors) was used, which will be called GST-TUBE in the following. GST-TUBE binds to lysine 6 (K6), lysine 11 (K11), lysine 48 (K48) and lysine 63 (K63) tetra-ubiquitin chains, and therefore protects proteins from degradation by the proteasome or lysosome or from de-ubiquitylation by de-ubiquitylating enzymes (DUBs). By performing pull-down experiments with the corresponding tag, polyubiquitylated proteins can be detected in subsequent Western blot analysis (see schematic figure in Fig. 4.2 B). HT1080 cells were treated with 10 µM proteasome inhibitor MG132 for 4 h. Extraction was carried out in the presence of GST-TUBE and GST-pull-down with subsequent Western blot analysis was performed (Fig. 4.2 C). Probing against BRCA2 showed that in MG132-treated cells BRCA2 was pulled down with GST-TUBE. Longer exposure revealed a faint band for BRCA2 in the non-treated sample, which was 20-fold less prominent than in the MG132-treated sample. As mentioned above, GST-TUBE recognizes ubiquitin chains linked via K6, K11, K48, and K63. K11, K48 and in a few cases also K63-linked polyubiquitin chains were found to target proteins for proteasomal degradation (Chau et al., 1989; Jin et al., 2008; Matsumoto et al., 2010; Saeki et al.,

2009; Thrower et al., 2000; Williamson et al., 2011). K48 and K63 have also been found to target proteins for lysosomal degradation (Zhang et al., 2013). However, the main function of K63 is thought to lie in its scaffolding role, e.g. in DNA damage, whereas the function of K6-linked polyubiquitin chains still unclear (Spence et al., 1995; VanDemark et al., 2001). However, increased co-pull-down of BRCA2 with GST-TUBE in the presence of MG132 indicates that BRCA2 is targeted for proteasomal degradation. The experiments described above were performed under non-denaturing conditions due to the presence of the GST-tag. A caveat of this procedure is that it cannot discriminate between a direct immunoprecipitation of BRCA2 with GST-TUBE and an indirect immunoprecipitated via one of BRCA2 binding partners. To eliminate this possibility, ubiquitin fused to a His-tag (6xHistidine tag) was used in subsequent experiments to allow pull-downs of ubiquitylated proteins under denaturing conditions. This method allowed the detection of directly ubiquitylated of BRCA2, as shown in section 4.6.

BRCA2 is a huge protein of 384 kDa, and hence it is difficult to detect posttranslational modifications by analysis of differences in the electrophoretic mobility shift of this protein. Nonetheless, attempts were made to overcome this problem by preparing a 7% SDS-polyacrylamide gel and separating proteins by SDS-PAGE overnight. GST-TUBE pull-down of ubiquitylated proteins was performed as described above, but lower amounts of GST-TUBE were used. In the Western blot analysis a slight shift of BRCA2 to a higher molecular weight was observed in the MG132 treated sample (Fig. 4.2 D), which further supports the notion that BRCA2 is ubiquitylated.

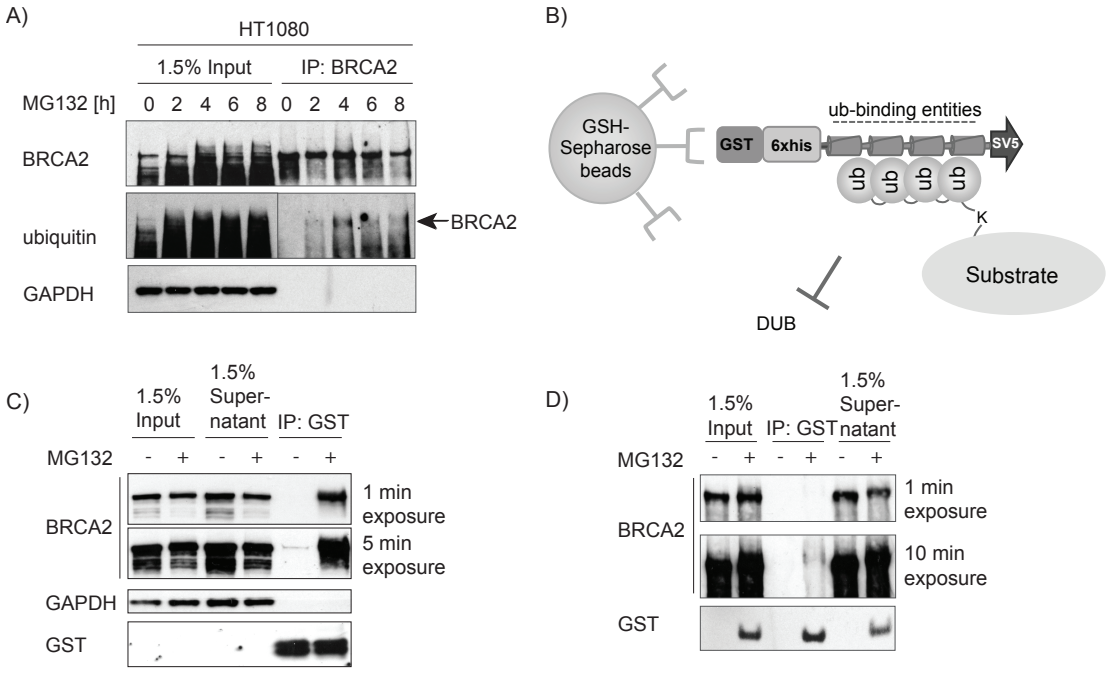

Figure 4.2: Detection of ubiquitylated BRCA2

A) HT1080 cells were incubated with 10 µM MG132. Whole cell extracts were prepared after 2, 4, 6 or 8 h treatment and subjected to immunoprecipitation (IP) with BRCA2 antibody. To detect ubiquitylated BRCA2, membranes were probed with ubiquitin antibody. B) Schematic figure of GST-TUBE 2 adapted from Lifesensors (Hjerpe et al., 2009). GST-TUBE contains 4 ubiquitin binding entities that are based on the ubiquitin associated (UBA1) domain from RAD23A. These UBA1 domains are attached to a GST, His- and SV5-tag, that can be used to purify ubiquitylated proteins. GST-TUBE recognizes K63 and K48-linked tetra-ubiquitin chains and protects proteins from degradation by the proteasome or lysosome and from de-ubiquitylation by de-ubiquitylating enzymes (DUB). C) Western blot analysis of HT1080 cells, mock treated (DMSO) or incubated with MG132, were lysed in the presence of GST-TUBE. GST-TUBE-ubiquitylated protein complexes were pulled-down using Glutathione Sepharose beads. D) As described in C, except for samples were separated by 7 % SDS-PAGE ON. Supernatant refers to the supernatant after GST-pull-down of GST-TUBE-ubiquitylated protein complexes.

4.3 BRCA2 ubiquitylation changes during cell cycle progression

The results in section 4.2 provide some evidences of BRCA2 ubiquitylation. In section 3.3 the cell cycle analysis showed that BRCA2 protein levels change during cell cycle (Fig. 3.3). Therefore, I questioned whether the ubiquitylation pattern of BRCA2 also changes during cell cycle. For this reason, proteins from synchronized cells were extracted at the indicated time points in the presence of GST-TUBE 2, and a GST-pull-down followed by Western blot analysis performed (Fig 4.3 A). In parallel, FACS cell cycle analysis was performed to monitor cell cycle progression and to confirm the corresponding cell cycle stages of the samples taken for the GST-TUBE pull-down (Fig.4.3 B). This analysis revealed that BRCA2 ubiquitylation indeed varied during the cell cycle. In agreement with previous observations (Fig. 4.2), in asynchronous MG132-treated cells BRCA2 showed strong interaction with GST-TUBE (Fig. 4.3 A). At 0 h and 4 h after release from a double thymidine block, less prominent BRCA2 bands were detected in GST-TUBE pull-down samples. By the 8 h time point, a clear five-fold increase in the BRCA2 signal was detected. According to the cell cycle progression data, by the 8 h time point cells began to exit mitosis and progressed into G1 phase (Fig. 4.3 B). This suggests that BRCA2 ubiquitylation begins in G1 phase.

The analysis of BRCA2 levels during cell cycle showed high BRCA2 levels in mitosis and a two-fold decrease of BRCA2 levels at the G1/S transition. Therefore, the increase in ubiquitylated BRCA2 could be due to higher amounts of BRCA2. However, this is unlikely, as the fold increase in BRCA2 ubiquitylation (five-fold) is higher than the increase in BRCA2 protein levels at 8 h after release (two-fold). To further assess the ubiquitylation pattern of BRCA2 during the cell cycle samples could be taken in shorter time intervals to obtain a more detailed picture of BRCA2

ubiquitylation. To perform further analysis of BRCA2 ubiquitylation, the generation of self-made GST-TUBE was attempted. However, though the generation of self-made GST-TUBE was successful, the efficiency of the self-made GST-TUBE was low and could not be used for this analysis (data not shown).

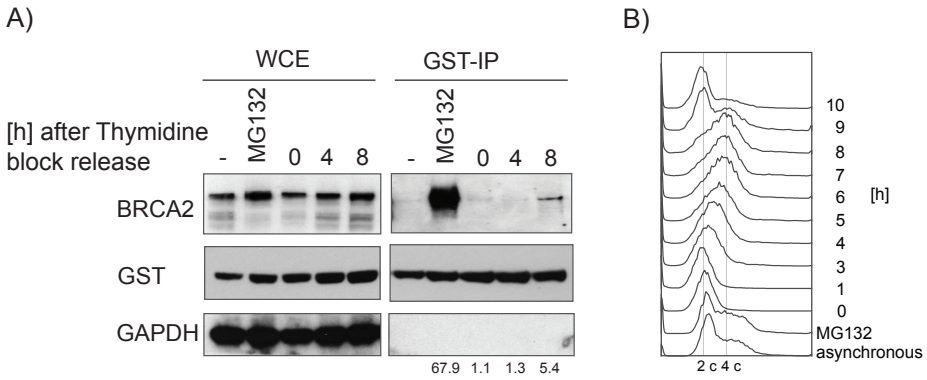

Figure 4.3: BRCA2 ubiquitylation changes during cell cycle
HT1080 cells were synchronized by double thymidine block and at 0, 4 and 8 h after release, cells were lysed in the presence of GST-TUBE and GST-pull-down was performed. As controls, asynchronous cells and cells treated with 10 µM MG132 for 4 h were used. A) Western blot analysis. Using ImageJ the intensities of the BRCA2 bands were determined. B) Cell cycle analysis by FACS of synchronized HT1080 cells.

4.4 Identification of candidate E3 ubiquitin ligases

As mentioned in Chapter 1.4.2, the amount of possible E3 ligases for one substrate is enormous as the human genome encodes more than 600 RING finger E3 ligases and around 30 HECT E3 ligases (Li et al., 2008). Given our interest in the cell cycle-dependent regulation of BRCA2 protein stability, I focused on two well characterized RING finger E3 ubiquitin ligases: the Skp1-Cullin1-F-box protein

complex (SCF) and the Anaphase Promoting Complex/Cyclosome (APC/C), which have been shown to be implicated in the regulation of cell cycle progression (Nakayama and Nakayama, 2006). Both E3 ligases are in complex with various exchangeable receptor proteins that mediate substrate specificity. The SCF and APC/C complexes are active at different stages of the cell cycle: the SCF complex is active from late G1 to early M phase, and the APC/C complex from early M phase to late G1 (see Fig. 1.4.4 and 4.4.1).

To identify E3 ligases involved in the cell cycle-dependent ubiquitylation of BRCA2, siRNA-mediated knockdown analyses were performed. In order to investigate whether down-regulation of SCF or APC/C subunits leads to stabilization of the BRCA2 protein, Dharmacon SMARTpool siRNAs were used to down-regulate Cullin1 (CUL1) the scaffolding subunit, and the SKP2, FBXW7, FBXO6, FBXO40 receptor proteins of the SCF complex, as well as for the receptor proteins of the APC/C (CDC20 and CDH1). These receptor proteins were chosen, because they all were reported to display activity at distinct stages of the cell cycle, with exception of FBXO40 (Fig.4.4.1).

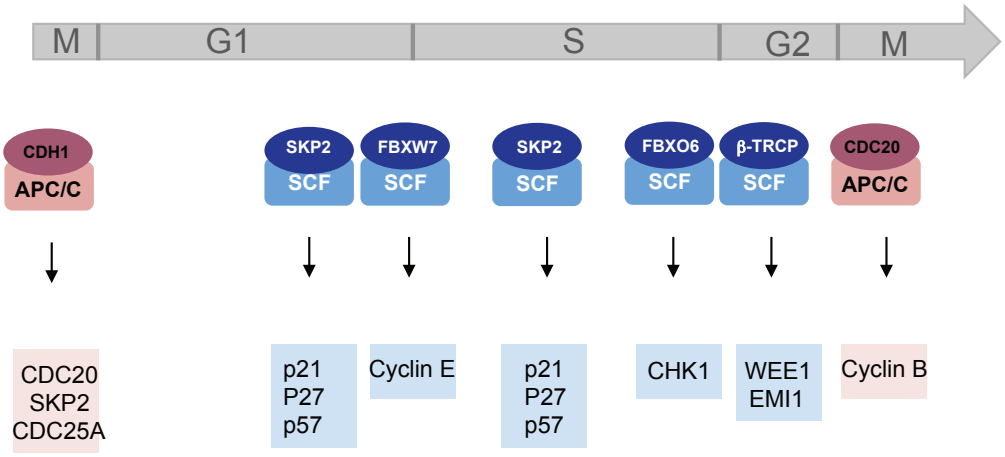

Figure 4.4.1: Schematic figure of activities of receptor proteins used
Letters on grey arrow represent the cell cycle phases. Pink-rosé coloured complexes show APC/C in complex with the receptor proteins CDH1 or CDC20, in dark and light blue the SCF complex in complex with the receptor proteins SKP2, FBXW7, FBXO6, β-TRCP is shown. Squares in pink represent substrates of the APC/C, squares in light blue represent substrates of SCF in complex with its receptor proteins.

First, single siRNA-mediated knockdowns of the listed proteins were performed and quantitatively analysed (Fig. 4.4.2 A, B). HT1080 cells were transfected with each individual siRNA for 24 h. As a control, expression of BRCA2, PALB2 and RAD51 was down regulated for 24 h. Using Western blot analysis and densitometric quantitation, the amount of BRCA2 and GAPDH were determined in each knockdown (Fig. 4.4.2 A). The quantitative analysis of the single knockdowns (Fig. 4.4.2 B) showed no significant changes in BRCA2 protein levels when HT1080 cells were treated with the siRNAs listed above. As overexpression of BRCA2 appears to be toxic to cells (Takata et al., 2002), BRCA2 levels may be efficiently regulated, which might have masked the change of protein stability in the siRNA knockdown analysis.

To circumvent this possibility, *de novo* protein synthesis of BRCA2 was blocked by simultaneous siRNA-mediated knockdown of BRCA2. Thus, combined

knockdowns of BRCA2 together with APC/C or SCF subunits were performed (Fig. 4.4.2 C, D), in which the change in residual protein amounts would allow to assess protein stability more directly.

Combined knockdowns in HT1080 cells with two siRNAs were performed using the same protocol as single knockdowns but twice the amount of total siRNA was used (final concentration of 200 nM siRNA). As control, a Universal negative control (Cntrl) (Sigma) was used in combination with BRCA2 siRNA. The quantitative data presented in Fig. 4.4.2 D represent the average of four independent experiments where BRCA2 was down-regulated in combination with subunits of the SCF and APC/C E3 ligases (Fig. 4.4.2 A). Reproducibly, a significant increase of the BRCA2 protein level in samples treated with siRNAs targeting CUL1, CDC20, CDH1 or FBXW7, was observed compared to the BRCA2 protein level present in combined knockdown of BRCA2 and Universal negative control. In combined knockdown with CUL1 a 2.4 fold increase of BRCA2 protein level with a p-value of 0.018 was obtained; with FBXW7 a nearly 3 fold increase with a p-value of 0.002; with CDC20 a 2 fold change with a p-value of 0.022; and with CDH1 a 2.3 fold increase and a p-value of 0.019. In combined knockdowns with SKP2, FBXO6 or FBXO40 no significant changes in BRCA2 level were detected. Nonetheless, a significant increase of BRCA2 protein levels was observed after down-regulation of the APC/C receptor proteins CDC20 and CDH1. However, APC/C is known to be in complex with CDC20 or CDH1 with which it is involved in the regulation of mitotic exit (García-Higuera et al., 2008). Since the cell cycle analysis revealed that BRCA2 levels change during the cell cycle, in particular that BRCA2 levels are increased in mitosis (Fig. 3.2), the possibility that the increase in BRCA2 levels as a result of cell cycle arrest in mitosis could not be excluded. Therefore, because the SCF in complex with FBXW7 is active from G1 (Koepp et al., 2001; Strohmaier et al., 2001), and BRCA2

levels start to decrease from G1, I focused on FBXW7 as a potential candidate E3 ligase for BRCA2.

To verify that the FBXW7 down-regulation performed did not impair cell cycle progression or display off-target effects on BRCA2, FBXW7 was down-regulated using the Dharmacon SMARTpool siRNA mix, which was used in the knockdowns shown in Figure 4.4.2 C, the four individual siRNAs that comprise the FBXW7 SMARTpool as well as a mixture of these four siRNAs. Combined knockdowns were performed as mentioned above. As individual siRNA knockdowns of FBXW7 did not have an effect on BRCA2 levels, an off-target effect of these siRNAs on BRCA2 is highly unlikely (Fig. 4.4.2 E). Additionally, the cell cycle analyses of FBXW7 knockdowns together with the Universal negative control (Cntrl) or BRCA2 (Fig. 4.4.2 F) showed similar cell cycle patterns, indicating that the increase in BRCA2 levels after FBXW7 knockdown is independent of a secondary cell cycle effect. In conclusion, these results suggest a potential role for the SCF complex (CUL1, FBXW7) in regulation of BRCA2 stability.

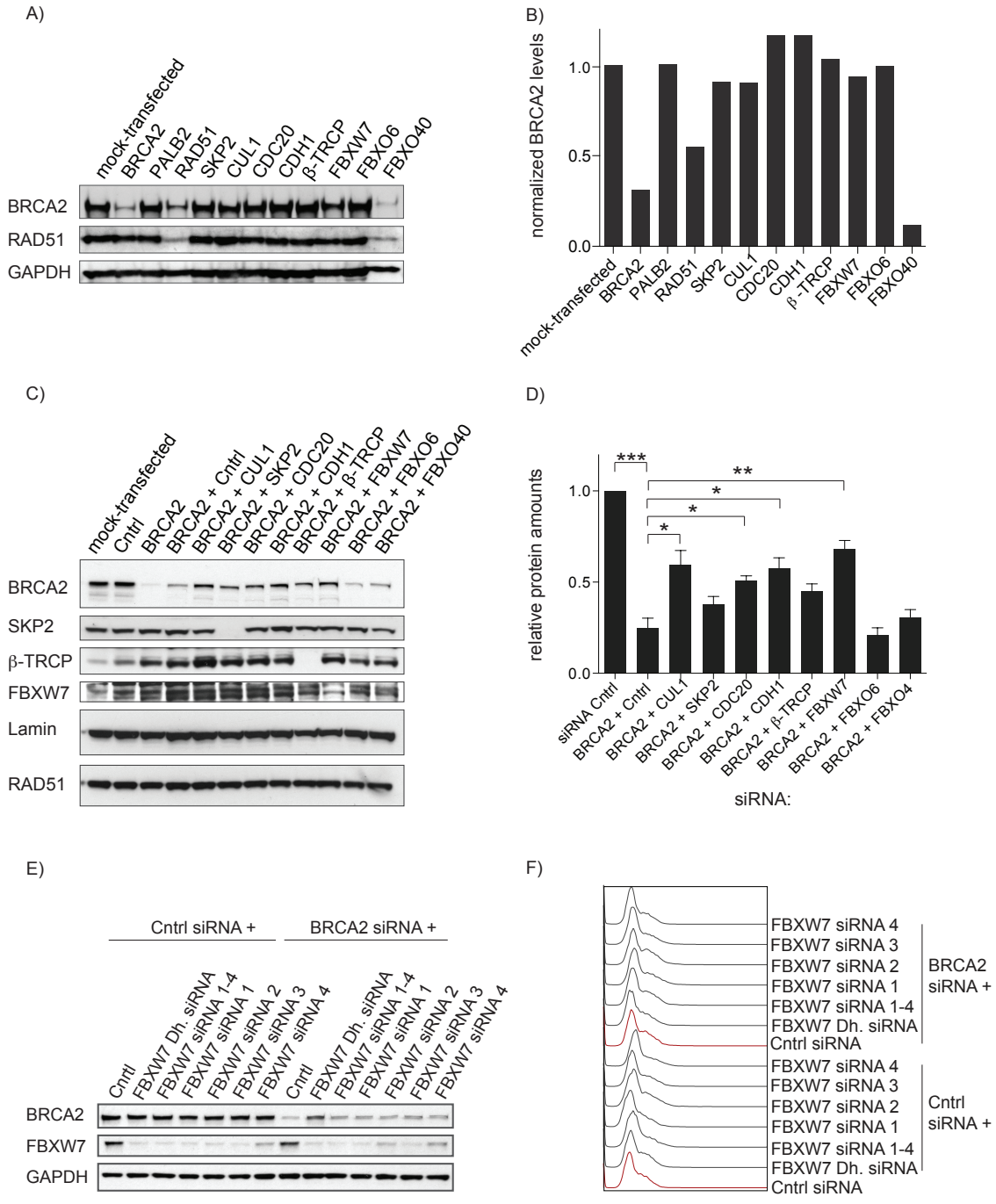

Figure 4.4.2: siRNA-mediated knockdowns of subunits of the E3 ligases SCF or APC/C

See next page for description

Figure 4.4.2: siRNA-mediated knockdowns of subunits of the E3 ligases SCF or APC/C

A) HT1080 cells were treated with a final concentration of 20 nM (BRCA2, RAD51) or 100 nM siRNA (PALB2, SKP2, CUL1, CDC20, CDH1, β-TRCP, FBXW7, FBXO6, FBXO40) for 24 h and Western blot analysis was performed. B) Quantitative analysis of siRNA knockdowns in A. Analysis was performed relative to the mock treated sample and normalized BRCA2 protein levels of BRCA2 are depicted. C) Western blot analysis of combined siRNA-mediated knockdowns. Subunits of the SCF or APC/C were down-regulated together with BRCA2. Down-regulation was performed as above, but in addition cells were also treated with siRNA for BRCA2, thus twice as much siRNA was used. D) Quantitative analysis of C. Depicted are the average means of four independent experiments, error bars represent the standard error of the mean, p-values were calculated using a paired two-tailed t-test. Asterisks indicate the t-test p-values: * < 0.05, ** < 0.01, *** < 0.001. Cntrl = Universal negative control (Sigma). E) Western blot analysis of siRNA-mediated knockdown of FBXW7 using the Dharmacon SMARTpool siRNA mix (FBXW7 Dh. siRNA), used in the previous experiments, the four individual siRNAs (FBXW7 siRNA 1, 2, 3, 4) that the SMARTpool siRNA mix is composed of and a mixture of the four individual siRNAs (FBXW7 siRNA 1-4). F) Cell cycle analysis after FBXW7 down-regulation using siRNAs in described in E using FACS.

4.5 BRCA2 ubiquitylation after siRNA-mediated down regulation of CUL1, FBXW7 and CDH1

The observation in section 4.4 that BRCA2 stability increased after siRNA-mediated down-regulation of the APC/C receptor proteins CDC20 and CDH1, and of the SCF scaffold protein CUL1 and receptor protein FBXW7 suggested a role for these complexes in BRCA2 ubiquitylation. To verify the effect of these E3 ligase complexes on BRCA2 protein stability, the ubiquitylation state of BRCA2 was assessed after depletion of these proteins.

In a preliminary experiment, HT1080 cells were subjected to siRNA-mediated knockdown of CUL1, FBXW7 and CDH1. As positive and negative controls, cells were treated with control siRNA and with or without MG132, respectively. After 24 h incubation, cells were harvested and following extraction in the presence of GST-TUBE to isolate ubiquitylated proteins GST-pull-downs were performed (Fig. 4.5). In this case, knockdown of the candidate E3 ligase should lead to a decrease in ubiquitylated BRCA2. The levels of BRCA2 in the input samples (no numbers) appear to be different between the different samples. This difference is due to a transfer problem such as a bubble, as the ponceau red staining did show no stain in that area. As shown before, in MG132-treated cells, ubiquitylated species of BRCA2 were pulled-down with GST-TUBE (lane 2). In addition, in comparison to the MG132-treated cells, lower amounts of ubiquitylated BRCA2 were also detected in cells treated with CDH1 siRNA (lane 5), suggesting that CDH1 is not responsible for BRCA2 ubiquitylation. No ubiquitylated BRCA2 species were detected in cells where CUL1 (lane 3) or FBXW7 (lane 4) were down-regulated, which supports the results observed above, that SCF^{FBXW7} is involved BRCA2 ubiquitylation. Probing against CUL1 (lane 8) and FBXW7 (lane 9) showed that the knockdowns were efficient.

In comparison to previous experiments with GST-TUBE (Fig. 4.2 C, D and Fig. 4.3 A), lower amounts of ubiquitylated BRCA2 were detected. A reason for this could be that lower amounts of GST-TUBE were used (25 µg/ml instead of the 100 µg/ml).

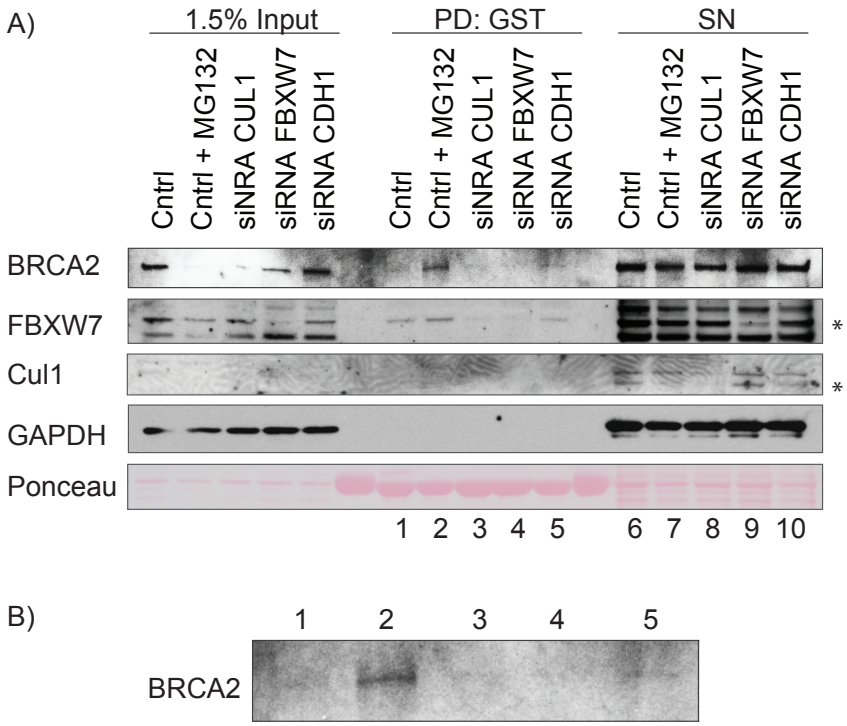

Figure 4.5: Ubiquitylation state of BRCA2 after down-regulation of CUL1, FBXW7 and CDH1 with siRNA

For CUL1, FBXW7 or CDH1 down-regulation, HT1080 cells were treated with siRNA for 24 h. As positive and negative controls, control siRNA treated cells were respectively treated with MG132 for 4 h or mock-treated with DMSO. Cells were lysed in the presence GST-TUBE 2 and GST-pull-down was performed. SN indicates supernatant, * represents specific bands. B) Magnification of the blot probed with BRCA2 antibody in panel A after GST-PD (Pull-down).

4.6 BRCA2 ubiquitylation by SCF^{FBXW7}

To address whether BRCA2 is directly ubiquitylated by SCF^{FBXW7} and to rule out the possibility that BRCA2 indirectly interacts with GST-TUBE (4.2), an *in vivo* ubiquitylation assay under denaturing conditions was performed.

To this end, a mammalian expression plasmid for 6xHistidine-tagged ubiquitin (His-ub) was generated and expressed in HEK293 Flp-In T-REx cells conditionally overexpressing the FLAG-EGFP tag (FE) or FE-BRCA2, and His-Talon affinity purifications were performed (Fig. 4.6).

Probing against FBXW7 revealed significant overexpression of FBXW7^{WT} in cells (lane 3 and 6). In cells treated with MG132 a faint band for BRCA2 was observed (lane 11). Increased amounts of BRCA2 were detected when FBXW7^{WT} was overexpressed in cells (lane 12). These results indicate that FBXW7 can target BRCA2 for ubiquitylation.

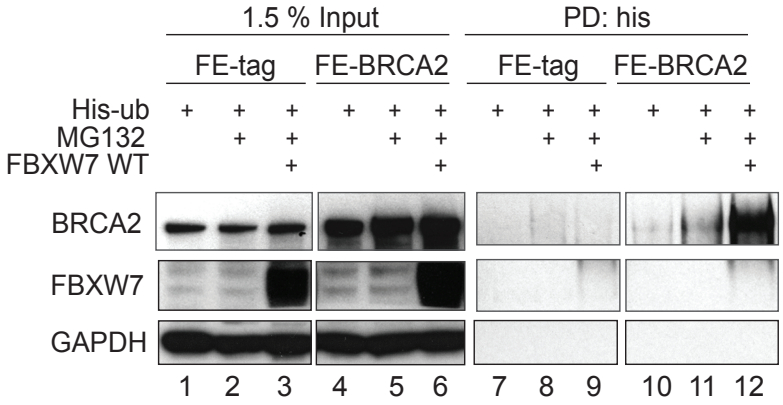

Figure 4.6: Overexpression of FBXW7 leads to increased ubiquitylation of BRCA2
Western blot analysis of his-pull down (PD) of HEK293T cells overexpressing either FLAG-EGFP tag (FE) or FLAG-EGFP-tagged BRCA2 (FEB) which were transfected with 6xHistindine-tagged ubiquitin (His-ub) and with or without FBXW7 wild type. Additionally cells were treated with 10 µM MG132 where indicated.

4.7 Summary and Discussion

The results obtained in section 3.3 suggested a role for the ubiquitin-proteasome system in BRCA2 regulation therefore, the ubiquitylation of BRCA2 was investigated. Two methods were applied to detect BRCA2 ubiquitylation. First, in the presence of the proteasome inhibitor, ubiquitylated BRCA2 was detected after a BRCA2-IP was performed (Fig. 4.2 A, S1). Second, BRCA2 co-pulled-down with GST-TUBE, in the presence of MG132, and third, a mobility shift of BRCA2 to higher molecular weight was observed in SDS-PAGE (Fig. 4.2 C, D). After longer exposure of the BRCA2 blot, a faint band for BRCA2 was also detected in the non-treated sample, which was 20-fold less prominent than in the MG132 treated sample. This shows that ubiquitylated BRCA2 species accumulate in the presence of MG132 indicating a role for the ubiquitin-proteasome system in the regulation of BRCA2 stability. Also, BRCA2 ubiquitylation during the cell cycle was investigated. Interestingly, in the pull-down of GST-TUBE the amount of BRCA2 that co-precipitated changed during the cell cycle. Low levels of BRCA2 were detected at 0 h and 4 h after release from the double thymidine block. After 8 h a clear increase in BRCA2 was detected (Fig. 4.3). According to the cell cycle analysis performed at 8 h, cells began to enter G1 phase at this point. To obtain a more detailed insight into the ubiquitylation pattern of BRCA2 during the cell cycle, this analysis could be performed taking samples in shorter time intervals from synchronized cells. This would also allow to verify if the increase seen in BRCA2 ubiquitylation after 8 h is in accordance with or independent of BRCA2 protein level detected during the cell cycle.

Furthermore, in subsequent analysis, ubiquitylation of BRCA2 could be investigated by mass-spectrometric analysis of BRCA2 purified from MG132-treated

cells. Indeed, mass-spectrometry analysis of FE-BRCA2 purified from HEK293 cells allowed the detection of ubiquitin in the gel slice corresponding to the molecular weight of BRCA2 (J.Y. Bleuyard and F. Esashi, unpublished).

Next, the identification of candidate E3 ligases responsible for BRCA2 ubiquitylation was attempted. To this end, siRNA-mediated knockdowns were performed, in which subunits or receptor proteins, which mediate substrate specificity for the E3 ligases, of SCF or APC/C were down-regulated. First, single knockdowns were tested, in which Cullin1 (CUL1) the scaffolding subunit, and the SKP2, FBXW7, FBXO6, FBXO40 receptor proteins of the SCF complex as well as the receptor proteins of the APC/C CDC20 and CDH1 were down-regulated individually (Fig. 4.4.2 A, B). The single knockdowns did not reveal significant changes in BRCA2 levels. As mentioned previously, high levels of BRCA2 were reported to suppress HR and BRCA2 levels decreased two-fold just before S phase where cells can employ HR repair, suggesting that high levels of BRCA2 are disadvantageous for cells. This is in agreement with observations that overexpression of BRCA2 is toxic to cells (Takata et al., 2002). Therefore, the tight regulation of BRCA2 levels might be necessary for the orderly function of BRCA2. As no significant changes after knockdown of single receptor proteins of SCF and APC/C, even for SKP2 which has been reported as a candidate F-box protein for BRCA2 degradation were observed (Arbini et al., 2011; Moro et al., 2006), it is possible to speculate that alternative E3 ligases are employed to maintain functional levels of BRCA2.

Therefore, another possibility to assess changes in protein stability is to carry out simultaneous inhibition of *de novo* protein synthesis together with siRNA-mediated knockdown of candidate E3 ligases. As CHX affects the cellular protein synthesis and secondary impacts that could affect the protein stability cannot be excluded (e.g. changes in posttranslational modifications), BRCA2 *de novo* synthesis

was inhibited directly by siRNA-mediated knockdown. For this reason, combined siRNA-mediated knockdowns were performed, in which both, the aforementioned E3 ligase subunits of the SCF complex and APC/C and BRCA2 were down-regulated together (Fig. 4.4.2 C, D). A significant increase in BRCA2 levels relative to the BRCA2 knockdown was observed when BRCA2 *de novo* synthesis was inhibited together with siRNA-mediated knockdown of CUL1, the scaffolding protein of the SCF complex, or FBXW7, a receptor protein of the SCF complex. Also, a significant increase was detected when the APC/C receptor proteins CDC20 or CDH1 were down-regulated together with BRCA2, though the highest increase in BRCA2 protein levels was observed after knockdown of CUL1 or FBXW7, which was 2.4 fold or nearly 3 fold, respectively.

APC/C^{CDC20} is active from metaphase-anaphase transition to late mitosis and APC/C^{CDH1} is activated in late mitosis and remains active until late G1 phase (Castro et al., 2005; Zheng et al., 2002b). The SCF in complex with its receptor proteins is active from late G1 phase to early M phase. In complex with FBXW7, SCF is thought to be active from late G1 phase, where it has been found to target Cyclin E, to trigger S phase (Koepp et al., 2001; Strohmaier et al., 2001). However, in regard to the cell cycle analysis of BRCA2 levels performed, this indicates that BRCA2 levels decrease when APC/C^{CDH1} or SCF^{FBXW7} are active. Because APC/C is known to regulate mitotic exit (García-Higuera et al., 2008), I focused on SCF^{FBXW7} as a potential candidate E3 ligase, as the increased amounts of BRCA2 after down-regulation of CDH1 could be due to the secondary effect of a cell cycle arrest in mitosis, where highest BRCA2 levels were detected (Fig. 3.2 B, C). This should be further verified by cell cycle analysis of cells down-regulated for CDH1.

To further investigate the effect of these identified proteins on BRCA2 stability, in a preliminary experiment, ubiquitylation of BRCA2 was assessed using

GST-TUBE in cells down-regulated for CUL1, FBXW7 and CDH1 (Fig. 4.5). Knockdown of the potential E3 ligase would lead to a decrease in ubiquitylated BRCA2 species. In cells down-regulated for CDH1 a faint band for BRCA2 was observed. In comparison, no BRCA2 was detected in CUL1 or FBXW7 down-regulated cells. Though the detection of BRCA2 was faint, due to low amounts of GST-TUBE used, this supports the notion that SCF^{FBXW7} might target BRCA2 for ubiquitylation. To further validate the results obtained here, this experiment could be repeated with increased amounts of GST-TUBE. Another possibility would be to express tagged ubiquitin in cells down regulated for CUL1, FBXW7 or CDH1 and to perform a pull-down experiment of tagged ubiquitin species under denaturing conditions to test whether ubiquitylation changes in CUL1 or FBXW7 down-regulated cells. Furthermore, the APC/C has been reported to generate K11-linked polyubiquitin chains whereas the SCF^{FBXW7} complex has been reported to generate K48-linked polyubiquitin chains. Though other E3 ligases might also be involved in the ubiquitylation of BRCA2 as well, detection of different linkage-types of polyubiquitin chains by linkage specific ubiquitin antibodies could provide additional information and allow to distinguish which of these two E3 ligases ubiquitylates BRCA2 (Jin et al., 2008; Matsumoto et al., 2010; Petroski and Deshaies, 2005b).

Since a pro-longed half-life of BRCA2 after simultaneous CHX and MG132 treatment was observed (Fig. 3.3), another intriguing experiment would be to assess BRCA2 half-life in cells down-regulated for CUL1, FBXW7, CDC20 or CDH1. This may allow to assess the effect of these subunits on BRCA2 stabilization in more detail.

Additionally, to verify the indications that SCF^{FBXW7} can target BRCA2 for ubiquitin-dependent proteasomal degradation, an *in vivo* ubiquitylation assay was performed. Therefore, 6xHis-ubiquitin and $FBXW7^{WT}$ were expressed in HEK293

cells overexpressing FE or FE-BRCA2 and His-ubiquitin was affinity purified. After the His-Talon purification a faint band for BRCA2 was detected in MG132 treated cells, indicating that using this methodology, ubiquitylated BRAC2 can be observed. Furthermore, this indicates the direct ubiquitylation of BRCA2. A five-fold increase in the intensity of the BRCA2 band was observed when FBXW7 was overexpressed in cells in comparison to cells treated with MG132 alone. As overexpression of receptor proteins can lead to non-physiological ubiquitylation of proteins or false positive results, this observation needs to be confirmed by performing the same approach in cells, which are down regulated for FBXW7. Furthermore, as mentioned above the half-life of BRCA2 could be analysed using the CHX-based approach in cells down-regulated for CUL1, FBXW7 or CDH1 to assess the effect of these proteins on BRCA2 stability.

Taken together, the results obtained in this chapter indicate that BRCA2 is targeted for ubiquitin-dependent proteasomal degradation and that the SCF in complex with FBXW7 can target BRCA2 for ubiquitylation.

5 Interaction of BRCA2 with SCF^{FBXW7}

5.1 Preface

The SCF can complex with a variety of F-box proteins, which mediate the substrate specificity of the SCF complex as well as determine its activity during the cell cycle (chapter 1.5.3). It has been shown that F-box proteins recognize their target proteins via a phospho-degron motif, a specific motif that contains a phosphorylated amino acid (Hao et al., 2007; Jin et al., 2005; Sundqvist et al., 2005; Welcker and Clurman, 2007; Welcker et al., 2004b; Yada et al., 2004). Many studies have focused on FBXW7 as it has been shown to act as a tumour suppressor by targeting oncoproteins for degradation. Known substrates include c-myc, cyclin E, c-Jun, Notch1 and Notch4 (Justice and Jan, 2002; Koepp et al., 2001; Nateri et al., 2004; Oberg et al., 2001; Strohmaier et al., 2001; Welcker et al., 2004a; Wu et al., 2001; Yada et al., 2004). The interaction of FBXW7 with its substrates is well studied. FBXW7 recognizes phosphorylated substrates via a phospho-degron motif which consists of hydrophobic residues and usually two critical phosphorylation sites at the 0 and +4 residue or a negatively charged residue at +4 site (Fig. 5.5 A) (Hao et al., 2007; Orlicky et al., 2003; Skowyra et al., 1997; Welcker et al., 2003; Ye et al., 2004). In the following chapter the interaction of SCF^{FBXW7} and BRCA2 was investigated.

5.2 BRCA2 and Cullin1 interact *in vivo*

The results in Chapter 4 indicate that BRCA2 can be targeted for ubiquitylation by SCF^{FBXW7}. Next, I addressed the question: do SCF^{FBXW7} and BRCA2 interact? The SCF complex belongs to the Cullin-RING family of E3 ligases and contains Cullin 1 as a scaffold protein. Therefore, the interaction of BRCA2 with the SCF complex was assessed *in vivo* using FLAG-tagged dominant negative (DN) Cullin 1 variant (Fig. 5.2 A). Wild type (WT) Cullins interact with the RING-finger protein RBX1 to form the core E3 ubiquitin ligase, which binds and activates the ubiquitin-conjugating enzyme E2 to transfer the ubiquitin onto the substrate (Skowyra et al., 1997; Zheng et al., 2002b). In DN Cullin variants, the Cullins are C-terminally truncated (Jin et al., 2005). They can still form an E3 ligase complex, which can also still interact with the substrate. However, due to the truncations, the Cullins can no longer interact with RBX1, thus interaction with the E2 enzyme is inhibited and the transfer of ubiquitin to the target protein is blocked. Expression of these FLAG-tagged DN Cullin variants in cells allows identification of binding partners and targets of the different Cullins by performing FLAG-immunoprecipitation.

To investigate the interaction of BRCA2 with the SCF complex *in vivo*, FLAG-tagged DN Cullin variants (see Fig. 5.2 and S3) were expressed in HEK293T cells and anti-FLAG immunoprecipitation was performed. As negative controls empty pcDNA3.1, FLAG-tagged CHK2 and FLAG-tagged DN Cullin 4b were expressed. FBXW7, a receptor protein of the SCF complex, co-immunoprecipitated with DN Cullin 1 demonstrating the efficiency of the FLAG-immunoprecipitation, which was confirmed in immunoprecipitations of all DN CUL variants (Fig. S3). Immunoprecipitations of the negative controls showed faint background bands for

BRCA2, however a distinct band was observed in immunoprecipitation with DN Cullin 1 (Fig. 5.2 B).

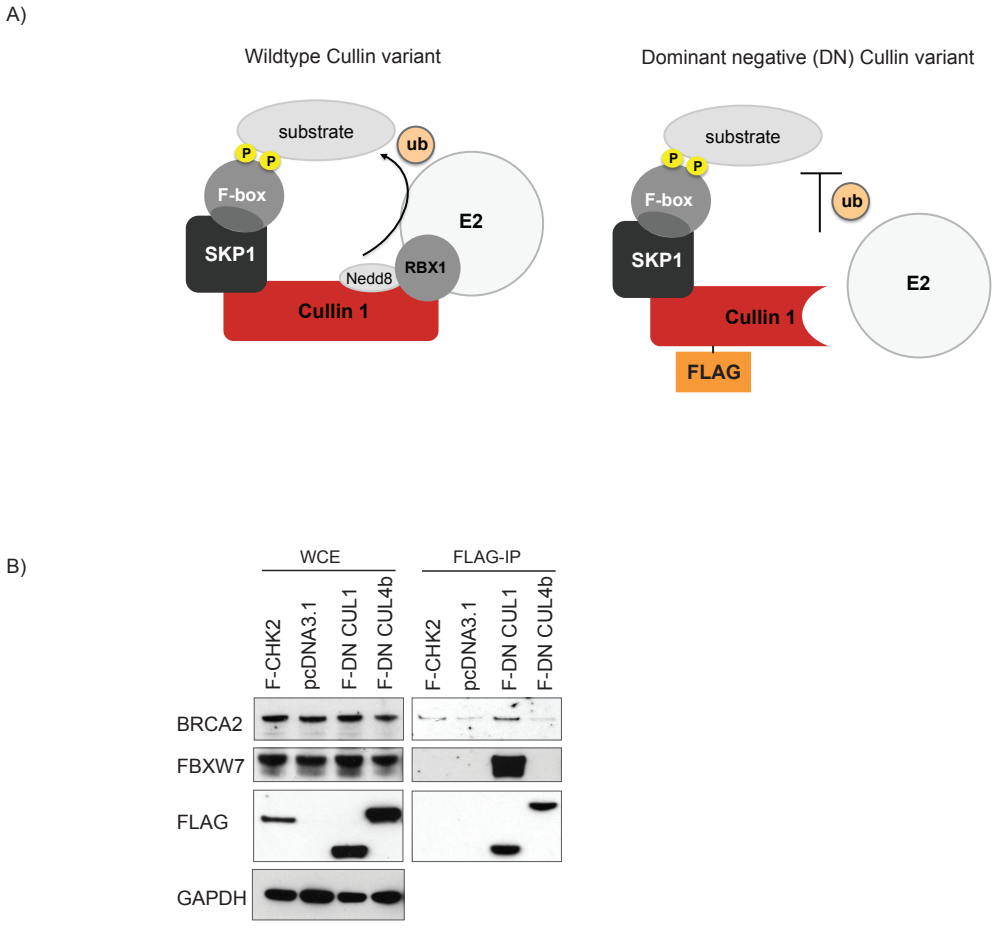

Figure 5.2: BRCA2 and Cullin 1 interact *in vivo*

A) Schematic figure of the mechanism of wild type (WT) Cullin variants and dominant negative (DN) Cullin (CUL) variants. See text for description. B) FLAG-immunoprecipitation of DN Cullin variants. FLAG tagged DN CUL1 and DN CUL4b - (F-DN) as well as empty vector (pcDNA3.1) and FLAG-tagged CHK2 as negative controls were expressed in HEK293T cells and FLAG-immunoprecipitation (IP) was performed.

5.3 BRCA2 and FBXW7 interact *in vivo*

Previously it was demonstrated that the SCF receptor protein FBXW7 is involved in the regulation of BRCA2 (chapter 4.4) and that FBXW7 can target BRCA2 for ubiquitylation (chapter 4.6). In chapter 5.2 the co-immunoprecipitation of BRCA2 with the DN Cullin1 variant was observed. As Cullin1 cannot directly bind to BRCA2 but via a receptor protein, the interaction of FBXW7 with BRCA2 was tested *in vivo*.

Therefore, FBXW7 and BRCA2 antibodies were cross-linked to Affi-Prep Protein A support (BioRad) and FBXW7- and BRCA2-immunoprecipitations were performed from HEK293T (Fig. 5.3 A) and HT1080 cells (Fig. 5.3 B). As controls, immunoprecipitations with beads cross-linked to mouse IgG were used. FBXW7 co-immunoprecipitated with BRCA2 but no band for BRCA2 was observed in the FBXW7-immunoprecipitation (Fig. 5.3 A). In HT1080 cells BRCA2 co-immunoprecipitated with FBXW7, and to a lesser extend FBXW7 with BRCA2 (Fig. 5.3 B). The efficiency of the immunoprecipitations in HEK293T and HT1080 were different, which might be a result of the difference in endogenous protein levels. However, the immunoprecipitations indicate that BRCA2 and FBXW7 do interact *in vivo*, which was further confirmed below (chapter 5.6).

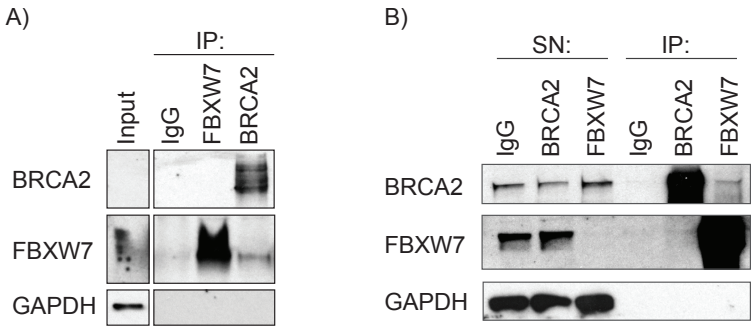

Figure 5.3: BRCA2 and FBXW7 interact *in vivo*
Immunoprecipitation of endogenous BRCA2 and FBXW7 in HEK293T (A) and HT1080 (B) cells. BRCA2 or FBXW7 antibodies were cross-linked to Affi-Prep Protein A support (BioRad) and immunoprecipitations performed. Interaction with endogenous FBXW7 or BRCA2 was detected by Western blot analysis of immunoprecipitation with anti-BRCA2 or FBXW7, respectively. SN = Supernatant.

5.4 Mapping the FBXW7 interaction site on BRCA2

To further characterize the interaction between BRCA2 and FBXW7, the interaction site of FBXW7 on BRCA2 was investigated. To this end, GFP-tagged BRCA2 fragments (B2-1 to B2-9), that encompass the whole length of BRCA2, were generated (Fig. 5.4 D). These GFP-BRCA2 fragments were expressed in HEK293T cells and GFP-pull-down using GFP-Nanotrap (Chromotek) and FBXW7-immunoprecipitation were performed (Fig. 5.4 B and C). As a negative control, HEK293T cells were transfected with empty vector (pDEST53).

Probing against GFP revealed that the expression of GFP-BRCA2 fragments (Fig. 5.4 A) and the efficiency of the GFP-pull-down (Fig. 5.4 B) were similar for all fragments. Also endogenous levels of RAD51 as well as FBXW7 were comparable (Fig. 5.4 A). Previous reports have shown that monomeric RAD51 interacts with

BRCA2 fragments B2-3 and B2-4 (Chen et al., 1998b; Esashi et al., 2005; Thorslund et al., 2007). In agreement with these reports RAD51 was detected when GFP-fusions of fragment B2-3 and B2-4 were immunoprecipitated, demonstrating the efficiency and specificity of the GFP-Pull-down (Fig. 5.4 B). FBXW7 was observed to co-pull-down with one BRCA2 fragment, the B2-2. When FBXW7-immunoprecipitation was performed three BRCA2 fragments B2-2, B2-6, and B2-9 co-immunoprecipitated with FBXW7 (Fig. 5.4 C). The B2-2 fragment was found to interact with FBXW7 in both reciprocal pull-downs, demonstrating that this interaction was most robust. For this reason I decided to further analyse the interaction of BRCA2 with FBXW7 by focusing on the region which is covered by the B2-2 as the potential area of FBXW7 interaction.

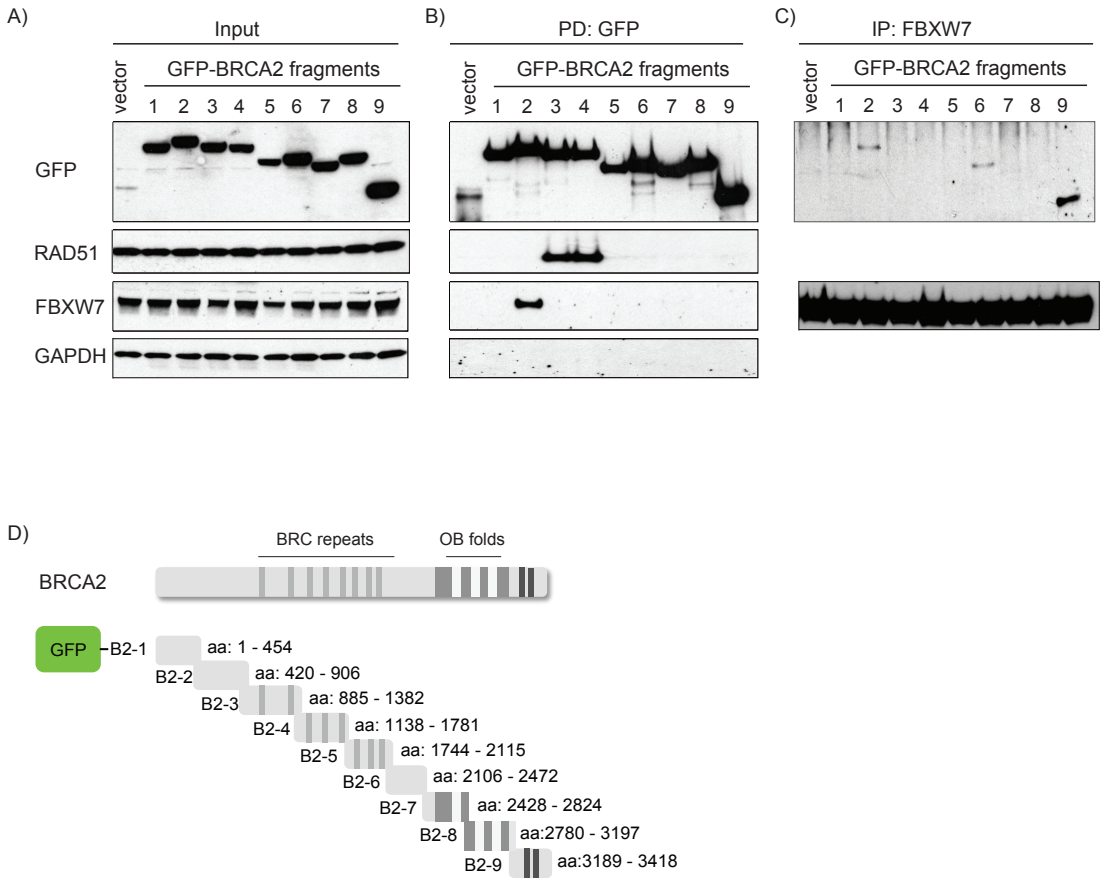

Figure 5.4: Mapping the interaction site on BRCA2 that FBXW7 interacts with GFP-tagged BRCA2 fragments (B2) 1-9 were expressed in HEK293T cells and immunoprecipitations were performed. A) 1.5% input. B) GFP-Pull-down. C) FBXW7-immunoprecipitation. D) Schematic diagram of full-length BRCA2 and GFP-tagged B2 fragments 1 – 9 aa = amino acids. Vector = pEYFP-C1

5.5 Analysis of the BRCA2 fragment B2-2 interaction with FBXW7

As mentioned above, extensive studies have been carried out to understand the recognition and interaction of FBXW7 with its substrates (chapter 1.7). FBXW7 recognizes phosphorylated substrates (Skowyra et al., 1997) via a phospho-degron motif which consists of hydrophobic residues and usually two critical phosphorylation

sites at the 0 and +4 residue or a negatively charged residue at +4 site (Fig. 5.5 A) (Hao et al., 2007; Orlicky et al., 2003; Welcker et al., 2003; Ye et al., 2004). Furthermore, it is known that FBW7-mediated degradation of substrates is triggered by glycogen synthase kinase 3 (GSK3) in most known FBXW7 substrates (Welcker and Clurman, 2008). However, for the FBXW7 substrate Cyclin E it has been shown that the phospho-degron is phosphorylated by both CDK2 and GSK3 (Welcker et al., 2003). GSK3 kinase is thought to require a priming phosphorylation event, which increases the specificity of GSK3 phosphorylation and substrate recognition (Cole et al., 2004; Haar et al., 2001).

The B2-2 fragment covers amino acids 420 to 906 of the BRCA2 protein. The B2-2 fragment contains two sites with hydrophobic residues and a TP site, which could be potential FBXW7 recognition sites. It is noteworthy, that another FBXW7 substrate, cyclin E, also contains two phospho-degron motifs (Fig 5.5 B) (Hao et al., 2007; Strohmaier et al., 2001; Ye et al., 2004). The alignment of B2-2 also shows that the threonine in the second degron motif T772 is highly conserved (Fig. 5.5 C). Since B2-2 and FBXW7 co-immunoprecipitated in the reciprocal pull-downs (Fig. 5.4) and B2-2 contains two potential FBXW7 phospho-degron motifs, the notion that B2-2 is the region where FBXW7 interacts with was supported. Therefore, I focused on B2-2 to investigate the interaction with FBXW7 further.

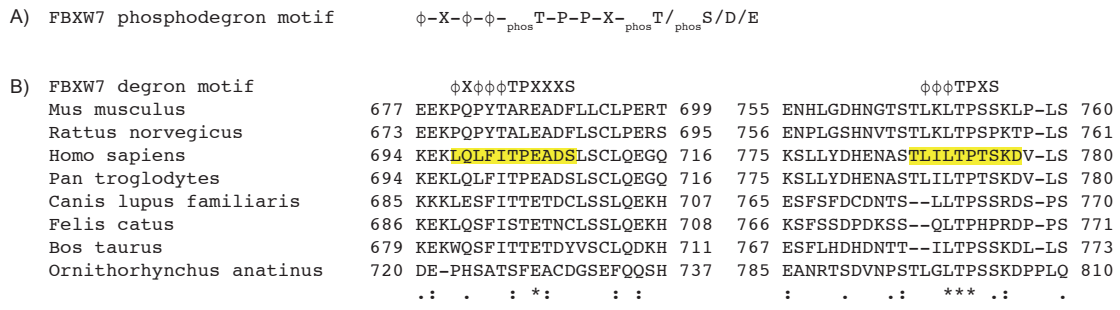

Figure 5.5: FBXW7 phospho-degron motif in B2-2

A) FBXW7 phospho-degron motif sequence. X denotes any amino acid, Φ hydrophobic amino acids, T threonine, S serine and P proline. B) Alignment of sections of the amino acid sequence of B2-2 that contain similar sequences to the FBXW7 phosphodegron motif. Similar sequences are highlighted yellow. Asterics "*" indicate identical residues, ":" conserved substitutions, "." semiconserved substitutions (See ClustalW).

5.5.1 Analysis of phosphorylation-dependent interaction of FBXW7 with B2-2 fragment *in vivo*

To first assess the phosphorylation-dependence of FBXW7 binding to BRCA2, GFP-tagged B2-2 fragment was pulled-down as above and the proteins on beads were treated with λ-phosphatase in the presence or absence of protein phosphatase inhibitors and the preservation of FBXW7-BRCA2 interaction was analysed (Fig. 5.5.1 A). Treatment of GFP-B2-2 pull-downs with λ-phosphatase or phosphatase inhibitors had no effect on the interaction of FBXW7 with B2-2. Similar amounts of FBXW7 were detected in all samples. This could indicate that the interaction of FBXW7 with B2-2 is phosphorylation independent or that binding of FBXW7 to B2-2 masks the phosphorylated residue. Masking the phosphorylated residue could block the phosphatase from accessing the residue, thus the

phosphorylation would not be removed. Therefore, the phosphorylation-dependency of FBXW7 binding to BRCA2 would not be visible.

To exclude the possibility, that the critical phosphorylated residue is masked, and to test whether GSK3 is the kinase responsible for the phosphorylation of BRCA2 B2-2 region, the effect of GSK3 inhibition on FBXW7 binding to B2-2 was analysed. Repeatedly, inhibition of GSK3, CDK or CDK1 and -2 did not affect FBXW7 interaction with B2-2 (Fig. S2). This further suggests that FBXW7 interaction with BRCA2 fragment B2-2 is phosphorylation independent.

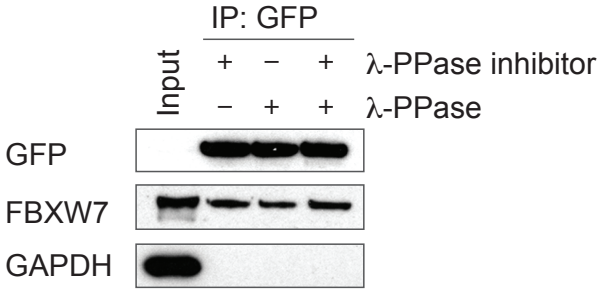

Figure 5.5.1: Analysis of phosphorylation dependent interaction of FBXW7 with B2-2 fragment *in vivo*

λ-phosphatase treatment of B2-2 fragment following GFP-immunoprecipitation. GFP-B2-2 was expressed in HEK293T cells and GFP-immunoprecipitation was performed. After non-treatment or treatment with λ-phosphatase or λ-phosphatase with phosphatase inhibitors FBXW7 co-immunoprecipitation with B2-2 was tested

5.5.2 Analysis of phosphorylation dependent interaction of FBXW7 with B2-2 fragment *in vitro*

Because no change in FBXW7 binding to B2-2 fragment was observed after λ-phosphatase treatment or in cells treated with kinase inhibitors (Fig. 5.5.1 and S4), the interaction of FBXW7 with B2-2 was tested *in vitro*. To this end, recombinant GST-tagged BRCA2 B2-2 fragment and recombinant his-tagged FBXW7 were generated and purified. Before assessing the phosphorylation-dependent interaction between B2-2 and FBXW7, GST-B2-2 was phosphorylated by the potential kinases.

The phosphorylation of B2-2 by different kinases was examined using CDK2/Cyclin A (generous gift from Jane Endicott), GSK3 kinase (Milipore), or a mixture of kinases from HeLa whole cell extract. To this end, purified GST-B2-2 was incubated with the corresponding kinase in the presence of 1 µCi γ^{32}P. If a protein was phosphorylated, the substrate should be labelled with γ^{32}P, thus be visible by autoradiography. As controls, RAD51, Histone H1, which is a known substrate of GSK3 kinase and CDK2 (Contreras et al., 2003; Happel et al., 2009), and B2-9, which is phosphorylated by CDK2 (Esashi et al., 2005), were tested.

Histone H1, B2-9 and B2-2 were efficiently phosphorylated by recombinant CDK2/CyclinA (Fig. 5.5.2 A) and RAD51 was weakly phosphorylated by CDK2/CyclinA. GSK3 phosphorylation analyses of the same proteins, showed that GSK3 efficiently phosphorylated Histone H1, as reported previously (Happel et al., 2009). Interestingly, RAD51 was also weakly phosphorylated, indicating that RAD51 might be a possible substrate for GSK3, which was previously unidentified. However, no GSK3 phosphorylation of B2-2 was detected (Fig. 5.5.2 B).

To test the possibility that other kinases may be involved in B2-2 phosphorylation, HeLa whole cell extract, which contains a cocktail of all kinases,

was used for the phosphorylation assay. Furthermore, because GSK3 needs prior priming phosphorylation of the substrate (Fiol et al., 1987; Welcker et al., 2003) using HeLa extract for phosphorylation might also contain the priming kinase as well as GSK3. Because the activity of the HeLa extract was not known, Histone H1 and B2-2 fragment were phosphorylated with 1 or 2 µl of HeLa whole cell lysate. Histone H1 as well as B2-2 were phosphorylated by the whole cell lysate, though Histone H1 was already highly phosphorylated by 1 µl of whole cell lysate (Fig. 5.5.2.C).

Although phosphorylation of B2-2 was detected after incubation with the HeLa whole cell lysate, the specificity of the phosphorylation could not be confirmed. For this reason, pre-phosphorylation by CDK2/CyclinA with subsequent phosphorylation by GSK-3 was intended to be tested next, but this sequential kinase reaction was not pursued further due to the results detailed in section 5.5.3.

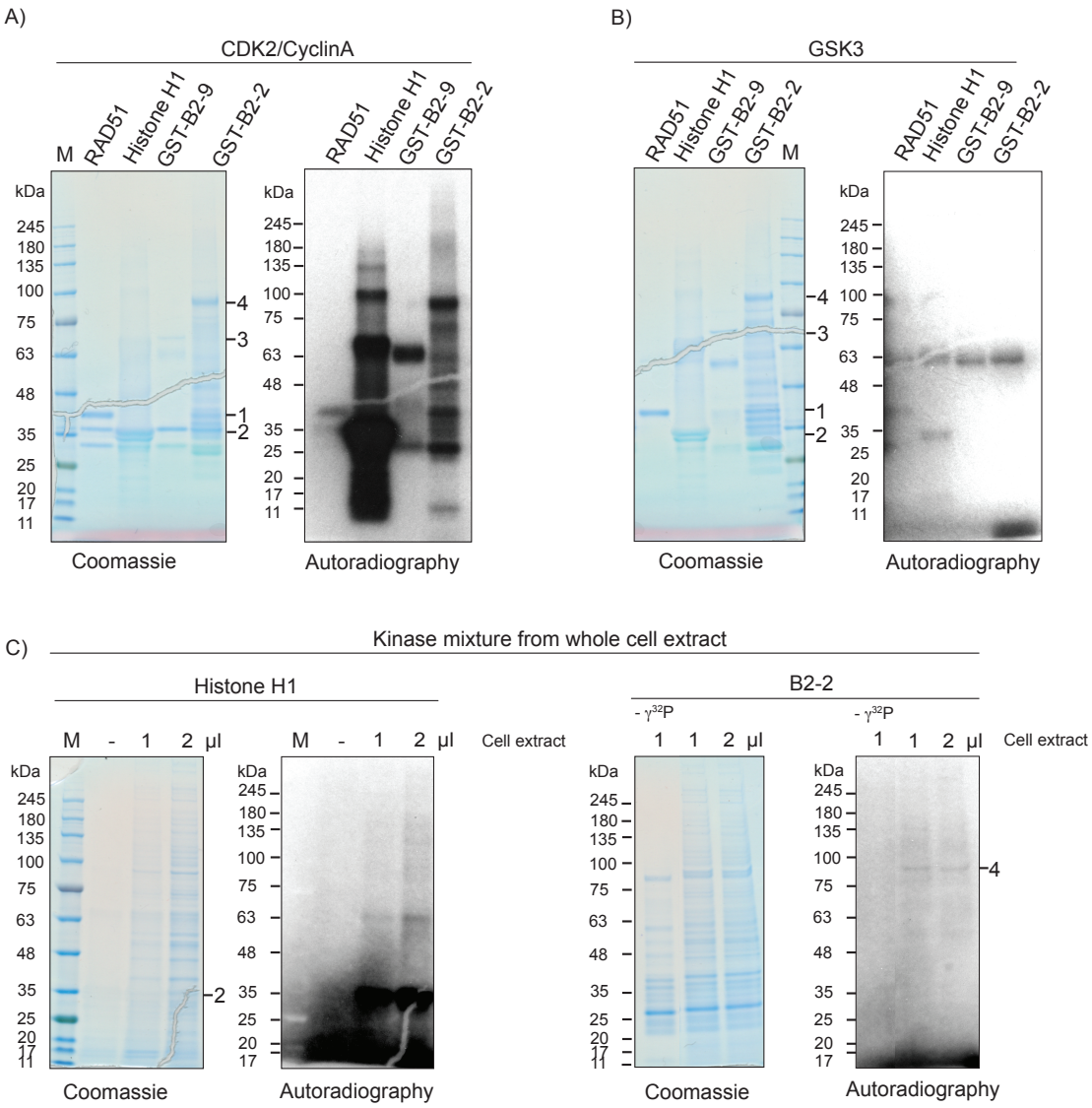

Figure 5.5.2: Analysis of phosphorylation of B2-2 fragment *in vitro*

A) Recombinant Histone H1, B2-9 and B2-2 and RAD51 were phosphorylated with recombinant CDK2/CyclinA in the presence of 1 µCi γ^{32}P ATP and analysed in SDS-PAGE (left) and autoradiography (right). B) Purified Histone H1, B2-9 and B2-2 and RAD51 were phosphorylated by GSK3 in the presence of 1 µCi and analysed in SDS-PAGE (left) and autoradiography (right). C) Histone H1 and B2-2 were incubated with 1 or 2 µl of whole cell lysate. As negative control only γ^{32}P ATP (in Histone H1 test, left) or only 1 µl of whole cell lysate without γ^{32}P ATP was loaded (in B2-2 test, right). Analyses were performed by SDS-PAGE (left) and autoradiography (right). Numbers indicate the proteins: 1 = RAD51, 2 = HistoneH1, 3 = GST-B2-9, 4 = GST-B2-2.

5.5.3 Interaction analysis of FBXW7 with B2-2 mutants

Another approach to assess the possibility of a phosphorylation-dependent interaction of FBXW7 with B2-2 was to generate mutants of B2-2 in which potential phosphorylatable residues are substituted with alanine, thus preventing phosphorylation.

To this end, GFP-B2-2 mutants T703A, T772A, T703A + T772A, S767A + T768A + 772A, T772A + T774A + S775A (Fig. 5.5.3 A) were generated. These residues represent potential phosphorylatable residues for CDKs or GSK3 within the FBXW7 phospho-degron motif and therefore were mutated to alanine. GFP-pull-down was performed as above (Fig. 5.5.3 A). As negative control the empty vector (pDEST53) was used. For all B2-2 mutants similar co-immunoprecipitation of FBXW7 was observed. The interaction of FBXW7 did not differ between the different mutants, indicating that these residues might not be critical for the interaction

For this reason I aimed to narrow down the region which is critical for B2-2 and FBXW7 interaction by generating smaller overlapping GFP-tagged B2-2 fragments (Fig. 5.5.3 C). These GFP-tagged smaller B2-2 fragments (1 – 5) as well as the empty vector and full length B2-2 were pulled-down as above. Probing with antibody against FBXW7 showed bands for full length B2-2 (lane 2) as well as bands in the lanes 3 and 4 at the molecular weight of B2-2-1 and B2-2-2 (Fig. 5.5.3 D). Probing the membrane with GFP antibody confirmed that these bands indeed represented B2-2-1 and B2-2-2. This indicates that the FBXW7 antibody cross-reacts with the N-terminal region of B2-2, in which no FBXW7 phospho-degron motif is located. The non-specific nature of this antibody was previously unidentified because FBXW7 and GFP-B2-2 run at the same molecular weight in SDS-PAGE. Furthermore, the antibody was tested beforehand with recombinant GST-B2-2,

where no cross-reactivity was observed (Fig. 5.5.3 E). This could be due to differences in the expression system, e.g. that protein is folded differently or that post-translational modification in cells produces an epitope that is recognized by the FBXW7 antibody.

As this was found out during the course of optimizing the *in vitro* phosphorylation assays, the optimization and further experiments were precluded and the data obtained so far were re-evaluated. Also the co-immunoprecipitation of full-length BRCA2 with FBXW7 antibody was re-assessed, as the antibody could bind to the region in BRCA2 that resembles the B2-2 area (Fig. 5.6). To test whether this is the case, Western blot analysis probing with FBXW7 antibody against full length BRCA2 could be performed. Furthermore, the unspecific detection of B2-2 also explains that no difference in FBXW7 co-pull-down with B2-2 was observed after λ-phosphatase treatment or in cells treated with kinase inhibitors.

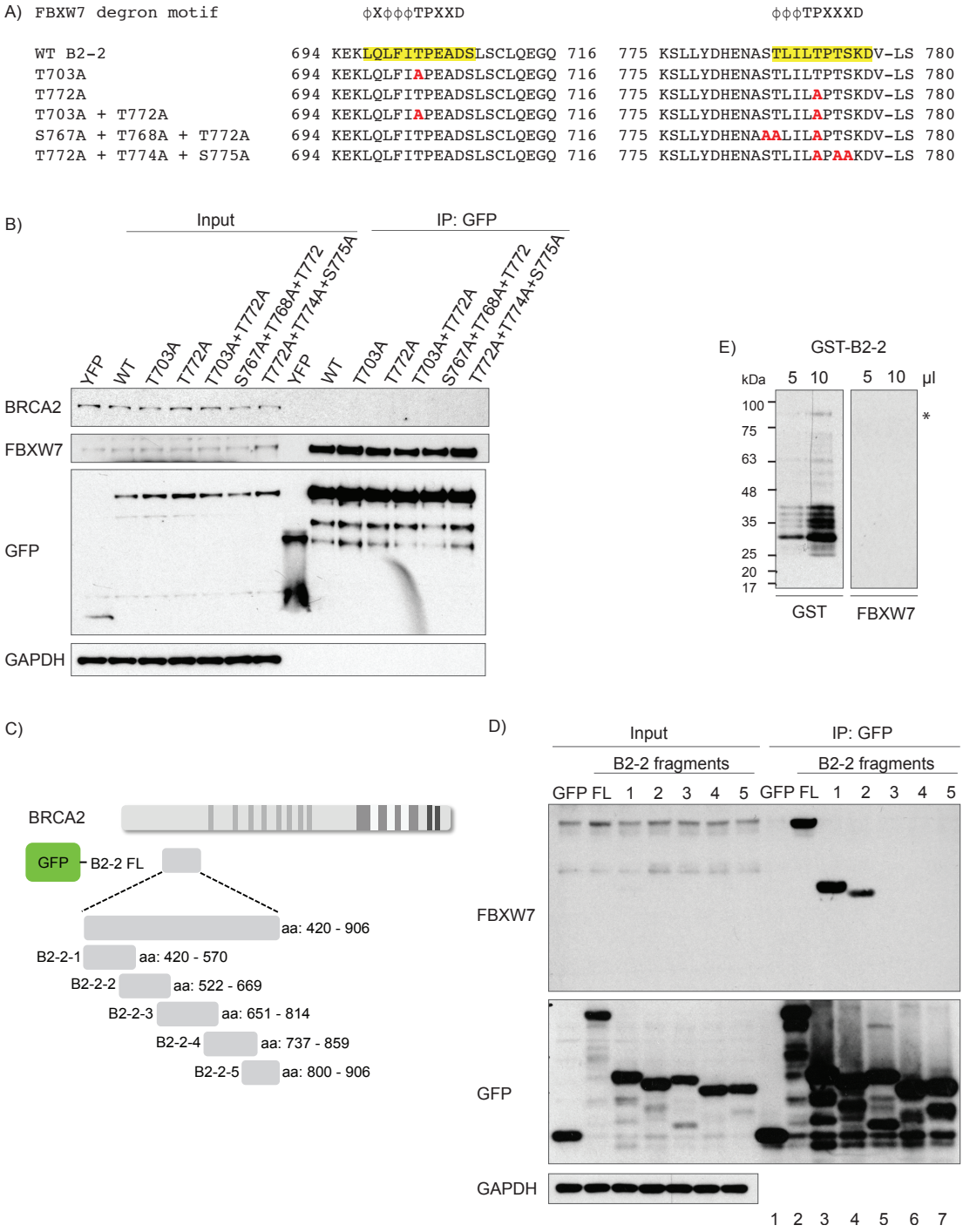

Figure 5.5.3: Interaction analysis of FBXW7 with B2-2 mutants

See description on next page.

Figure 5.5.3: Interaction analysis of FBXW7 with B2-2 mutants

A, B) Interaction of FBXW7 with B2-2 mutants and WT. A) Alignment of the B2-2 sequence with the FBXW7 degron motif with potential FBXW7 motifs in the B2-2 WT highlighted in yellow. X denotes any amino acid, Φ hydrophobic amino acids, T threonine, S serine and P proline. Below the generated B2-2 mutants with potential phosphorylatable residues highlighted in red: T703A, T772A, T703A + T772A, 767A + 768A + 772A, T772A + T774A + S775A. B) Western blot analysis of GFP-pull-down of B2-2 mutants expressed in HEK293T cells tested for FBXW7 co-pull-down. C) Schematic illustration of smaller GFP-tagged B2-2 fragments B2-2-1 - 5. . FL = full length, aa = amino acid. D) Interaction of FBXW7 with smaller B2-2 fragments. GFP-pull-down of smaller B2-2 fragments expressed in HEK293T cells tested for FBXW7 co-immunoprecipitation. E) 5 or 10 µl purified GST-B2-2 was separated on SDS-PAGE and Western blot analysis performed to test co-reactivity of the FBXW7 antibody with B2-2. * represents the molecular weight of GST-B2-2.

5.6 Analysis of the interaction of BRCA2, B2-6 and B2-9 fragments with FBXW7

Because the FBXW7 antibody was found to cross-react with the BRCA2 fragment B2-2, previous results were re-evaluated. In Fig. 4.5 C I observed that besides B2-2, also the fragments B2-6 and B2-9 co-immunoprecipitated with FBXW7. In both fragments sequence similarities to the FBXW7 phospho-degron motif can be found. In B2-6 two phospho-degron motifs can be found: TPXXT (aa 2310 – 2314) and SPXXS (2152 – 2156); in B2-9 four motifs: ΦXTPXXD (aa 3185 – 3191), ΦΦΦXSPXXE (aa 3215 – 3223), ΦXXXΦSPICT (aa 3279 – 3288), and ΦXSPXXT (aa 3311 – 3317) (Fig. 5.6 A). More interestingly, some of these motifs contain conserved TP/SP sites: 2310TP (B2-6), 3284SP (B2-9) and 3313SP (B2-9) that could potentially be phosphorylated by CDKs or GSK3. Therefore, the interaction between FBXW7 and these two fragments was further analysed. Additionally, two smaller fragments, within the B2-9 sequence were used: TR1 (aa 3189 – 3274) and TR2 (aa 3265 – 3330) (Fig. 5.6 B). To assess the phosphorylation dependency of the interaction with these fragments FE, FE-BRCA2 as well as empty vector (pDEST53) as a negative control and GFP-tagged B2-6, GFP-B2-9, GFP-TR1, and GFP-TR2 were expressed in HEK293T cells. Whole cell lysates from HEK293T cells expressing FE and FE-BRCA2 were subjected to FBXW7-immunoprecipitation directly. Cell lysates expressing GFP, B2-6, B2-9, TR1, TR2 were first divided into two, then treated or not treated with λ-phosphatase before addition of FBXW7 antibody cross-linked beads. As control whole cell lysates were also incubated with empty non-linked beads. The input samples represent input of immunoprecipitations performed with non-linked beads (odd numbered lanes) and

input of immunoprecipitations with FBXW7 (even numbered lanes) (Fig. 5.6 C). Expression of all proteins was successful, with the exception of GFP (lanes 5, 6). FBXW7-immunoprecipitations was similarly efficient in all samples. Interestingly, in FE (lane 16) and FE-BRCA2 (lane 18) expressing cells BRCA2 immunoprecipitated with FBXW7. Also, immunoprecipitations of cells expressing the empty vector (lanes 19) or B2-9 (26) showed that BRCA2 immunoprecipitated with FBXW7, whereby this could be due to the unspecific recognition by the FBXW7 antibody. Nonetheless, the interaction was diminished after treatment with λ-phosphatase (lanes 20, 27). This indicates that λ-phosphatase treatment disrupted the interaction between FBXW7 and BRCA2, and suggests that the interaction observed here is a specific phosphorylation-dependent interaction of BRCA2 with FBXW7 protein rather than cross-reaction with the FBXW7 antibody.

B2-6 (lane 23) and B2-9 (lane 26) also co-immunoprecipitated with FBXW7 confirming the results obtained above. Treatment with λ-phosphatase led to reduced interaction of B2-9 (lane 27), but not B2-6, indicating that the interaction of B2-9 with FBXW7 is phosphorylation-dependent. Furthermore, the C-terminal fragments TR1 (29) and TR2 (32) also co-immunoprecipitated with FBXW7. Treatment with λ-phosphatase did not impair the interaction of TR1 with FBXW7 (lane 30) but led to a decreased interaction of TR2 with FBXW7 (lane 33). This suggests that the interaction of BRCA2 with FBXW7 is phosphorylation dependent (lanes 19, 20, 26, 27 and 32,33). That B2-6 also immunoprecipitated with FBXW7 could be due to the sequence similarity to the degron motif, though this region as a potential interaction site for FBXW7 is unlikely as FBXW7 is known to recognize a phosphorylated motif and a change in interaction after phosphatase treatment was not observed. The possibility of cross-reaction of this antibody with these fragments still has to be considered, though as these fragments have not been detected with the FBXW7

antibody before, it is likely that the FBXW7 only recognized modified B2-2 but not any of the other fragments. For this reason, as the interaction of B2-9 (lanes 26, 27) was affected by λ-phosphatase treatment, the critical phosphorylation should be in the C-terminal region, which was further confirmed by reduced interaction of TR2 after phosphatase treatment (lanes 32, 33). Thus the critical residue is likely to be located within the sequence of BRCA2 ranging from amino acid 3265 to 3330.

FBXW7 phosphodegron motif ϕ-X-ϕ-ϕ-$_{phos}$T/$_{phos}$S-P-X-X-$_{phos}$T/$_{phos}$S/D/E

A) BRCA2 fragment B2-6

```
                                TPXXT                                                SPXXS
Mus musculus                2248 KGKSLTPSKSTPDGTVKDRSLFTHH 2272  2095 SSGNTQSIEVSLQLSQMERNQDTQLVL 2121
Rattus norvegicus           2263 KGKSLTPSKSTPDGTIKDRRLFTHH 2287  2110 SSGNTQSLEVSPQLSQMERKQETQSVL 2136
Homo sapiens                2300 QEKSLKASKSTPDGTIKDRRLFMHH 2324  2142 SSENNHSIKVSPYLSQFQQDKQ-QLVL 2167
Pan troglodytes             2300 QEKSLKASKSTPDGTIKDRRLFMHH 2324  2142 SSENNHSIKVSPYLSQFQQDKQ-QLVL 2167
Canis lupus familiaris      2317 QETSLKASKSTPDGILKDRSLFMHH 2341  2139 SSENHHSIKVSPCPSQLKRDKP-QLLV 2184
Felis catus                 2242 QEKSLKASKSTPDGIIKDRSLFMHH 2266  2088 SSEN-HSVQVSPYPSQFKQDK--QLIQ 2111
Bos taurus                  2306 QGKSLKASKSTPDGAMKDRRLFMHH 2330  2149 SSENNHSIKVSSYLSEFKQDQQ-QSVL 2174
Ornithorhynchus anatinus    2396 EKSSLKASRSTPEGTMKDRRMCTNH 2420  2251 SSEDSRHIQVS-------RNRDEQLSL 2270
                                 : .**..*:***:* :*** :  :*                ** : : ::**      :.:  *
```

B) BRCA2 fragment B2-9

```
                                ϕXTPXXD                                ϕϕϕXSPXXE
Mus musculus                3107 SQVSTPNKDPTREPHAASTCCASDLLGSGGQFLRISPTGQQSYQSPLSHC 3156
Rattus norvegicus           3116 PKWSTPNKDPTREPYPASTCSASDLAS-GGQLPRSSPTDQQSYRSPLSCC 3164
Homo sapiens                3189 PKWSTPTKDCTSGPYTAQIIPG-----TGNKLLMSSPNCEIYYQSPLSLC 3233
Pan troglodytes             3189 PKWSTPTKDCTSGPYAAQIIPG-----TGNKLLMSSPNCEIYYQSPLSLC 3233
Canis lupus familiaris      3208 PKLSTPTKDYASEPHTAQIVLG-----IGNKFLMSSPNNEMNYQSPLSLC 3252
Felis catus                 3133 PKVSTPMKDYASEPHTIQTVLG-----LGNKLSMSSPNSEMNYQSPLSLC 3177
Bos taurus                  3187 PKWSTPTKDCTSAPPTAQTVLG-----SGNKFPLSSPSSEMNYQSPLSLC 3231
Ornithorhynchus anatinus    3295 PSWSHRAADGSLEPPTP----------HGRFDLMPPKSEAGPSP-----  3325
                                 .. *    * :  * .                .::   .*. :    .
                                      ϕXXXϕSPICT                                ϕXSPXXT
Mus musculus                3196 LSRLPLPSPVSPICTFVSPAAQKAFQP 3223  3229 ATPIKKE-PSSPR-RTPFQKTSGVSL 3255
Rattus norvegicus           2204 LSRLPLPPPLSPVCTFVSPAAQKAFQP 3231  3239 PTPLKKEGPSSPWSRAPFQKASGVSL 3265
Homo sapiens                3273 LSRLPLPPPVSPICTFVSPAAQKAFQP 3300  3307 ETPIKKKELNSPQ-MTPFKKFNEISL 3333
Pan troglodytes             3273 LSRLPLPPPVSPICTFVSPAAQKAFQP 3300  3307 ETPIKKKELNSPQ-MTPFKKFNEISL 3333
Canis lupus familiaris      3292 LSRVPLPPSVSPICTFVSPAAQKAFQP 3320  3325 ETLMKK-ELNSPQ-MTP-RKFNDLSL 3351
Felis catus                 3217 LSRLPLPPPVSPICTFVSPAAQKAFQP 3245  3251 ETPIKKRELNSPQ-MTP-LKFNDTSL 3277
Bos taurus                  3271 LSRLPVPPPVSPICTFVSQAAQKAFQP 3299  3306 ETPMKKNELNSPQ-MTPRKKFNDISL 3332
Ornithorhynchus anatinus    3365 LSRIPSPPPVSPLCASVSPALKKAFQP 3393  3395 STPVQR--PSSPR----EGSAQSPPP 3421
                                 ***:* *..:**:*: ** * :*****          * :::   .**      . .  .
```

See description on page 151

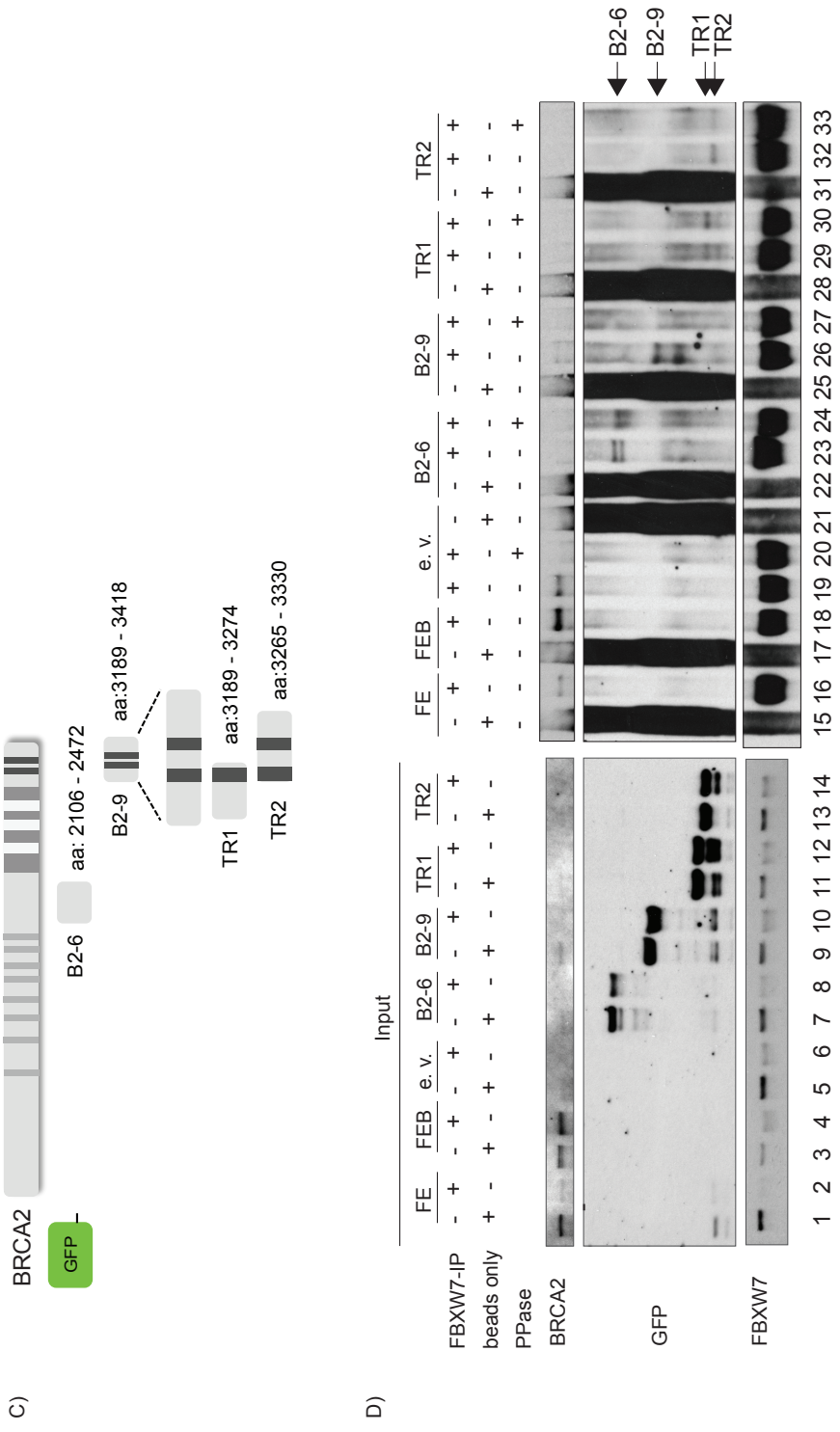

See description on page 151

Figure 5.6: Analysis of the interaction of BRCA2, B2-6 and B2-9 fragments with FBXW7

A) Alignment of the B2-6 sequence with the potential FBXW7 degron motifs highlighted in yellow. B) Alignment of the B2-9 sequence with potential FBXW7 degron motifs highlighted in yellow. Asterisk "*" describe identical residues, ":" conserved substitutions, "." semiconserved substitutions. X denotes any amino acid, Φ hydrophobic amino acid, T threonine, S serine and P proline, D aspartate, E glutamate. C) Schematic picture of GFP-tagged B2-6, B2-9, TR1 and TR2. aa = amino acids. D) Western blot analysis of interaction of D) Western blot analysis of interaction of BRCA2, B2-6, B2-9, TR1 and TR2 with FBXW7 and its phosphorylation dependency. FE, FEB (FE-BRCA2), pDEST53 (e.v.) as a negative control and GFP-tagged B2-6, GFP-B2-9, TR1, and TR2 were transiently expressed in HEK293T cells. The left panel shows input for the immunoprecipitations (IPs). Odd numbered lanes are input for IPs with empty non-linked beads (lanes 1, 3, 5, 7, 9, 11, 13), even numbered lanes depict inputs that were used for FBXW7-IPs (lanes 2, 4, 6, 8, 10, 12, 14). The right panel shows the IPs performed with empty beads (lane 15, 17, 21, 22, 25, 28, 31) and FBXW7 cross-linked beads, where samples were non-treated (lanes 16, 18, 19, 23, 26, 29, 32) or treated with λ-phosphatase (lanes 20, 24, 27, 30, 33). The arrows indicate the height of bands for B2-6, B2-9, TR1 and TR1 in the corresponding lanes.

5.7 Summary and Discussion

In Chapter 5 the interaction of BRCA2 with FBXW7 was analysed. BRCA2 co-immunoprecipitated with DN CUL1 showing that BRCA2 and Cullin1 interact *in vivo* (Fig. 5.2 B). Furthermore, the interaction of endogenous FBXW7 with BRCA2 was observed by immonoprecipitation (Fig. 5.3 A, B). In the course of investigation a cross-reaction of FBXW7 antibody with the N-terminal region of BRCA2-fragment B2-2, which does not contain a canonical FBXW7 phospho-degron motif, was discovered (Fig. 5.5 D). This suggests, that the interaction between FBXW7 and full-length BRCA2 might be unspecific. Although the antibody might cross-react with modified BRCA2 fragment B2-2, the analysis of the phosphorylation-dependency of the interaction suggests that BRCA2 specifically co-immunoprecipitates with FBXW7 protein rather than unspecifically with the antibody (Fig. 5.6). Therefore, the interaction seen here, is likely through specific interaction of BRCA2 with FBXW7 protein, and this will be discussed further below.

Next, the region on BRCA2 that FBXW7 interacts with was mapped. For this reason smaller GFP-tagged BRCA2 fragments (B2-1 – 9), covering the full sequence of BRCA2 were generated and subjected to FBXW7-immunoprecipitation and GFP-pull-down. The FBXW7-immunoprecipitation revealed that the fragments B2-2, B2-6 and B2-9 interact with FBXW7 (Fig. 5.4 C). However, the GFP-pull-down showed that FBXW7 only co-immunoprecipitated with B2-2 suggesting the sequence covered by B2-2 as the potential region that FBXW7 interacts with (Fig. 5.4 B). For this reason, I focused on the B2-2 fragment to analyse the mechanism of interaction. As described above, FBXW7 is known to recognize a phosphorylated degron motif, hence the involvement of phosphorylation in BRCA2-FBXW7 interaction was assessed using different methods (5.5.1 A, B). However, no phosphorylation-

dependent binding of FBXW7 to BRCA2 was observed, even mutations of putative critical residues within the potential phospho-degron motif of BRCA2 did not reveal a phosphorylation-dependent interaction (Fig. 5.5.3 B). Therefore, I tried to refine the binding region on BRCA2 that FBXW7 may bind to, using smaller fragments of B2-2 and discovered that the FBXW7 antibody used in this study cross-reacts with the N-terminal region of the BRCA2 fragment B2-2, that does not contain sequence similarities to the FBXW7 degron motif (Fig. 5.5.3 D). Therefore, the analysis of FBXW7 interaction with the BRCA2 B2-2 fragment was not carried out further, and previously obtained results were reassessed. As mentioned above, in addition to the B2-2 also the fragments B2-6 and B2-9 also co-immunoprecipitated with FBXW7 in the FBXW7-immunoprecipitation (Fig. 5.4 C). FBXW7 was reported to moderately bind to substrates, therefore it is possible that in the GFP-pull-down of BRCA2 fragments no interaction of FBXW7 with these fragments was detected due to the limited amount of FBXW7, together with possibly moderate binding affinities (Welcker and Clurman, 2007). However, both fragments contain sequences similar to the FBXW7 degron motif (Fig. 5.4 A, B, C), therefore the phosphorylation-dependent interaction with FBXW7 was tested. This analysis showed that full length BRCA2 co-immunoprecipitated with FBXW7 (Fig. 5.6 lane 16, 18, 19, 26). Because FBXW7 antibody was found to cross-react with BRCA2-fragment B2-2, the specificity of this observation is not decisive. However, interestingly, the interaction of full length BRCA2 with FBXW7 was abolished after treatment with λ-phosphatase (Fig. 5.6 lanes 20, 27). The effect of λ-phosphatase treatment on the interaction between BRCA2 and FBXW7 suggests, that the interaction observed is a phosphorylation-dependent interaction of BRCA2 with FBXW7 protein and not a cross-reaction with the FBXW7 antibody and the phosphorylation site responsible for this interaction remains to be determined.

Also, B2-9 (Fig. 5.6 lane 26, 27), but not B2-6 (Fig. 5.6 lane 23, 24), interaction with FBXW7 decreased after treatment with λ-phosphatase. Furthermore, using smaller fragments within the B2-9 sequence (TR1, TR2), a decrease in interaction was observed after λ-phosphatase treatment for TR2 (Fig. 5.6 lane 32, 33), which covers the middle part of B2-9 (aa 3265 – 3330). This indicates that the residues critical for the interaction of FBXW7 are located within this TR2 region. Since these fragments were not detected by the FBXW7 antibody before, this interaction is likely to be specific.

To further analyse the phosphorylation-dependency of the interaction between BRCA2 and FBXW7, BRCA2 mutants in which putative critical phosphorylatable residues are mutated to alanine, thus blocking phosphorylation-dependent interaction could be used for immunoprecipitation. Also it would be interesting to see whether a BRCA2 mutant that fails to interact with FBXW7 is more stable than wild type BRCA2, as SCF^{FBXW7} likely targets BRCA2 for ubiquitin-dependent proteasomal degradation. Additionally, to investigate the phosphorylation-dependency of the interaction and to determine the kinase responsible for the phosphorylation in BRCA2 that leads to FBXW7 recognition, interaction of FBXW7 with B2-9 or TR2 fragments could be assessed in cells treated with kinase inhibitors. Furthermore, *in vitro* kinase assays, as above, with subsequent FBXW7 interaction assays could be performed.

6 Investigation of the impact of SCF^{FBXW7} on DNA damage repair

6.1 Preface

BRCA2 plays a key role in DNA double strand break repair by HR. BRCA2-deficient cells show increased sensitivity to ionizing radiation, defects in HR, RAD51 foci formation and DNA replication, and accumulate chromosomal breaks (Lomonosov et al., 2003; Moynahan et al., 2001; Sharan et al., 1997; Yu et al., 2000; Yuan et al., 1999). However, it has also been suggested that high levels of BRCA2 suppress RAD51-mediated homologous recombination (Magwood et al., 2012). These reports revealed that the loss of BRCA2 function as well as increased levels of BRCA2 impair the repair of DNA damage by HR suggesting that levels of BRCA2 have to be tightly controlled.

Recent evidence highlights ubiquitylation events as key regulatory mechanisms in the DNA damage response (chapter 1.4 and 1.9). As previously mentioned, BRCA2 has been shown to interact with the proteasome components DSS1, RPN3 and RPN7 (Gudmundsdottir et al., 2007). Furthermore, ubiquitylation of BRCA2 by the SCF^{SKP2} complex has been suggested (Arbini et al., 2011; Moro et al., 2006) and Schoenfeld et al. showed that *in vivo* ubiquitylated BRCA2 interacts with the de-ubiquitylating enzyme USP11 (Schoenfeld et al., 2004). In the previous chapters, *in vivo* ubiquitylation of BRCA2 was examined and a candidate approach-based identification of E3 ligases was performed. These analyses suggested that

BRCA2 is targeted for ubiquitin-dependent degradation (chapters 4.2 and 4.6) and BRCA2 is ubiquitylated by SCF^{FBXW7} (chapters 4.4 and 5.6).

Since the reports mentioned above indicate that the control of BRCA2 level is crucial for the orderly process of HR repair, the following chapter investigates the involvement of SCF^{FBXW7} in HR repair to address the question whether FBXW7 may regulate BRCA2 level by promoting its degradation.

6.2 Phenotypic analyses of isogenic *FBXW7*^{WT} and *FBXW7*$^{-/-}$ HCT116 cells

To analyse the impact of FBXW7 on homology directed repair as well as BRCA2 regulation, isogenic mutants of the karyotypically stable colon carcinoma cell line HCT116 were used (Jallepalli et al., 2001). First, phenotypic analysis of FBXW7 wild type (WT) and null (-/-) HCT116 isogenic cells was performed. To assess whether expression of functional or non-functional FBXW7 results in changes in BRCA2 levels the wild type FBXW7 ($FBXW7^{WT}$) and a FBXW7 R465C mutant ($FBXW7^{R465C}$) were expressed in cells. Although three arginine residues have been reported to be important for substrate recognition by FBXW7, the substitution of arginine 465 by a cysteine (R465C) was found to abolish FBXW7-mediated degradation of its substrate cyclin E (Hao et al., 2007).

To this end, $FBXW7^{WT}$ and $FBXW7^{R465C}$ mutant were transiently expressed in HT1080, and the isogenic *FBXW7*^{WT} and *FBXW7*$^{-/-}$ cells. Western blot analysis showed that expression of $FBXW7^{WT}$ and $FBXW7^{R465C}$ mutant was similar in all cell lines (Fig. 6.2). In HT1080 cells, overexpression of $FBXW7^{WT}$ or $FBXW7^{R465C}$ did not

result in changes in BRCA2 levels. In all HCT116 cell lines, BRCA2 levels were similar in non-transfected cells. Also, neither the expression of $FBXW7^{WT}$ nor $FBXW7^{R465C}$ led to changes in the BRCA2 levels in comparison to the non-transfected cells or to the other cell lines. In order to test whether these cells depict normal physiological behaviour e.g. no changes in kinase activities, a previously observed phosphorylation of BRCA2 on S3291 by CDKs in M phase was tested (Esashi et al., 2005). Interestingly, in *FBXW7*$^{-/-}$ cells increased S3291 phosphorylation of BRCA2 was observed in comparison to *FBXW7*^{WT}, which did not change when $FBXW7^{WT}$ or $FBXW7^{R465C}$ mutant were expressed. Furthermore, probing against the mitotic marker pH3 revealed that fewer *FBXW7*$^{-/-}$ cells were in mitosis in comparison to the other HCT116 cell lines. This observation was independent of $FBXW7^{WT}$ or $FBXW7^{R465C}$ mutant expression. Intriguingly, in HT1080 cells overexpressing $FBXW7^{WT}$ and $FBXW7^{R465C}$ mutant much weaker signals for pH3 were detected, in comparison to non-transfected cells, which might indicate a FBXW7-induced cell cycle defect. This is in agreement with the FACS cell cycle analysis of *FBXW7*^{WT} and *FBXW7*$^{-/-}$ HCT116 cells, which showed that loss of FBXW7 results in a cell cycle defect (Fig. 6.2 B). In *FBXW7*^{WT} cells, most cells were observed in G1 and G2/M phases, with less cells being in S phase. In comparison, in *FBXW7*$^{-/-}$ HCT116 cells, only a minor population of cells was observed in G2/M phases, and most cells were in G1 phase. This appears to be in agreement with the reported function of FBXW7, which triggers S phase entry by degrading cyclin E (Koepp et al., 2001; Strohmaier et al., 2001). Thus loss of FBXW7 can lead to accumulation of cells in G1 in *FBXW7*$^{-/-}$ HCT116 cells. Overexpression of FBXW7 in HT1080 resulted in a decrease in pH3 detection, suggesting that overexpression of FBXW7 impairs the ability of cells to progress into mitosis. This is in line with previous observations that FBXW7 can target Aurora-A, a kinase crucial for mitotic entry (Fujii et al., 2006;

Kwon et al., 2012). Overexpression of FBXW7 was reported to result in decreased Aurora-A levels (Fujii et al., 2006; Kwon et al., 2012) possibly leading to defect in mitotic entry, which will be discussed in the summary.

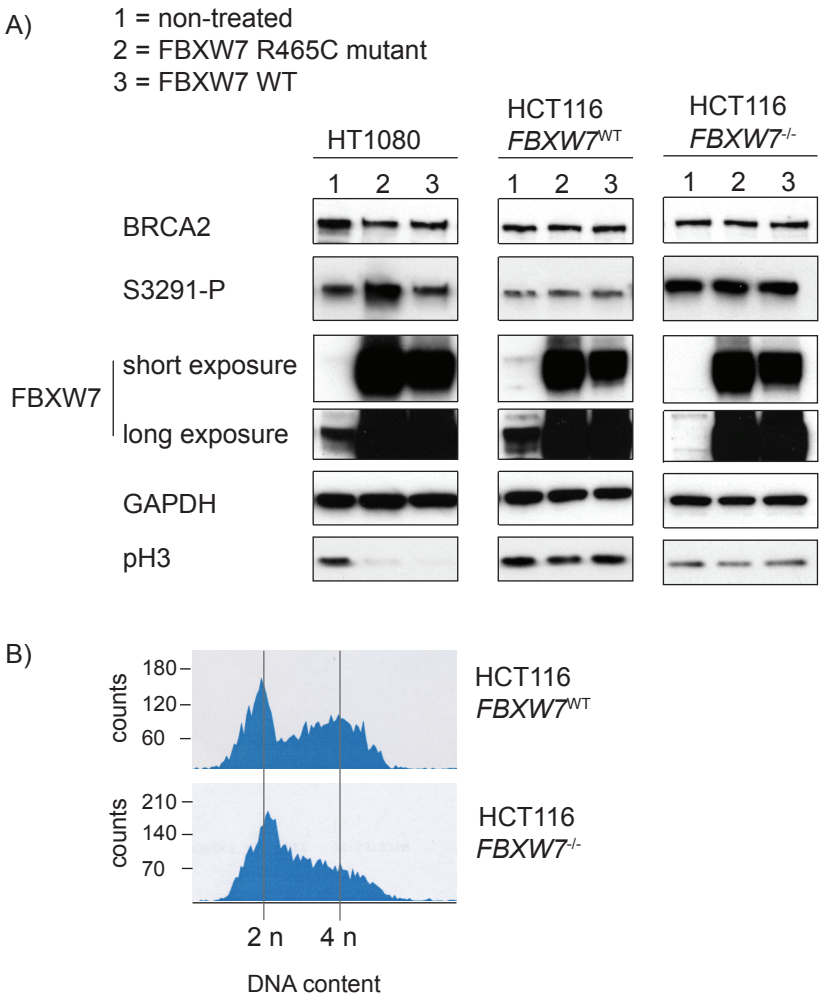

Figure 6.2: Phenotypic analysis of isogenic *FBXW7*^{WT} and *FBXW7*$^{-/-}$ HCT116 cell lines

A) FBXW7^{WT} and FBXW7^{R465C} mutant were expressed in HT1080, *FBXW7*^{WT} and *FBXW7*$^{-/-}$ isogenic cell lines and Western blot analysis was performed. B) FACS cell cycle analysis of *FBXW7*^{WT} and *FBXW7*$^{-/-}$ HCT116 cell lines.

6.3 IR sensitivity clonogenic assays

To investigate the effect that FBXW7 may have on DNA repair, clonogenic cell survival assays were performed and the damage sensitivity of FBXW7 knockout cells to ionizing radiation (IR) was assessed. Clonogenic cell survival assays enable one to determine the sensitivity of cells to exogenous stress by analysis of the ability of cells to proliferate and to form colonies, after exposure to the DNA damaging agent.

For this analysis, *FBXW7*^{WT} and *FBXW7*$^{-/-}$ HCT116 cells were irradiated with 1, 2 and 4 Gy of IR. The survival analysis revealed that *FBXW7*$^{-/-}$ HCT116 cells indeed exhibited a higher sensitivity towards IR than *FBXW7*^{WT} HCT116 cells (Fig. 6.3). At 1 Gy *FBXW7*^{WT} HCT116 cells showed similar sensitivity to IR. However, at higher doses of 2 and 4 Gy a significant reduction in survival of homozygous knockout cells was observed in comparison to cells expressing wild type FBXW7. This indicates that loss of FBXW7 leads to a higher sensitivity of cells to IR, thus a higher sensitivity towards DNA double strand breaks.

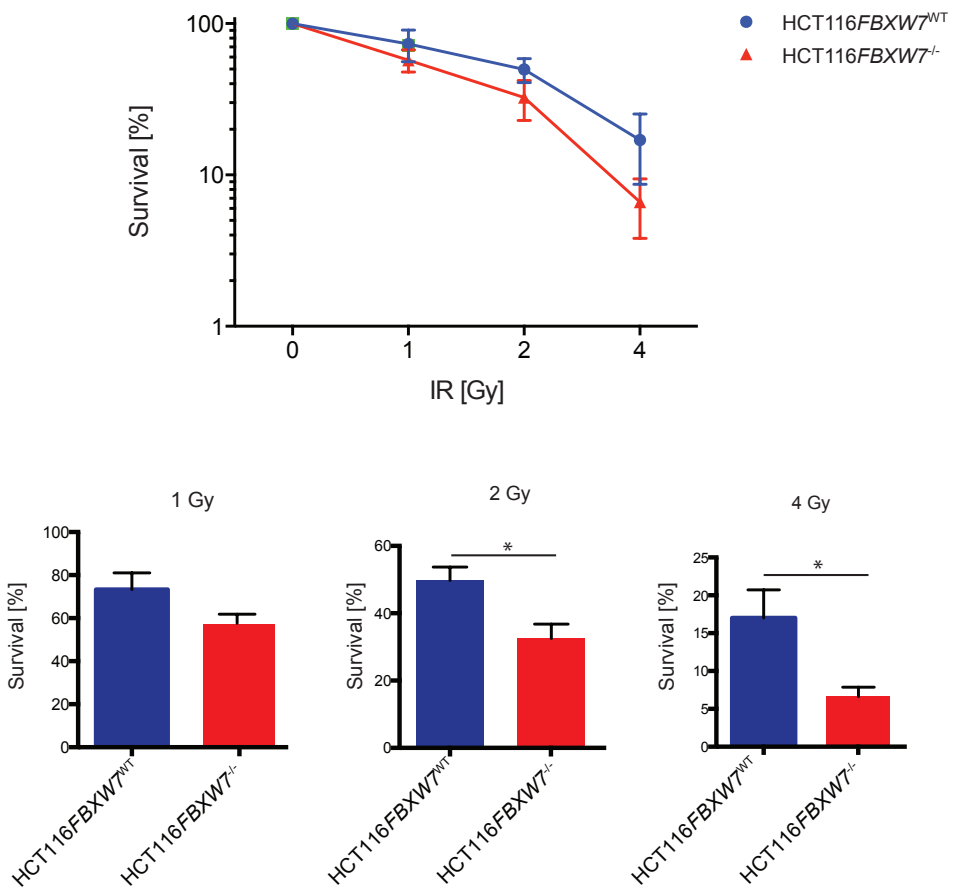

Figure 6.3: Clonogenic cell survival assays after IR exposure of *FBXW7*^{WT} and *FBXW7*$^{-/-}$ HCT116 cells

Cellular survival of *FBXW7* wild type (WT) and null (-/-) isogenic HCT116 cells was analysed after exposure to 1, 2 or 4 Gy of IR. Depicted are the average means of five independent experiments performed in triplicates. Error bars represent the standard error of the mean, p-values were calculated using a paired two-tailed t-test, * represents a significance below 0.05 $p < 0.05$.

6.4 Double stand break-induced gene conversion assay

To further analyse the effect of FBXW7 on HR-directed repair, a gene conversion assay was performed using U2OS-SCR＃18 cells (a generously gift by Ralph Scully), which encode for one 5'-truncated GFP-protein and one mutated GFP, which contains an ISceI-endonuclease restriction site. After introduction of site-specific DNA double strand breaks by ISceI-endonuclease, gene conversion or homologous recombination could result in a functional GFP. Gene conversion can then be measured by detection of GFP positive cells in FACS analysis (Puget et al., 2005).

To investigate whether SCF^{FBXW7} plays a role in HR-dependent repair, siRNA-mediated knockdowns of FBXW7, BRCA2 or FBXW7 together with BRCA2 were performed and GFP-positive cells were measured by FACS analysis (Fig. 6.4 A). The analysis showed an approximately two fold decrease in GFP-positive cells when BRCA2 was down-regulated, which is in agreement with previous observations and its reported function in homology-directed repair (Moynahan et al., 2001). Down-regulation of FBXW7 or FBXW7 together with BRCA2 led to a subtle but not significant decrease in GFP-positive cells in comparison to cells treated with control siRNA (Cntrl, Universal negative control), indicating that FBXW7 has no marked impact on gene conversion. Furthermore, in *FBXW7* homozygous knockout HCT116 cells, the cell cycle analysis revealed an increase in G1 population, which could also occur in U2OS-SCR cells treated with FBXW7 siRNA. Therefore, cell cycle analysis of non-treated U2OS-SCR cells and cells treated with Universal negative control, BRCA2, FBXW7 or FBXW7 together with BRCA2 siRNAs was performed. The analysis did not reveal differences between non-treated cells and the different

treatments with siRNA or ISceI nuclease, indicating that no cell cycle defect in response to siRNA knockdowns or nuclease treatment occurred (Fig. 6.4 B, C).

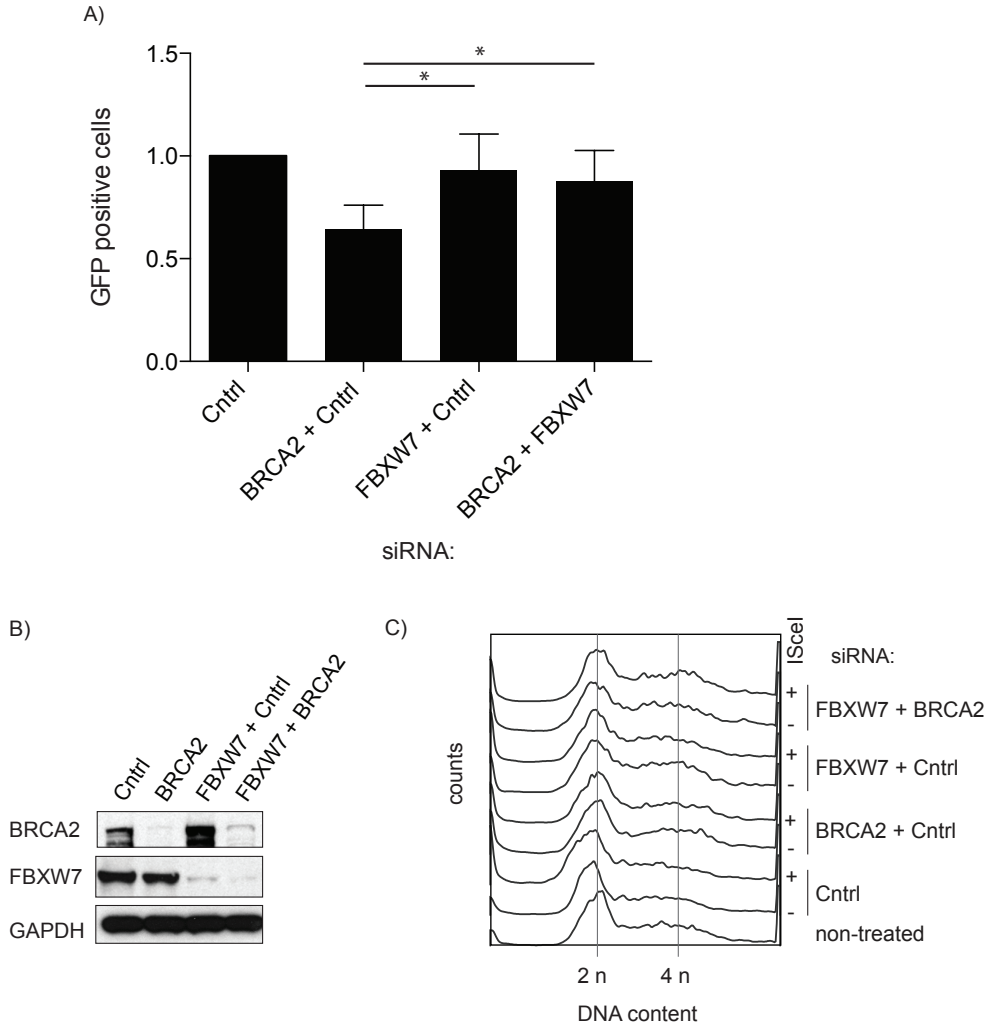

Figure 6.4: Analysis of gene conversion after down-regulation of FBXW7 and BRCA2 A) U2OS-SCR cells were treated with siRNA against Universal negative control (Cntrl), BRCA2 and Cntrl, FBXW7 and Cntrl, and BRCA2 together with FBXW7 and gene conversion was analysed by measuring GFP-positive cells in FACS. Depicted are the average means of four independent experiments. Error bars represent the standard error of the mean, p-values were calculated using a paired two-tailed t-test, * represents p-values < 0.05. B) Western blot analysis of siRNA-mediated knockdowns for Universal negative control (Cntrl), BRCA2 and Cntrl, FBXW7 and Cntrl, and BRCA2 together with FBXW7 in U2OS-SCR cells. C) FACS cell cycle analysis of U2OS-SCR cells were treated with siRNA against Universal negative control (Cntrl), BRCA2 and Cntrl, FBXW7 and Cntrl, and BRCA2 together with FBXW7.

6.5 RAD51 foci formation after IR

Upon DNA damage, DNA damage repair proteins accumulate at sites of DNA damage and form discrete accumulations called foci (Haaf et al., 1995; Scully et al., 1997). The amount of foci and the size of foci change over time and can be visualized by immunocytochemistry (van Veelen et al., 2005). RAD51 has been found to accumulate at sites of DNA damage creating visible foci in the cell nucleus after DNA damage (Haaf et al., 1995).

Since increased sensitivity to IR in cells lacking FBXW7 was observed, I analysed the ability of *FBXW7*^{WT} and *FBXW7*$^{-/-}$ HCT116 cells to form RAD51 foci following IR treatment. Cells were exposed to 4 Gy IR and 2.5 h post exposure cells were fixed and immunocytochemistry was performed (Fig. 6.5 A). In comparison to *FBXW7*^{WT} HCT116 cells, less RAD51 foci positive cells were observed for *FBXW7*$^{-/-}$ HCT116 cells, *FBXW7*$^{-/-}$ cells showed even an eight-fold reduction in RAD51 foci positive cells, indicating that loss of FBXW7 leads to impaired RAD51 foci formation.

To further investigate RAD51 foci formation in cells, independent of cell cycle arrest due to the loss of FBXW7, RAD51 foci positive cells were analysed using HT1080 cells, which showed no detectable effect on cell cycle progression after down-regulation of FBXW7 (Fig. 4.4). HT1080 cells treated with siRNA against FBXW7 or FBXW7 together with BRCA2 were exposed to 4 Gy of IR and immunocytochemistry was performed 2.5 h after IR treatment (Fig. 6.5 C). In comparison to cells transfected with Universal negative control (Cntrl) in cells down-regulated for FBXW7 or FBXW7 together with BRCA2, a two fold decrease in RAD51 foci positive cells was detected. Since a decrease in RAD51 foci positive cells was detected in HT1080 cells down-regulated for FBXW7 or FBXW7 together with BRCA2 as wells as in *FBXW7*$^{-/-}$ HCT116 cells this also suggests that loss of FBXW7

impairs the ability of cells to form RAD51 foci. The higher decrease in RAD51 positive cells observed in *FBXW7*$^{-/-}$ HCT116 cells in comparison to siRNA-mediated knockdown of FBXW7 in HT1080 cells could occur as an additional result of a cell cycle progression defect in these cells.

To gain a deeper insight into the different abilities of the HCT116 cell lines to form RAD51 foci, e.g. whether the temporal rate of RAD51 foci formation is different between the cell lines, a time course was taken to analyse RAD51 foci formation at 2, 4 and 6 h after exposure to IR. Since the clonogenic survival assay showed the best cellular survival of *FBXW7*^{WT} and *FBXW7*$^{-/-}$ HCT116 cells was observed at 1 Gy, this analysis was performed after exposure to 1 Gy. In addition, the formation of γH2AX, a DNA damage marker was also analysed (Fig. 6.5 C). Histone H2AX is phosphorylated on serine139 in response to DNA damage and is then called γH2AX (Rogakou et al., 1998). In *FBXW7*^{WT} HCT116 cells a three-fold decrease in γH2AX foci positive cells was observed over the time course. In contrast, γH2AX foci positive cells appeared to be persistent in *FBXW7*$^{-/-}$ HCT116 cells. Also, in both cell lines, a decrease in RAD51 foci positive cells was observed during the time course, whereas, for *FBXW7*^{WT} HCT116 cells less RAD51 foci positive cells were detected than for *FBXW7*$^{-/-}$ HCT116 cells. Taken together these results suggest, that in *FBXW7*^{WT} HCT116 cells, repair can be performed most efficiently as RAD51 foci positive γH2AX foci positive cells decreased over the time course. In *FBXW7*$^{-/-}$ cells, higher amounts of RAD51 foci positive cells and persistent γH2AX foci positive cells were detected, which may indicate that the repair of DNA damage is less effective. This could suggest that loss of FBXW7 leads to impaired repair of DNA damage and a possibly positive effect of FBXW7 on DNA damage repair. However, a cell cycle effect on the impaired DNA repair cannot be excluded.

To avoid cell cycle defects observed in HCT116 *FBXW7* homozygous knockout cells, other homozygous FBXW7 knockout cell lines were tested. To this end, phenotypic analyses of the isogenic *FBXW7*^{WT} and *FBXW7*$^{-/-}$ colorectal adenocarcinoma DLD-1 cell lines were performed (S5). No differences in cell cycle progression were observed between *FBXW7*^{WT} and *FBXW7*$^{-/-}$ DLD-1 cells. Furthermore, BRCA2 levels were similar, though S3291 phosphorylation was decreased in *FBXW7*$^{-/-}$ DLD-1 cells in comparison to *FBXW7*^{WT} DLD-1 cells. However, further analysis, such as RAD51 foci analyses, could not be performed due to time constraints.

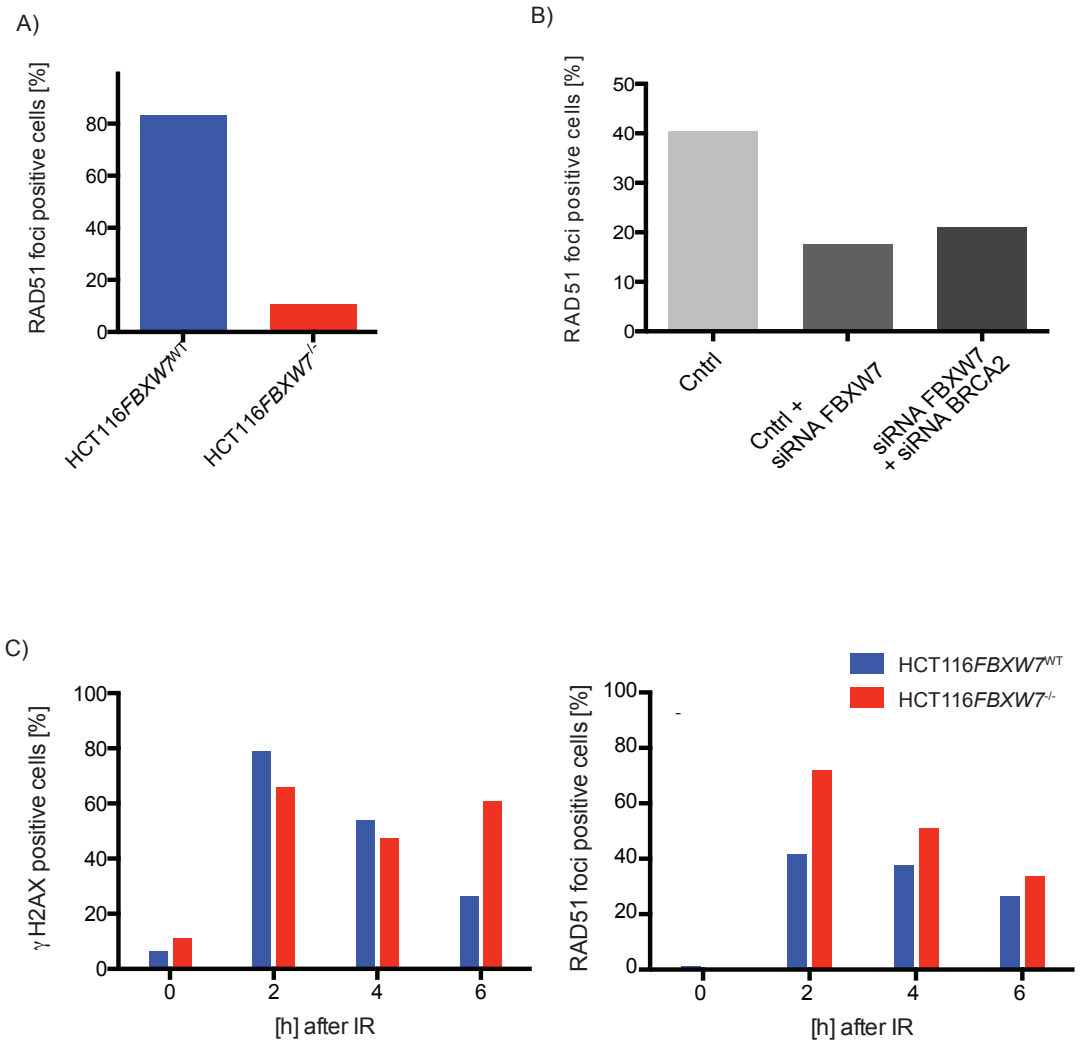

Figure 6.5: Analysis of RAD51 foci positive cells in *FBXW7*^{WT} and *FBXW7*$^{-/-}$ HCT116 cell lines and in HT1080 after siRNA-mediated knockdowns of FBXW7 and FBXW7 together with BRCA2

See description on next page.

Figure 6.5: Analysis of RAD51 foci positive cells in $FBXW7^{WT}$ and $FBXW7^{-/-}$ HCT116 cell lines and in HT1080 after siRNA-mediated knockdowns of FBXW7 and FBXW7 together with BRCA2

A) RAD51 foci positive $FBXW7^{WT}$ and $FBXW7^{-/-}$ HCT116 cells were analysed 2.5 h after exposure to 4 Gy of IR. Depicted are the percentages of RAD51 foci positive cells. At least 200 cells were counted. B) Analysis of RAD51 foci positive HT1080 cells siRNA treated with Universal negative control (Cntrl, Sigma), FBXW7 and FBXW7 together with BRCA2. 2.5 h after exposure to 4 Gy of IR cells were fixed. Depicted are the percentages of RAD51 foci positive cells. More than 100 cells were counted. C) Analysis of γH2AX (left) and RAD51 (right) foci positive $FBXW7^{WT}$ and $FBXW7^{-/-}$ HCT116 cells 2, 4, and 6 h after exposure to 1 Gy of IR. Depicted are the percentages of γH2AX or RAD51 foci positive cells. At least 200 cells were counted. Cells were counted positive for γH2AX or RAD51 foci when more than 10 foci were detected per nucleus.

6.6 Summary and Discussion

In Chapter 6, the impact of FBXW7 on DNA repair was assessed. DNA damage sensitivity was first assessed in clonogenic cell survival assays using *FBXW7*^{WT} and *FBXW7*$^{-/-}$ HCT116 cells. The clonogenic assay showed that at higher doses of IR (2 and 4 Gy) survival of *FBXW7*$^{-/-}$ HCT116 cells significantly decreased in comparison to *FBXW7*^{WT} HCT116 cells, indicating that loss of FBXW7 results in increased sensitivity towards IR (Fig. 6.3). As no differences in BRCA2 levels were observed between these cell lines, even after overexpression of FBXW7, the increased sensitivity towards IR is likely to be independent of BRCA2. This can be supported by the observation that *FBXW7*$^{-/-}$ HCT116 cells exhibit a cell cycle defect, resulting in accumulation of cells in G1, where no BRCA2-dependent HR repair occurs (Fig. 6.2). Because cells accumulated in G1 and HR repair can only be employed in S and G2 phases an effect of FBXW7 on BRCA2 and HR repair cannot be completely excluded either.

To investigate whether FBXW7 has an impact on HR-directed repair, gene conversion assays were performed in which gene conversion can be measured by detection of GFP positive cells. Down-regulation of BRCA2 led to a two-fold decrease in GFP-positive cells in comparison to the control siRNA treated cells. In cells down-regulated for FBXW7 or FBXW7 together with BRCA2 a minor decrease in GFP-positive cells was observed in comparison to the control (Fig. 6.4 A). Since no cell cycle defect was observed in U2OS-SCR cells after treatments with siRNA and ISceI nuclease (Fig. 6.4 B), this indicates that down-regulation of FBXW7 has no detectable effect on gene conversion using this system.

Together, the above results did not provide direct evidence that FBXW7 is involved in HR-directed repair. Further investigations are required to

comprehensively analyse the effect of FBXW7 on homology-directed repair. An alternative approach would be to employ the zinc finger nuclease-mediated gene-targeting assay in HT1080 cells, a cell line in which FBXW7 down-regulation also has been shown not to affect cell cycle progression (Fig. 4.4). The zinc finger methodology allows the assessment of HR-directed gene-targeting. Cells are transfected with the zinc finger nuclease and a donor plasmid, which acts as a HR template. The donor plasmid is flanked by sequences homologous to each side of the zinc finger nuclease cleavage site. Therefore, DNA double strand breaks, introduced by the zinc finger nuclease, can be targeted by homology-directed recombination using the donor plasmid as a template. Homology-directed recombination of the DNA double strand break integrates GFP under a functional promoter and thus can be measured by detection of fluorescent signals (Hockemeyer et al., 2009).

Another, indirect approach to analyse HR repair in cells is to assess the ability of cells to form damaged-induced RAD51 nuclear foci, which accumulate at sites of DNA damage (van Veelen et al., 2005). Analysis of IR-induced RAD51 foci formation at 4 Gy revealed a nearly complete disappearance in RAD51 foci positive cells in *FBXW7*$^{-/-}$ HCT116 cells in comparison to *FBXW7*^{WT} HCT116 cells (Fig. 6.5 A). Also in HT1080 cells a decrease in RAD51 foci positive cells was detected after down-regulation of FBXW7 or FBXW7 together with BRCA2 (Fig. 6.5) indicating that loss of FBXW7 leads to an impaired ability of cells to form RAD51 foci. To further investigate the impact of FBXW7 DNA damage repair and on the ability to form RAD51 foci, RAD51 foci positive cells and γH2AX foci formation were analysed at different times after exposure to 1 Gy IR. γH2AX foci positive cells decreased over time after IR treatment in *FBXW7*^{WT} HCT116 cells, whereas in *FBXW7*$^{-/-}$ HCT116 cells γH2AX foci positive cells were sustained up to 6 hours. At 1 Gy of IR in both cell

lines RAD51 foci positive cells decreased after 2 h of induction. Surprisingly, in comparison to homozygous FBXW7 knockout cells, less RAD51 foci positive cells were detected in *FBXW7*^{WT} HCT116 cells. This could indicate that DNA damage is efficiently repaired in *FBXW7*^{WT} HCT116 cells, as a decrease in γH2AX foci positive cells was observed over time. In *FBXW7*$^{-/-}$ HCT116 cells persistent amounts of γH2AX foci positive cells were detected, which could indicate that loss of FBXW7 leads to impaired repair of DNA damage. This is strengthened by the observation that more RAD51 foci where observed in *FBXW7*$^{-/-}$ HCT116 cells. A possible reason for this might be, that at 1 Gy of IR the threshold of DNA damage is low, therefore replication forks progress unperturbed whereas at 4 DSBs occur resulting in activation of the intra S phase checkpoint (Groth et al., 2012). Therefore it might be that unperturbed replication forks that are independent of IR-induced checkpoint control hit IR-induced DNA damage, thus resulting in replication associated one-ended DSBs (Groth et al., 2012). As BRCA2 as well as RAD51 have been proposed to be involved in replication fork protection, it might be possible that the foci detected here represent RAD51 accumulations at replication forks and that depletion of FBXW7 leads to impaired control of RAD51 loading or unloading on DNA at replication forks and repair and therefore to persistent γH2Ax foci (González-Prieto et al., 2013; Liberi et al., 2005; Schlacher et al., 2011).

The data obtained in this chapter indicate that loss of FBXW7 leads to an increased sensitivity of cells to IR and to impaired repair of DNA damage, which was assessed by γH2AX staining. Nonetheless, whether this increased sensitivity is a result of BRCA2 de-regulation due to loss of FBXW7 needs to be further investigated. As *FBXW7*$^{-/-}$ HCT116 cells show a different phenotype than *FBXW7*^{WT} HCT116 cells it is conceivable, that during generation of the HCT116 isogenic cell lines, cells acquired the ability to circumvent the loss of FBXW7, so different cell lines

could be used for further analyses. A BRCA2 mutant that cannot interact with FBXW7, e.g. due to mutation of the crucial phosphorylated residue (see chapter 5.6 and 5.7), could be expressed in BRCA2 depleted cells and clonogenic survival assays after IR, aphidicolin or HU treatment, ZFN assays or aphidicolin or HU - induced RAD51 foci analyses could be performed.

7 Discussion

In summary, this study revealed that BRCA2 can be targeted for ubiquitin-dependent proteasomal degradation. Total BRCA2 levels changed during the cell cycle, decreasing two-fold at the G1/S phase transition. Interestingly, BRCA2 ubiquitylation also changed during the cell cycle. Furthermore, the results presented here suggest that BRCA2 can be targeted for ubiquitin-dependent degradation by SCF^{FBXW7} in a phosphorylation-dependent manner. These data suggest that BRCA2 levels are tightly regulated.

In addition to the approximately two-fold decrease of BRCA2 levels before S phase (Fig. 3.2) a two-fold decrease of BRCA2 levels was observed after IR exposure, which is in agreement with previous observations (Fig. S2) (Schoenfeld et al., 2004; Wang et al., 2001). The decrease in BRCA2 levels after DNA damage as well as during S phase where homologous recombination (HR) can be employed was unexpected, as BRCA2 is a key player in DSB repair by HR. In line with this observation, it has been reported that increased level of *BRCA2* mRNA correlates with poor cancer prognosis and that high levels of BRCA2 protein can suppress RAD51-mediated HR (Bièche et al., 1999; Magwood et al., 2012). Furthermore, it has been shown that exogenous overexpression of the BRC4 motif can interfere with the function of BRCA2; in particular, it impairs the recruitment of RAD51 to sites of DNA damage and nucleoprotein filament formation (Chen et al., 1998b; Davies et al., 2001; Pellegrini et al., 2002). More recently, the importance of the molecular ratio of RAD51 to peptides containing BRC4 or BRC1-8 has emerged, as BRC4 and BRC1-8 were found to stimulate RAD51-mediated strand exchange at low concentrations, but decreased RAD51 nucleation rate at higher concentration (Carreira et al., 2009;

Shivji et al., 2006). This suggests that an appropriate amount of BRCA2 is critical for its function; optimal amounts of BRCA2 facilitate RAD51 nucleofilament formation, whereas elevated levels of BRCA2 block the formation of RAD51 nucleoprotein filaments.

A major regulatory system that controls protein levels in cells is the ubiquitin-proteasome system. It has been reported that BRCA2 mRNA levels peak at the G1/S phase transition, remain high during S phase and decrease towards mitosis (Vaughn et al., 1996a), which does not correlate with the BRCA2 protein levels observed here. In addition, BRCA2 level decreased two-fold within 4 h of exposure to IR, and a fast decrease of BRCA2 protein levels was observed at the G1/S transition; within 1 h of release from a double thymidine block in HT1080 and 2-4 h of release in HeLa cells, a two-fold decrease of BRCA2 levels was observed (Fig. 3.2). These results suggest the presence of an active mechanism for the regulation of BRCA2 protein levels such as degradation by the ubiquitin-proteasome system. In line with this idea, BRCA2 protein half-life was prolonged in the presence of the proteasome inhibitor MG132 (Fig. 3.3), and ubiquitylated BRCA2 was detected in pull-downs from MG132-treated cells (Fig. 4.2). Interestingly, ubiquitylation of BRCA2 also changed during the cell cycle (Fig. 4.3). BRCA2 ubiquitylation was low during S phase and increased when cells began to enter G1, which is in agreement with observed BRCA2 levels in the cell cycle analyses, where BRCA2 levels began to decrease in G1 phase. These data suggest the ubiquitin-dependent proteasomal degradation of BRCA2 during the cell cycle.

A candidate-based approach to identify an E3 ligase responsible for BRCA2 ubiquitylation during the cell cycle highlighted the potential involvement of SCF^{FBXW7} as an E3 ligase that targets BRCA2 for ubiquitylation-dependent proteasomal degradation (Fig. 4.4.2). Remarkably, the decrease of BRCA2 levels at the G1/S

transition (Fig. 3.2) coincides with the phase of the cell cycle where SCF^{FBXW7} is known to be active, targeting cyclin E for proteasomal degradation (Klotz et al., 2009). Moreover, in a preliminary experiment, ubiquitylation of BRCA2 was still detectable after siRNA-mediated down-regulation of CDH1, but not when CUL1 or FBXW7 were down-regulated (Fig. 5.3). Conversely, increased *in vivo* ubiquitylation of BRCA2 was observed when FBXW7 was overexpressed (Fig. 4.6). A role of SCF^{FBXW7} in BRCA2 ubiquitylation was additionally supported by the finding that FBXW7 interacts with the C-terminal region of BRCA2 (probably within residues 3265 – 3330) likely in a phosphorylation-dependent manner (Fig. 5.2, 5.4 and 5.6). Therefore, it can be proposed that BRCA2 level can be regulated by the action of SCF^{FBXW7} to maintain optimal levels of BRCA2 during S phase.

Interestingly, the candidate-based approach performed to identify an E3 ligase that targets BRCA2 for ubiquitin-dependent degradation, only resulted in a mild increase of BRCA2 protein stability after down-regulation of the receptor proteins. This raises the possibility that SCF^{FBXW7} is just one of several E3 ligases that targets BRCA2 for proteasomal degradation. For example, SKP2 was proposed to be involved in BRCA2 degradation in previous studies (Arbini et al., 2011; Malone et al., 2009; Moro, 2006). Notably, we and others observed that exogenous overexpression of BRCA2 under a strong promoter (CMV) leads to maximal 2 – 3 fold increase of BRCA2 protein levels, therefore it was proposed, that overexpression of BRCA2 is toxic to cells (Takata et al., 2002). If high cellular levels of BRCA2 are deleterious, down-regulation of one E3 ligase might lead to activation of alternative E3 ligases that ubiquitylate BRCA2 and target BRCA2 for proteasomal degradation. It is also possible to speculate that several E3 ligases act sequentially or in concert during the cell cycle to maintain appropriate levels of BRCA2 during S phase.

In the future, BRCA2-IP from synchronized cells followed by mass-spectrometry, or an unbiased siRNA-mediated screen for BRCA2 E3 ligases would likely provide better insights into the possibility of a regulation of BRCA2 protein stability during the cell cycle.

In order to investigate the impact of FBXW7-dependent regulation of BRCA2 on HR repair, the sensitivity of colorectal carcinoma HCT116 cell lines with homozygous (-/-) knockout of *FBXW7* or wild type (WT) *FBXW7* to IR was analysed by clonogenic survival assays (Fig. 6.3). At 2 and 4 Gy of IR, *FBXW7*$^{-/-}$ HCT116 cells showed a significant decrease in cellular survival in comparison to cells expressing wild type *FBXW7*. In addition, persistent amounts of γH2AX foci positive cells were detected in *FBXW7*$^{-/-}$ HCT116 cells (Fig. 6.5). This could indicate that loss of FBXW7 leads to impaired repair of DNA damage. However, the analyses of IR-induced RAD51 foci formation in *FBXW7*$^{-/-}$ HCT116 cells at 4 and 1 Gy or in HT1080 cells down-regulated for FBXW7 or the analysis of homology-directed gene conversion in U2OS-SCR cells down-regulated for FBXW7 did not provide clear evidence for an impact of FBXW7-mediated BRCA2 regulation in HR (Fig. 6.4, 6.5).

Intriguingly, *FBXW7*$^{-/-}$ HCT116 cells show an increased population of cells in G1 phase, when DSBs are repaired by NHEJ and not by HR (Fig. 6.2). Therefore, it is difficult to directly assess the effect of FBXW7 on BRCA2-dependent homology-directed repair as this occurs in S and G2 phases of the cell cycle. Hence, it would be premature, at this stage of investigation, to completely exclude a role for FBXW7-dependent regulation of BRCA2 in HR. Nonetheless, the increased sensitivity to IR could also be a result of the accumulation of cells in G1 phase, in which cells are more sensitive to IR (Iwabuchi et al., 2006; Nghiem et al., 2001).

In addition, treatment of cells with IR leads to checkpoint activation that results in S phase arrest and inhibition of origin firing (Jazayeri et al., 2006; Merrick

et al., 2004). Groth et al. showed that IR treatment did not affect ongoing replication forks suggesting that fork progression is independent of IR-induced checkpoint control and proposed that unperturbed post-DNA damage replication forks possibly collide with persistent DNA damage resulting in replication associated one-ended DSBs, so-called secondary DSBs (Groth et al., 2012). Therefore it could be proposed here, that at 4 Gy DSBs occur that lead to activation of the intra-S phase checkpoint causing a block in origin firing. In contrast at 1 Gy of IR, the DNA damage threshold might be too low so that the checkpoint is not activated resulting in the occurrence of secondary DSBs due to continuous origin firing. As RAD51 has been shown to be involved in replication fork protection it might be possible that the foci detected represent RAD51 accumulations at replication forks and secondary DSBs (González-Prieto et al., 2013; Liberi et al., 2005). This possibly could explain the decrease in RAD51 foci formation at 4 Gy (Fig. 6.5 A) yet increased RAD51 foci formation at 1 Gy in *FBXW7*$^{-/-}$ HCT116 cells (Fig. 6.5 C) leading to speculate three hypotheses: First, it might be possible that during generation *FBXW7*$^{-/-}$ HCT116 cells acquired defects in checkpoint activation leading continuous origin firing; second, that FBXW7 might play a role in checkpoint activation; or third, that depletion of FBXW7 results in defects in controlled RAD51 loading and unloading onto nascent DNA at replication forks, thereby blocking repair of secondary DSBs and thus increased RAD51 foci and persistent γH2AX formation. Although these hypotheses might explain the differences observed in RAD51 foci formation at 1 and 4 Gy of IR further analyses are required, e. g. analysis of checkpoint activation in *FBXW7*$^{-/-}$ HCT116 cells or in cells down-regulated for FBXW7, DNA fiber analysis in FBXW7 depleted cells after treatment with the two replication inhibitors aphidicolin or hydroxyurea.

Another mechanism in cells to modulate protein function is the post-

translational modification of proteins, such as phosphorylations. BRCA2 can be phosphorylated by CDKs on S3291, when cells progress towards mitosis, which blocks RAD51 interaction with the C-terminal region of BRCA2, thereby inhibiting RAD51 nucleoprotein filament formation (Esashi et al., 2005). Intriguingly, preliminary data from our group and others indicate that S3291 phosphorylation also controls stability of BRCA2; a BRCA2 fragment with a mutation (P3292L) that prevents S3291 phosphorylation shows reduced stability in cells, whereas a phospho-mimetic mutation at S3291 (S3291E) significantly stabilises the fragment (Esashi, unpublished; Malone et al., 2009). It is notable that S3291 phosphorylation is low during S phase and after DNA damage but increases towards M phase (Esashi et al., 2005). Remarkably, in *FBXW7*$^{-/-}$ HCT116 cells an increased G1 population and higher amounts of BRCA2 S3291 phosphorylation were observed (Fig. 6.2). As S3291 phosphorylation is proposed to block BRCA2 interaction with RAD51 and RAD51 nucleofilament formation in G2 and M phase (Esashi et al., 2005) this BRCA2 phosphorylation in *FBXW7*$^{-/-}$ HCT116 appears to be independent of the cell cycle. Therefore it could be proposed, that S3291 phosphorylation of BRCA2 can be used as a mechanism to control BRCA2 function in homology-directed repair in the absence of a regulatory mechanism for BRCA2 stability.

Given the observations obtained in this study and reported observations showing that excess of BRC motifs and increased levels of BRCA2 suppress HR, it can be speculated that an appropriate amount of BRCA2 is critical for its function also in HR-independent roles of BRCA2 (Carreira et al., 2009; Chen et al., 1999a; 1998b; Davies and Pellegrini, 2007; Esashi et al., 2005; Esashi et al., 2007; Galkin, 2005; Magwood et al., 2012; Shivji et al., 2006; Thorslund et al., 2010).

Therefore, a hypothesis can be proposed that cells ensure the tight regulation of BRCA2 function on two levels: one level represents the control of BRCA2

abundance by the ubiquitin proteasome system (quantitative control), the second level represents the regulation of BRCA2 function by post-translational modification (quality control) (Fig. 7.1).

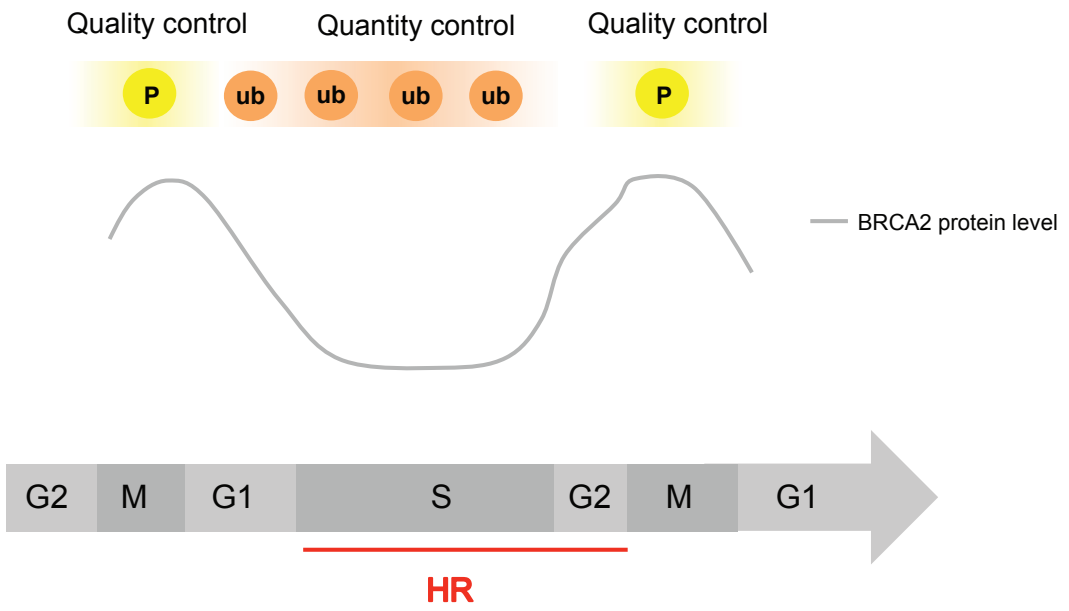

Figure 7.1: A model of BRCA2 regulation

BRCA2 function is regulated by two mechanisms; one regulates the availability of BRCA2 protein, which is mediated by the ubiquitin-proteasome system (quantity control, depicted in orange), the second regulates BRCA2 function by posttranslational modifications (quantity control, depicted in yellow). Grey line represents BRCA2 protein levels during the cell cycle, letters within the grey arrow represent cell cycle phases G1 (gap 1), S (synthesis), G2 (gap 2), M (mitosis). The red line shows when homologous recombination (HR) can be employed.

References

Agarwal, M.L., Agarwal, A., Taylor, W.R., and Stark, G.R. (1995). p53 controls both the G2/M and the G1 cell cycle checkpoints and mediates reversible growth arrest in human fibroblasts. Proceedings of the National Academy of Sciences of the United States of America *92*, 8493–8497.

Akhoondi, S., Sun, D., Lehr, von der, N., Apostolidou, S., Klotz, K., Maljukova, A., Cepeda, D., Fiegl, H., Dafou, D., Dofou, D., et al. (2007). FBXW7/hCDC4 is a general tumor suppressor in human cancer. Cancer Research *67*, 9006–9012.

Andersen, S.L., Bergstralh, D.T., Kohl, K.P., LaRocque, J.R., Moore, C.B., and Sekelsky, J. (2009). Drosophila MUS312 and the vertebrate ortholog BTBD12 interact with DNA structure-specific endonucleases in DNA repair and recombination. Molecular Cell *35*, 128–135.

Arbini, A.A., Greco, M., Yao, J.L., Bourne, P., Marra, E., Hsieh, J.-T., di Sant'agnese, P.A., and Moro, L. (2011). Skp2 overexpression is associated with loss of BRCA2 protein in human prostate cancer. Am. J. Pathol. *178*, 2367–2376.

Aylon, Y., Liefshitz, B., and Kupiec, M. (2004). The CDK regulates repair of double-strand breaks by homologous recombination during the cell cycle. The EMBO Journal *23*, 4868–4875.

Bahassi, E.M., Ovesen, J.L., Riesenberg, A.L., Bernstein, W.Z., Hasty, P.E., and Stambrook, P.J. (2008). The checkpoint kinases Chk1 and Chk2 regulate the functional associations between hBRCA2 and Rad51 in response to DNA damage. Oncogene *27*, 3977–3985.

Bahram, F., Lehr, von der, N., Cetinkaya, C., and Larsson, L.G. (2000). c-Myc hot spot mutations in lymphomas result in inefficient ubiquitination and decreased proteasome-mediated turnover. Blood *95*, 2104–2110.

Bai, C., Sen, P., Hofmann, K., Ma, L., Goebl, M., Harper, J.W., and Elledge, S.J. (1996). SKP1 connects cell cycle regulators to the ubiquitin proteolysis machinery through a novel motif, the F-box. Cell *86*, 263–274.

Bakkenist, C.J., and Kastan, M.B. (2003). DNA damage activates ATM through intermolecular autophosphorylation and dimer dissociation. Nature *421*, 499–506.

Barbash, O., Zamfirova, P., Lin, D.I., Chen, X., Yang, K., Nakagawa, H., Lu, F., Rustgi, A.K., and Diehl, J.A. (2008). Mutations in Fbx4 inhibit dimerization of the SCF(Fbx4) ligase and contribute to cyclin D1 overexpression in human cancer. Cancer Cell *14*, 68–78.

Barber, L.J., Youds, J.L., Ward, J.D., McIlwraith, M.J., O'Neil, N.J., Petalcorin, M.I.R., Martin, J.S., Collis, S.J., Cantor, S.B., Auclair, M., et al. (2008). RTEL1 maintains genomic stability by suppressing homologous recombination. Cell *135*, 261–271.

Bashir, T., Dorrello, N.V., Amador, V., Guardavaccaro, D., and Pagano, M. (2004). Control of the SCF(Skp2-Cks1) ubiquitin ligase by the APC/C(Cdh1) ubiquitin ligase. Nature *428*, 190–193.

Beijersbergen, R.L., and Bernards, R. (1996). Cell cycle regulation by the retinoblastoma family of growth inhibitory proteins. Biochim. Biophys. Acta *1287*, 103–120.

Bekker-Jensen, S., Rendtlew Danielsen, J., Fugger, K., Gromova, I., Nerstedt, A., Lukas, C., Bartek, J., Lukas, J., and Mailand, N. (2010). HERC2 coordinates ubiquitin-dependent assembly of DNA repair factors on damaged chromosomes. Nat. Cell Biol. *12*, 80–6–suppp1–12.

Ben-Aroya, S., Agmon, N., Yuen, K., Kwok, T., McManus, K., Kupiec, M., and Hieter, P. (2010). Proteasome nuclear activity affects chromosome stability by controlling the turnover of Mms22, a protein important for DNA repair. PLoS Genetics *6*, e1000852.

Ben-Saadon, R., Zaaroor, D., Ziv, T., and Ciechanover, A. (2006). The polycomb protein Ring1B generates self atypical mixed ubiquitin chains required for its in vitro histone H2A ligase activity. Molecular Cell *24*, 701–711.

Bienvenu, F., Jirawatnotai, S., Elias, J.E., Meyer, C.A., Mizeracka, K., Marson, A., Frampton, G.M., Cole, M.F., Odom, D.T., Odajima, J., et al. (2010). Transcriptional role of cyclin D1 in development revealed by a genetic-proteomic screen. Nature *463*, 374–378.

Bièche, I., Noguès, C., and Lidereau, R. (1999). Overexpression of BRCA2 gene in sporadic breast tumours. Oncogene *18*, 5232–5238.

Bignell, G., Micklem, G., Stratton, M.R., Ashworth, A., and Wooster, R. (1997). The BRC repeats are conserved in mammalian BRCA2 proteins. Hum. Mol. Genet. *6*, 53–58.

Blickwedehl, J., Agarwal, M., Seong, C., Pandita, R.K., Melendy, T., Sung, P., Pandita, T.K., and Bangia, N. (2008). Role for proteasome activator PA200 and postglutamyl proteasome activity in genomic stability. Proceedings of the National Academy of Sciences *105*, 16165–16170.

Boisvert, F.-M., Ahmad, Y., Gierliński, M., Charrière, F., Lamont, D., Scott, M., Barton, G., and Lamond, A.I. (2012). A quantitative spatial proteomics analysis of proteome turnover in human cells. Mol. Cell Proteomics *11*, M111.011429.

Bork, P., Blomberg, N., and Nilges, M. (1996). Internal repeats in the BRCA2 protein sequence. Nature Genetics *13*, 22–23.

Bosu, D.R., Feng, H., Min, K., Kim, Y., Wallenfang, M.R., and Kipreos, E.T. (2010). C. elegans CAND-1 regulates cullin neddylation, cell proliferation and morphogenesis in specific tissues. Developmental Biology *346*, 113–126.

Bradford, M.M. (1976). A rapid and sensitive method for the quantitation of microgram quantities of protein utilizing the principle of protein-dye binding. Anal. Biochem. *72*, 248–254.

Brzovic, P.S., Keeffe, J.R., Nishikawa, H., Miyamoto, K., Fox, D., Fukuda, M., Ohta, T., and Klevit, R. (2003). Binding and recognition in the assembly of an active BRCA1/BARD1 ubiquitin-ligase complex. Proceedings of the National Academy of Sciences of the United States of America *100*, 5646–5651.

Bugreev, D.V., Yu, X., Egelman, E.H., and Mazin, A.V. (2007). Novel pro- and anti-recombination activities of the Bloom's syndrome helicase. Genes & Development *21*, 3085–3094.

Bulavin, D.V., Higashimoto, Y., Demidenko, Z.N., Meek, S., Graves, P., Phillips, C., Zhao, H., Moody, S.A., Appella, E., Piwnica-Worms, H., et al. (2003). Dual phosphorylation controls Cdc25 phosphatases and mitotic entry. Nat. Cell Biol. *5*, 545–551.

Butler, L.R., Densham, R.M., Jia, J., Garvin, A.J., Stone, H.R., Shah, V., Weekes, D., Festy, F., Beesley, J., and Morris, J.R. (2012). The proteasomal de-ubiquitinating enzyme POH1 promotes the double-strand DNA break response. The EMBO Journal *31*, 3918–3934.

Carreira, A., and Kowalczykowski, S.C. (2011). Two classes of BRC repeats in BRCA2 promote RAD51 nucleoprotein filament function by distinct mechanisms. Proceedings of the National Academy of Sciences *108*, 10448–10453.

Carreira, A., Hilario, J., Amitani, I., Baskin, R.J., Shivji, M.K.K., Venkitaraman, A.R., and Kowalczykowski, S.C. (2009). The BRC repeats of BRCA2 modulate the DNA-binding selectivity of RAD51. Cell *136*, 1032–1043.

Carroll, C.W., Enquist-Newman, M., and Morgan, D.O. (2005). The APC subunit Doc1 promotes recognition of the substrate destruction box. Current Biology : CB *15*, 11–18.

Castro, A., Arlot-Bonnemains, Y., Vigneron, S., Labbé, J.-C., Prigent, C., and Lorca, T. (2002). APC/Fizzy-Related targets Aurora-A kinase for proteolysis. EMBO Reports *3*, 457–462.

Castro, A., Bernis, C., Vigneron, S., Labbé, J.-C., and Lorca, T. (2005). The anaphase-promoting complex: a key factor in the regulation of cell cycle. Oncogene *24*, 314–325.

Chan, F.K., Zhang, J., Cheng, L., Shapiro, D.N., and Winoto, A. (1995). Identification of human and mouse p19, a novel CDK4 and CDK6 inhibitor with homology to p16ink4. Molecular and Cellular Biology *15*, 2682–2688.

Chance, B., Sies, H., and Boveris, A. (1979). Hydroperoxide metabolism in mammalian organs. Physiol. Rev. *59*, 527–605.

Chao, W.C.H., Kulkarni, K., Zhang, Z., Kong, E.H., and Barford, D. (2012). Structure of the mitotic checkpoint complex. Nature *484*, 208–213.

Chapman, J.R., and Jackson, S.P. (2008). Phospho-dependent interactions between NBS1 and MDC1 mediate chromatin retention of the MRN complex at sites of DNA damage. EMBO Reports *9*, 795–801.

Chapman, J.R., Taylor, M.R.G., and Boulton, S.J. (2012). Playing the end game: DNA double-strand break repair pathway choice. Molecular Cell *47*, 497–510.

Chau, V., Tobias, J.W., Bachmair, A., Marriott, D., Ecker, D.J., Gonda, D.K., and Varshavsky, A. (1989). A multiubiquitin chain is confined to specific lysine in a targeted short-lived protein. Science (New York, N.Y.) *243*, 1576–1583.

Chen, C.F., Chen, P.L., Zhong, Q., Sharp, Z.D., and Lee, W.H. (1999a). Expression of BRC repeats in breast cancer cells disrupts the BRCA2-Rad51 complex and leads to radiation hypersensitivity and loss of G(2)/M checkpoint control. The Journal of Biological Chemistry *274*, 32931–32935.

Chen, J.J., Silver, D., Cantor, S., Livingston, D.M., and Scully, R. (1999b). BRCA1, BRCA2, and Rad51 operate in a common DNA damage response pathway. Cancer Research *59*, 1752s–1756s.

Chen, J., Silver, D.P., Walpita, D., Cantor, S.B., Gazdar, A.F., Tomlinson, G., Couch, F.J., Weber, B.L., Ashley, T., Livingston, D.M., et al. (1998a). Stable interaction between the products of the BRCA1 and BRCA2 tumor suppressor genes in mitotic and meiotic cells. Molecular Cell *2*, 317–328.

Chen, P.L., Chen, C.F., Chen, Y., Xiao, J., Sharp, Z.D., and Lee, W.H. (1998b). The BRC repeats in BRCA2 are critical for RAD51 binding and resistance to methyl methanesulfonate treatment. Proceedings of the National Academy of Sciences of the United States of America *95*, 5287–5292.

Ciccia, A., and Elledge, S.J. (2010). The DNA damage response: making it safe to play with knives. Molecular Cell *40*, 179–204.

Cimprich, K.A., and Cortez, D. (2008). ATR: an essential regulator of genome integrity. Nature Reviews. Molecular Cell Biology *9*, 616–627.

Ciosk, R., Zachariae, W., Michaelis, C., Shevchenko, A., Mann, M., and Nasmyth, K. (1998). An ESP1/PDS1 complex regulates loss of sister chromatid cohesion at the metaphase to anaphase transition in yeast. Cell *93*, 1067–1076.

Cohen-Fix, O., Peters, J.M., Kirschner, M.W., and Koshland, D. (1996). Anaphase initiation in Saccharomyces cerevisiae is controlled by the APC-dependent degradation of the anaphase inhibitor Pds1p. Genes & Development *10*, 3081–3093.

Cole, A., Frame, S., and Cohen, P. (2004). Further evidence that the tyrosine phosphorylation of glycogen synthase kinase-3 (GSK3) in mammalian cells is an autophosphorylation event. Biochem. J. *377*, 249–255.

Connor, F., Bertwistle, D., Mee, P.J., Ross, G.M., Swift, S., Grigorieva, E., Tybulewicz, V.L., and Ashworth, A. (1997). Tumorigenesis and a DNA repair defect in mice with a truncating Brca2 mutation. Nature Genetics *17*, 423–430.

Contreras, A., Hale, T.K., Stenoien, D.L., Rosen, J.M., Mancini, M.A., and Herrera, R.E. (2003). The dynamic mobility of histone H1 is regulated by cyclin/CDK phosphorylation. Molecular and Cellular Biology *23*, 8626–8636.

Cooper, E.M., Boeke, J.D., and Cohen, R.E. (2010). Specificity of the BRISC deubiquitinating enzyme is not due to selective binding to Lys63-linked polyubiquitin. Journal of Biological Chemistry *285*, 10344–10352.

Couch, F.J., Farid, L.M., DeShano, M.L., Tavtigian, S.V., Calzone, K., Campeau, L., Peng, Y., Bogden, B., Chen, Q., Neuhausen, S., et al. (1996). BRCA2 germline mutations in male breast cancer cases and breast cancer families. Nature Genetics *13*, 123–125.

Dalton, W.B., Nandan, M.O., Moore, R.T., and Yang, V.W. (2007). Human cancer cells commonly acquire DNA damage during mitotic arrest. Cancer Research *67*, 11487–11492.

Daniels, M.J., Wang, Y., Lee, M., and Venkitaraman, A.R. (2004). Abnormal cytokinesis in cells deficient in the breast cancer susceptibility protein BRCA2. Science *306*, 876–879.

Davies, A.A., Masson, J.Y., McIlwraith, M.J., Stasiak, A.Z., Stasiak, A., Venkitaraman, A.R., and West, S.C. (2001). Role of BRCA2 in control of the RAD51 recombination and DNA repair protein. Molecular Cell *7*, 273–282.

Davies, O.R., and Pellegrini, L. (2007). Interaction with the BRCA2 C terminus protects RAD51-DNA filaments from disassembly by BRC repeats. Nature Structural & Molecular Biology *14*, 475–483.

Davies, T.G., Bentley, J., Arris, C.E., Boyle, F.T., Curtin, N.J., Endicott, J.A., Gibson, A.E., Golding, B.T., Griffin, R.J., Hardcastle, I.R., et al. (2002). Structure-based design of a potent purine-based cyclin-dependent kinase inhibitor. Nat. Struct. Biol. *9*, 745–749.

Dawson, I.A., Roth, S., and Artavanis-Tsakonas, S. (1995). The Drosophila cell cycle gene fizzy is required for normal degradation of cyclins A and B during mitosis and has homology to the CDC20 gene of Saccharomyces cerevisiae. J. Cell Biol. *129*, 725–737.

de Jager, M., van Noort, J., van Gent, D.C., Dekker, C., Kanaar, R., and Wyman, C. (2001). Human Rad50/Mre11 is a flexible complex that can tether DNA ends. Molecular Cell *8*, 1129–1135.

de Sousa Abreu, R., Penalva, L.O., Marcotte, E.M., and Vogel, C. (2009). Global signatures of protein and mRNA expression levels. Mol Biosyst *5*, 1512–1526.

Deng, L., Wang, C., Spencer, E., Yang, L., Braun, A., You, J., Slaughter, C., Pickart, C., and Chen, Z.J. (2000). Activation of the IkappaB kinase complex by TRAF6 requires a dimeric ubiquitin-conjugating enzyme complex and a unique polyubiquitin chain. Cell *103*, 351–361.

Deshaies, R.J., and Joazeiro, C.A.P. (2009). RING domain E3 ubiquitin ligases. Annu. Rev. Biochem. *78*, 399–434.

Di Leonardo, A., Linke, S.P., Clarkin, K., and Wahl, G.M. (1994). DNA damage triggers a prolonged p53-dependent G1 arrest and long-term induction of Cip1 in normal human fibroblasts. Genes & Development *8*, 2540–2551.

Doil, C., Mailand, N., Bekker-Jensen, S., Menard, P., Larsen, D.H., Pepperkok, R., Ellenberg, J., Panier, S., Durocher, D., Bartek, J., et al. (2009). RNF168 binds and amplifies ubiquitin conjugates on damaged chromosomes to allow accumulation of repair proteins. Cell *136*, 435–446.

Duda, D.M., Borg, L.A., Scott, D.C., Hunt, H.W., Hammel, M., and Schulman, B.A. (2008). Structural insights into NEDD8 activation of cullin-RING ligases: conformational control of conjugation. Cell *134*, 995–1006.

Dulić, V., Kaufmann, W.K., Wilson, S.J., Tlsty, T.D., Lees, E., Harper, J.W., Elledge, S.J., and Reed, S.I. (1994). p53-dependent inhibition of cyclin-dependent kinase activities in human fibroblasts during radiation-induced G1 arrest. Cell *76*, 1013–1023.

Dulić, V., Lees, E., and Reed, S.I. (1992). Association of human cyclin E with a periodic G1-S phase protein kinase. Science (New York, N.Y.) *257*, 1958–1961.

Eden, E., Geva-Zatorsky, N., Issaeva, I., Cohen, A., Dekel, E., Danon, T., Cohen, L., Mayo, A., and Alon, U. (2011). Proteome half-life dynamics in living human cells. Science *331*, 764–768.

Egawa, C., Miyoshi, Y., Taguchi, T., Tamaki, Y., and Noguchi, S. (2002). High BRCA2 mRNA expression predicts poor prognosis in breast cancer patients. International Journal of Cancer. Journal International Du Cancer *98*, 879–882.

Ekholm, S.V., Zickert, P., Reed, S.I., and Zetterberg, A. (2001). Accumulation of cyclin E is not a prerequisite for passage through the restriction point. Molecular and Cellular Biology *21*, 3256–3265.

Esashi, F., Christ, N., Gannon, J., Liu, Y., Hunt, T., Jasin, M., and West, S.C. (2005). CDK-dependent phosphorylation of BRCA2 as a regulatory mechanism for recombinational repair. Nature *434*, 598–604.

Esashi, F., Galkin, V.E., Yu, X., Egelman, E.H., and West, S.C. (2007). Stabilization of RAD51 nucleoprotein filaments by the C-terminal region of BRCA2. Nature Structural & Molecular Biology *14*, 468–474.

Escribano-Diaz, C., and Durocher, D. (2013). DNA repair pathway choice--a PTIP of the hat to 53BP1. EMBO Reports *14*, 665–666.

Fabre, F., Chan, A., Heyer, W.-D., and Gangloff, S. (2002). Alternate pathways involving Sgs1/Top3, Mus81/ Mms4, and Srs2 prevent formation of toxic recombination intermediates from single-stranded gaps created by DNA replication. Proceedings of the National Academy of Sciences of the United States of America *99*, 16887–16892.

Falck, J., Coates, J., and Jackson, S.P. (2005). Conserved modes of recruitment of ATM, ATR and DNA-PKcs to sites of DNA damage. Nature *434*, 605–611.

Falck, J., Forment, J.V., Coates, J., Mistrik, M., Lukas, J., Bartek, J., and Jackson, S.P. (2012). CDK targeting of NBS1 promotes DNA-end resection, replication restart and homologous recombination. EMBO Reports *13*, 561–568.

Fang, G., Yu, H., and Kirschner, M.W. (1998). Direct binding of CDC20 protein family members activates the anaphase-promoting complex in mitosis and G1. Molecular Cell *2*, 163–171.

Fekairi, S., Scaglione, S., Chahwan, C., Taylor, E.R., Tissier, A., Coulon, S., Dong, M.-Q., Ruse, C., Yates, J.R., Russell, P., et al. (2009). Human SLX4 is a Holliday junction resolvase subunit that binds multiple DNA repair/recombination endonucleases. Cell *138*, 78–89.

Fiol, C.J., Mahrenholz, A.M., Wang, Y., Roeske, R.W., and Roach, P.J. (1987). Formation of protein kinase recognition sites by covalent modification of the substrate. Molecular mechanism for the synergistic action of casein kinase II and glycogen synthase kinase 3. The Journal of Biological Chemistry *262*, 14042–14048.

Fisher, R.D., Wang, B., Alam, S.L., Higginson, D.S., Robinson, H., Sundquist, W.I., and Hill, C.P. (2003). Structure and ubiquitin binding of the ubiquitin-interacting motif. The Journal of Biological Chemistry *278*, 28976–28984.

Freemont, P.S., Hanson, I.M., and Trowsdale, J. (1991). A novel cysteine-rich sequence motif. Cell *64*, 483–484.

Friedberg, E.C., Aguilera, A., Gellert, M., Hanawalt, P.C., Hays, J.B., Lehmann, A.R., Lindahl, T., Lowndes, N., Sarasin, A., and Wood, R.D. (2006). DNA repair: from molecular mechanism to human disease. DNA Repair *5*, 986–996.

Fujii, Y., Yada, M., Nishiyama, M., Kamura, T., Takahashi, H., Tsunematsu, R., Susaki, E., Nakagawa, T., Matsumoto, A., and Nakayama, K.I. (2006). Fbxw7 contributes to tumor suppression by targeting multiple proteins for ubiquitin-dependent degradation. Cancer Sci. *97*, 729–736.

Funabiki, H., Yamano, H., Kumada, K., Nagao, K., Hunt, T., and Yanagida, M. (1996). Cut2 proteolysis required for sister-chromatid seperation in fission yeast. Nature *381*, 438–441.

Galanty, Y., Belotserkovskaya, R., Coates, J., and Jackson, S.P. (2012). RNF4, a SUMO-targeted ubiquitin E3 ligase, promotes DNA double-strand break repair. Genes & Development *26*, 1179–1195.

Galkin, V.E. (2005). BRCA2 BRC motifs bind RAD51-DNA filaments. Proceedings of the National Academy of Sciences *102*, 8537–8542.

García-Higuera, I., Manchado, E., Dubus, P., Cañamero, M., Méndez, J., Moreno, S., and Malumbres, M. (2008). Genomic stability and tumour suppression by the APC/C cofactor Cdh1. Nat. Cell Biol. *10*, 802–811.

Garnett, M.J., Mansfeld, J., Godwin, C., Matsusaka, T., Wu, J., Russell, P., Pines, J., and Venkitaraman, A.R. (2009). UBE2S elongates ubiquitin chains on APC/C substrates to promote mitotic exit. Nat. Cell Biol. *11*, 1363–1369.

Geley, S., Kramer, E., Gieffers, C., Gannon, J., Peters, J.M., and Hunt, T. (2001). Anaphase-promoting complex/cyclosome-dependent proteolysis of human cyclin A starts at the beginning of mitosis and is not subject to the spindle assembly checkpoint. J. Cell Biol. *153*, 137–148.

Glotzer, M., Murray, A.W., and Kirschner, M.W. (1991). Cyclin is degraded by the ubiquitin pathway. Nature *349*, 132–138.

Goldenberg, S.J., Cascio, T.C., Shumway, S.D., Garbutt, K.C., Liu, J., Xiong, Y., and Zheng, N. (2004). Structure of the Cand1-Cul1-Roc1 complex reveals regulatory mechanisms for the assembly of the multisubunit cullin-dependent ubiquitin ligases. Cell *119*, 517–528.

González-Prieto, R., Muñoz-Cabello, A.M., Cabello-Lobato, M.J., and Prado, F. (2013). Rad51 replication fork recruitment is required for DNA damage tolerance. The EMBO Journal *32*, 1307–1321.

Gravel, S., Chapman, J.R., Magill, C., and Jackson, S.P. (2008). DNA helicases Sgs1 and BLM promote DNA double-strand break resection. Genes & Development *22*, 2767–2772.

Groth, P., Orta, M.L., Elvers, I., Majumder, M.M., Lagerqvist, A., and Helleday, T. (2012). Homologous recombination repairs secondary replication induced DNA double-strand breaks after ionizing radiation. Nucleic Acids Research *40*, 6585–6594.

Gu, Y., Turck, C.W., and Morgan, D.O. (1993). Inhibition of CDK2 activity in vivo by an associated 20K regulatory subunit. Nature *366*, 707–710.

Guan, K.L., Jenkins, C.W., Li, Y., Nichols, M.A., Wu, X., O'Keefe, C.L., Matera, A.G., and Xiong, Y. (1994). Growth suppression by p18, a p16INK4/MTS1- and p14INK4B/MTS2-related CDK6 inhibitor, correlates with wild-type pRb function. Genes & Development *8*, 2939–2952.

Gudmundsdottir, K., Lord, C.J., and Ashworth, A. (2007). The proteasome is involved in determining differential utilization of double-strand break repair pathways. Oncogene *26*, 7601–7606.

Gygi, S.P., Rochon, Y., Franza, B.R., and Aebersold, R. (1999). Correlation between protein and mRNA abundance in yeast. Molecular and Cellular Biology *19*, 1720–1730.

Haaf, T., Golub, E.I., Reddy, G., Radding, C.M., and Ward, D.C. (1995). Nuclear foci of mammalian Rad51 recombination protein in somatic cells after DNA damage and its localization in synaptonemal complexes. Proceedings of the National Academy of Sciences of the United States of America *92*, 2298–2302.

Haar, ter, E., Coll, J.T., Austen, D.A., Hsiao, H.M., Swenson, L., and Jain, J. (2001). Structure of GSK3beta reveals a primed phosphorylation mechanism. Nat. Struct. Biol. *8*, 593–596.

Haglund, K., Sigismund, S., Polo, S., Szymkiewicz, I., Di Fiore, P.P., and Dikic, I. (2003). Multiple monoubiquitination of RTKs is sufficient for their endocytosis and degradation. Nat. Cell Biol. *5*, 461–466.

Hanahan, D., and Weinberg, R.A. (2000). The hallmarks of cancer. Cell *100*, 57–70.

Hannon, G.J., and Beach, D. (1994). p15INK4B is a potential effector of TGF-beta-induced cell cycle arrest. Nature *371*, 257–261.

Hansen, D.V., Loktev, A.V., Ban, K.H., and Jackson, P.K. (2004). Plk1 regulates activation of the anaphase promoting complex by phosphorylating and triggering SCFbetaTrCP-dependent destruction of the APC Inhibitor Emi1. Mol. Biol. Cell *15*, 5623–5634.

Hao, B., Oehlmann, S., Sowa, M.E., Harper, J.W., and Pavletich, N.P. (2007). Structure of a Fbw7-Skp1-cyclin E complex: multisite-phosphorylated substrate recognition by SCF ubiquitin ligases. Molecular Cell *26*, 131–143.

Happel, N., Stoldt, S., Schmidt, B., and Doenecke, D. (2009). M phase-specific phosphorylation of histone H1.5 at threonine 10 by GSK-3. Journal of Molecular Biology *386*, 339–350.

Harper, J.W., Adami, G.R., Wei, N., Keyomarsi, K., and Elledge, S.J. (1993). The p21 Cdk-interacting protein Cip1 is a potent inhibitor of G1 cyclin-dependent kinases. Cell *75*, 805–816.

Hashimoto, Y., Ray Chaudhuri, A., Lopes, M., and Costanzo, V. (2010). Rad51 protects nascent DNA from Mre11-dependent degradation and promotes continuous DNA synthesis. Nature Structural & Molecular Biology *17*, 1305–1311.

Hershko, A., and Ciechanover, A. (1998). The ubiquitin system. Annu. Rev. Biochem. *67*, 425–479.

Hershko, A., Heller, H., Elias, S., and Ciechanover, A. (1983). Components of ubiquitin-protein ligase system. Resolution, affinity purification, and role in protein breakdown. The Journal of Biological Chemistry *258*, 8206–8214.

Hirai, H., Roussel, M.F., Kato, J.Y., Ashmun, R.A., and Sherr, C.J. (1995). Novel INK4 proteins, p19 and p18, are specific inhibitors of the cyclin D-dependent kinases CDK4 and CDK6. Molecular and Cellular Biology *15*, 2672–2681.

Hjerpe, R., Aillet, F., Lopitz-Otsoa, F., Lang, V., England, P., and Rodriguez, M.S. (2009). Efficient protection and isolation of ubiquitylated proteins using tandem ubiquitin-binding entities. EMBO Reports *10*, 1250–1258.

Hockemeyer, D., Soldner, F., Beard, C., Gao, Q., Mitalipova, M., DeKelver, R.C., Katibah, G.E., Amora, R., Boydston, E.A., Zeitler, B., et al. (2009). Efficient targeting of expressed and silent genes in human ESCs and iPSCs using zinc-finger nucleases. Nat. Biotechnol. *27*, 851–857.

Hoeijmakers, J.H.J. (2009). DNA damage, aging, and cancer. N. Engl. J. Med. *361*, 1475–1485.

Huen, M.S.Y., Grant, R., Manke, I., Minn, K., Yu, X., Yaffe, M.B., and Chen, J. (2007). RNF8 transduces the DNA-damage signal via histone ubiquitylation and checkpoint protein assembly. Cell *131*, 901–914.

Huertas, P., and Jackson, S.P. (2009). Human CtIP Mediates Cell Cycle Control of DNA End Resection and Double Strand Break Repair. Journal of Biological Chemistry *284*, 9558–9565.

Hughes-Davies, L., Huntsman, D., Ruas, M., Fuks, F., Bye, J., Chin, S.-F., Milner, J., Brown, L.A., Hsu, F., Gilks, B., et al. (2003). EMSY links the BRCA2 pathway to sporadic breast and ovarian cancer. Cell *115*, 523–535.

Hussain, S., Wilson, J.B., Medhurst, A.L., Hejna, J., Witt, E., Ananth, S., Davies, A., Masson, J.-Y., Moses, R., West, S.C., et al. (2004). Direct interaction of FANCD2 with BRCA2 in DNA damage response pathways. Hum. Mol. Genet. *13*, 1241–1248.

Hussain, S., Witt, E., Huber, P.A.J., Medhurst, A.L., Ashworth, A., and Mathew, C.G. (2003). Direct interaction of the Fanconi anaemia protein FANCG with BRCA2/FANCD1. Hum. Mol. Genet. *12*, 2503–2510.

Ira, G., Pellicioli, A., Balijja, A., Wang, X., Fiorani, S., Carotenuto, W., Liberi, G., Bressan, D., Wan, L., Hollingsworth, N.M., et al. (2004). DNA end resection, homologous recombination and DNA damage checkpoint activation require CDK1. Nature *431*, 1011–1017.

Iwabuchi, K., Hashimoto, M., Matsui, T., Kurihara, T., Shimizu, H., Adachi, N., Ishiai, M., Yamamoto, K.-I., Tauchi, H., Takata, M., et al. (2006). 53BP1 contributes to survival of cells irradiated with X-ray during G1 without Ku70 or Artemis. Genes Cells *11*, 935–948.

Jackson, S.P., and Bartek, J. (2009). The DNA-damage response in human biology and disease. Nature *461*, 1071–1078.

Jacquemont, C., and Taniguchi, T. (2007). Proteasome function is required for DNA damage response and fanconi anemia pathway activation. Cancer Research *67*, 7395–7405.

Jallepalli, P.V., Waizenegger, I.C., Bunz, F., Langer, S., Speicher, M.R., Peters, J.M., Kinzler, K.W., Vogelstein, B., and Lengauer, C. (2001). Securin is required for chromosomal stability in human cells. Cell *105*, 445–457.

Jaspersen, S.L., Charles, J.F., and Morgan, D.O. (1999). Inhibitory phosphorylation of the APC regulator Hct1 is controlled by the kinase Cdc28 and the phosphatase Cdc14. Current Biology : CB *9*, 227–236.

Jazayeri, A., Falck, J., Lukas, C., Bartek, J., Smith, G.C.M., Lukas, J., and Jackson, S.P. (2006). ATM- and cell cycle-dependent regulation of ATR in response to DNA double-strand breaks. Nat. Cell Biol. *8*, 37–45.

Jensen, R.B., Carreira, A., and Kowalczykowski, S.C. (2010). Purified human BRCA2 stimulates RAD51-mediated recombination. Nature *467*, 678–683.

Jin, J., Ang, X.L., Shirogane, T., and Wade Harper, J. (2005). Identification of substrates for F-box proteins. Meth. Enzymol. *399*, 287–309.

Jin, J., Cardozo, T., Lovering, R.C., Elledge, S.J., Pagano, M., and Harper, J.W. (2004). Systematic analysis and nomenclature of mammalian F-box proteins. Genes & Development *18*, 2573–2580.

Jin, L., Williamson, A., Banerjee, S., Philipp, I., and Rape, M. (2008). Mechanism of ubiquitin-chain formation by the human anaphase-promoting complex. Cell *133*, 653–665.

Johnson, E.S., Ma, P.C., Ota, I.M., and Varshavsky, A. (1995). A proteolytic pathway that recognizes ubiquitin as a degradation signal. The Journal of Biological Chemistry *270*, 17442–17456.

Justice, N.J., and Jan, Y.N. (2002). Variations on the Notch pathway in neural development. Curr. Opin. Neurobiol. *12*, 64–70.

Kim, H., Chen, J., and Yu, X. (2007). Ubiquitin-binding protein RAP80 mediates BRCA1-dependent DNA damage response. Science *316*, 1202–1205.

Kim, S., Mohapatra, G., and Haber, D.A. (2008). In vitro phosphorylation of BRCA2 by the checkpoint kinase CHEK2. Br. J. Cancer *99*, 1302–1306.

Kinzler, K.W., and Vogelstein, B. (1996). Lessons from hereditary colorectal cancer. Cell *87*, 159–170.

Kirisako, T., Kamei, K., Murata, S., Kato, M., Fukumoto, H., Kanie, M., Sano, S., Tokunaga, F., Tanaka, K., and Iwai, K. (2006). A ubiquitin ligase complex assembles linear polyubiquitin chains. The EMBO Journal *25*, 4877–4887.

Kitagawa, R., Bakkenist, C.J., McKinnon, P.J., and Kastan, M.B. (2004). Phosphorylation of SMC1 is a critical downstream event in the ATM-NBS1-BRCA1 pathway. Genes & Development *18*, 1423–1438.

Klotz, K., Cepeda, D., Tan, Y., Sun, D., Sangfelt, O., and Spruck, C. (2009). SCF(Fbxw7/hCdc4) targets cyclin E2 for ubiquitin-dependent proteolysis. Exp. Cell Res. *315*, 1832–1839.

Koepp, D.M., Schaefer, L.K., Ye, X., Keyomarsi, K., Chu, C., Harper, J.W., and Elledge, S.J. (2001). Phosphorylation-dependent ubiquitination of cyclin E by the SCFFbw7 ubiquitin ligase. Science (New York, N.Y.) *294*, 173–177.

Kojic, M., Zhou, Q., Lisby, M., and Holloman, W.K. (2005). Brh2-Dss1 interplay enables properly controlled recombination in Ustilago maydis. Molecular and Cellular Biology *25*, 2547–2557.

Kolas, N.K., Chapman, J.R., Nakada, S., Ylanko, J., Chahwan, R., Sweeney, F.D., Panier, S., Mendez, M., Wildenhain, J., Thomson, T.M., et al. (2007). Orchestration of the DNA-damage response by the RNF8 ubiquitin ligase. Science *318*, 1637–1640.

Komander, D., Reyes-Turcu, F., Licchesi, J.D.F., Odenwaelder, P., Wilkinson, K.D., and Barford, D. (2009). Molecular discrimination of structurally equivalent Lys 63-linked and linear polyubiquitin chains. EMBO Reports *10*, 466–473.

Kraft, C., Herzog, F., Gieffers, C., Mechtler, K., Hagting, A., Pines, J., and Peters, J.-M. (2003). Mitotic regulation of the human anaphase-promoting complex by phosphorylation. The EMBO Journal *22*, 6598–6609.

Kramer, E.R., Gieffers, C., Hölzl, G., Hengstschläger, M., and Peters, J.M. (1998). Activation of the human anaphase-promoting complex by proteins of the CDC20/Fizzy family. Current Biology : CB *8*, 1207–1210.

Kristensen, C.N., Bystol, K.M., Li, B., Serrano, L., and Brenneman, M.A. (2010). Depletion of DSS1 protein disables homologous recombinational repair in human cells. Mutat. Res. *694*, 60–64.

Krogan, N.J., Lam, M.H.Y., Fillingham, J., Keogh, M.-C., Gebbia, M., Li, J., Datta, N., Cagney, G., Buratowski, S., Emili, A., et al. (2004). Proteasome involvement in the repair of DNA double-strand breaks. Molecular Cell *16*, 1027–1034.

Kulukian, A., Han, J.S., and Cleveland, D.W. (2009). Unattached kinetochores catalyze production of an anaphase inhibitor that requires a Mad2 template to prime Cdc20 for BubR1 binding. Dev. Cell *16*, 105–117.

Kwon, Y.-W., Kim, I.-J., Wu, D., Lu, J., Stock, W.A., Liu, Y., Huang, Y., Kang, H.C., DelRosario, R., Jen, K.-Y., et al. (2012). Pten regulates Aurora-A and cooperates with Fbxw7 in modulating radiation-induced tumor development. Mol. Cancer Res. *10*, 834–844.

Laemmli, U.K. (1970). Cleavage of structural proteins during the assembly of the head of bacteriophage T4. Nature *227*, 680–685.

Landy, A. (1989). Dynamic, structural, and regulatory aspects of lambda site-specific recombination. Annu. Rev. Biochem. *58*, 913–949.

Lee, J.-H., and Paull, T.T. (2005). ATM activation by DNA double-strand breaks through the Mre11-Rad50-Nbs1 complex. Science *308*, 551–554.

Lee, M.H., Reynisdóttir, I., and Massagué, J. (1995). Cloning of p57KIP2, a cyclin-dependent kinase inhibitor with unique domain structure and tissue distribution. Genes & Development *9*, 639–649.

Lee, M., Daniels, M.J., and Venkitaraman, A.R. (2004). Phosphorylation of BRCA2 by the Polo-like kinase Plk1 is regulated by DNA damage and mitotic progression. Oncogene *23*, 865–872.

Lee, S., Tsai, Y.C., Mattera, R., Smith, W.J., Kostelansky, M.S., Weissman, A.M., Bonifacino, J.S., and Hurley, J.H. (2006). Structural basis for ubiquitin recognition and autoubiquitination by Rabex-5. Nature Structural & Molecular Biology *13*, 264–271.

Levy-Barda, A., Lerenthal, Y., Davis, A.J., Chung, Y.M., Essers, J., Shao, Z., van Vliet, N., Chen, D.J., Hu, M.C.-T., Kanaar, R., et al. (2011). Involvement of the nuclear proteasome activator PA28γ in the cellular response to DNA double-strand breaks. Cell Cycle *10*, 4300–4310.

Li, W., Bengtson, M.H., Ulbrich, A., Matsuda, A., Reddy, V.A., Orth, A., Chanda, S.K., Batalov, S., and Joazeiro, C.A.P. (2008). Genome-wide and functional annotation of human E3 ubiquitin ligases identifies MULAN, a mitochondrial E3 that regulates the organelle's dynamics and signaling. PLoS ONE *3*, e1487.

Li, W., Tu, D., Brunger, A.T., and Ye, Y. (2007). A ubiquitin ligase transfers preformed polyubiquitin chains from a conjugating enzyme to a substrate. Nature *446*, 333–337.

Li, Y., and Hao, B. (2010). Structural basis of dimerization-dependent ubiquitination by the SCF(Fbx4) ubiquitin ligase. Journal of Biological Chemistry *285*, 13896–13906.

Liberi, G., Maffioletti, G., Lucca, C., Chiolo, I., Baryshnikova, A., Cotta-Ramusino, C., Lopes, M., Pellicioli, A., Haber, J.E., and Foiani, M. (2005). Rad51-dependent DNA structures accumulate at damaged replication forks in sgs1 mutants defective in the yeast ortholog of BLM RecQ helicase. Genes & Development *19*, 339–350.

Lim, H.H., Goh, P.Y., and Surana, U. (1998). Cdc20 is essential for the cyclosome-mediated proteolysis of both Pds1 and Clb2 during M phase in budding yeast. Current Biology : CB *8*, 231–234.

Limbo, O., Chahwan, C., Yamada, Y., de Bruin, R.A.M., Wittenberg, C., and Russell, P. (2007). Ctp1 Is a Cell-Cycle-Regulated Protein that Functions with Mre11 Complex to Control Double-Strand Break Repair by Homologous Recombination. Molecular Cell *28*, 134–146.

Lin, H.-R., Ting, N.S.Y., Qin, J., and Lee, W.-H. (2003). M phase-specific phosphorylation of BRCA2 by Polo-like kinase 1 correlates with the dissociation of the BRCA2-P/CAF complex. The Journal of Biological Chemistry *278*, 35979–35987.

Lindahl, T., and Barnes, D.E. (2000). Repair of endogenous DNA damage. Cold Spring Harb. Symp. Quant. Biol. *65*, 127–133.

Lindon, C., and Pines, J. (2004). Ordered proteolysis in anaphase inactivates Plk1 to contribute to proper mitotic exit in human cells. J. Cell Biol. *164*, 233–241.

Listovsky, T., Oren, Y.S., Yudkovsky, Y., Mahbubani, H.M., Weiss, A.M., Lebendiker, M., and Brandeis, M. (2004). Mammalian Cdh1/Fzr mediates its own degradation. The EMBO Journal *23*, 1619–1626.

Liu, J., Furukawa, M., Matsumoto, T., and Xiong, Y. (2002). NEDD8 modification of CUL1 dissociates p120(CAND1), an inhibitor of CUL1-SKP1 binding and SCF ligases. Molecular Cell *10*, 1511–1518.

Liu, J., Doty, T., Gibson, B., and Heyer, W.-D. (2010). Human BRCA2 protein promotes RAD51 filament formation on RPA-covered single-stranded DNA. Nature Structural & Molecular Biology *17*, 1260–1262.

Liu, Z., Wu, J., and Yu, X. (2007). CCDC98 targets BRCA1 to DNA damage sites. Nature Structural & Molecular Biology *14*, 716–720.

Lomonosov, M., Anand, S., Sangrithi, M., Davies, R., and Venkitaraman, A.R. (2003). Stabilization of stalled DNA replication forks by the BRCA2 breast cancer susceptibility protein. Genes & Development *17*, 3017–3022.

Lorca, T., Castro, A., Martinez, A.M., Vigneron, S., Morin, N., Sigrist, S., Lehner, C., Dorée, M., and Labbé, J.C. (1998). Fizzy is required for activation of the APC/cyclosome in Xenopus egg extracts. The EMBO Journal *17*, 3565–3575.

Lord, C.J., and Ashworth, A. (2012). The DNA damage response and cancer therapy. Nature *481*, 287–294.

Lovejoy, C.A., and Cortez, D. (2009). Common mechanisms of PIKK regulation. DNA Repair *8*, 1004–1008.

Lowenfels, A.B., and Maisonneuve, P. (2005). Risk factors for pancreatic cancer. J. Cell. Biochem. *95*, 649–656.

Lu, H., Guo, X., Meng, X., Liu, J., Allen, C., Wray, J., Nickoloff, J.A., and Shen, Z. (2005). The BRCA2-interacting protein BCCIP functions in RAD51 and BRCA2 focus formation and homologous recombinational repair. Molecular and Cellular Biology *25*, 1949–1957.

Lundgren, K., Walworth, N., Booher, R., Dembski, M., Kirschner, M., and Beach, D. (1991). mik1 and wee1 cooperate in the inhibitory tyrosine phosphorylation of cdc2. Cell *64*, 1111–1122.

Lyapina, S., Cope, G., Shevchenko, A., Serino, G., Tsuge, T., Zhou, C., Wolf, D.A., Wei, N., Shevchenko, A., and Deshaies, R.J. (2001). Promotion of NEDD-CUL1 conjugate cleavage by COP9 signalosome. Science (New York, N.Y.) *292*, 1382–1385.

Magwood, A.C., Mundia, M.M., and Baker, M.D. (2012). High Levels of Wild-Type BRCA2 Suppress Homologous Recombination. Journal of Molecular Biology *421*, 38–53.

Maier, T., Güell, M., and Serrano, L. (2009). Correlation of mRNA and protein in complex biological samples. FEBS Lett. *583*, 3966–3973.

Mailand, N., Falck, J., Lukas, C., Syljuâsen, R.G., Welcker, M., Bartek, J., and Lukas, J. (2000). Rapid destruction of human Cdc25A in response to DNA damage. Science (New York, N.Y.) *288*, 1425–1429.

Mailand, N., Bekker-Jensen, S., Faustrup, H., Melander, F., Bartek, J., Lukas, C., and Lukas, J. (2007). RNF8 ubiquitylates histones at DNA double-strand breaks and promotes assembly of repair proteins. Cell *131*, 887–900.

Mailand, N., Podtelejnikov, A.V., Groth, A., Mann, M., Bartek, J., and Lukas, J. (2002). Regulation of G(2)/M events by Cdc25A through phosphorylation-dependent modulation of its stability. The EMBO Journal *21*, 5911–5920.

Malone, J.L., Nelson, A.C., Lieberman, R., Anderson, S., and Holt, J.T. (2009). Oestrogen-mediated phosphorylation and stabilization of BRCA2 protein in breast. The Journal of Pathology *217*, 380–388.

Malumbres, M., Harlow, E., Hunt, T., Hunter, T., Lahti, J.M., Manning, G., Morgan, D.O., Tsai, L.-H., and Wolgemuth, D.J. (2009). Cyclin-dependent kinases: a family portrait. Nat. Cell Biol. *11*, 1275–1276.

Mao, J.-H., Perez-Losada, J., Wu, D., DelRosario, R., Tsunematsu, R., Nakayama, K.I., Brown, K., Bryson, S., and Balmain, A. (2004). Fbxw7/Cdc4 is a p53-dependent, haploinsufficient tumour suppressor gene. Nature *432*, 775–779.

Margottin-Goguet, F., Hsu, J.Y., Loktev, A., Hsieh, H.M., Reimann, J.D.R., and Jackson, P.K. (2003). Prophase destruction of Emi1 by the SCF(betaTrCP/Slimb) ubiquitin ligase activates the anaphase promoting complex to allow progression beyond prometaphase. Dev. Cell *4*, 813–826.

Marmorstein, L.Y., Kinev, A.V., Chan, G.K., Bochar, D.A., Beniya, H., Epstein, J.A., Yen, T.J., and Shiekhattar, R. (2001). A human BRCA2 complex containing a structural DNA binding component influences cell cycle progression. Cell *104*, 247–257.

Marston, N.J., Richards, W.J., Hughes, D., Bertwistle, D., Marshall, C.J., and Ashworth, A. (1999). Interaction between the product of the breast cancer susceptibility gene BRCA2 and DSS1, a protein functionally conserved from yeast to mammals. Molecular and Cellular Biology *19*, 4633–4642.

Maser, R.S., Choudhury, B., Campbell, P.J., Feng, B., Wong, K.-K., Protopopov, A., O'Neil, J., Gutierrez, A., Ivanova, E., Perna, I., et al. (2007). Chromosomally unstable mouse tumours have genomic alterations similar to diverse human cancers. Nature *447*, 966–971.

Matsumoto, M.L., Wickliffe, K.E., Dong, K.C., Yu, C., Bosanac, I., Bustos, D., Phu, L., Kirkpatrick, D.S., Hymowitz, S.G., Rape, M., et al. (2010). K11-linked polyubiquitination in cell cycle control revealed by a K11 linkage-specific antibody. Molecular Cell *39*, 477–484.

Matsuoka, S., Edwards, M.C., Bai, C., Parker, S., Zhang, P., Baldini, A., Harper, J.W., and Elledge, S.J. (1995). p57KIP2, a structurally distinct member of the p21CIP1 Cdk inhibitor family, is a candidate tumor suppressor gene. Genes & Development *9*, 650–662.

Merrick, C.J., Jackson, D., and Diffley, J.F.X. (2004). Visualization of altered replication dynamics after DNA damage in human cells. The Journal of Biological Chemistry *279*, 20067–20075.

Milner, J., Ponder, B., Hughes-Davies, L., Seltmann, M., and Kouzarides, T. (1997). Transcriptional activation functions in BRCA2. Nature *386*, 772–773.

Minella, A.C., Welcker, M., and Clurman, B.E. (2005). Ras activity regulates cyclin E degradation by the Fbw7 pathway. Proceedings of the National Academy of Sciences of the United States of America *102*, 9649–9654.

Moro, L. (2006). Up-regulation of Skp2 after Prostate Cancer Cell Adhesion to Basement Membranes Results in BRCA2 Degradation and Cell Proliferation. Journal of Biological Chemistry *281*, 22100–22107.

Moro, L., Arbini, A.A., Marra, E., and Greco, M. (2006). Up-regulation of Skp2 after prostate cancer cell adhesion to basement membranes results in BRCA2 degradation and cell proliferation. The Journal of Biological Chemistry *281*, 22100–22107.

Moynahan, M.E., Pierce, A.J., and Jasin, M. (2001). BRCA2 is required for homology-directed repair of chromosomal breaks. Molecular Cell *7*, 263–272.

Mukhopadhyay, D., and Riezman, H. (2007). Proteasome-independent functions of ubiquitin in endocytosis and signaling. Science *315*, 201–205.

Murakawa, Y., Sonoda, E., Barber, L.J., Zeng, W., Yokomori, K., Kimura, H., Niimi, A., Lehmann, A., Zhao, G.Y., Hochegger, H., et al. (2007). Inhibitors of the proteasome suppress homologous DNA recombination in mammalian cells. Cancer Research *67*, 8536–8543.

Nakayama, K.I., and Nakayama, K. (2006). Ubiquitin ligases: cell-cycle control and cancer. Nature Reviews. Cancer *6*, 369–381.

Nash, P., Tang, X., Orlicky, S., Chen, Q., Gertler, F.B., Mendenhall, M.D., Sicheri, F., Pawson, T., and Tyers, M. (2001). Multisite phosphorylation of a CDK inhibitor sets a threshold for the onset of DNA replication. Nature *414*, 514–521.

Nateri, A.S., Riera-Sans, L., Da Costa, C., and Behrens, A. (2004). The ubiquitin ligase SCFFbw7 antagonizes apoptotic JNK signaling. Science *303*, 1374–1378.

Nghiem, P., Park, P.K., Kim, Y., Vaziri, C., and Schreiber, S.L. (2001). ATR inhibition selectively sensitizes G1 checkpoint-deficient cells to lethal premature chromatin condensation. Proceedings of the National Academy of Sciences of the United States of America *98*, 9092–9097.

Nigg, E.A. (2001). Mitotic kinases as regulators of cell division and its checkpoints. Nature Reviews. Molecular Cell Biology *2*, 21–32.

Nishikawa, H., Ooka, S., Sato, K., Arima, K., Okamoto, J., Klevit, R.E., Fukuda, M., and Ohta, T. (2004). Mass spectrometric and mutational analyses reveal Lys-6-linked polyubiquitin chains catalyzed by BRCA1-BARD1 ubiquitin ligase. The Journal of Biological Chemistry *279*, 3916–3924.

O'Gorman, S., Fox, D.T., and Wahl, G.M. (1991). Recombinase-mediated gene activation and site-specific integration in mammalian cells. Science (New York, N.Y.) *251*, 1351–1355.

Oberg, C., Li, J., Pauley, A., Wolf, E., Gurney, M., and Lendahl, U. (2001). The Notch intracellular domain is ubiquitinated and negatively regulated by the mammalian Sel-10 homolog. The Journal of Biological Chemistry *276*, 35847–35853.

Olsen, J.V., Vermeulen, M., Santamaria, A., Kumar, C., Miller, M.L., Jensen, L.J., Gnad, F., Cox, J., Jensen, T.S., Nigg, E.A., et al. (2010). Quantitative phosphoproteomics reveals widespread full phosphorylation site occupancy during mitosis. Sci Signal *3*, ra3.

Orlicky, S., Tang, X., Willems, A., Tyers, M., and Sicheri, F. (2003). Structural basis for phosphodependent substrate selection and orientation by the SCFCdc4 ubiquitin ligase. Cell *112*, 243–256.

Osman, F., Dixon, J., Doe, C.L., and Whitby, M.C. (2003). Generating crossovers by resolution of nicked Holliday junctions: a role for Mus81-Eme1 in meiosis. Molecular Cell *12*, 761–774.

Pagano, M., Pepperkok, R., Verde, F., Ansorge, W., and Draetta, G. (1992). Cyclin A is required at two points in the human cell cycle. The EMBO Journal *11*, 961–971.

Parker, L.L., and Piwnica-Worms, H. (1992). Inactivation of the p34cdc2-cyclin B complex by the human WEE1 tyrosine kinase. Science (New York, N.Y.) *257*, 1955–1957.

Parker, L.L., Atherton-Fessler, S., and Piwnica-Worms, H. (1992). p107wee1 is a dual-specificity kinase that phosphorylates p34cdc2 on tyrosine 15. Proceedings of the National Academy of Sciences of the United States of America *89*, 2917–2921.

Passmore, L.A., McCormack, E.A., Au, S.W.N., Paul, A., Willison, K.R., Harper, J.W., and Barford, D. (2003). Doc1 mediates the activity of the anaphase-promoting complex by contributing to substrate recognition. The EMBO Journal *22*, 786–796.

Patel, K.J., Yu, V.P., Lee, H., Corcoran, A., Thistlethwaite, F.C., Evans, M.J., Colledge, W.H., Friedman, L.S., Ponder, B.A., and Venkitaraman, A.R. (1998). Involvement of Brca2 in DNA repair. Molecular Cell *1*, 347–357.

Pellegrini, L., Yu, D.S., Lo, T., Anand, S., Lee, M., Blundell, T.L., and Venkitaraman, A.R. (2002). Insights into DNA recombination from the structure of a RAD51--BRCA2 complex. Nature *420*, 1–7.

Penengo, L., Mapelli, M., Murachelli, A.G., Confalonieri, S., Magri, L., Musacchio, A., Di Fiore, P.P., Polo, S., and Schneider, T.R. (2006). Crystal structure of the ubiquitin binding domains of rabex-5 reveals two modes of interaction with ubiquitin. Cell *124*, 1183–1195.

Peng, J., Schwartz, D., Elias, J.E., Thoreen, C.C., Cheng, D., Marsischky, G., Roelofs, J., Finley, D., and Gygi, S.P. (2003). A proteomics approach to understanding protein ubiquitination. Nat. Biotechnol. *21*, 921–926.

Petroski, M.D., and Deshaies, R.J. (2003). Context of multiubiquitin chain attachment influences the rate of Sic1 degradation. Molecular Cell *11*, 1435–1444.

Petroski, M.D., and Deshaies, R.J. (2005a). Function and regulation of cullin-RING ubiquitin ligases. Nature Reviews. Molecular Cell Biology *6*, 9–20.

Petroski, M.D., and Deshaies, R.J. (2005b). Mechanism of lysine 48-linked ubiquitin-chain synthesis by the cullin-RING ubiquitin-ligase complex SCF-Cdc34. Cell *123*, 1107–1120.

Pfleger, C.M., and Kirschner, M.W. (2000). The KEN box: an APC recognition signal distinct from the D box targeted by Cdh1. Genes & Development *14*, 655–665.

Pierce, N.W., Lee, J.E., Liu, X., Sweredoski, M.J., Graham, R.L.J., Larimore, E.A., Rome, M., Zheng, N., Clurman, B.E., Hess, S., et al. (2013). Cand1 promotes assembly of new SCF complexes through dynamic exchange of F box proteins. Cell *153*, 206–215.

Polo, S. (2012). Signaling-mediated control of ubiquitin ligases in endocytosis. BMC Biol. *10*, 25.

Polyak, K., Lee, M.H., Erdjument-Bromage, H., Koff, A., Roberts, J.M., Tempst, P., and Massagué, J. (1994). Cloning of p27Kip1, a cyclin-dependent kinase inhibitor and a potential mediator of extracellular antimitogenic signals. Cell *78*, 59–66.

Popov, N., Herold, S., Llamazares, M., Schülein, C., and Eilers, M. (2007). Fbw7 and Usp28 regulate myc protein stability in response to DNA damage. Cell Cycle *6*, 2327–2331.

Puget, N., Knowlton, M., and Scully, R. (2005). Molecular analysis of sister chromatid recombination in mammalian cells. DNA Repair *4*, 149–161.

Punga, T., Bengoechea-Alonso, M.T., and Ericsson, J. (2006). Phosphorylation and ubiquitination of the transcription factor sterol regulatory element-binding protein-1 in response to DNA binding. The Journal of Biological Chemistry *281*, 25278–25286.

Rahighi, S., Ikeda, F., Kawasaki, M., Akutsu, M., Suzuki, N., Kato, R., Kensche, T., Uejima, T., Bloor, S., Komander, D., et al. (2009). Specific recognition of linear ubiquitin chains by NEMO is important for NF-kappaB activation. Cell *136*, 1098–1109.

Raiborg, C., Bache, K.G., Gillooly, D.J., Madshus, I.H., Stang, E., and Stenmark, H. (2002). Hrs sorts ubiquitinated proteins into clathrin-coated microdomains of early endosomes. Nat. Cell Biol. *4*, 394–398.

Rajagopalan, H., Jallepalli, P.V., Rago, C., Velculescu, V.E., Kinzler, K.W., Vogelstein, B., and Lengauer, C. (2004). Inactivation of hCDC4 can cause chromosomal instability. Nature *428*, 77–81.

Rajan, J.V., Wang, M., Marquis, S.T., and Chodosh, L.A. (1996). Brca2 is coordinately regulated with Brca1 during proliferation and differentiation in mammary epithelial cells. Proceedings of the National Academy of Sciences of the United States of America *93*, 13078–13083.

Reczek, C.R., Szabolcs, M., Stark, J.M., Ludwig, T., and Baer, R. (2013). The interaction between CtIP and BRCA1 is not essential for resection-mediated DNA repair or tumor suppression. J. Cell Biol. *201*, 693–707.

Reimann, J.D., Freed, E., Hsu, J.Y., Kramer, E.R., Peters, J.M., and Jackson, P.K. (2001). Emi1 is a mitotic regulator that interacts with Cdc20 and inhibits the anaphase promoting complex. Cell *105*, 645–655.

Ren, S., and Rollins, B.J. (2004). Cyclin C/cdk3 promotes Rb-dependent G0 exit. Cell *117*, 239–251.

Reviews, C.T., Walter, P., Alberts, B., Alberts, Al, E., Johnson, A., Lewis, J., and Raff, M. (2002). Molecular Biology of the Cell, Ise (Garland Science).

Rodrigo-Brenni, M.C., and Morgan, D.O. (2007). Sequential E2s drive polyubiquitin chain assembly on APC targets. Cell *130*, 127–139.

Rogakou, E.P., Pilch, D.R., Orr, A.H., Ivanova, V.S., and Bonner, W.M. (1998). DNA double-stranded breaks induce histone H2AX phosphorylation on serine 139. The Journal of Biological Chemistry *273*, 5858–5868.

Rosenblatt, J., Gu, Y., and Morgan, D.O. (1992). Human cyclin-dependent kinase 2 is activated during the S and G2 phases of the cell cycle and associates with cyclin A. Proceedings of the National Academy of Sciences of the United States of America *89*, 2824–2828.

Rother, K., Kirschner, R., Sänger, K., Böhlig, L., Mössner, J., and Engeland, K. (2007). p53 downregulates expression of the G1/S cell cycle phosphatase Cdc25A. Oncogene *26*, 1949–1953.

Rouet, P., Smih, F., and Jasin, M. (1994). Introduction of double-strand breaks into the genome of mouse cells by expression of a rare-cutting endonuclease. Molecular and Cellular Biology *14*, 8096–8106.

Rudner, A.D., and Murray, A.W. (2000). Phosphorylation by Cdc28 activates the Cdc20-dependent activity of the anaphase-promoting complex. J. Cell Biol. *149*, 1377–1390.

Russell, P., and Nurse, P. (1986). cdc25+ functions as an inducer in the mitotic control of fission yeast. Cell *45*, 145–153.

Russell, P., and Nurse, P. (1987). Negative regulation of mitosis by wee1+, a gene encoding a protein kinase homolog. Cell *49*, 559–567.

Saeki, Y., Kudo, T., Sone, T., Kikuchi, Y., Yokosawa, H., Toh-e, A., and Tanaka, K. (2009). Lysine 63-linked polyubiquitin chain may serve as a targeting signal for the 26S proteasome. The EMBO Journal *28*, 359–371.

Sage, J. (2004). Cyclin C makes an entry into the cell cycle. Dev. Cell *6*, 607–608.

Saha, A., and Deshaies, R.J. (2008). Multimodal activation of the ubiquitin ligase SCF by Nedd8 conjugation. Molecular Cell *32*, 21–31.

Sambrook, J., and Russell, D.W. (2001). [CITATION][C].

Scheffner, M., and Staub, O. (2007). HECT E3s and human disease. BMC Biochem. *8 Suppl 1*, S6.

Schlacher, K., Christ, N., Siaud, N., Egashira, A., Wu, H., and Jasin, M. (2011). Double-strand break repair-independent role for BRCA2 in blocking stalled replication fork degradation by MRE11. Cell *145*, 529–542.

Schoenfeld, A.R., Apgar, S., Dolios, G., Wang, R., and Aaronson, S.A. (2004). BRCA2 Is Ubiquitinated In Vivo and Interacts with USP11, a Deubiquitinating Enzyme That Exhibits Prosurvival Function in the Cellular Response to DNA Damage. Molecular and Cellular Biology *24*, 7444–7455.

Schwechheimer, C., Serino, G., Callis, J., Crosby, W.L., Lyapina, S., Deshaies, R.J., Gray, W.M., Estelle, M., and Deng, X.W. (2001). Interactions of the COP9 signalosome with the E3 ubiquitin ligase SCFTIRI in mediating auxin response. Science (New York, N.Y.) *292*, 1379–1382.

Scully, R., Chen, J., Ochs, R.L., Keegan, K., Hoekstra, M., Feunteun, J., and Livingston, D.M. (1997). Dynamic changes of BRCA1 subnuclear location and phosphorylation state are initiated by DNA damage. Cell *90*, 425–435.

Serrano, M., Hannon, G.J., and Beach, D. (1993). A new regulatory motif in cell-cycle control causing specific inhibition of cyclin D/CDK4. Nature *366*, 704–707.

Sharan, S.K., Morimatsu, M., Albrecht, U., Lim, D.S., Regel, E., Dinh, C., Sands, A., Eichele, G., Hasty, P., and Bradley, A. (1997). Embryonic lethality and radiation hypersensitivity mediated by Rad51 in mice lacking Brca2. Nature *386*, 804–810.

Shi, W., Ma, Z., Willers, H., Akhtar, K., Scott, S.P., Zhang, J., Powell, S., and Zhang, J. (2008). Disassembly of MDC1 foci is controlled by ubiquitin-proteasome-dependent degradation. The Journal of Biological Chemistry *283*, 31608–31616.

Shin, S., and Verma, I.M. (2003). BRCA2 cooperates with histone acetyltransferases in androgen receptor-mediated transcription. Proceedings of the National Academy of Sciences of the United States of America *100*, 7201–7206.

Shirayama, M., Zachariae, W., Ciosk, R., and Nasmyth, K. (1998). The Polo-like kinase Cdc5p and the WD-repeat protein Cdc20p/fizzy are regulators and substrates of the anaphase promoting complex in Saccharomyces cerevisiae. The EMBO Journal *17*, 1336–1349.

Shivji, M.K.K., Davies, O.R., Savill, J.M., Bates, D.L., Pellegrini, L., and Venkitaraman, A.R. (2006). A region of human BRCA2 containing multiple BRC repeats promotes RAD51-mediated strand exchange. Nucleic Acids Research *34*, 4000–4011.

Sigrist, S., Jacobs, H., Stratmann, R., and Lehner, C.F. (1995). Exit from mitosis is regulated by Drosophila fizzy and the sequential destruction of cyclins A, B and B3. The EMBO Journal *14*, 4827–4838.

Simard, J., Dumont, M., Labuda, D., Sinnett, D., Meloche, C., El-Alfy, M., Berger, L., Lees, E., Labrie, F., and Tavtigian, S.V. (2003). Prostate cancer susceptibility genes: lessons learned and challenges posed. Endocr. Relat. Cancer *10*, 225–259.

Skaar, J.R., Pagan, J.K., and Pagano, M. (2013). Mechanisms and function of substrate recruitment by F-box proteins. Nature Reviews. Molecular Cell Biology *14*, 369–381.

Skowyra, D., Craig, K.L., Tyers, M., Elledge, S.J., and Harper, J.W. (1997). F-box proteins are receptors that recruit phosphorylated substrates to the SCF ubiquitin-ligase complex. Cell *91*, 209–219.

Sobhian, B., Shao, G., Lilli, D.R., Culhane, A.C., Moreau, L.A., Xia, B., Livingston, D.M., and Greenberg, R.A. (2007). RAP80 targets BRCA1 to specific ubiquitin structures at DNA damage sites. Science *316*, 1198–1202.

Sowa, M.E., Bennett, E.J., Gygi, S.P., and Harper, J.W. (2009). Defining the human deubiquitinating enzyme interaction landscape. Cell *138*, 389–403.

Spence, J., Sadis, S., Haas, A.L., and Finley, D. (1995). A ubiquitin mutant with specific defects in DNA repair and multiubiquitination. Molecular and Cellular Biology *15*, 1265–1273.

Spruck, C.H., Strohmaier, H., Sangfelt, O., Müller, H.M., Hubalek, M., Müller-Holzner, E., Marth, C., Widschwendter, M., and Reed, S.I. (2002). hCDC4 gene mutations in endometrial cancer. Cancer Research *62*, 4535–4539.

Stewart, G.S., Panier, S., Townsend, K., Al-Hakim, A.K., Kolas, N.K., Miller, E.S., Nakada, S., Ylanko, J., Olivarius, S., Mendez, M., et al. (2009). The RIDDLE syndrome protein mediates a ubiquitin-dependent signaling cascade at sites of DNA damage. Cell *136*, 420–434.

Stewart, S., and Fang, G. (2005). Destruction box-dependent degradation of aurora B is mediated by the anaphase-promoting complex/cyclosome and Cdh1. Cancer Research *65*, 8730–8735.

Strohmaier, H., Spruck, C.H., Kaiser, P., Won, K.A., Sangfelt, O., and Reed, S.I. (2001). Human F-box protein hCdc4 targets cyclin E for proteolysis and is mutated in a breast cancer cell line. Nature *413*, 316–322.

Stucki, M., Clapperton, J.A., Mohammad, D., Yaffe, M.B., Smerdon, S.J., and Jackson, S.P. (2005). MDC1 directly binds phosphorylated histone H2AX to regulate cellular responses to DNA double-strand breaks. Cell *123*, 1213–1226.

Sudakin, V., Chan, G.K., and Yen, T.J. (2001). Checkpoint inhibition of the APC/C in HeLa cells is mediated by a complex of BUBR1, BUB3, CDC20, and MAD2. J. Cell Biol. *154*, 925–936.

Sudakin, V., Ganoth, D., Dahan, A., Heller, H., Hershko, J., Luca, F.C., Ruderman, J.V., and Hershko, A. (1995). The cyclosome, a large complex containing cyclin-selective ubiquitin ligase activity, targets cyclins for destruction at the end of mitosis. Mol. Biol. Cell *6*, 185–197.

Sundqvist, A., Bengoechea-Alonso, M.T., Ye, X., Lukiyanchuk, V., Jin, J., Harper, J.W., and Ericsson, J. (2005). Control of lipid metabolism by phosphorylation-dependent degradation of the SREBP family of transcription factors by SCF(Fbw7). Cell Metab. *1*, 379–391.

Svendsen, J.M., Smogorzewska, A., Sowa, M.E., O'Connell, B.C., Gygi, S.P., Elledge, S.J., and Harper, J.W. (2009). Mammalian BTBD12/SLX4 assembles a Holliday junction resolvase and is required for DNA repair. Cell *138*, 63–77.

Swanson, K.A., Kang, R.S., Stamenova, S.D., Hicke, L., and Radhakrishnan, I. (2003). Solution structure of Vps27 UIM-ubiquitin complex important for endosomal sorting and receptor downregulation. The EMBO Journal *22*, 4597–4606.

Sy, S.M.-H., Huen, M.S.Y., and Chen, J. (2009). PALB2 is an integral component of the BRCA complex required for homologous recombination repair. Proceedings of the National Academy of Sciences *106*, 7155–7160.

Taguchi, S.I., Honda, K., Sugiura, K., Yamaguchi, A., Furukawa, K., and Urano, T. (2002). Degradation of human Aurora-A protein kinase is mediated by hCdh1. FEBS Lett. *519*, 59–65.

Takata, M., Tachiiri, S., Fujimori, A., Thompson, L.H., Miki, Y., Hiraoka, M., Takeda, S., and Yamazoe, M. (2002). Conserved domains in the chicken homologue of BRCA2. Oncogene *21*, 1130–1134.

Tang, X., Orlicky, S., Lin, Z., Willems, A., Neculai, D., Ceccarelli, D., Mercurio, F., Shilton, B.H., Sicheri, F., and Tyers, M. (2007). Suprafacial orientation of the SCFCdc4 dimer accommodates multiple geometries for substrate ubiquitination. Cell *129*, 1165–1176.

Tarsounas, M., Davies, D., and West, S.C. (2003). BRCA2-dependent and independent formation of RAD51 nuclear foci. Oncogene *22*, 1115–1123.

Teixeira, L.K., and Reed, S.I. (2013). Ubiquitin ligases and cell cycle control. Annu. Rev. Biochem. *82*, 387–414.

Thorslund, T., Esashi, F., and West, S.C. (2007). Interactions between human BRCA2 protein and the meiosis-specific recombinase DMC1. The EMBO Journal *26*, 2915–2922.

Thorslund, T., McIlwraith, M.J., Compton, S.A., Lekomtsev, S., Petronczki, M., Griffith, J.D., and West, S.C. (2010). The breast cancer tumor suppressor BRCA2 promotes the specific targeting of RAD51 to single-stranded DNA. Nature Structural & Molecular Biology *17*, 1263–1265.

Thrower, J.S., Hoffman, L., Rechsteiner, M., and Pickart, C.M. (2000). Recognition of the polyubiquitin proteolytic signal. The EMBO Journal *19*, 94–102.

Tomashevski, A., Webster, D.R., Grammas, P., Gorospe, M., and Kruman, I.I. (2010). Cyclin-C-dependent cell-cycle entry is required for activation of non-homologous end joining DNA repair in postmitotic neurons. Cell Death Differ. *17*, 1189–1198.

Tron, A.E., Arai, T., Duda, D.M., Kuwabara, H., Olszewski, J.L., Fujiwara, Y., Bahamon, B.N., Signoretti, S., Schulman, B.A., and DeCaprio, J.A. (2012). The glomuvenous malformation protein Glomulin binds Rbx1 and regulates cullin RING ligase-mediated turnover of Fbw7. Molecular Cell *46*, 67–78.

Tutt, A. (2001). Mutation in Brca2 stimulates error-prone homology-directed repair of DNA double-strand breaks occurring between repeated sequences. The EMBO Journal *20*, 4704–4716.

Tutt, A., Gabriel, A., Bertwistle, D., Connor, F., Paterson, H., Peacock, J., Ross, G., and Ashworth, A. (1999). Absence of Brca2 causes genome instability by chromosome breakage and loss associated with centrosome amplification. Current Biology : CB *9*, 1107–1110.

Uhlmann, F., Lottspeich, F., and Nasmyth, K. (1999). Sister-chromatid separation at anaphase onset is promoted by cleavage of the cohesin subunit Scc1. Nature *400*, 37–42.

Ustrell, V., Hoffman, L., Pratt, G., and Rechsteiner, M. (2002). PA200, a nuclear proteasome activator involved in DNA repair. The EMBO Journal *21*, 3516–3525.

Uziel, T., Lerenthal, Y., Moyal, L., Andegeko, Y., Mittelman, L., and Shiloh, Y. (2003). Requirement of the MRN complex for ATM activation by DNA damage. The EMBO Journal *22*, 5612–5621.

van Veelen, L.R., Cervelli, T., van de Rakt, M.W.M.M., Theil, A.F., Essers, J., and Kanaar, R. (2005). Analysis of ionizing radiation-induced foci of DNA damage repair proteins. Mutat. Res. *574*, 22–33.

VanDemark, A.P., Hofmann, R.M., Tsui, C., Pickart, C.M., and Wolberger, C. (2001). Molecular insights into polyubiquitin chain assembly: crystal structure of the Mms2/Ubc13 heterodimer. Cell *105*, 711–720.

Vaughn, J.P., Cirisano, F.D., Huper, G., Berchuck, A., Futreal, P.A., Marks, J.R., and Iglehart, J.D. (1996a). Cell cycle control of BRCA2. Cancer Research *56*, 4590–4594.

Vaughn, J.P., Davis, P.L., Jarboe, M.D., Huper, G., Evans, A.C., Wiseman, R.W., Berchuck, A., Iglehart, J.D., Futreal, P.A., and Marks, J.R. (1996b). BRCA1 expression is induced before DNA synthesis in both normal and tumor-derived breast cells. Cell Growth & Differentiation : the Molecular Biology Journal of the American Association for Cancer Research *7*, 711–715.

Venkitaraman, A.R. (2002). Cancer susceptibility and the functions of BRCA1 and BRCA2. Cell *108*, 171–182.

Visintin, R., Prinz, S., and Amon, A. (1997). CDC20 and CDH1: a family of substrate-specific activators of APC-dependent proteolysis. Science (New York, N.Y.) *278*, 460–463.

Vogel, C., and Marcotte, E.M. (2012). Insights into the regulation of protein abundance from proteomic and transcriptomic analyses. Nat. Rev. Genet. *13*, 227–232.

Waizenegger, I.C., Hauf, S., Meinke, A., and Peters, J.M. (2000). Two distinct pathways remove mammalian cohesin from chromosome arms in prophase and from centromeres in anaphase. Cell *103*, 399–410.

Wang, B., and Elledge, S.J. (2007). Ubc13/Rnf8 ubiquitin ligases control foci formation of the Rap80/Abraxas/Brca1/Brcc36 complex in response to DNA damage. Proceedings of the National Academy of Sciences *104*, 20759–20763.

Wang, H., Shi, L.Z., Wong, C.C.L., Han, X., Hwang, P.Y.-H., Truong, L.N., Zhu, Q., Shao, Z., Chen, D.J., Berns, M.W., et al. (2013). The interaction of CtIP and Nbs1 connects CDK and ATM to regulate HR-mediated double-strand break repair. PLoS Genetics *9*, e1003277.

Wang, Q., Young, P., and Walters, K.J. (2005). Structure of S5a bound to monoubiquitin provides a model for polyubiquitin recognition. Journal of Molecular Biology *348*, 727–739.

Wang, S.C., Lin, S.H., Su, L.K., and Hung, M.C. (1997). Changes in BRCA2 expression during progression of the cell cycle. Biochem. Biophys. Res. Commun. *234*, 247–251.

Wang, S.-C., Makino, K., Su, L.-K., Pao, A.Y., Kim, J.S., and Hung, M.-C. (2001). Ultraviolet irradiation induces BRCA2 protein depletion through a p53-independent and protein synthesis-dependent pathway.

Wang, X., and D'Andrea, A.D. (2004). The interplay of Fanconi anemia proteins in the DNA damage response. DNA Repair *3*, 1063–1069.

Watanabe, N., Arai, H., Nishihara, Y., Taniguchi, M., Watanabe, N., Hunter, T., and Osada, H. (2004). M-phase kinases induce phospho-dependent ubiquitination of somatic Wee1 by SCFbeta-TrCP. Proceedings of the National Academy of Sciences of the United States of America *101*, 4419–4424.

Wei, W., Ayad, N.G., Wan, Y., Zhang, G.-J., Kirschner, M.W., and Kaelin, W.G. (2004). Degradation of the SCF component Skp2 in cell-cycle phase G1 by the anaphase-promoting complex. Nature *428*, 194–198.

Wei, W., Jin, J., Schlisio, S., Harper, J.W., and Kaelin, W.G. (2005). The v-Jun point mutation allows c-Jun to escape GSK3-dependent recognition and destruction by the Fbw7 ubiquitin ligase. Cancer Cell *8*, 25–33.

Wei, Y., Yu, L., Bowen, J., Gorovsky, M.A., and Allis, C.D. (1999). Phosphorylation of histone H3 is required for proper chromosome condensation and segregation. Cell *97*, 99–109.

Welcker, M., and Clurman, B.E. (2005). The SV40 large T antigen contains a decoy phosphodegron that mediates its interactions with Fbw7/hCdc4. The Journal of Biological Chemistry *280*, 7654–7658.

Welcker, M., and Clurman, B.E. (2007). Fbw7/hCDC4 dimerization regulates its substrate interactions. Cell Div *2*, 7.

Welcker, M., and Clurman, B.E. (2008). FBW7 ubiquitin ligase: a tumour suppressor at the crossroads of cell division, growth and differentiation. Nature Reviews. Cancer *8*, 83–93.

Welcker, M., Orian, A., Grim, J.E., Grim, J.A., Eisenman, R.N., and Clurman, B.E. (2004a). A nucleolar isoform of the Fbw7 ubiquitin ligase regulates c-Myc and cell size. Current Biology : CB *14*, 1852–1857.

Welcker, M., Orian, A., Jin, J., Grim, J.E., Grim, J.A., Harper, J.W., Eisenman, R.N., and Clurman, B.E. (2004b). The Fbw7 tumor suppressor regulates glycogen synthase kinase 3 phosphorylation-dependent c-Myc protein degradation. Proceedings of the National Academy of Sciences of the United States of America *101*, 9085–9090.

Welcker, M., Singer, J., Loeb, K.R., Grim, J., Bloecher, A., Gurien-West, M., Clurman, B.E., and Roberts, J.M. (2003). Multisite phosphorylation by Cdk2 and GSK3 controls cyclin E degradation. Molecular Cell *12*, 381–392.

Weng, A.P., Ferrando, A.A., Lee, W., Morris, J.P., Silverman, L.B., Sanchez-Irizarry, C., Blacklow, S.C., Look, A.T., and Aster, J.C. (2004). Activating mutations of NOTCH1 in human T cell acute lymphoblastic leukemia. Science *306*, 269–271.

Wickliffe, K.E., Lorenz, S., Wemmer, D.E., Kuriyan, J., and Rape, M. (2011). The mechanism of linkage-specific ubiquitin chain elongation by a single-subunit E2. Cell *144*, 769–781.

Williamson, A., Banerjee, S., Zhu, X., Philipp, I., Iavarone, A.T., and Rape, M. (2011). Regulation of ubiquitin chain initiation to control the timing of substrate degradation. Molecular Cell *42*, 744–757.

Williamson, A., Wickliffe, K.E., Mellone, B.G., Song, L., Karpen, G.H., and Rape, M. (2009). Identification of a physiological E2 module for the human anaphase-promoting complex. Proceedings of the National Academy of Sciences *106*, 18213–18218.

Wohlbold, L., Merrick, K.A., De, S., Amat, R., Kim, J.H., Larochelle, S., Allen, J.J., Zhang, C., Shokat, K.M., Petrini, J.H.J., et al. (2012). Chemical genetics reveals a specific requirement for Cdk2 activity in the DNA damage response and identifies Nbs1 as a Cdk2 substrate in human cells. PLoS Genetics *8*, e1002935.

Wong, A.K., Pero, R., Ormonde, P.A., Tavtigian, S.V., and Bartel, P.L. (1997). RAD51 interacts with the evolutionarily conserved BRC motifs in the human breast cancer susceptibility gene brca2. The Journal of Biological Chemistry *272*, 31941–31944.

Wong, C., and Stearns, T. (2005). Mammalian cells lack checkpoints for tetraploidy, aberrant centrosome number, and cytokinesis failure. BMC Cell Biol. *6*, 6.

Wooster, R., Bignell, G., Lancaster, J., Swift, S., Seal, S., Mangion, J., Collins, N., Gregory, S., Gumbs, C., Micklem, G., et al. (1995). Identification of the breast cancer susceptibility gene BRCA2. Nature *378*, 789–792.

Wu, G., Lyapina, S., Das, I., Li, J., Gurney, M., Pauley, A., Chui, I., Deshaies, R.J., and Kitajewski, J. (2001). SEL-10 is an inhibitor of notch signaling that targets notch for ubiquitin-mediated protein degradation. Molecular and Cellular Biology *21*, 7403–7415.

Wu, J., Zhang, X., Zhang, L., Wu, C.-Y., Rezaeian, A.H., Chan, C.-H., Li, J.-M., Wang, J., Gao, Y., Han, F., et al. (2012). Skp2 E3 ligase integrates ATM activation and homologous recombination repair by ubiquitinating NBS1. Molecular Cell *46*, 351–361.

Wu, L., Bachrati, C.Z., Ou, J., Xu, C., Yin, J., Chang, M., Wang, W., Li, L., Brown, G.W., and Hickson, I.D. (2006). BLAP75/RMI1 promotes the BLM-dependent dissolution of homologous recombination intermediates. Proceedings of the National Academy of Sciences of the United States of America *103*, 4068–4073.

Wu, S., Zhu, W., Nhan, T., Toth, J.I., Petroski, M.D., and Wolf, D.A. (2013). CAND1 controls in vivo dynamics of the cullin 1-RING ubiquitin ligase repertoire. Nat Commun *4*, 1642.

Xia, F., Taghian, D.G., DeFrank, J.S., Zeng, Z.C., Willers, H., Iliakis, G., and Powell, S.N. (2001). Deficiency of human BRCA2 leads to impaired homologous recombination but maintains normal nonhomologous end joining. Proceedings of the National Academy of Sciences of the United States of America *98*, 8644–8649.

Xu, M., Skaug, B., Zeng, W., and Chen, Z.J. (2009). A ubiquitin replacement strategy in human cells reveals distinct mechanisms of IKK activation by TNFalpha and IL-1beta. Molecular Cell *36*, 302–314.

Yada, M., Hatakeyama, S., Kamura, T., Nishiyama, M., Tsunematsu, R., Imaki, H., Ishida, N., Okumura, F., Nakayama, K., and Nakayama, K.I. (2004). Phosphorylation-dependent degradation of c-Myc is mediated by the F-box protein Fbw7. The EMBO Journal *23*, 2116–2125.

Yang, H., Jeffrey, P.D., Miller, J., Kinnucan, E., Sun, Y., Thomä, N.H., Zheng, N., Chen, P.-L., Lee, W.-H., and Pavletich, N.P. (2002). BRCA2 Function in DNA Binding and Recombination from a BRCA2-DSS1-ssDNA Structure. Science (New York, N.Y.) *297*, 1837–1848.

Yata, K., Lloyd, J., Maslen, S., Bleuyard, J.-Y., Skehel, M., Smerdon, S.J., and Esashi, F. (2012). Plk1 and CK2 Act in Concert to Regulate Rad51 during DNA Double Strand Break Repair. Molecular Cell *45*, 371–383.

Ye, X., Nalepa, G., Welcker, M., Kessler, B.M., Spooner, E., Qin, J., Elledge, S.J., Clurman, B.E., and Harper, J.W. (2004). Recognition of phosphodegron motifs in human cyclin E by the SCF(Fbw7) ubiquitin ligase. The Journal of Biological Chemistry *279*, 50110–50119.

Yen, H.-C.S., Xu, Q., Chou, D.M., Zhao, Z., and Elledge, S.J. (2008). Global protein stability profiling in mammalian cells. Science *322*, 918–923.

Yin, Y., Seifert, A., Chua, J.S., Maure, J.-F., Golebiowski, F., and Hay, R.T. (2012). SUMO-targeted ubiquitin E3 ligase RNF4 is required for the response of human cells to DNA damage. Genes & Development *26*, 1196–1208.

Ying, S., Hamdy, F.C., and Helleday, T. (2012). Mre11-dependent degradation of stalled DNA replication forks is prevented by BRCA2 and PARP1. Cancer Research *72*, 2814–2821.

Youds, J.L., Mets, D.G., McIlwraith, M.J., Martin, J.S., Ward, J.D., O'Neil, N.J., Rose, A.M., West, S.C., Meyer, B.J., and Boulton, S.J. (2010). RTEL-1 enforces meiotic crossover interference and homeostasis. Science *327*, 1254–1258.

Yu, D.S., Sonoda, E., Takeda, S., Huang, C.L.H., Pellegrini, L., Blundell, T.L., and Venkitaraman, A.R. (2003). Dynamic control of Rad51 recombinase by self-association and interaction with BRCA2. Molecular Cell *12*, 1029–1041.

Yu, V.P., Koehler, M., Steinlein, C., Schmid, M., Hanakahi, L.A., van Gool, A.J., West, S.C., and Venkitaraman, A.R. (2000). Gross chromosomal rearrangements and genetic exchange between nonhomologous chromosomes following BRCA2 inactivation. Genes & Development *14*, 1400–1406.

Yu, X., and Chen, J. (2004). DNA damage-induced cell cycle checkpoint control requires CtIP, a phosphorylation-dependent binding partner of BRCA1 C-terminal domains. Molecular and Cellular Biology *24*, 9478–9486.

Yu, X., Fu, S., Lai, M., Baer, R., and Chen, J. (2006). BRCA1 ubiquitinates its phosphorylation-dependent binding partner CtIP. Genes & Development *20*, 1721–1726.

Yuan, S.S., Lee, S.Y., Chen, G., Song, M., Tomlinson, G.E., and Lee, E.Y. (1999a). BRCA2 is required for ionizing radiation-induced assembly of Rad51 complex in vivo. Cancer Research *59*, 3547–3551.

Yuan, S.S., Lee, S.Y., Chen, G., Song, M., Tomlinson, G.E., and Lee, E.Y. (1999b). BRCA2 is required for ionizing radiation-induced assembly of Rad51 complex in vivo. Cancer Research *59*, 3547–3551.

Yun, M.H., and Hiom, K. (2009). CtIP-BRCA1 modulates the choice of DNA double-strand-break repair pathway throughout the cell cycle. Nature *459*, 460–463.

Zachariae, W., Schwab, M., Nasmyth, K., and Seufert, W. (1998). Control of cyclin ubiquitination by CDK-regulated binding of Hct1 to the anaphase promoting complex. Science (New York, N.Y.) *282*, 1721–1724.

Zemla, A., Thomas, Y., Kedziora, S., Knebel, A., Wood, N.T., Rabut, G., and Kurz, T. (2013). CSN- and CAND1-dependent remodelling of the budding yeast SCF complex. Nat Commun *4*, 1641.

Zhang, F., Fan, Q., Ren, K., and Andreassen, P.R. (2009a). PALB2 functionally connects the breast cancer susceptibility proteins BRCA1 and BRCA2. Mol. Cancer Res. *7*, 1110–1118.

Zhang, F., Ma, J., Wu, J., Ye, L., Cai, H., Xia, B., and Yu, X. (2009b). PALB2 links BRCA1 and BRCA2 in the DNA-damage response. Current Biology : CB *19*, 524–529.

Zhang, L., Xu, M., Scotti, E., Chen, Z.J., and Tontonoz, P. (2013). Both K63 and K48 ubiquitin linkages signal lysosomal degradation of the LDL receptor. J. Lipid Res. *54*, 1410–1420.

Zhang, W., and Koepp, D.M. (2006). Fbw7 isoform interaction contributes to cyclin E proteolysis. Mol. Cancer Res. *4*, 935–943.

Zheng, J., Yang, X., Harrell, J.M., Ryzhikov, S., Shim, E.H., Lykke-Andersen, K., Wei, N., Sun, H., Kobayashi, R., and Zhang, H. (2002a). CAND1 binds to unneddylated CUL1 and regulates the formation of SCF ubiquitin E3 ligase complex. Molecular Cell *10*, 1519–1526.

Zheng, N., Wang, P., Jeffrey, P.D., and Pavletich, N.P. (2000). Structure of a c-Cbl-UbcH7 complex: RING domain function in ubiquitin-protein ligases. Cell *102*, 533–539.

Zheng, N., Schulman, B.A., Song, L., Miller, J.J., Jeffrey, P.D., Wang, P., Chu, C., Koepp, D.M., Elledge, S.J., Pagano, M., et al. (2002b). Structure of the Cul1-Rbx1-Skp1-F boxSkp2 SCF ubiquitin ligase complex. Nature *416*, 703–709.

Zhou, Q., Kojic, M., Cao, Z., Lisby, M., Mazloum, N.A., and Holloman, W.K. (2007). Dss1 interaction with Brh2 as a regulatory mechanism for recombinational repair. Molecular and Cellular Biology *27*, 2512–2526.

Zierhut, C., and Diffley, J.F.X. (2008). Break dosage, cell cycle stage and DNA replication influence DNA double strand break response. The EMBO Journal *27*, 1875–1885.

Appendices

S1 Detection of ubiquitylated BRCA2 in HEK293T cells using GST-TUBE

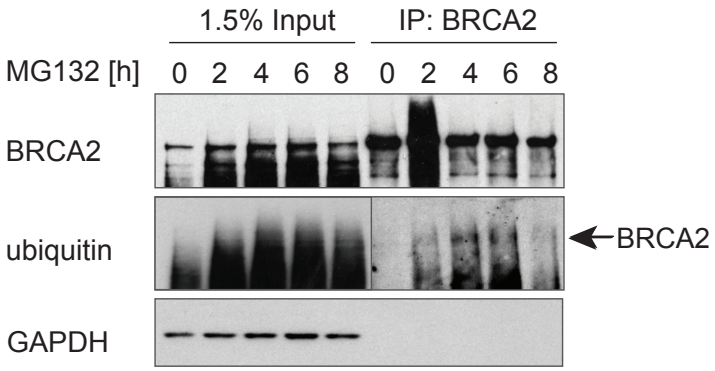

Figure S1: Detection of ubiquitylated BRCA2 in HEK293T

A) HEK293T cells were incubated with 10 µM MG132. Whole cell extracts were prepared after 2, 4, 6 or 8 h treatment and subjected to immunoprecipitation with BRCA2 antibody. To detect ubiquitylated BRCA2, membranes were probed with ubiquitin antibody.

S2 Analysis of BRCA2 level after DNA damage

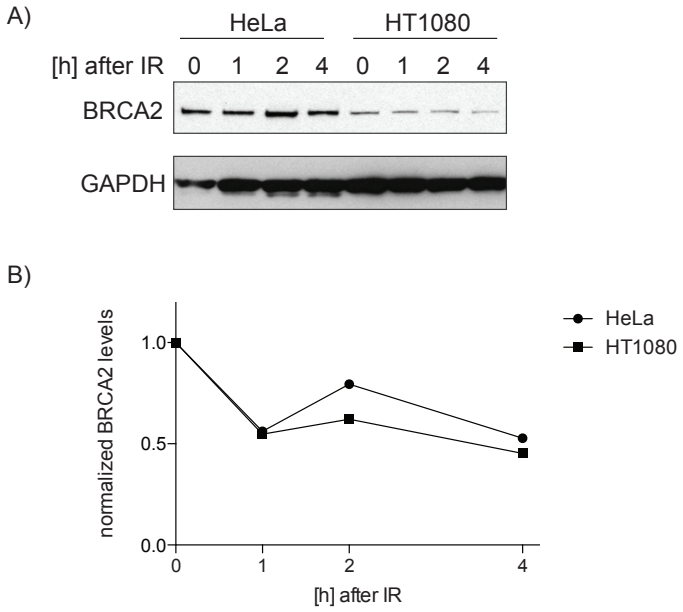

Figure S2: BRCA2 protein levels decrease after DNA damage

HeLa and HT1080 cells were exposed to IR (4 Gy) and BRCA2 protein levels were followed taking samples at 0, 1, 2, and 4 h after IR. A) BRCA2 levels were detected by Western blot analysis. B) Quantitative analysis of BRCA2 level. Detected BRCA2 was normalized against the loading control (GAPDH) and plotted against the time after IR (h).

S3 Analysis of phosphorylation dependent interaction of FBXW7 with B2-2 fragment *in vivo* in cells treated with kinase inhibitors

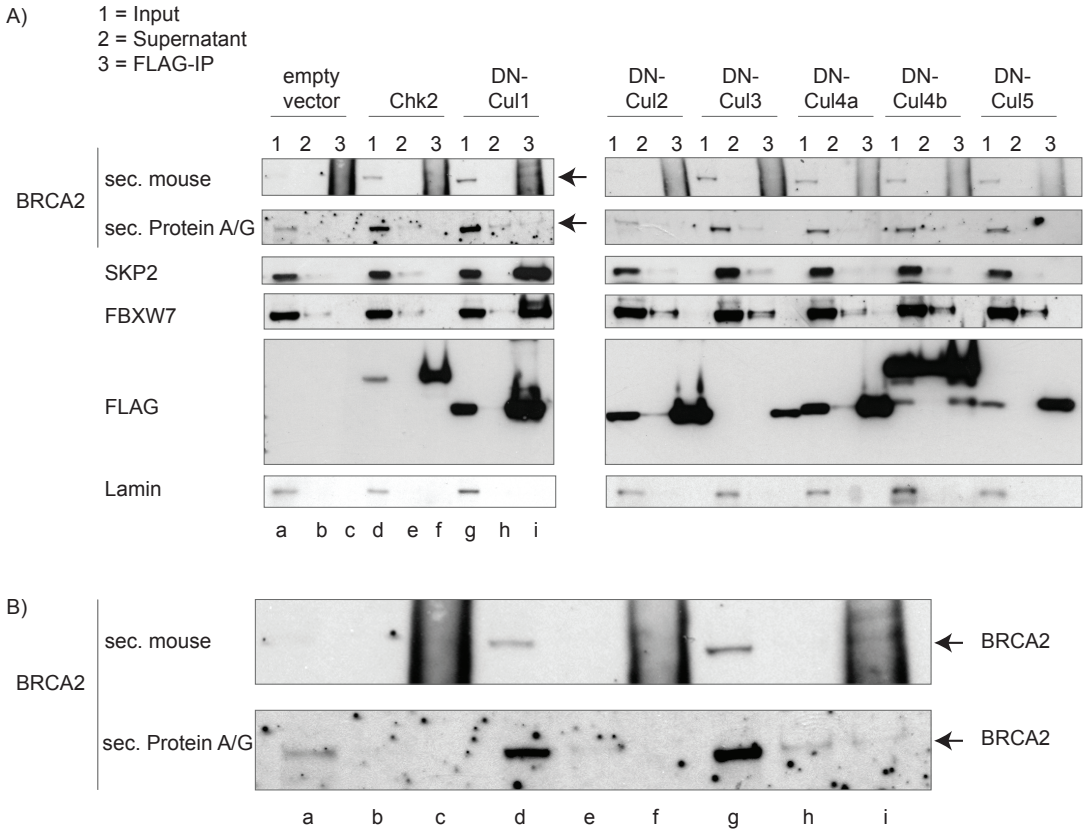

Figure S3: BRCA2 and Cullin 1 interact *in vivo*

A) FLAG-immunoprecipitation of DN Cullin variants (F-DN) as well as empty vector (pcDNA3.1) and FLAG-tagged CHK2 as negative controls were expressed in HEK293T cells and FLAG-immunoprecipitation (IP) was performed. Extraction of proteins was performed using HEPES-based extraction buffer. B) Magnification of BRCA2 probed blot of FLAG-immunoprecipitation of empty vector (a-c), FLAG-tagged CHK2 (d-f), and F-DN CUL1 (g-i).

S4 Analysis of phosphorylation-dependent interaction of FBXW7 with B2-2 fragment *in vivo* in cells treated with kinase inhibitors

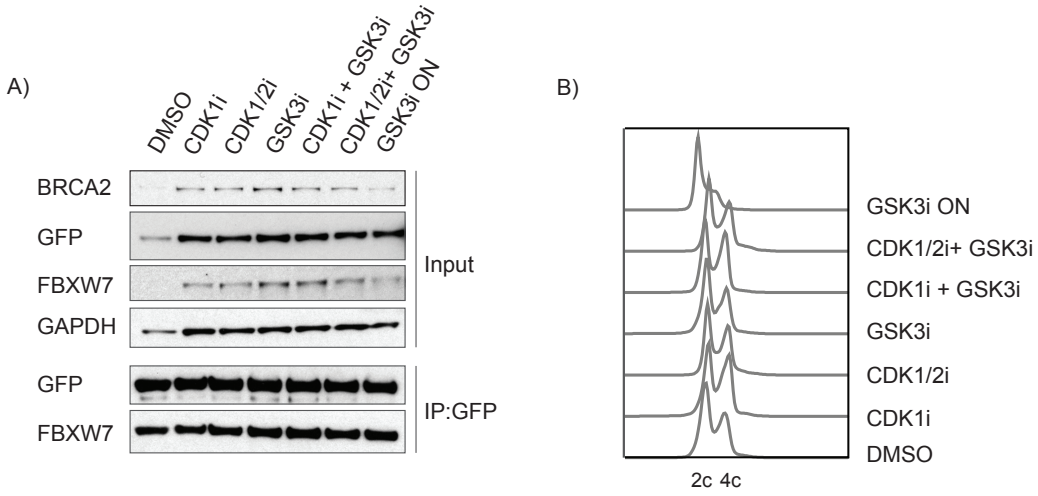

Figure S4: Analysis of phosphorylation-dependent interaction of FBXW7 with B2-2 *in vivo* in cells treated with kinase inhibitors

A) GFP-immunoprecipitation of B2-2 fragment expressed in HEK293T cells, which were treated with different kinase inhibitors. HEK293T cells were transfected with B2-2 fragment for 24 h and treated for 4 h with DMSO, CDK1i (RO-3306), CDK1i + CDK2i (NU6102), GSK-3i (IX), CDK1i + GSK-3i (RO-3306 + IX), CDK1i + CDK2i + GSK-3i (NU6102 + IX) or GSK-3i (IX) ON (16 h). B2-2 was immunoprecipitated by GFP-IP and interaction with FBXW7 was tested. B) Cell cycle analysis of inhibitor treated cells.

S5 Phenotypic analysis of DLD-1

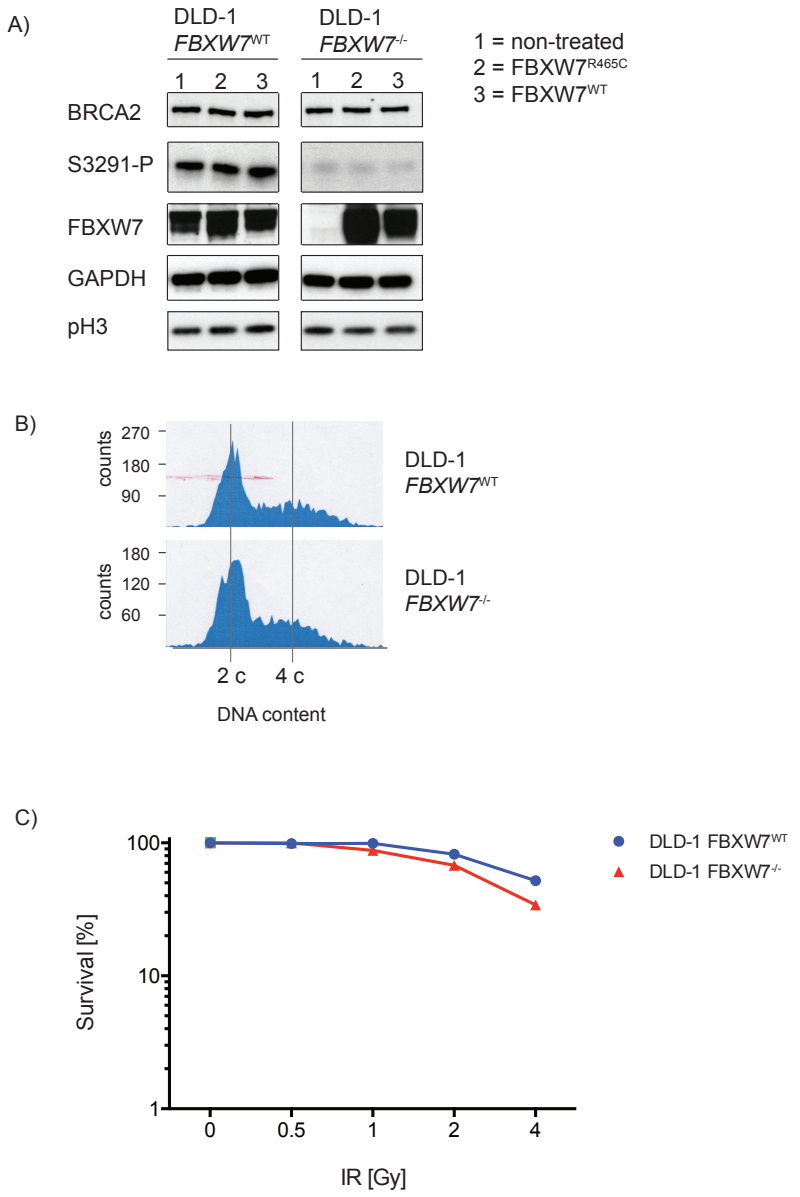

Figure S5: Phenotypic analysis of isogenic *FBXW7*^{WT} and *FBXW7*$^{-/-}$ DLD-1 cell lines A) FBXW7^{WT} and FBXW7^{R465C} mutant were expressed in *FBXW7*^{WT} and *FBXW7*$^{-/-}$ DLD-1 isogenic cell lines and Western blot analysis was performed. B) FACS cell cycle analysis of *FBXW7*^{WT} and *FBXW7*$^{-/-}$ DLD-1 cell lines. C) Cellular survival of *FBXW7* wild type (WT) and null (-/-) isogenic HCT116 cells was analysed after exposure to 1, 2, 4 Gy of IR in clonogenic cell survival assay. Depicted are the average means of 1 triplicate experiment.